HAI Project #1DTG00001.002

Forensic Analysis of Ignitable Liquid Fuel Fires in Buildings

FINAL

Grant No. 2009-DN-BX-K232

Prepared by

Christopher L. Mealy, Andrew J. Wolfe and Daniel T. Gottuk
Hughes Associates, Inc.
3610 Commerce Drive, Suite 817
Baltimore, MD 21227
Ph. 410-737-8677 FAX 410-737-8688
www.haifire.com

February 15, 2013

ABSTRACT

An experimental study of liquid fuel fires (Class B) in enclosures with Class A combustibles was conducted to 1) characterize the differences in fire dynamics and fire damage between ignitable liquid fuel fires in compartments versus in the open, and 2) to evaluate the reliability of fire patterns and fire debris sampling for ignitable liquid residue analysis. The experimental work included an evaluation of patterns within enclosure fires, including fuel spill patterns and clean burns and an analysis of calcination of gypsum wallboard**.** A reliable and accurate method of obtaining calcinations depth surveys with a new portable hand-held tool was developed. The utility of calcination depth surveys was evaluated with respect to assessing the compartment fire dynamics and fire origin. The impact of water spray on the accuracy of calcination depth measurements was also assessed. The persistence of ignitable liquid residue was evaluated in a controlled, small-scale environment and in full-scale enclosure fires to identify optimum sampling locations within a given scenario.

TABLE OF CONTENTS

TABLE OF FIGURES

Page

TABLE OF TABLES

Page

ACKNOWLEDGEMENTS

This project was supported by Award No. 2009-DN-BX-K232 awarded by the National Institute of Justice, Office of Justice Programs, U.S. Department of Justice. The opinions, findings, and conclusions or recommendations expressed in this publication/program/exhibition are those of the author(s) and do not necessarily reflect those of the Department of Justice. The authors would also like to thank the assistance of the ATF Fire Laboratory for providing support with the full-scale enclosure fires.

LIST OF ACRONYMS

ATF	Bureau of Alcohol, Tobacco, and Firearms
FTIR	Fourier transform infrared spectroscopy
GWB	Gypsum Wallboard
ILR	Ignitable Liquid Residue

EXECUTIVE SUMMARY

Liquid fuel fires represent the initiating fire hazard in many applications ranging from accidents at industrial plants to arson fires. A previous NIJ grant evaluated the burning dynamics and resulting patterns from liquid fuel spill fires in the open. These scenarios are relevant to outside fires and fires in large spaces where ceilings and upper gas layers have no significant effects and air supply is not limited. However, many fire events will include ignitable liquids used in smaller rooms with varying amounts of ventilation. For example, half (54%) of intentional structure fires and four out of five civilian deaths (85%) and civilian injuries (82%) occur in homes. Therefore, there was a need to expand on the past liquid fuel fire project with a program of compartment fires that evaluate fire development and fire scene analysis including damage patterns, fire debris sampling techniques and ignitable liquid residue (ILR) measurements.

Although there have been various projects addressing fire patterns in general, there has been limited work done to evaluate the effect of compartment fire conditions on the comparison of ignitable liquid fire patterns and other Class A fire patterns. More work was needed to understand the reliability of pattern analysis and ignitable liquid residue testing for a range of compartment fires with ignitable liquids and Class A fuels. Therefore, the objectives of this work were to: 1) characterize the differences in fire dynamics and fire damage between ignitable liquid fuel fires in compartments versus in the open, and 2) to evaluate the reliability of fire patterns and fire debris sampling analysis using GC/MS ILR testing to identify the presence of ignitable liquid fuel in compartment fires relative to a range of fuel types, flooring materials, and thermal conditions.

These objectives were evaluated through a series of small and full-scale fire tests. Comparisons between the burning dynamics of liquid and Class A fuels in both the open and within an enclosure are provided in a parallel report. This report addresses the forensic analysis of the large-scale fires and addresses pattern formation, evaluation of the utility of calcination measurements of gypsum wallboard, and the persistence of ignitable liquid residues. The report is divided into three sections that discuss each of these subjects.

The calcination of gypsum wallboard (GWB) was studied with the intent to 1) develop an objective tool and method of quantifying in situ calcination depths, 2) assess the utility of calcination depth surveys as a means to understand fire origin and fire development within an enclosure, and 3) characterize the impact of water spray on the accuracy of calcination depth measurements.

Small-scale cone calorimeter testing was used to create varying degrees of calcination within GWB samples. Using visual observations to quantify calcination depth based on color or texture variations proved inconclusive, as none of these changes could be consistently correlated to calcination, moreover a specific depth. However, using these samples, a hand-held tool was developed to measure calcination depth based on an evaluation which identified a probe pressure that was sufficient to penetrate all degrees of calcination but not sufficient to penetrate virgin GWB. The tool consists of a digital force gauge to which a 2 mm hex key is attached to serve as the probe. A probe force of 3kg (6.6 lbs) was determined to be the appropriate force to completely penetrate calcined material without penetrating uncalcined material. The 3 kg force with the specified probe equates to a probe pressure of 0.86 kg/mm^2 (1175 psi). Using this

probing technique, the calcination depths of all small-scale samples were measured and tabulated. The calcination depths for the corresponding total heat exposures were in good agreement to a recent study by a Mann & Putaansuu [2010], in which the authors characterized calcination depth using an FTIR chemical analysis. The similarity between the depths measured in this study and those quantified by Mann serve as validation of the technique developed in this work. From this small-scale data set it was also determined that a total heat exposure of approximately 36 MJ/m^2 was required to achieve complete calcination of GWB samples with a thickness of 12.7 mm (0.5 in.) and approximately 90 MJ/m^2 was required to achieve complete calcination of samples with a thickness of 15.9 mm (0.625 in.) samples.

With a hand-held tool and appropriate technique developed, a series of calcination depth surveys of full-scale room fire enclosures were conducted. Surveys were conducted after six different full-scale enclosure fires with varying ignition and ventilation scenarios. The benefit of the calcination depth survey was realized primarily for the tests where visual patterns were not obvious. In these scenarios, the interior surfaces of the enclosure were heavily sooted with no visual indications of any fire patterns. However, after collecting calcination depths at set intervals and plotting these values, a contour plot of the data provided valuable insight into the areas within the enclosure that were subjected to the most severe thermal damage. In general, the areas in which the initiating (or primary first fuel) fire occurred could be identified based on differences in damage patterns relative to adjacent areas. From these full-scale calcination depth surveys it was concluded that the utility of this technique is greatest when visible patterns are not present. In the event that visual patterns were present, calcination depth surveys provided minimal additional insight into the fire scenario. However, further study of the relationship between calcination and total heat exposure could enhance the utility of these surveys by providing fire investigators a means of estimating fire growth scenarios based on thermal damage to the GWB.

The impact of water spray on the measurement of calcination depth was also evaluated. From these tests, it was concluded that the application of water alters the measured depth of calcination. An average increase in depth of approximately 18 percent was calculated for measurements collected 24 hours after fire exposure and application of the water. This difference fell to less than five percent after the samples were left to dry for a period of 30 days. This data suggests that if measurements are to be collected in areas that have been wetted by suppression activities for any extended period of time, it would be advisable to delay measurements until the water has been removed. However, based on the limited water application (1.25 and 5 gal/ft^2), even at 24 hours, the expected error (~18%) is reasonable if the main purpose of the depth survey is to identify heat patterns.

Gasoline spill fire scenarios were conducted on carpet and vinyl flooring in the open and in rooms with other Class A combustibles. The enclosure fires in this study included flashover conditions (full door vented fires) and fully involved fires that did not actually flashover (slit vent cases). In both types of fires, most combustibles in the room had pyrolized or burned. Exposure durations ranged from 60–300 seconds for open burning scenarios, 1–6 minutes for post-flashover scenarios, and 7–12 minutes for the limited ventilation scenarios.

In general, the utility of floor patterns was minimal for all scenarios except those conducted in the open. Due to the extensive thermal damage within the enclosure fires, patterns initially

formed by gasoline spill fires were destroyed. For vinyl floor scenarios, the brevity of the spill fire was such that the surface charring and thermal discoloration produced by the spill fires were quickly overwhelmed by the ignition and burning of the material. Furthermore, the impermeable nature of the vinyl was such that the subfloor was not impacted in any way by the initial spill fire, therefore when the vinyl flooring was consumed, the subfloor showed no evidence of the initiating fire scenario.

For carpet scenarios, the persistence and utility of the patterns was slightly better than that of vinyl floors. In both the open burning and enclosed scenario with no Class A materials present, the carpet flooring showed evidence of the gasoline spill fire in the form of a doughnut pattern. However, this type of pattern was not observed in any of the enclosure tests conducted with Class A fuels present. In these tests, patterns remaining on the flooring materials were primarily a result of the burning Class A materials inducing ignition and flame spread on the flooring material. As a result of this, when the carpet flooring was not completely thermally degraded, the largest and most severe areas of burning were generally located proximate to the larger Class A furnishings (i.e., upholstered sofa and chair).

Based on these flooring evaluations, the persistence of a fire pattern from an initiating fire source requires that the damage from the source be greater than that from the pursuant enclosure fire and that the substrate be resilient enough to survive both exposures. Spill fires in rooms with large volumes relative to the fire size are candidate scenarios in which fuel spill patterns may have a chance to persist, particularly for floor materials that can absorb liquid fuel. Unless there are areas of undamaged or marginally damaged flooring, initial spill fire patterns are not expected to remain post-fire. Based on the tests conducted with fully involved, limited ventilation fires and full door vented flashed over fires, spill patterns did not persist due to the widespread thermal degradation of the floor.

In the nine Class A fire enclosure tests, the most easily identifiable patterns were characterized by the relative absence of soot compared to adjacent areas. Traditionally, these patterns are referred to as clean burns and are associated with the thermal oxidation of soot (i.e., removal of soot due to high temperature exposure). Clean burns are also typically associated with areas that are stark white in contrast to adjacent areas that are blackened due to soot deposition. However, clean burns can exhibit a range of colors from dark gray to white as the pattern forms with increasing heat exposure. These patterns will also range from a finely speckled appearance to fully cleared areas of white gypsum.

Numerous wall patterns were identified behind the smaller fuel packages (i.e., upholstered chair and baby seat) which were offset from the enclosure wall. These patterns were not completely clean (white) but showed signs of soot oxidation. Within the boundary of these clean burn patterns, soot was still present, but to varying degrees of gray. As the fire exposed the gypsum wallboard, the paper face would pyrolize (thermally degrade, char). Pyrolysis of materials can transition to flaming combustion, but it can also progress as charring or smoldering combustion. The result of the pyrolysis or burning of the gypsum wallboard paper was ash. Ash was present both with and without soot (i.e., black and white). Clean burns occurred with white ash present and sometimes with no ash at all, just the underlying gypsum.

These tests showed that clean burn patterns can be formed on walls in areas that do not have a Class A fuel source directly adjacent to them. As noted by other investigators, clean burns can be formed on walls and ceilings in areas dictated by the supply of air due to local ventilation flows. In several of the tests, large areas in which soot had been removed were not associated with fire exposure. Although these white patterns had similar appearances to clean burn patterns, they had notable differences upon closer examination. These patterns were characterized by a splatter appearance (larger whitish spots) around the periphery with the center consisting of larger areas of soot removal, sometimes with signs of a smeared, directional appearance. These patterns were the result of suppression activities on both walls and ceilings. In some cases, particularly walls, watermarks were observable (i.e., water drip marks). Besides the characteristics noted above, the suppression patterns were also verified by the visual presence of a green tint to the pattern that was associated with the chemical treatment of the suppression water at the fire lab. The means of differentiating clean burn and suppression patterns based on the characteristics described in this report would be enhanced by further systematic testing. These tests showed that the characteristics are distinct. However, for the case of complete soot and ash removal with large white patterns, there may be circumstances that the absence of either the speckled pattern associated with clean burn development or splatter patterns associated with water extinguishment cause uncertainty in determining the source of the white pattern. In addition, depending on the quality and resolution of photographs, it is possible to have water spray patterns appear as indistinguishable from clean burns in photos.

A total of 52 small- and full-scale fire tests were conducted to study the persistence of an ignitable liquid residue on several different substrates subjected to varying fire conditions and to identify optimum locations from within fire patterns for ILR sampling. The focus of the small-scale testing was to characterize the persistence of an ignitable liquid residue on four different substrates exposed to four different total heat exposures. The substrates evaluated varied in porosity and propensity to burn and represented typical building materials (composite furniture materials, plywood, vinyl and carpet/pad). The results from this testing demonstrated that the likelihood of an ILR persisting within a given substrate was dependent upon both the total heat exposure and the ability of the substrate to absorb the ignitable liquid. Absorbent materials such as carpet flooring and plywood retained ILR under more severe thermal exposures than impermeable substrates, such as vinyl.

The absorbency of the ignitable liquid substrate was not the only factor identified as playing a key role in the persistence of ILR on the material. The combustibility of the material (i.e., how readily it burns) impacted the persistence of the ILR. The prime example of this was the composite furniture material. This material was the most absorbent material tested, however, it was also the most readily combusted (i.e., greatest mass loss at a given heat flux), which resulted in the material being the least likely to contain ILR after the thermal exposure. Based on the small-scale test results, gasoline was most persistent when spilled onto carpet and pad flooring. The likelihood of residue remaining on the other substrates tested was found to be progressively less probable for plywood, vinyl, and the furniture material, respectively. From these tests, approximate total heat exposure thresholds were calculated based on the exposure severity and exposure duration. The thresholds were calculated to provide estimates of the total amount of heat needed to consume the ILR present within the samples tested. A threshold was not established for carpet (i.e., ILR was always identified for the four total heat exposures considered, up to 39 MJ/m^2). The threshold for plywood is between 18–39 MJ/m^2. The threshold

for vinyl and the furniture material was between 3.6–7.8 MJ/m^2. It should be noted that this threshold is most likely dependent on the volume of ILR applied to the substrate with greater volumes requiring larger total heat exposures and vice versa. However, this variable was not explored in this work.

Full-scale testing was conducted to identify optimum sampling locations within fuel spill fire patterns. Open-burning and enclosed scenarios, with and without Class A furnishings, were evaluated. ILR results from open burning tests showed that in these scenarios the thermal insult from the spill fire alone is generally not sufficient to consume the ignitable liquid residue present within a given pattern. Samples were collected at edge, mid-point, and center locations for both carpet and vinyl substrates.

The results from open burning spill fires on carpet showed that in the absence of an external heat source, samples can be collected from anywhere within the original spill area to obtain positive ILR results. It should be noted that in many cases, even open burns with extended burning duration, the initial spill area is not readily identifiable. Consequently, for carpet scenarios, sampling from the center of the pattern provides the highest likelihood of positive ILR identification, if an ignitable liquid was initially present. This approach is supported by the fire dynamics that are required to form the doughnut pattern, a well-established fire pattern associated with liquid fuel spills on carpet flooring. The phenomenon that forms this pattern requires that the ILR persist the longest at the center of the pattern to the limited burning of material during the initial stage of the fire because of wicking of the gasoline through the carpet fibers. Essentially, the liquid fuel keeps the center of the spill area cool even though it has the greatest incident heat flux from the flame compared to the edges of the fire area. The higher probability of ILR in the center is contrary to the conclusion of O'Donnell [1985]. In O'Donnell's tests, the carpet flooring did not have padding beneath it (i.e., less absorption), and his results are not consistent with the formation of doughnut patterns.

For the open burning spill fires on vinyl, the majority of the sampling locations were positively identified as containing ILR. However, in three of the tests, ILR was not identified at the center sampling location. These results indicate that for impermeable substrates, sampling along the edge, or at least away from the center should provide the highest likelihood of positive ILR identification if an ignitable liquid was initially present. This result is consistent with the recommendations of Stauffer et al. [2008]. The preferential degradation of the ILR at the center of the vinyl spill fire pattern is attributed to greater heat fluxes in the center than at the edges.

Within an enclosure without additional Class A combustibles present, the presence of ILR was found to be substantially less prevalent than was observed for open burning tests. This decrease in ILR persistence is attributed to the additional heat imposed by the hot upper layer within the enclosure. This hot layer not only caused additional fuel to be evaporated from the substrate, but also resulted in the involvement of the substrate in the fire. For the vinyl substrate, despite the fact that a 2.0 L (0.53 gal) gasoline spill was used, no positive ILR samples were identified. For the carpet scenarios, three of the nine samples collected were identified as containing ILR. All of these samples were collected from the center of the pattern, which is consistent with the findings of the open-burning tests. These tests demonstrated the negative impact that an enclosure has on the persistence of ILR.

Within an enclosure with Class A combustibles present, the persistence of ILR on both carpet and vinyl flooring was dependent on numerous factors that affect the total heat exposure to the material with the ILR. These factors can include the hot upper layer, radiation from fire plumes of burning Class A material and ventilation that creates intensified combustion regions. From these tests, it was determined that identifying ILR sampling locations from enclosure fires with severe fire conditions (i.e., near or post-flashover) is very challenging for two primary reasons: the first being that the patterns created by the spill fires did not persist through the fire event and the second being the thermal exposure created by the enclosure fire consumed the ILR in many samples. In general, upholstered furnishing debris (i.e., wood/particle board framing materials) had the highest likelihood of retaining an ILR when compared to samples collected from flooring materials (i.e., carpet or vinyl) Based on the fact that fuel spill patterns generally may not be identifiable at fire scenes with substantial damage (e.g., flashed over conditions), areas should be surveyed for ILR using a systematic approach (i.e., a grid network across the whole space) to ensure representative results. However, particular attention may be given to areas around furniture or other fuel sources that were known to exist in the room. Without a systematic survey approach, the chances are high that an investigator will miss a positive ILR sample location if relying on a visual indicator. This concept reinforces the findings of this work that the absence of ILR in samples collected from a fire scene is not a confirmation that an ignitable liquid was not initially present.

1.0 INTRODUCTION

Liquid fuel fires represent the initiating fire hazard in many applications ranging from accidents at industrial plants to arson fires. Although there are a number of studies that address liquid fuel fires, there is limited work available on liquid spill fires, which represent the majority of actual fire incidents [Putorti 2001, Modak 1981, Gottuk & White 2002, Stensaas et al. 1999]. It is noted that a pool fire is characterized by a confined body of fuel that typically has a depth of greater than 1 cm [Gottuk & White 2002]. A pool can result due to a spill that collects in a low spot, such as a trench, or can exist as a result of normal storage of fuels in tanks and containers. An unconfined fuel spill is generally associated with fuel that is released with no physical boundaries and results in a liquid layer that is thin compared to a pool.

A previous NIJ grant evaluated the burning dynamics and resulting patterns from liquid fuel spill fires in the open [Mealy et al. 2011]. These scenarios are relevant to outside fires and fires in large spaces where ceilings and upper gas layers have no significant effects and air supply is not limited. However, many fire events will include ignitable liquids used in smaller rooms with varying amounts of ventilation. For example, half (54%) of intentional structure fires and four out of five civilian deaths (85%) and civilian injuries (82%) occur in homes [Flynn 2009]. Therefore, there was a need to expand on the past liquid fuel fire project with a program of compartment fires that evaluate fire development and fire scene analysis including damage patterns, fire debris sampling techniques and ignitable liquid residue measurements.

Although there have been various projects addressing fire patterns in general [Putorti 2001, Hopkins et al. 2008, Gorbett et al. 2006, Mealy et al. 2006], there has been limited work done to evaluate the effect of compartment fire conditions on the comparison of ignitable liquid fire patterns and other Class A fire patterns [Stensaas et al. 1999 and Shanely 1997]. More work was needed to understand the reliability of pattern analysis and ignitable liquid residue testing for a range of compartment fires with ignitable liquids and Class A fuels. Therefore, the objectives of this work were to: 1) characterize the differences in fire dynamics and fire damage between ignitable liquid fuel fires in compartments versus in the open, and 2) to evaluate the reliability of fire patterns and fire debris sampling analysis using GC/MS ILR testing to identify the presence of ignitable liquid fuel in compartment fires relative to a range of fuel types, flooring materials, and thermal conditions.

These objectives were evaluated through a series of small and full-scale fire tests. Comparisons between the burning dynamics of liquid and Class A fuels in both the open and within an enclosure are provided in a parallel report [Mealy et al. 2013]. This report addresses the forensic analysis of the large-scale fires and addresses pattern formation, evaluation of the utility of calcination measurements of gypsum wallboard, and the persistence of ignitable liquid residues. The report is divided into three sections that discuss each of these subjects.

2.0 CALCINATION DEPTH STUDY

2.1 Literature Review

Gypsum wallboard is a building material used for walls, ceilings and partitions in residential and commercial buildings. It has been present in the vast majority of new construction in the

United States since 1945. Gypsum wallboard consists of a gypsum core that is most often enclosed by a paper covering on either side. Gypsum is a naturally occurring substance consisting of approximately 79 percent calcium sulphate and 21 percent chemically bound water. As gypsum is heated it undergoes several phase changes that can be associated with different temperature thresholds. The heating of gypsum results in the removal of both free and chemically-bound water in a process known as calcination. The temperature thresholds commonly associated with the calcination of the material range from 52–130ºC (125–266ºF) [Mann & Putaansuu 2010, Schroeder 1999]. At these temperatures, the water contained within the material will begin to dissociate and gradually be completely removed from the gypsum material. The dehydrated gypsum continues to adhere to the undamaged gypsum behind it but is considered calcined. Calcined gypsum is less dense, than virgin gypsum; the softened, calcined material can be penetrated to a deeper depth when pushed on with a thin probe.

The prevalence of gypsum wallboard in fire scenes makes it a potentially valuable source of information to fire investigators when assessing a fire scene. The exposure of gypsum wallboard to heat from a fire can result in calcination, which in turn can theoretically be correlated to the total heat exposure to that area. Therefore, if properly characterized, a calcination depth profile of a given enclosure could provide fire investigators with a detailed history of the total heat exposure to the walls and ceiling of the space. This history, when combined with other findings, could provide valuable insight as to where the area of origin was located or how the fire developed. Despite the fact that calcination depth surveys are a relatively well-known fire investigation tool, there has been very limited research conducted to develop a technical basis and standardized methodology for understanding and collecting these measurements in realistic scenarios.

The purpose of this study was to expand upon the current methodologies, recommendations, and general information available to fire investigators choosing to investigate the calcination depth of gypsum wallboard in fire scenes. The approach presented in this section was designed to incorporate small-, intermediate-, and full-scale testing to develop an objective method for measuring the calcination depth of gypsum wallboard (GWB). Small-scale testing was conducted to expose samples to known heat fluxes for various durations. These samples were then used to develop a tool and the associated technique needed to accurately measure calcination depth. Once this tool and technique were developed and validated, they were used to perform calcination depth surveys on several different full-scale enclosures exposed to various fire scenarios. The data from these surveys was tabulated and used to compare measured damage trends (i.e., calcination depths) to visual observations/patterns to assess the utility of the measurements collected. Finally, a series of controlled intermediate-scale furnace exposures was conducted to assess the impact of wetting of the GWB on the accuracy of calcination depth measurements. Understanding this impact is essential because in most real-world fire scenarios, it can be assumed that fire suppression activities wet surfaces of the enclosure that could be used for calcination depth measurements. Calcination depths were collected within 24 hours of wetting as well as 30 days after wetting. Companion measurements from the non-wetted (i.e., dry) side of the GWB were collected at these time intervals as well.

The relationship between total heat exposure (i.e., time v. temperature) and the calcination of the gypsum wallboard was first identified by Posey & Posey [1983]. In this work, the authors suggested that a series of visual observations, noting the depth of calcination, could be used by

fire investigators to identify thermal exposures within a given space. The authors recommended that sections of the gypsum wallboard be removed and broken in half. Posey & Posey defined calcination as the layer of color differentiation visible in the cross section of the gypsum material. Technical rationale for this differentiation was not provided and no experimental verification was performed in this early work.

DeHaan [1997] expanded the discussion of the utility of calcination measurements and provided a simple description of the chemical make-up of gypsum and the dehydration process. While discussing the topic he also cautioned against the application of the technique to characterize fire intensity. Again, no experimental verification was performed.

The first systematic investigation into the physical measurement of calcination depth was performed by McGraw [1998]. McGraw exposed GWB samples to three different thermal exposures for three different durations to induce varying degrees of calcination. In this work, the depth of calcination was measured in two ways: cracking and moisture content. The cracking method consisted of breaking a sample in half and measuring calcination depth along the broken edge of the sample using vernier calipers. The calipers provided greater accuracy and allowed for multiple depths to be measured and averaged. In this work, the author reported that a visible ridge or fracture line could be identified within the samples. The author attributed this line to the dehydration front (i.e., calcination depth). The author also reported that samples exposed to the highest thermal exposures exhibited no line, which was attributed to complete calcination. The moisture method utilized mass loss data and equated mass loss to moisture loss. This method assumed complete dehydration of the sample up to the calcination front and no dehydration beyond the front.

When comparing the depths measured using the cracking method and moisture methods, no consistent trends were identified. In five of the nine comparisons, a greater depth was measured using the cracking method. In these cases, the average difference in measured depth was 1 mm. The moisture method produced the greatest depths in the remaining four comparisons with an average difference of 1.7 mm. Differences in calcination depths for these two methods ranged from 0.4–3.4 mm. From this work, the author concluded that the depth of calcination is dependent on the exposure severity and duration. It was also concluded that more severe, longer duration exposures produce deeper layers of calcination. However, a correlation between the thermal insult and the depth of calcination was not identified and confirmation that the visual indicator truly represented the calcination depth was not obtained.

The first attempt to quantitatively analyze the depth of calcination of gypsum wallboard as it relates to forensic fire reconstruction was performed by Schroeder [1999]. This work differs from that of McGraw in that the measurement of calcination depth was based on a phenomenological change in the material as opposed to a visual observation. In this work, the author examined GWB samples from both experimental thermal exposures and real-world fire exposures in an attempt to quantify the extent of calcination as a function of thermal exposure severity. Experimental samples were created by exposing 0.1 m (4 in.) square sections of GWB to various thermal insults using the ASTM E1354 radiant heater. Calcined GWB samples were also generated using a computerized display furnace. The corresponding calcination profiles from the experimental samples were quantified using both visual and analytical techniques. Schroeder demonstrated that the crystalline change that occurs in GWB when heated can provide

a distinct change in texture and color that can be visually detected by investigators. This conclusion was supported using x-ray diffraction techniques. Schroeder also states that in samples taken from actual fire exposures, numerous colors can be present making it more challenging to identify a clear depth. Based on his results, Schroeder concluded that the thermal exposure to a given section of GWB can be deduced from the measurement of calcination depth. In this work, Schroeder demonstrated the potential utility of calcination depth measurements using small-scale thermal exposures and analytical material characterization techniques. However, the author did not provide a reasonable approach for making such measurements. Given that calcination depth measurements are typically evaluated on a relative basis (i.e., comparisons between samples to identify areas of increased thermal damage) the removal of sections of wall material, as suggested by Schroeder, from numerous different locations does not lend itself to an efficient processing of a fire scene.

Kennedy et al. [2003] studied the practical use of calcination depth measurements to identify/illustrate fire patterns for fire origin determination. In this work, the authors used both a probe survey technique as well as visual cross-section inspection. When evaluating calcination depth using visual inspection, the depth was characterized based on color change in the material. According to the authors, the probe survey was based on techniques typically used in depth of char analyses, which have been used by fire investigators since the 1950's [Kennedy & Kennedy 1962]. The principle of the probe survey was to identify the depth at which the density of the material changes thereby identifying the point at which calcination progression through the material ceased. In this work, the participants used a probe depth gauge marketed for measuring the depth of sprayed-on thermal insulation. The probe had a circular cross-section steel probe of 0.127 cm (0.05 in.) diameter with a slightly chiseled tip. The device recorded depth measurements in 0.1 mm increments. Participants were instructed to apply a uniform force for all measurements and to apply the probe until a noticeable change in resistance was observed.

GWB samples were created during full-scale fire testing and calcination measurements were collected by numerous fire investigators with varying levels of experience. From this work, the authors concluded that the probe survey method of calcination depth analysis produced accurate and reproducible results in that the survey results were claimed to be representative of the fire origin and fire growth patterns observed during testing. Results of this work also showed that the probe measurements of calcinations depth were consistently less than those obtained from visual analysis of the cross-section. Despite the fact that numerous calcination depth measurements were collected by several different operators in this work, the accuracy of the depth measurements (i.e., were the depths measured representative of the actual calcination depth of the material) was never discussed or considered. Instead, the authors evaluated the utility of the method based on relative differences only.

Chu [2004] developed power law correlation between the calcination of GWB and the total heat exposure for various types and thicknesses of material. Plots of the measured calcination depths and associated thermal exposures from Chu [2004] are presented in Figure 1.

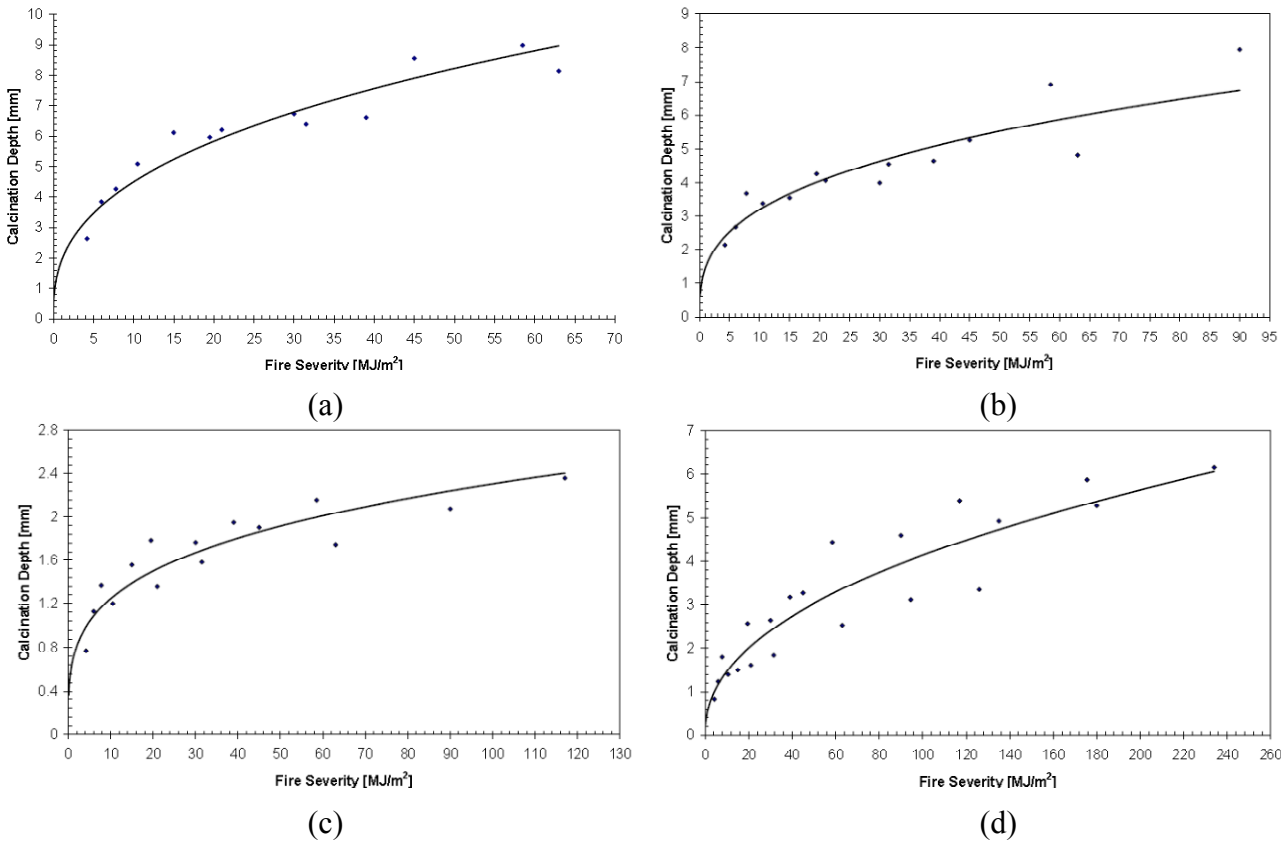

Figure 1. Summary of calcination depth versus fire severity correlations for (a) 10 mm standard board, (b) 10 mm Fireline board, (c) 10 mm Noiseline board, and (d) 19 mm Fireline board developed by Chu [2004].

Chu attempted to develop a practical tool, referred to as a constant force probe, that could be used to accurately and reliably measure calcination depth [Chu 2004]. He exposed small-scale samples of GWB to radiant heating using the ASTM E1354 cone calorimeter. The heated materials were then evaluated for calcination depth using two different techniques: hand scraping and probe survey. Visual observation of calcination depth was considered by Chu [2004], but determined to be too labor intensive, time consuming, and subjective relative to the investigator. Hand scraping was also used in this study to evaluate calcination depth. With this approach the operator removed the calcined material, via a flat-head screw driver by hand until a 'reasonable' hard plane was reached. The depth of this plane was associated with the depth of calcination. The author noted that this approach required the operator to become acclimated to the 'feel' between the two layers of material. Measurement consistency between these techniques varied. The development of the practical tool was comprised of evaluating both an appropriate probe cross-section as well as an appropriate probe force. Based on comparisons to hand scraping depths collected, the author concluded that a force of 6.6 N when applied to a blunt tip probe with a diameter of 1.45 mm (0.057 in.) was the most appropriate force to obtain representative calcination depths. This combination results in a probe pressure of 4.04 N/mm^2 (586 psi). In conclusion, the author states that while the visual measurement and hand-scraping techniques provide calcination depths that can be used to make relative determinations regarding fire severity, both of these techniques have drawbacks with respect to both accuracy and execution of

the measurement techniques. Chu [2004] concluded that only the constant force probe technique provides measurements that can be correlated to actual thermal exposures. While the author of this work provided a wealth of data regarding the calcination of various types of gypsum material relative to varying thermal exposures and started to characterize the force needed to characterize the depth of calcination, he did not extend the utility of these data sets and probing forces to full-scale, real-world exposures.

Mealy et al. [2006] collected calcination depth measurements from a series of full-scale enclosure fires. Probe measurements were taken manually using a depth gauge commonly used when measuring insulation thickness. The operators inserted the small area steel probe into the calcined material until a noticeable change in force was noted, at which point the probing was stopped and penetration depth measured. The work concluded that the contour plots of calcination measurements provided no more information than the visually observed fire patterns. An example of a calcination probe survey (contour plot) and the corresponding fire pattern photograph are provided in Figure 2. Other contour plots and photos are available in Mealy et al. [2006].

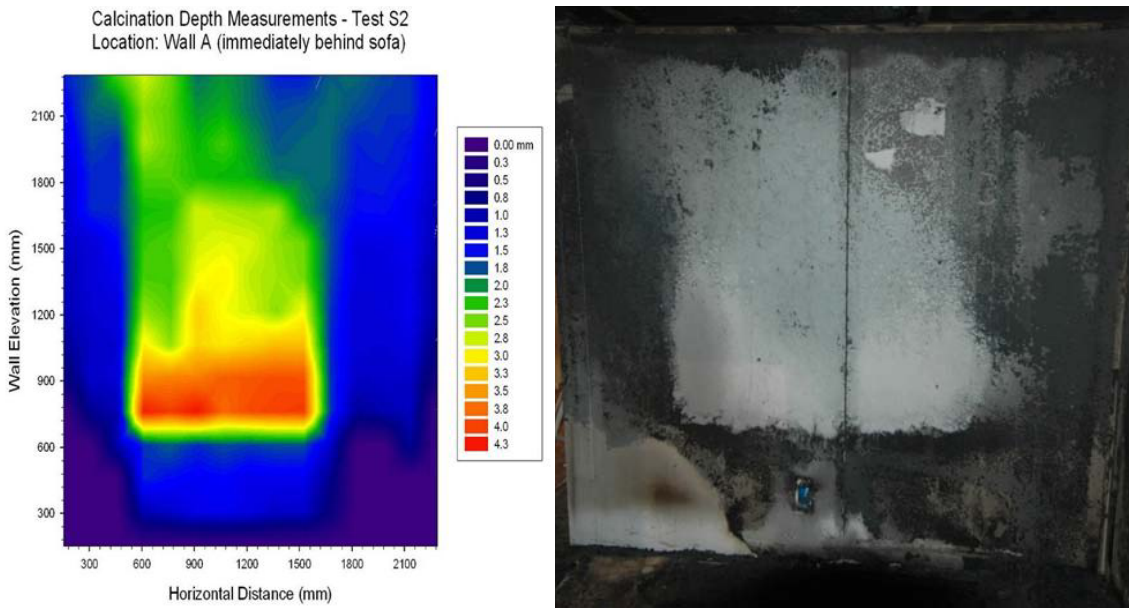

Figure 2. Comparison between calcination probe survey illustration (left) and photograph of fire pattern (right) from Test S2 [Mealy et al. 2006].

Mann & Putaansuu [2010] studied the dehydration/calcination of gypsum wallboard using both Fourier transform infrared spectroscopy (FTIR) as well as developing a technique to accurately measure calcination depth. The authors used FTIR measurements to distinguish between the different hydrated forms of the calcium sulfate present in GWB. Reagent grade standards of calcium sulfate di-hydrate, hemihydrate and anhydrous were used to confirm findings within actual GWB samples. Using this analytical technique, the authors were able to identify physical changes within the GWB due to dehydration and thereby identify the depths to which the material was calcined. Test data was used by Mann & Putaansuu [2010] to develop a probing tool and to explore several different probe forces to determine which force resulted in the depth measurements comparable to those obtained analytically. From this work, the authors

concluded that the optimal probe configuration was a blunt tip probe having a surface area of 3.12 mm^2 (0.005 $in.^2$). Furthermore, they found that using an application pressure of 0.9 kg/mm^2 (1230 psi) resulted in calcination depth measurements consistent (i.e., with 0.7 mm) with those obtained using the FTIR analysis. Mann & Putaansuu [2010] took the work of Schroeder [2001] and Chu [2004] one-step further by combining an analytical characterization of heated GWB with the development of a tool that can be used to accurately quantify calcination depth. However, the tool developed by the author required that samples be removed from a fire scene, as opposed to allowing in situ measurements to be collected.

Currently, Section 17.4.4.2 of NFPA 921, *Guide for Fire and Explosion Investigations* [2011] provides guidance for characterizing calcination depths, but this guidance is limited to the use of a "small-cross section probe" at intervals of no more than one foot while applying a "consistent" force. Under this guidance, the size of the probe and the force used by the investigator are completely subjective and other than making relative comparisons of depth (assuming consistent force is applied), the measurements collected provide no additional information as to the total heat exposure to the wall.

Despite the fact that all of the research described above relates to calcination of gypsum wallboard as a result of exposure to heat, there are two differing approaches to the utilization of calcination depth measurements. Up until the work of Kennedy et al. [2003], the focus of studying calcination was specifically to understand/develop the correlation between heat exposure and depth of calcination with the thought that this correlation could be used to characterize the fire environment. The stated intent of the Kennedy et al. [2003] work was to demonstrate the utility of the technique as it relates to identifying fire origin and movement patterns. The primary difference between these approaches is that the prior requires an accurate measurement of the calcination depth to quantify thermal insult while the latter only requires consistency throughout all measurements collected because a relative assessment is all that is needed.

The utility of calcination depth measurements as it relates to forensic fire investigation has been an ongoing debate/study for nearly three decades. The goal of this work was to assess under what conditions calcination depth surveys are of sufficient value to warrant the time and effort involved in conducting a survey. The potential value of a calcination depth survey was considered to be either its usefulness in identification of patterns or as a quantitative assessment of the amount heat exposure to a wall of ceiling based on the depth of calcinations. In order to meet this goal, particularly in evaluating the heat exposures, it was necessary to develop a tool that could be used by fire investigators to collect quantitatively accurate, in situ calcination depth measurements. At the start of this study, no such tool had been developed and validated. Building off the work of Chu [2004], a series of tests were conducted in this program to develop a probe and to assess the correct force that should be applied to accurately correlate the probe measurement to the true calcination depth. Part way through this program, the work of Mann & Putaansuu [2010] was obtained and served as an additional source for guidance and validation of this work.

2.2 Small-scale Exposure Study

The first series of calcination tests were conducted using the ASTM E1354 [2010] cone calorimeter as the exposure source. This test apparatus provided a means of applying a known heat flux that was uniformly distributed over a 0.1 m (4 in.) square surface area. The controlled nature of these tests was ideal for the development of a consistent, objective approach to measuring calcination depth in gypsum wallboard (GWB). The intent of these tests was to expose GWB samples to known total heat values (i.e., [incident heat flux] x [time]) and to quantify the extent of calcination via visual observations, manual probing, and mass loss. The mass loss of all samples was collected to determine if the change in mass of the material could be correlated to the total heat exposure. A description of the findings of this small-scale exposure study is provided in this section.

2.2.1 Small-scale Experimental Approach

All small-scale testing was conducted using the cone calorimeter located in the Hughes Associates Inc. small-scale test laboratory. The cone was constructed and maintained in general accordance with ASTM E1354 [2010]. This test method is designed to provide a small-scale test procedure to measure the ignitability, heat release rate, mass loss rate, and combustion product generation rate of a material exposed to a specified irradiance level. For the purposes of this testing, the heat release and combustion product generation features of the apparatus were not utilized. During each test, a 0.1 m (4 in.) square sample was placed beneath a conical shaped heater that provided a uniform irradiance on the sample surface, see Figure 3. Sample mass was continuously monitored using a load cell.

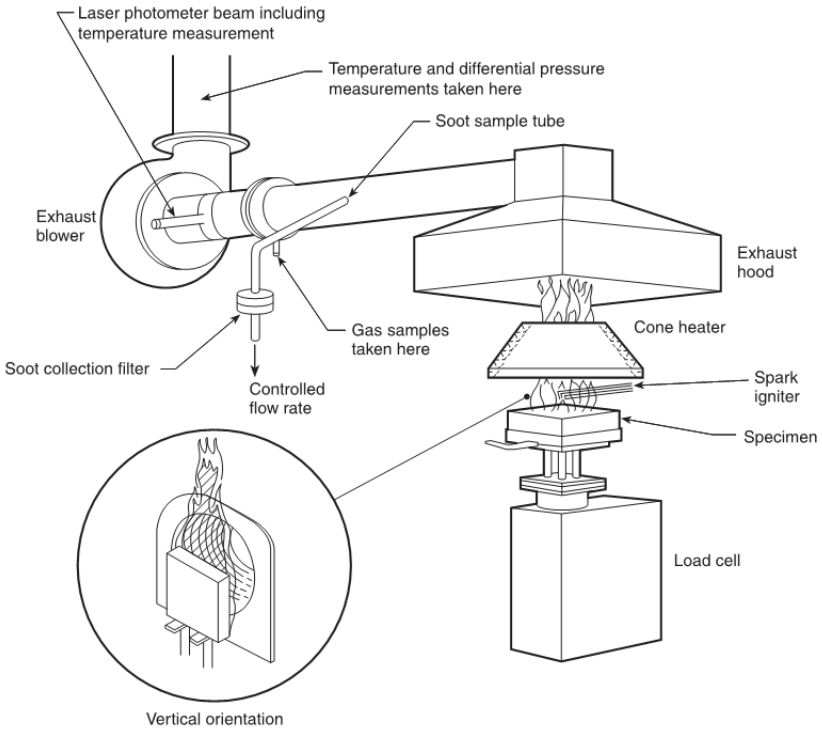

Figure 3. Illustration of the ASTM E 1354 cone calorimeter.

The GWB used in these tests was purchased from a local home improvement store and cut to size using a band-saw. United States Gypsum Sheetrock brand gypsum wallboard sheets were used for all tests. GWB thicknesses of both 12.7 mm (0.5 in.) and 15.9 mm (0.625 in.) were evaluated. After being cut to size, an initial sample mass was measured and recorded using a Sartorious Model YACO1LP load cell with 16 kg (35 lbs.) capacity and 0.1 g (0.0002 lbs.) resolution. Once weighed, the samples were wrapped in a single layer of aluminum foil as required in ASTM E1354 [2010]. Wrapped samples were then placed onto a 12.7 mm (0.5 in.) layer of ceramic fiber insulation and into a steel sample holder (i.e., a square pan).

Prior to each test, the desired heat flux was measured using a Medtherm Model GTW-10-32-485A, Schmidt-Boelter, water-cooled, heat flux transducer with a range of 0–75 kW/m^2. The transducer was installed beneath the conical heater at the same elevation as the samples were exposed (i.e., 25.4 mm (1 in.) below the conical heater). After reaching the desired heat flux, the heater was permitted to stabilize for a minimum of ten minutes to ensure a constant exposure.

After this period of stabilization, the GWB was placed beneath the conical heater for the specified period of time. At the end of each exposure, the final mass of the GWB was recorded and the sample was permitted to return to ambient conditions. After twenty-four hours, the calcined samples were evaluated using both probing and visual analysis techniques.

2.2.2 Development of Methodology and Technique

The objective of initial testing was to develop a methodology and technique for analyzing the calcination depth of GWB after heat exposure. Two methods were explored: visual analysis of the GWB after exposure and calcination depth probing with a force gauge.

2.2.2.1 Visual Analysis

Literature [Posey et al. 1983, NFPA 921 2011, Schroeder 2001] suggests that visual observations of calcination depth measurements can be collected based on relative differences in color across the cross-section of the GWB. Schroeder [2001] attributes this change in color to changes in the chemical structure of the GWB material. It is this change in structure that can produce distinct changes in texture and color, which can be visually detectable. However, it has been noted by several authors [Schroeder 2001, Mann & Putaansuu 2010] that smoke staining due to combustion of the gypsum wallboard paper or combustibles within the room can make the identification of a clear line of demarcation challenging. This program found little change in texture of the GWB after exposure, but did note soot staining due to the paper of the GWB.

2.2.2.1.1 Visual Analysis Technique

In testing this methodology, the cross-section of the GWB samples was evaluated to determine the calcination depth based on color or texture change in the gypsum. Samples of USG Sheetrock GWB were exposed to heat as outlined in Section 2.2.1. The 15.9 mm (5/8 inch) board was Type X, which includes reinforcing fibers in the gypsum. A range of heat fluxes and exposure durations were evaluated with the intent of developing varying degrees of calcination. A summary of these exposure severities and durations is provided in Table 1. A total of nine different thermal exposures were used. Samples were exposed to three different heat fluxes (20, 65, and 100 kW/m^2) for durations of 5, 10, 15, 20 and 30 minutes. These heat fluxes were identified as

being representative of the heat fluxes to the interior surfaces of an enclosure during the evolution of a fire from just prior to flashover to fully involved burning conditions. The durations were selected to induce varying degrees of calcination.

Table 1. Summary of small-scale calcination exposure severities and durations for visual inspection.

Sample Thickness (mm)	Heat Flux (kW/m^2)	Exposure Time (min)	Total Heat Exposure (MJ/m^2)
12.7	20	5	6
		10	12
		30	36
	65	5	20
		10	39
		30	117
	100	5	30
		10	60
		15	90
15.9	20	5	6
		10	12
		30	36
	65	5	20
		10	39
		30	117
	100	5	30
		10	60
		15	90

After exposure, the cross sections of the samples were exposed and analyzed. The cross sections were documented using a Dino-Lite Model AD4013MTL digital microscope capable of 20–90x zoom and 1.3 MP image resolutions. Each image of the calcined GWB cross-section was captured with a millimeter rule in the field of view. Samples were inspected for changes in color or texture in relation to unexposed GWB. A photograph of an uncalcined GWB cross-section is provided in Figure 4. The uncalcined gypsum is characterized by color consistency (i.e., white throughout) and uniformity of texture (i.e., small bubbles throughout the cross section). If variations were noted, the depth of the variations were recorded.

Two different techniques were used to expose the cross-section of the samples: 1) cutting with a bandsaw and 2) manually scoring and breaking the samples. Initially, these samples were cut using a JET Model JWBS-16B bandsaw. However, after preliminary inspections, it was determined that the blade of the saw was compacting and smoothing the gypsum material along the cross section (see top of Figure 5). This effect prevented any visual analysis/measurement from being properly performed. The first approach to solving this problem consisted of manually scraping the cut edge with a razor blade after the sample was cut with the bandsaw. This

technique gradually revealed the texture and discoloration of the gypsum material; however, it was also very destructive, in some cases removing large sections of material. Other scraping and brushing techniques did not prove useful. The second approach that was adopted consisted of scoring paper on the backside of the samples with a utility knife and manually breaking them along this seam. This technique did not disturb the cross-section, and provided a consistent profile that could be focused on during documentation. As can be seen below in the lower half of Figure 5, this method provided a much more representative cross-section, which allowed for visual analysis.

Figure 4. Cross-section of uncalcined USG Sheetrock GWB showing the gypsum sandwiched between the paper face on each side of the photo.

Figure 5. Gypsum wallboard cross section exposed by cutting (top half of picture) and breaking (bottom half of picture)

2.2.2.1.2 Visual Inspection Observations

In this work, no visible changes were noted in the texture of the GWB after exposure. Figure 6 shows three GWB samples. Figure 6(a) is unexposed and therefore, uncalcined. Throughout the cross section, there are numerous small indentations. Figure 6(b) and 6(c) show GWB that was exposed to a total heat exposure of 6 and 12 MJ/m^2, respectively. The exposed side of the samples is to the right. After exposure, the indentations are still present, and do not noticeably change size or general quantity. The rough edges on the right side of the sample in 6c are due to the sample crumbling slightly when broken. The center of sample 6c shows the calcination depth probe mark from the right side.

(a) (b) (c)

Figure 6. Cross-sections of 12.7 mm (0.5 in.) USG Sheetrock GWB: (a) unexposed, (b) 6 MJ/m^2, and (c) 12 MJ/m^2.

Although no texture changes were noted, color variations were noted during some of the tests. Figure 7 shows the cross-section of a gypsum wallboard sample after it was exposed to 65 kW/m^2 for 10 minutes in the cone calorimeter. Multiple color bands were observed which complicated the calcination depth determination. The first 1–2 mm of the incident side (right side) of the GWB cross-section sample changed to a dark gray color. The next 5–6 mm of the sample center was light gray in color and the last 3–4 mm of the sample was darker brown in color. It was theorized (and later demonstrated via results below), that these different color bands were attributed more to soot staining from the thermal decomposition and burning of the paper faces than it was due to calcination.

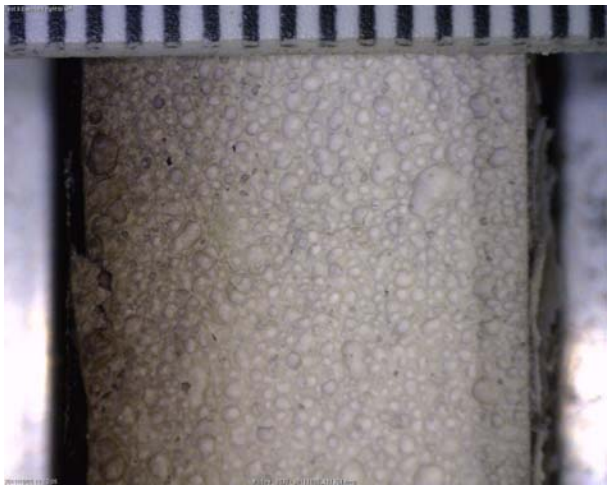

Figure 7. Multiple areas of discoloration within the cross-section of 12.7 mm (0.5 in.) USG Sheetrock GWB exposed on right side to 65 kW/m^2 for 10 minutes (39 MJ/m^2).

The progression of the color bands was associated with the progression of heat through the GWB sample. Initially, the exposed surface of the sample was heated to temperatures at or above the 52–130ºC (126–266ºF) threshold associated with calcination. During this progression, the exposed surface (i.e., white paper surface) continuously increased in temperature until the paper was thermally degraded. Thermal degradation of the exposed paper face of GWB occurs at temperatures around 412ºC (774ºF) [SFPE 2002]. The dark gray layer on the exposed side of the sample was attributed to soot staining from the combustion of the white paper face. The discoloration on the unexposed side of the GWB sample was also attributed to the soot staining from the thermal decomposition and burning of the brown paper facing. Just as described for the exposed face, the gypsum core was initially calcined and later as the isotherm progressed to the unexposed side and gradually increased, the paper was degraded and this combustion resulted in staining of the calcined material. The greater discoloration thickness observed at the unexposed face was attributed to the horizontal orientation of the test sample confined in the pan, which forced confined combustion gases up into the calcined material. The evolution of these color bands within the GWB samples was documented by exposing samples to a common heat flux for varying durations. In Figure 8, photographs of samples exposed to 65 kW/m^2 for 5, 10, and 30 minutes are presented. These samples had average calcination depth measurements of 11.4, 12.7 and 12.7 mm, respectively. In these photographs, the presence of three distinct color bands is visible. However, the color and depth of these bands varies depending upon the exposure duration.

For the five-minute exposure, the dark gray (1–2 mm) band nearest the exposed surface is evident. This band immediately transitions to a light gray band that extends 3–4 mm further into the depth of the sample. The remaining 6–8 mm of the GWB remained white in color. It should be noted that the last 1–2 mm of the sample is the back (unexposed side) paper facing and does not represent soot staining. In addition, it should be noted that the sample shown in Figure 8(a) was cut using a band-saw, which accounts for the variation in texture from the other samples.

For the ten-minute exposure (Figure 8(b)), the dark gray band identified in the previous photograph was lighter in color. The thickness of the band remained approximately 1–2 mm. The

center was relatively white/lighter gray, and the back 3–4 mm of the sample thickness was dark in color. Due to the preferential nature of the discoloration at the exposed and unexposed faces, these areas of discoloration were attributed to smoke staining. It can also be seen on the left side of the sample that the brown paper had been consumed.

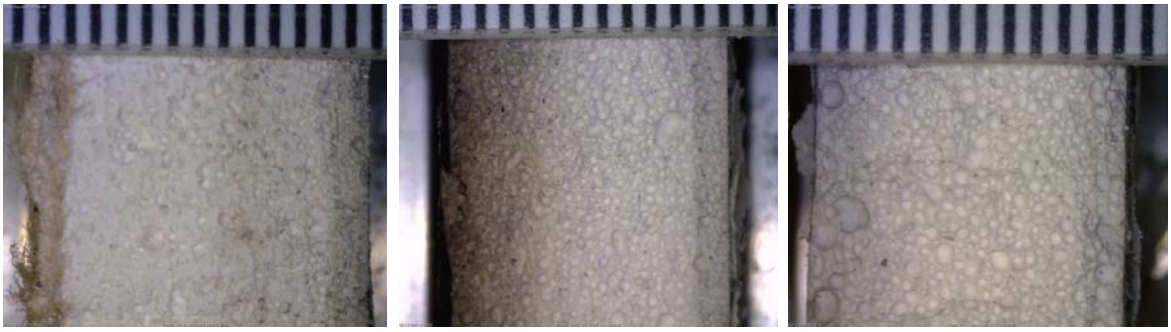

(a) (b) (c)

Figure 8. Cross-sections of 12.7 mm (0.5 in.) USG Sheetrock GWB exposed, from the right, to 65 kW/m^2 for (a) 5 min. (20 MJ/m^2), (b) 10 min. (39 MJ/m^2), and (c) 30 min. (117 MJ/m^2).

For the thirty-minute exposure, the distinct banding was lessened and the entire cross-section transitioned to a more uniform light gray color. Both sides of the sample showed a slightly darker gray color than the center, but there were less distinct lines of demarcation. The loss of soot staining for the thirty minute test was attributed to the fact that during the 30 minute exposure, these samples reached temperatures in excess of 450ºC (842ºF) which are sufficient to begin to thermally oxidize the soot that stained the calcined material earlier in the exposure. Similar observations were made for testing conducted at 20 kW/m^2 for exposure durations of 5, 10, and 30 minutes. Similar observations were also noted for tests using GWB from different manufacturers. GWB surface temperatures were measured at the exposed face using an optical pyrometer. Backside temperatures were not collected in this study.

Six additional tests were conducted with the intention of isolating soot staining as the primary reason for color change within the GWB cross section during exposure. Samples of 12.7 mm (0.5 in.) CertainTeed GWB were exposed to three levels of heat as outlined in Table 2. For each exposure, one sample was tested normally, with the paper in tact on the sample. The other sample per the same exposure had the top and bottom layers of paper removed. The paper was removed using a band saw. Using this technique, the overall thickness of the sample was reduced from 12.7 mm to an average of 9.7 mm. After exposure, the samples were broken and the cross section examined. Figures 9 (a)–(f) show a side by side comparison of the results of these tests. Figure 9(a), exposed to 18 MJ/m^2 has a distinct band of darkened material extending from the front paper layer (bottom of photo) into the GWB, as the soot from the paper begins to penetrate the gypsum material. In contrast Figure 9(b), exposed to the same heat, has no darkening and remains uniform in color throughout. Figure 9(c) shows darkening extending from the front (bottom) and back (top) faces of the GWB, indicating that the back paper layer has begun to thermally decompose. Figure 9(d), although exposed to the same 39 MJ/m^2, shows no darkening, remaining relatively white throughout the cross section. Figure 9(e) shows a small amount of light grey demarcation on the back side (top). At this level of exposure, the soot has been almost completely burned away, leaving only the small, faint area of demarcation on the rear face. Like

the other paperless samples, Figure 9(f) shows no sign of demarcation. It should be noted that all six samples were fully calcined.

Table 2. Summary of soot staining follow-up tests.

Manufacturer and Date	Sample Thickness (mm)	Heat Flux (kW/m^2)	Exposure Time (min)	Total Heat Exposure (MJ/m^2)	Paper?
CertainTeed – 2012	12.7	20	15	18	Yes
		20	15	18	No
		65	10	39	Yes
		65	10	39	No
		100	15	90	Yes
		100	15	90	No

(a) 18 MJ/m^2 – With Paper (b) 18 MJ/m^2 – Without Paper (c) 39 MJ/m^2 – With Paper

(d) 39 MJ/m^2 – Without Paper (e) 90 MJ/m^2 With Paper (f) 90 MJ/m^2 – Without paper

Figure 9. Side by side comparison of CertainTeed GWB exposed to 18, 39, and 90 MJ/m^2 with and without paper facing.

From these comparisons, it is concluded that the principle cause for discoloration in GWB samples during exposure is soot staining caused by thermal degradation of the paper barriers. In addition, these tests reinforce the previous findings of the progression of the soot staining through the GWB as the total heat exposure increases. In addition, the results show that similar soot staining occurs in GWB from different manufacturers.

Visual differences in the cross-section of the GWB samples were not noted for different thermal exposures, excluding soot staining that was determined to be from the GWB paper. The

texture of the material was unchanged for the various heat exposures. In addition, no correlations have actually been verified to relate specific colors or surface features to calcination. The following observations were made during the visual inspection and characterization of the GWB samples heated in the cone calorimeter:

- Bands of discoloration (dark gray or brown) only occurred in regions close to the surfaces with paper facing and are attributable to soot staining from the thermal degradation of the paper facing.
- As the samples were continuously heated, the extent of discoloration at both the exposed and unexposed surfaces was diminished. This reduction in color is associated with the thermal oxidation of the soot within the sample as material temperatures reach approximately 450ºC (842ºF). Temperatures in excess of 450ºC (842ºF) were measured at the exposed face of samples using an optical pyrometer. Backside temperatures were not collected in this study.

Based on these findings it was concluded that visual indicators could not be used to consistently assess depth of calcination or be correlated to the total thermal exposure.

2.2.2.2 Manual Probing Tool/Technique Development

The probing tool and technique developed in this work was based on the findings of previous researchers [Mann & Putaansuu 2010, Chu 2004] as well as data collected from small-scale cone calorimeter testing. The goal was to develop a technique and accompanying tool that could be easily constructed and used by fire investigators to characterize in situ calcination depths at fire scenes. As described above, the original intent of the preliminary tests was to quantify an appropriate probing force using visual observations of calcination depth and measuring the force needed for the probe to reach this depth. However, this approach was abandoned early on in testing due to the inability to visually distinguish between calcined and uncalcined gypsum material. In the absence of visual measurements, an appropriate probing force was derived based on the measureable difference in force needed to probe uncalcined GWB compared to calcined GWB. The development of the probing tool, probing force, and probing technique are described in this section.

2.2.2.2.1 Manual Probing Tool

The probing tool developed in this work consisted of a hand-held force gauge outfitted with a steel probe. The force gauge used was a Shimpo Model FGV-100X digital force gauge with a capacity of 45.4 kg (100 lbs) and a resolution of 0.01 kg (0.02 lbs). The steel probe used was a 2.0 mm hex key cut to a length of 25.4 mm (1 in.) and attached to the force gauge. The selection of this hex key was in part based on the work of both Chu [2004] and Mann & Putaansuu [2010]. Chu recommended that a flat tip probe be used to prevent piercing the uncalcined layer and ensure that the measurements were representative of the depth of calcination. The hex key provided a flat tip probe that was structurally sound (i.e., no flexure when pressure was applied), readily available, and inexpensive. The size of the hex key (2.0 mm [0.08 in.]), which constitutes an impacting surface area of 3.46 mm^2 (0.005 $in.^2$) was selected because the impacting surface area was comparable to that identified by Mann & Putaansuu [2010]. Photographs of the hand-held calcination depth probe are provided in Figure 10.

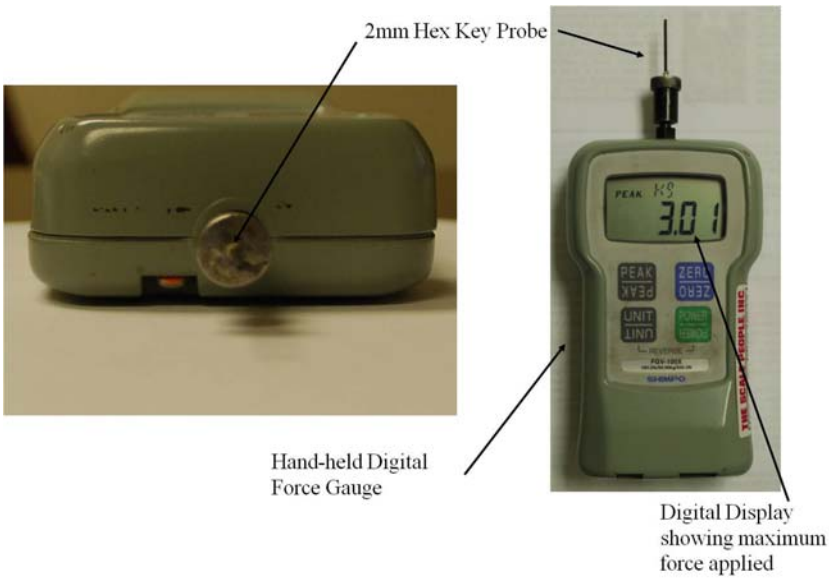

Figure 10. Hand-held calcination depth probe.

Construction of the tool consisted of attaching the hex key probe to the measuring tip of the force gauge. As shown in Figure 10, the probe was attached using a screw-on cap accessory that came with the force gauge. For initial tests, the probe was bonded to this cap using JB Weld, a two-part epoxy. The probe was bonded to the cap such that it was exactly perpendicular to the top of the cap and force gauge. For later tests, a screw cap chuck accessory was used.

2.2.2.2.2 Calcination Depth Probing Technique

Once constructed, the probe was used to quantify calcination depth for a variety of samples ranging from small- to large-scale. A preliminary set of probing tests were conducted to determine an appropriate probe force. These tests consisted of identifying a force that would penetrate calcined gypsum but would not penetrate uncalcined material. Therefore, the use of this force with the specified probe would penetrate only to a depth where the gypsum was calcined (the calcinations depth) and would stop at the uncalcined material. Once this force was developed, it was incorporated into the probing technique. To probe the GWB samples, the 3.46 mm^2 (0.005 $in.^2$) flat cross-section of the hex key was placed against the surface of the sample. Force was then manually applied to the probe perpendicular to the GWB surface. Prior to establishing a prescribed force, several different probing approaches were explored.

The first series of probing tests was designed to quantify the probe force needed to travel through the GWB material at various stages of thermal degradation ranging from uncalcined to fully calcined. This force was determined by applying the probe to a given sample with the force gauge set to record a peak value. Force was then applied until the penetration into the sample was achieved and the probe entered the gypsum core (i.e., the probe traveled through the material). Once movement was observed the test operator would cease applying pressure, remove the probe, and record the maximum force applied. These force measurements were collected for both 12.7 mm (0.5 in.) and 15.9 mm (0.625 in.) GWB thicknesses. For these tests, the digital force gauge was set to a "PEAK" setting; such that only the maximum force applied during any given probe effort was retained on the LCD screen. Three force measurements were

collected for each sample and the average force to penetrate the sample was calculated. The average probe force required to penetrate both 12.7 mm (0.5 in.) and 15.9 mm (0.625 in.) uncalcined (virgin) GWB material was 4 kg (8.8 lbs), which equates to a probe pressure of 1.16 kg/mm^2 (1585 psi) based on the 3.46 mm^2 (0.005 in.^{2}) probe area. A summary of the maximum probe forces for the thermally degraded samples is provided in Table 3. A plot of these results are presented in Figure 11 along with a best fit logarithmic trend line of the average probe force as a function of total heat exposure. This fit was used to estimate the force needed to penetrate virgin gypsum material such that a comparison to experimental results could be made.

Table 3. Average penetration forces.

Sample Thickness (mm)	Heat Flux (kW/m^2)	Exposure Time (min)	Total Heat Exposure (MJ/m^2)	Average Penetration Force (kg)	Std Dev. (kg)
12.7	0	0	0	3.9	0.1
15.9				4.0	0.1
12.7	20	5	6	1.88	0.08
		10	12	1.48	0.06
		30	36	0.82	0.08
	65	5	20	1.19	0.05
		10	39	0.75	0.04
		30	117	0.69	0.04
	100	5	30	0.98	0.07
		10	60	0.72	0.06
		15	90	0.72	0.07
15.9	20	5	6	2.59	0.14
		10	12	2.4	0.13
		30	36	1.48	0.07
	65	5	20	2.15	0.36
		10	39	1.36	0.23
		30	117	1.18	0.12
	100	5	30	1.67	0.15
		10	60	1.1	0.07
		15	90	1.09	0.06

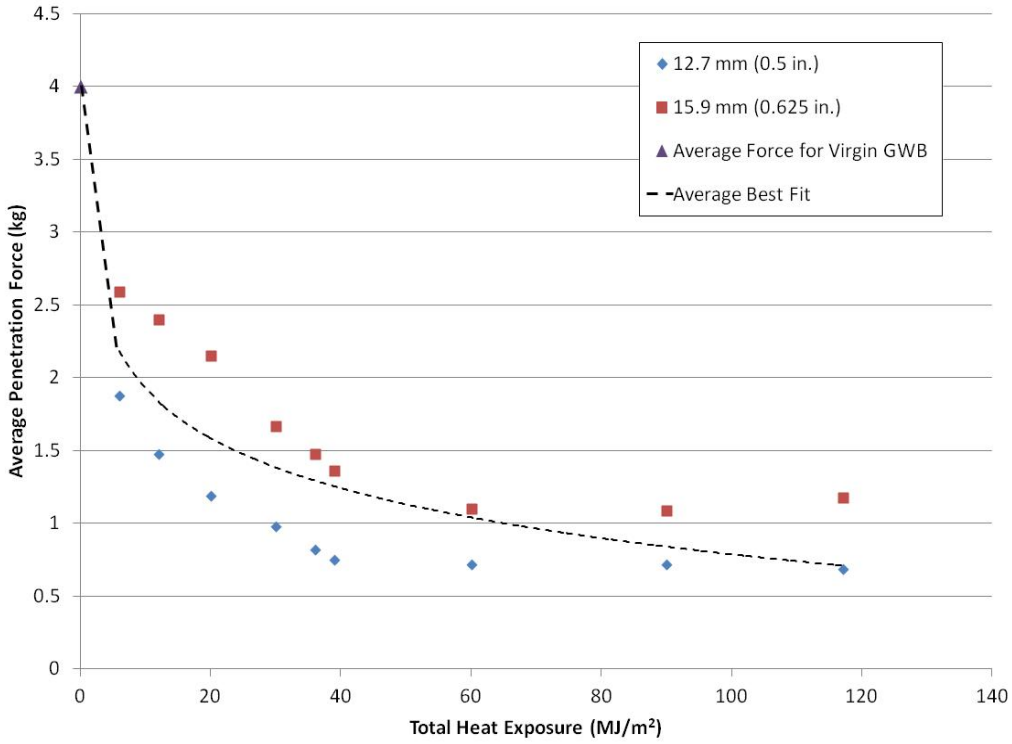

Figure 11. Penetration force as a function of heat exposure for small-scale GWB samples.

Due to the various heat fluxes and exposure times considered in this testing, sample results were compared on the basis of the total heat exposure. This value is the product of the heat flux per unit area provided by the cone calorimeter (kW/m^2) divided by the time of exposure(s).

$$\text{Total Exposure } (MJ/m^2) = \text{H. F.} \left(\frac{kJ}{m^2 s}\right) * \text{ (1 MJ/ 1000 kJ) / Exposure Time (s)} \qquad \text{Eq. 1}$$

For both GWB thicknesses, the probe force required to penetrate the calcined gypsum layer was inversely proportional to the total heat exposure. Compared to the 12.7 mm (0.5 in.) GWB, the 15.9 mm (0.625 in.) material required an average of 0.65 kg (1.4 lbs) of additional force to penetrate the calcined material. This additional force could be the result of the fiberglass that is added to the thicker material for added structural performance. When subjected to more than 40 MJ/m^2 of total heat, the forces required to penetrate both GWB thicknesses stabilized around 1 kg (2.2 lbs) with the force to penetrate the thicker material being consistently higher (~30 percent greater) than that required to penetrate the 12.7 mm (0.5 in.) material. The highest forces required to penetrate the heat samples ranged from 1.9–2.6 kg (4.2–5.7 lbs). The average of the force measurements collected at each total heat exposure was used to develop a logarithmic trend line (shown in Figure 11). This trend line provides a means of determining an appropriate penetration force for a given thermal exposure. However, since there will be a range of thermal exposures to GWB in fire events and the exposure will not be known, a probe force that is sufficient to penetrate all calcined materials, regardless of exposure, was selected. This force was 3 kg (6.6 lbs), which correlates to a pressure of 0.86 kg/mm^2 (1175 psi). This value is consistent with the optimum force and corresponding pressure that was identified by Mann & Putaansuu [2010]. Mann & Putaansuu [2010] concluded that a 2.7 kg (6 lbs) force applied over a 3.12 mm^2 (0.005 $in.^2$) area

was sufficient to overcome the resistance of the paper surface and fully penetrate both the anhydrous and hemihydrate (calcined material) without penetrating the diydrate (uncalcined) material. It should also be noted that the trend line developed from the penetration force data, collected in this work, when extrapolated back to a thermal exposure of zero (i.e., uncalcined material) is generally consistent with the penetration force measurements collected for the virgin gypsum material evaluated in this work.

The inverse relationship between penetration force and total heat exposure as well as the plateau of penetration force at total heat exposures above 40 MJ/m^2 is attributed to the progressive loss of water mass by the GWB samples as the thermal exposure increased (shown in Figure 12). A summary of the mass loss percentages for these samples is provided in Table 4. The water content of the GWB is generally associated with the structural integrity of the material (i.e., the adhesion between the gypsum particles). As both the free- and chemically-bound water is driven out, the remaining gypsum material is more easily penetrated due to lack of adhesion.

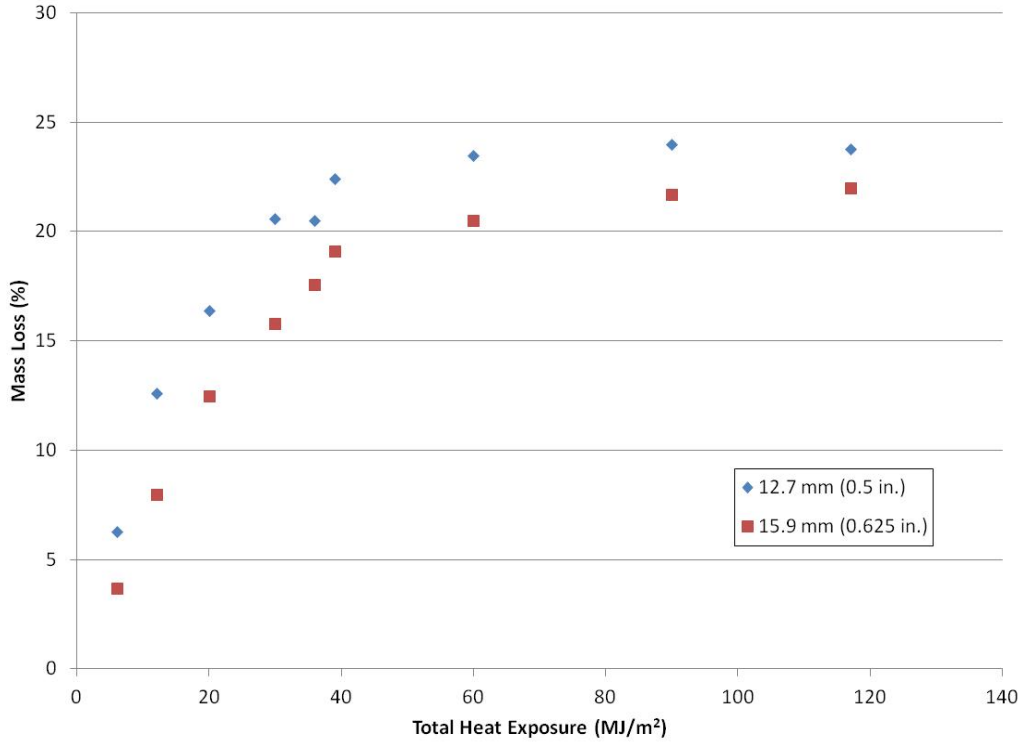

Figure 12. Mass loss as a function of heat exposure for small-scale GWB samples.

Table 4. Summary of average mass loss percentages.

Sample Thickness (mm)	Heat Flux (kW/m^2)	Exposure Time (min)	Average Mass Loss (%)
12.7	20	5	6.3
		10	12.6
		30	20.5
	65	5	16.4
		10	22.4
		30	23.8
	100	5	20.6
		10	23.5
		15	24.0
15.9	20	5	3.7
		10	8.0
		30	17.6
	65	5	12.5
		10	19.1
		30	22.0
	100	5	15.8
		10	20.5
		15	21.7

As shown in Figure 12, up until approximately 40 MJ/m^2, as the total heat exposure increased, so did the mass loss percentages for the GWB samples. This trend shows the progressive loss of bound water within the GWB material. After this threshold (40 MJ/m^2), the mass loss percentage reached a plateau ranging between 20–24 percent. This range of mass loss is consistent with the mass loss percentage of a 12.7 mm GWB sample that was heated in a 150ºC (302ºF) oven for 48 hours to remove all water from the sample. This baked sample had a total mass loss of 25 percent. Based on these results, a total heat exposure of greater than 40 MJ/m^2 is sufficient to remove the majority of the bound water within gypsum wallboard samples evaluated in small-scale testing.

Using the probing tool penetration force of 3 kg (6.6 lbs), a calcination depth survey was completed for each of the samples. The survey consisted of four depth measurements, one in the center of each of the four quadrants of the sample. In these surveys, once the 3 kg (6.6 lbs) force was applied, the penetration depth was temporarily marked on the hex key probe using adhesive tape that was applied to the probe at the surface of the GWB. Once marked, the probe was removed and the distance between the tape and the impacting surface of the probe was measured using digital calipers (Westward Model 1AAU4) with a measurement resolution of 0.01 mm. A summary of the average calcination depth measurement and the associated standard deviation is provided in Table 5.

Table 5. Probe measured calcination depths using a 3 kg (6.6 lbs) probing force.

Sample Thickness (mm)	Heat Flux (kW/m^2)	Exposure Time (min)	Total Heat Exposure (MJ/m^2)	Average Depth (mm)	Std. Dev. (mm)
12.7	20	5	6	4.4	0.1
		10	12	8.3	0.4
		30	36	12.6	0.1
	65	5	20	11.4	0.4
		10	39	12.7	0.0
		30	117	12.7	0.0
	100	5	30	11.0	0.1
		10	60	12.7	0.0
		15	90	12.7	0.0
15.9	20	5	6	2.9	0.1
		10	12	6.4	0.7
		30	36	10.3	0.2
	65	5	20	7.8	0.2
		10	39	13.3	0.7
		30	117	15.9	0.0
	100	5	30	8.6	0.1
		10	60	13.7	0.1
		15	90	15.9	0.0

As shown in Table 5, the standard deviations for the depth measurements collected from the small-scale samples were relatively small ranging from 0.0–0.7 mm which, at worst, represents approximately 10 percent of the average value. The trend in calcination depths was similar to that of the mass loss data in that the depth of calcination consistently increased as total heat exposure increased until leveling off at a peak threshold (see Figure 13). As shown in Figure 13 for 12.7 mm (0.5 in.) thick samples, this threshold was approximately 36 MJ/m^2 and for 15.9 mm (0.625 in.) samples, this threshold was approximately 90 MJ/m^2. It should be noted that complete calcination of the samples (i.e., full penetration) was measured for several of the samples evaluated (i.e., samples with total heat exposures at or above the peak threshold). Complete calcination was established when the probe penetrated through the unexposed side of the sample indicating that no virgin material remained. Compared to depth data collected by other authors using similar material and total heat exposures, the consistency between data sets varied.

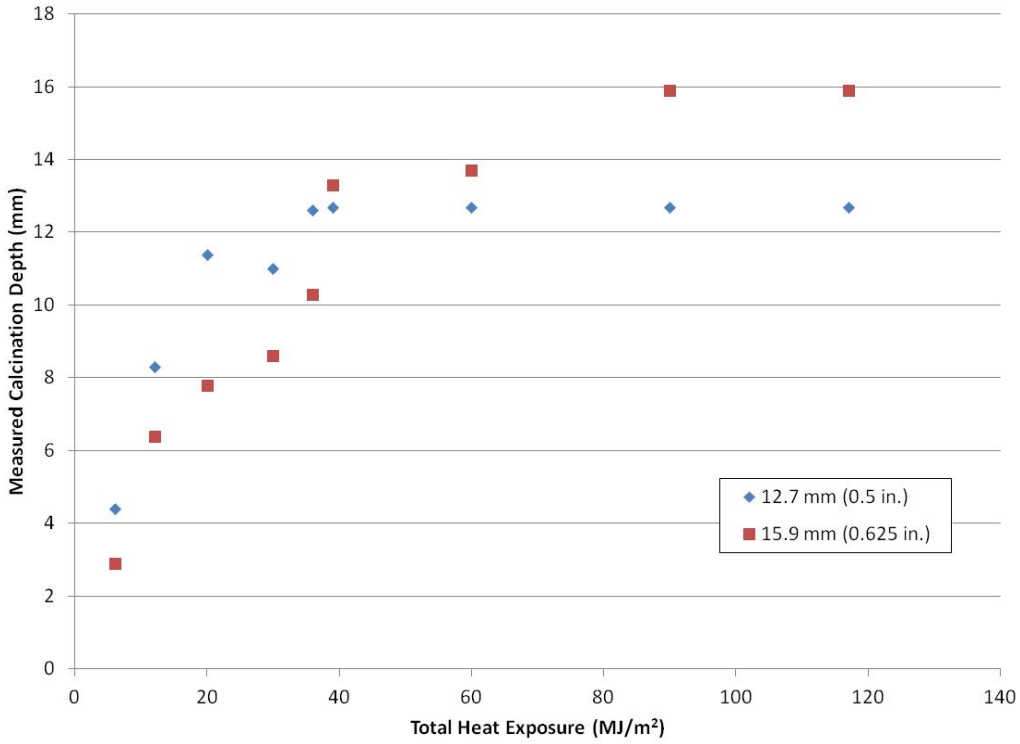

Figure 13. Calcination depths for increasing heat exposures, obtained using a 3 kg (6.6 lbs) probe force.

Chu [2004] presents depth data for 10 mm thick, standard gypsum wallboard subjected to 30 and 60 MJ/m^2 exposures in the cone calorimeter. These samples were the same size as used in this program and reported above. In these scenarios, Chu reports calcination depths of 6.5 and 8.8 mm. These values are less than the depths measured in the current testing for similar exposures. At these exposures, the depths measured for the 12.7 mm (0.5 in.) thick material were 11.4 mm and 11 mm, respectively. For the 15.9 mm (0.625 in.) material, depths of 7.8 and 8.6 mm were measured, respectively. The differences between depth measurements in these tests are most likely due to the different probing forces used but could also be a result of different material construction. Chu [2004] used a probing pressure of 0.4 kg/mm^2 (586 psi) and used material that was purchased in New Zealand while the material used in this work was purchased locally in the U.S. and was probed using a force of 0.86 kg/mm^2 (1175 psi). The use of a lower probe pressure is consistent with Chu obtaining smaller calcinations depths.

Mann & Putaansuu [2010] presents calcinations depths for 12.7 mm (0.5 in.) gypsum wallboard subjected to 5, 10, and 15 MJ/m^2 exposures in the cone calorimeter. In these scenarios, depths of 4, 6, and 8 mm were measured using FTIR analysis and depths of 3, 6, and 7 mm, respectively, were measured using a probe pressure of 0.9 kg/mm^2 (1230 psi). Compared to similar thermal exposures conducted in the current work (i.e., 6 and 12 MJ/m^2), measured depths were generally consistent with values of 4.4 and 8.3 mm, respectively. The consistency of the depth values, measured using the probing tool, to the values measured using the FTIR analysis indicates that the probing method developed provides a means of accurately characterizing calcination depth.

As presented earlier, the similarity between the mass loss data (Figure 12) and the calcination depths (Figure 13) was expected since the progression of calcination is dependent on the loss of moisture content in the gypsum. As shown in Figure 14, the linear relationship between the mass loss data and calcination depth data for both the 12.7 mm (0.5 in.) and 15.9 mm (0.625 in.) samples confirms this.

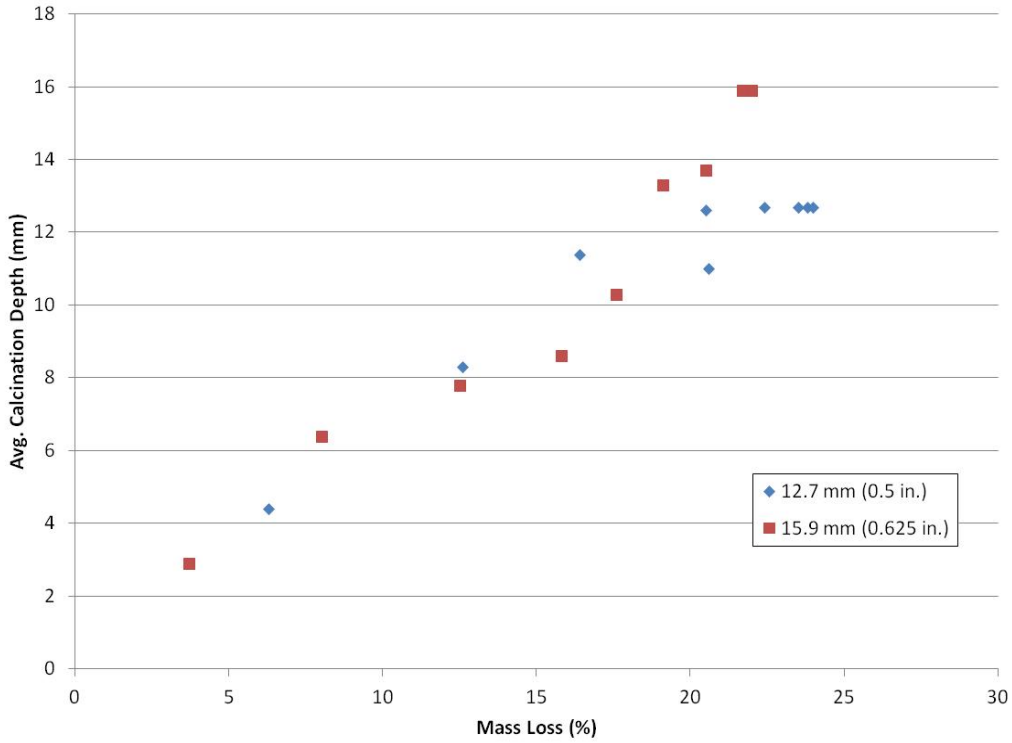

Figure 14. Calcination depths in relation to mass loss percentages.

2.2.2.2.3 Blind Calcination Depth Survey

The motivation for this small-scale calcination work was to develop an objective method for quantifying the extent of calcination of GWB. With the development of a measurement tool and appropriate penetration force, a series of depth measurements were collected by one of the authors and several other engineers working at Hughes Associates, Inc. In order to assess the applicability of this method to any operator, a blind study was conducted whereby two additional operators, unfamiliar with the procedure, were asked to perform calcination depth surveys on a selected subset of the GWB samples. The samples used in this blind testing were a subset of the samples discussed in this section. The additional operators were instructed to apply a 3.0 kg (6.6 lbs) force perpendicular to the GWB surface but were given no context as to the extent of heat exposure and calcination of the samples. A summary of the thermal exposures and resulting depth measurements for the six samples used in this blind study is provided in Table 6. The samples evaluated in this testing were 15.9 mm (0.625 in.) thick USG Type X Sheetrock. The measurements collected by these 'blind' operators were compared to those collected by the author to assess the applicability of the tool and technique developed in this work (see Figure 15).

Table 6. Summary of thermal exposure conditions for blind study samples.

Sample ID	Heat Flux (kW/m^2)	Exposure Time (min)	Total Heat Exposure (MJ/m^2)	Avg. Depth from Operator 1 (mm)	Avg. Depth from Operator 2 (mm)	Avg. Depth from Operator 3 (mm)
A-1	20	10	12	7.1	5.8	7.2
A-2				6.5	6.2	7.1
A-3				7	6.3	7.0
B-1	65	5	20	9.2	8.5	8.4
B-2				9.5	8.3	8.2
B-3				8.7	8.0	8.1

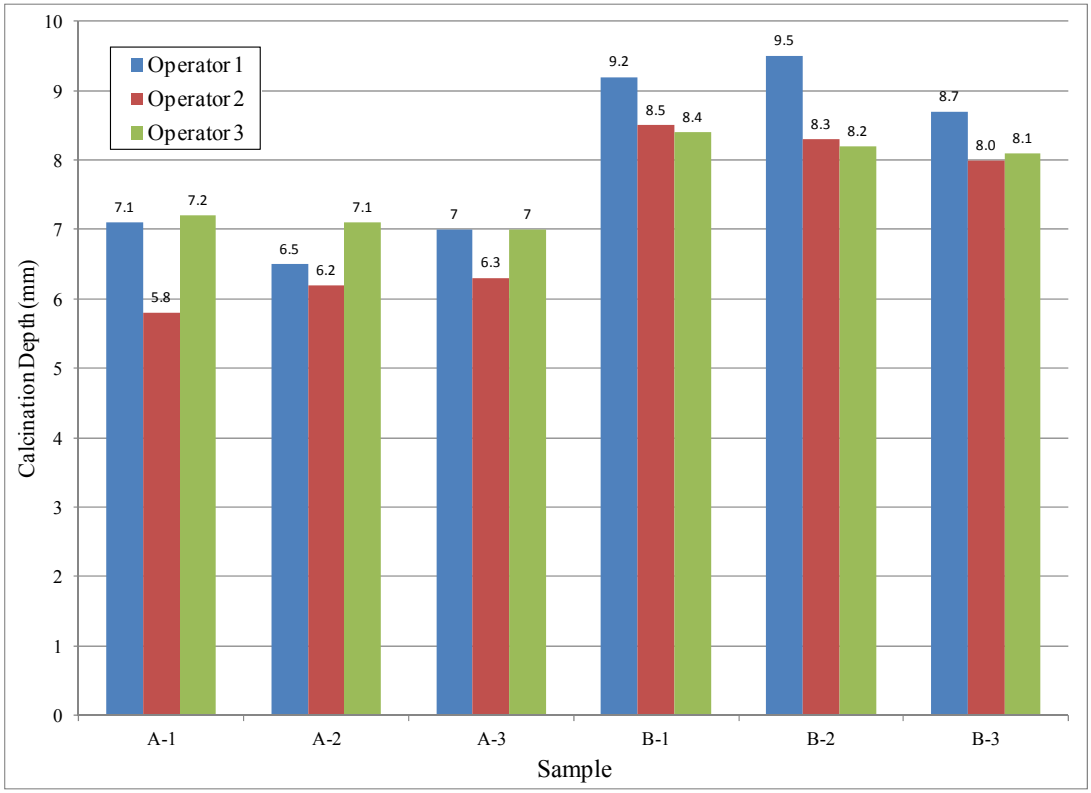

Figure 15. Comparison of calcination depth measurements collected by three different operators.

The maximum difference between operators was 1.48 mm with an average difference of less than 1.0 mm. When considered in relation to the average calcination depth measurement for a given sample, the variance between operators was less than 15 percent. As shown in Figure 15, there were no consistent differences in calcination depth measurements from operator to operator (i.e., no operator consistently measured higher values for all samples). This is an indication that the subjectivity of the measurements has been removed. The differences between measurements, while reasonable, could in part be attributed to the varying location of the measurement for each operator. Measurements could not be collected from the same location on the sample due to the

nature of the probing. Consequently, the calcination depth measurements being compared were collected from different locations on the surface of the sample. While it is assumed that the sample was exposed to a uniform heat flux over the entire surface, non-uniformity within the sample could result in slightly different depths of calcination across the sample. This variability was characterized, to some extent, in Table 5, which showed that the standard deviations between measurements collected from the same sample by the same operator ranged from 0.0–0.7 mm (max 10% variation). Taking into account this inherent variability within a given sample, the differences between operators presented above is negligible. In summary, the tool and technique developed in this work provide an objective means of accurately characterizing the calcination depth of GWB that has been exposed to heat.

2.2.2.3 Methodology and Technique Development Summary

This work determined that a visual analysis of the cross section of a sample of GWB after heat exposure is not a dependable way of determining the calcination depth or severity of exposure. Some discoloration was observed, but was attributed to soot staining caused by thermal degradation of the paper barriers. A manual probing technique using a force of 3 kg was developed and found to be an accurate way of determining calcination depth. The manual probing method was used in a blind study which yielded results which confirm its viability.

2.2.3 Application of Probing Technique and Methodology

Using the methodology and technique developed in Section 2.2.2.2, this work sought to expand on the application of the probing technique to a wider range of GWB, including different manufacturers and manufacturing dates, and to attempt to establish a correlation between calcination depth measurements and total heat exposure. Three manufactures were used: USG, CertainTeed, and National Gypsum. Both CertainTeed and National Gypsum Samples were manufactured in 2012. For USG, samples manufactured in 2002, 2005, and 2010 were used.

2.2.3.1 Test Method

Using the procedure outlined in Section 2.2.1, a total of 42 GWB samples were tested using various heat exposures. Table 7 details the samples and exposures. These samples included the 18 tests previously used to develop the probing methodology, and 24 samples from other manufacturers and manufacturing dates. The 24 additional samples were exposed in the same manner as the previous samples. After exposure, the samples were placed in ambient conditions for 24 hours, and then probed in six locations. After probing, the samples were broken and the cross sections analyzed. The probe and break locations are shown in Figure 16. The cross sectional analysis reaffirmed the observations in Section 2.2.2.1 that visual analysis is not an accurate way to determine calcination depth or exposure. The results of the probing method are tabulated below in Table 7.

Table 7. Summary of exposures and calcination depths.

Manufacturer – Date	Sample Thickness (mm)	Heat Flux (kW/m^2)	Exposure Time (min)	Total Heat Exposure (MJ/m^2)	Average Probe Depth (mm)	Probe Depth Standard Deviation
USG – 2010	12.7	20	5	6	4.4	0.1
			10	12	8.3	0.4
			30	36	12.6	0.1
		65	5	20	11.4	0.4
			10	39	12.7	0.0
			30	117	12.7	0.0
		100	5	30	11.0	0.1
			10	60	12.7	0.0
			15	90	12.7	0.0
	15.9	20	5	6	2.9	0.1
			10	12	6.4	0.7
			30	36	10.3	0.2
		65	5	20	7.8	0.2
			10	39	13.3	0.7
			30	117	15.9	0.0
		100	5	30	8.6	0.1
			10	60	13.7	0.1
			15	90	15.9	0.0
USG – 2005	12.7	10	5	3	3.2	0.1
			7.5	4.5	5.1	0.1
		20	5	6	8.4	0.4
			7.5	9	12.7	0.0
			10	12	12.7	0.0
USG – 2002	12.7	10	5	3	3.2	0.3
			7.5	4.5	4.6	0.3
		20	5	6	7.8	0.3
			6.5	7.8	8.6	0.1
			8	9.6	12.7	0.0
CertainTeed – 2012	12.7	10	5	3	3.2	0.4
			7.5	4.5	4.1	0.4
		20	5	6	7.5	0.2
			7.5	9	8.1	0.1
			8.5	10.2	9.0	0.1
			10	12	10.7	0.4
			15	18	12.5	0.0
National – 2012	12.7	10	5	3	3.9	0.3
			7.5	4.5	4.9	0.1
			8.5	5.1	5.4	0.4
		20	5	6	10.8	0.2
			7.5	9	12.4	0.0
			10	12	12.4	0.0
			15	18	12.4	0.0

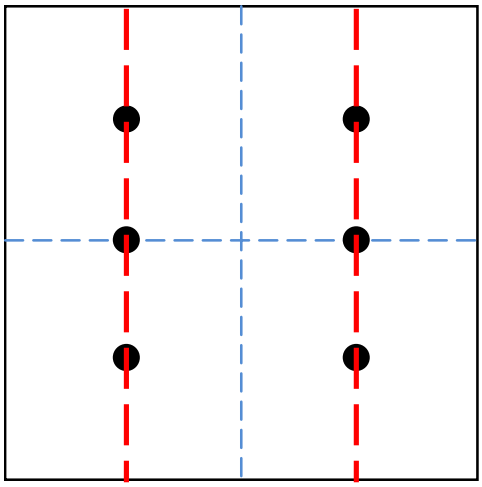

Figure 16. Probe (black circles) and break (red dashed line) locations. Centerlines (blue dashed line) shown for reference.

It should be noted that between testing of the first 18 samples (USG 2010 samples) and the remaining 24 samples, the handheld probing device was altered slightly. Instead of attaching a hex key to an adapter with JB Weld, a new adapter was found that featured a chuck that holds the hex key in place. The chuck attachment offered better stability and longevity as opposed to the JB Weld, and was used for all subsequent testing. The chuck attachment is shown in Figure 17.

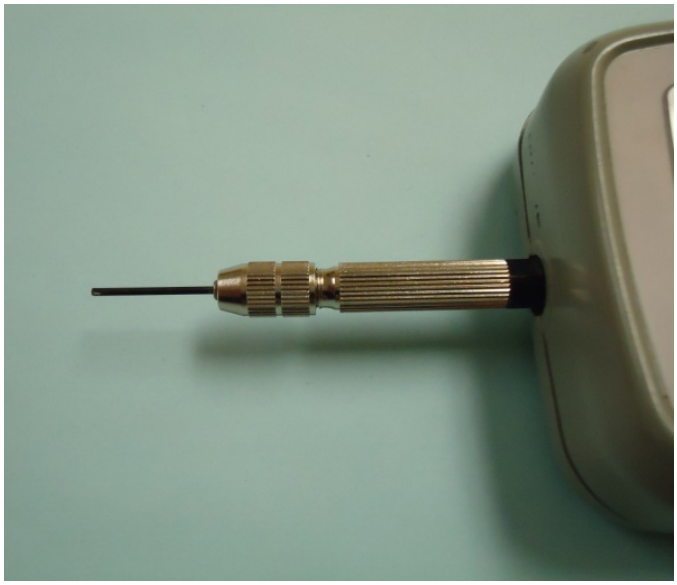

Figure 17. Chuck Attachment with Hex Key

To verify that the 3 kg technique was valid for all types of GWB used, each type was probed prior to exposure. A minimum force needed to penetrate the gypsum core was recorded with and without paper present. Across all manufacturers and manufacturing dates, with and without paper, the force needed to penetrate was between 3.5 and 4 kg, thus validating that the probing method developed was applicable for GWB from different manufacturers.

2.2.3.2 Total Heat Exposure Correlations

Using the data in Table 7, a correlation between total heat exposure and calcination depth was generated for each manufacturer/manufacturing date set of GWB samples. These correlations can be seen in Figure 18 and Figure 19. The correlations only include data points that were not completely calcined and the first completely calcined data point. Other completely calcined data points at higher heat exposures were not included in the correlation curves.

In general, the correlation curves follow a similar progression. The grouping of data is considerably closer at low heat exposures, and diverges substantially as the heat exposure increases. Although all manufacturers and manufacturing dates do not line up perfectly, a general range can be established. For instance, if an unknown sample of 12.7 mm thick drywall is probed to a depth of 6 mm, a general assumption can be made that the sample was exposed to a range of approximately 5 to 8 MJ/m^2. In addition, it can be inferred that complete calcination will not occur below a total heat exposure of 9 to 10 MJ/m^2.

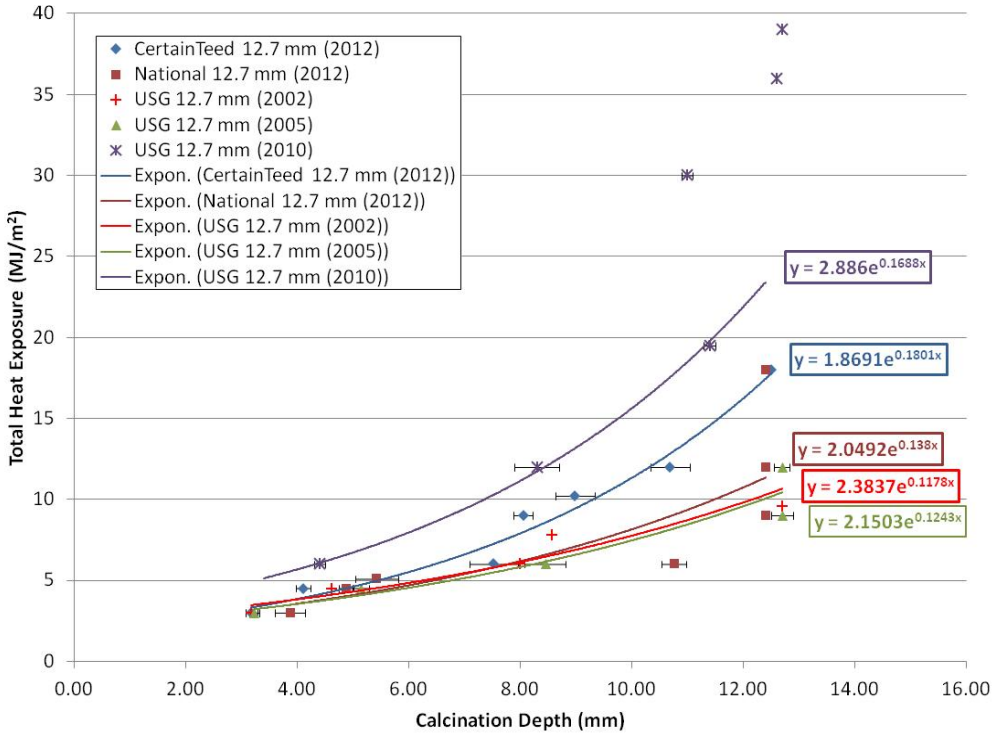

Figure 18. Calcination Depth and Heat Exposure Correlation (12.7 mm thickness only)

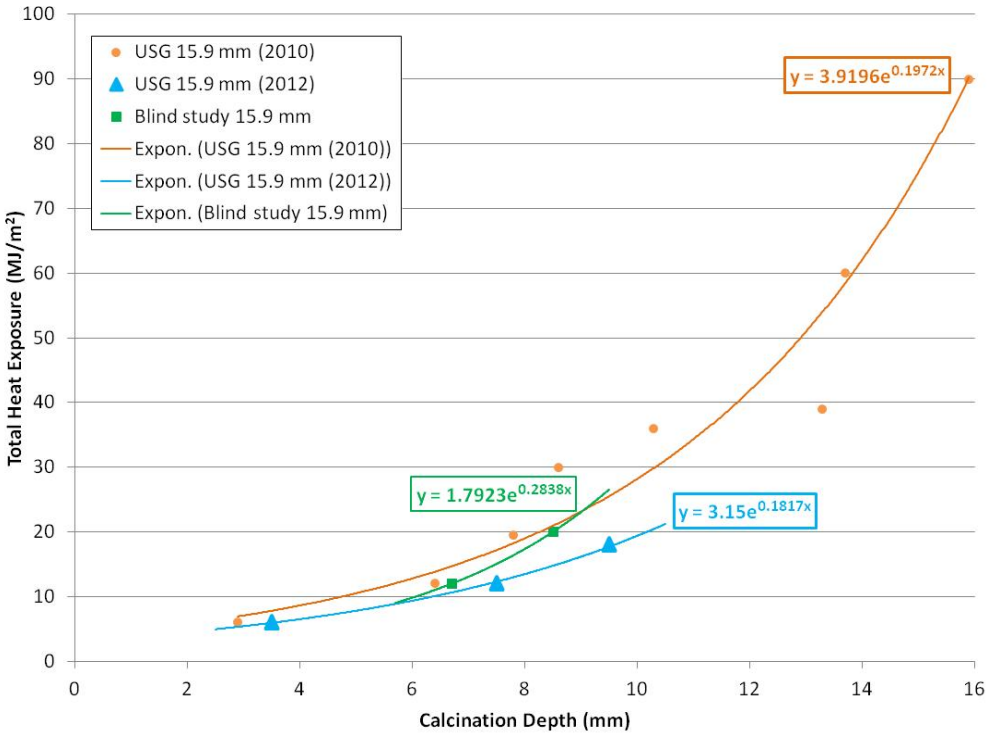

Figure 19. Calcination Depth and Heat Exposure Correlation (15.9 mm thickness only)

2.2.4 General Conclusions and Observations

2.2.4.1 Cross Sectional Uniformity

By breaking each sample twice, the uniformity of the cross section could be analyzed. Overall, the cross sections of the exposed samples showed relative uniformity. There were no color or textural differences along the two cross sections sampled. In addition, calcination depth measurements were generally uniform across both cross sections sampled. A sample of the cross sectional analysis is shown below in Figure 20. Further examples can be found in Appendix A.

2.2.4.2 Visual Effects

Visual effects of heat, although not useful in determining a level of calcination, can still be a useful aid in determining heat exposure. The progression of damage on the face of the GWB, as well as soot staining throughout the cross section, can aid in determining a general level of heat exposure. Figure 21 shows a side-by-side comparison of all CertainTeed GWB samples tested in this work, after exposure. The top row of pictures shows the face of the drywall, while the bottom row of pictures shows the cross section, with the exposure side oriented to the bottom of the photo.

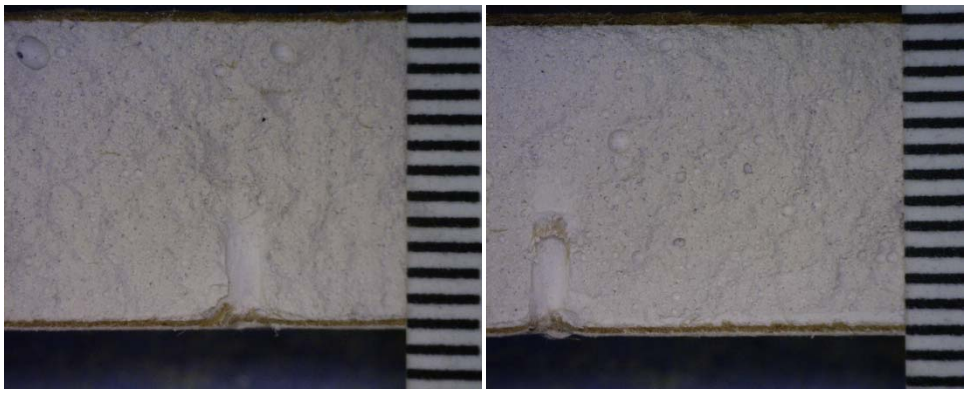

(a) CertainTeed – 3 MJ/m^2

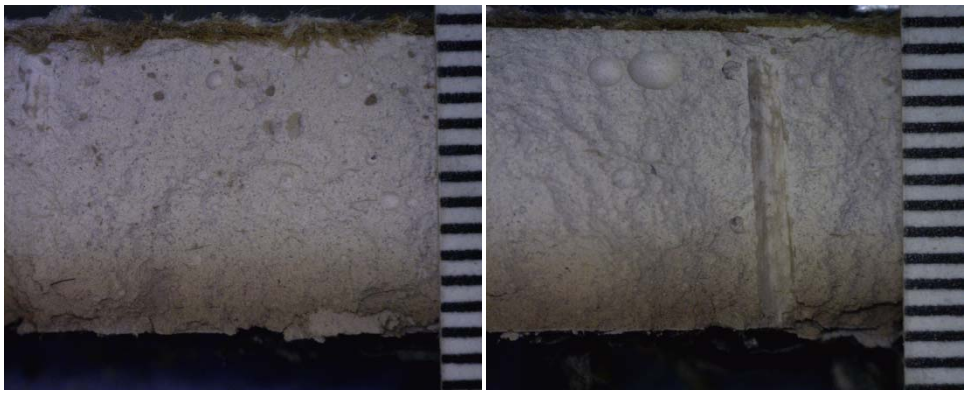

(b) National Gypsum – 12 MJ/m^2

Figure 20. Cross Sectional Analysis of GWB

Heat exposures of 3 and 4.5 MJ/m^2 yield little visual changes. There is slight browning of the front paper facing. An exposure of 6 MJ/m^2 begins to char and crack the front paper, and the first signs of soot staining are observed. From 9 through 18 MJ/m^2, the paper continues to crack and char, and dark soot staining extends further into the cross section. As the paper chars it turns to ash which is initially black and then turns white with increasing heat. By 39 MJ/m^2, the soot on the front face is burned clean with only flaky white ash remaining on a light gray gypsum background. In the cross section, the soot staining in the front of the cross section has largely burned away, while soot staining can now be observed at the rear face, indicating that the back paper facing has begun to thermally degrade. At 90 MJ/m^2, the soot on the front face has been completely burned off, and the gypsum surface and ash are very white. In the cross section, only minimal soot staining remains at the back face, indicating that the back paper has been completely consumed and the soot has been burned off. Samples from other manufacturers followed this same general trend.

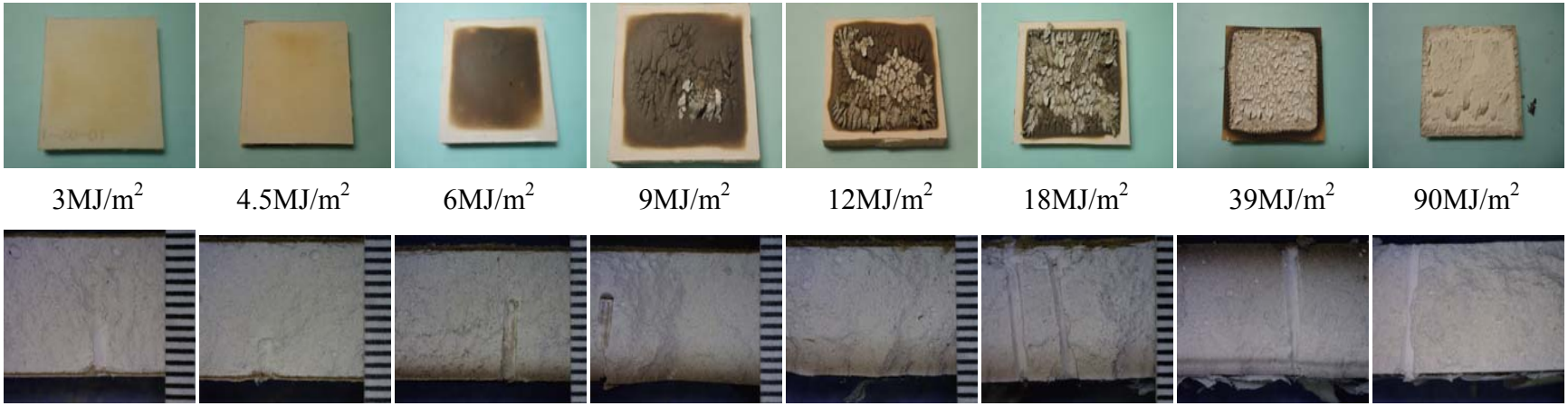

Figure 21. Visual progression of CertainTeed GWB face and cross section.

2.2.4.3 Lightweight Drywall

The major focus of this work was on traditional, non-lightweight GWB, as this type of drywall is most prevalent in existing structures. However, use of lightweight GWB is becoming more and more common in new construction. This work briefly explored the utility of the manual probing method on 12.7 mm (0.5 in.) USG Ultralight (2011) GWB.

Three tests were performed using the test method outlined in Section 2.2.3.1. The results are tabulated below in Table 8. Using the 3 kg force manual probing method developed in this work, all samples appeared to be fully calcined. This result is different from all other GWB types sampled, especially for the 6 MJ/m^2 heat exposure.

Table 8. Lightweight drywall results.

Manufacturer and Date	Sample Thickness (mm)	Heat Flux (kW/m^2)	Exposure Time (min)	Total Heat Exposure (MJ/m^2)	Probe Average Depth (mm)	Probe Depth Standard Deviation
USG Ultralight – 2011	12.7	20	5	6	12.7	0
			8.5	10.2	12.7	0
			12.5	15	12.7	0

It was determined that the lightweight GWB may need a lesser amount of force to penetrate uncalcined GWB. With paper on the lightweight GWB, a force of 3 to 3.5 kg was needed to penetrate into the USG Ultralight GWB samples. However, in the absence of paper, only 2.5 to 3 kg of force was needed to penetrate. Thus, the use of a 3 kg force on the Ultralight GWB will tend to overestimate calcination, particularly if the paper has been degraded.

This discovery, however, is not comprehensive. Due to the small sample size and the fact that the composition of lightweight drywall has undergone changes since its introduction, this finding may not necessarily apply to all brands or manufacturing dates of lightweight GWB. Further research is needed in determining the appropriate penetration force for probing lightweight GWB.

2.2.4.4 Effects of Solid Backing

The method for probing samples in this work was to place the sample on a table to probe for calcination depth. It was found that when the GWB is backed by a solid, flat surface, such as the table, the probe may not penetrate completely even though the sample is fully calcined. In some instances of fully calcined samples, the solid backing can prevent the material ahead of the probe from being expelled out of the back side, and thus is compacted ahead of the probe between it and the table. When this occurred, the the measurement inaccurately indicated a probe depth a few millimeters less than the GWB thickness instead of it being fully calcined.

Several instances of this were observed. By raising the sample a small distance off the table, the probe penetrated the sample fully. It was found that anything measured over 10.5 to 11 mm

calcined, when backed by the table, was able to be fully penetrated fully when raised off of the table. Measurements under 10.5 mm calcined were generally unaffected by the table backing. In real world applications, this means that measurements should be avoided in locations where GWB is backed by a board.

2.2.4.5 Exposure Variance

To achieve a specific total heat exposure, different combinations of heat flux and exposure time can be used. For example, a total heat exposure of 12 MJ/m^2 can be achieved by exposing a sample to 20 kW/m^2 for 10 minutes, or 40 kW/m^2 for 5 minutes. Six tests were performed to analyze the effect of different methods of achieving a desired total heat exposure on calcination depth measurements. These tests were performed with 15.9 mm (0.625 in.) USG Type X Sheetrock. The results of the tests are tabulated below in Table 9. The measurements of the samples with the same total heat exposure were generally within 10% of the measured calcination depth. This indicates that the method of heating does not significantly affect the results as long as the same total heat exposure is achieved.

Table 9. Exposure variance results.

Manufacturer and Date	Sample Thickness (mm)	Heat Flux (kW/m^2)	Exposure Time (min)	Total Heat Exposure (MJ/m^2)	Probe Average Depth (mm)	Probe Depth Standard Deviation
USG – 2012	15.9	10	10	6	3.48	0.27
		20	5	6	3.95	0.17
		20	10	12	7.61	0.15
		40	5	12	7.01	0.11
		30	10	18	9.95	0.15
		60	5	18	9.30	0.10

2.3 Full-scale Exposure Study

Using the calcination depth measurement tool/technique developed in small-scale testing, a total of six calcination depth surveys were completed within the full-scale fire tests described for Test Series 6 in the companion report [Mealy et al. 2013]. Three of the nine full-scale enclosure fire tests conducted in Test Series 6 were not characterized with a calcination depth survey. In these tests, the damage to the GWB lining material was either too severe (Test 6-0) or the GWB was damaged during suppression and therefore accurate measurements could not be collected (Test 6-1 and Test 6-3). The details of these tests are described in brief in this report. The reader is referred to the companion report for complete description of the fire development in these tests.

These surveys were performed on select GWB surfaces within the test enclosure (i.e., walls and/or ceiling) for select tests and were conducted using a 0.3 m (1 ft) measurement grid. The grid was put in place over top of the GWB surfaces using chalk lines that were snapped at the

appropriate distances both horizontally and vertically. A representative photograph of the gridded fire test enclosure is provided in Figure 22. Calcination depth measurements were collected at each grid intersection point.

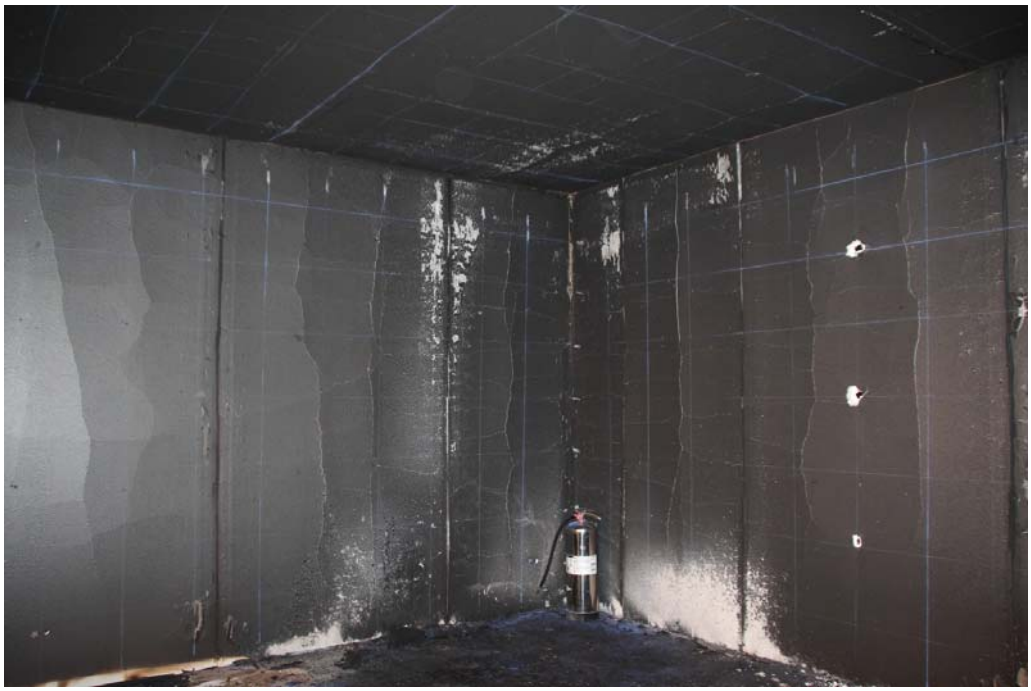

Figure 22. Chalk line grid (blue) installed over top of thermally damaged GWB for calcination depth survey.

The objective of these tests was to assess the utility of the calcination depth survey by comparing measured calcination depth contour plots (i.e., damage patterns) to visual patterns. With this in mind and based on the findings of Mealy et al. [2006], full-room surveys were only conducted after Tests 6-2 and 6-6. The ceiling of the enclosure was the only surface characterized in all other tests. In the majority of tests, the surface of most interest was determined to be the ceiling of the enclosure. In many cases, the ceiling was heavily sooted and patterns of any sort, if present, were not visually identifiable.

2.3.1 Test 6-2: Gasoline on Carpet Floor with Slit Vent Opening

The first test in which a calcination depth survey was conducted was Test 6-2. In this test, the fire was initiated using a 2.0 L (0.53 gal) gasoline spill in the aisle between the upholstered sofa and table. After the test burned for a period of approximately eight minutes, the fire was manually extinguished. Fire patterns were visually identified in several locations on the walls of the enclosure (see Section 3.3.2.7), but no patterns were identified on the ceiling. The ceiling was uniformly coated with soot with no visually identifiable pattern of any sort. Based on the lack of information visually available, a survey of the ceiling was conducted whereby a total of 132 calcination depth measurements were collected and tabulated. As shown in Figure 23, this data was used to create a contour plot of the thermal damage to the ceiling.

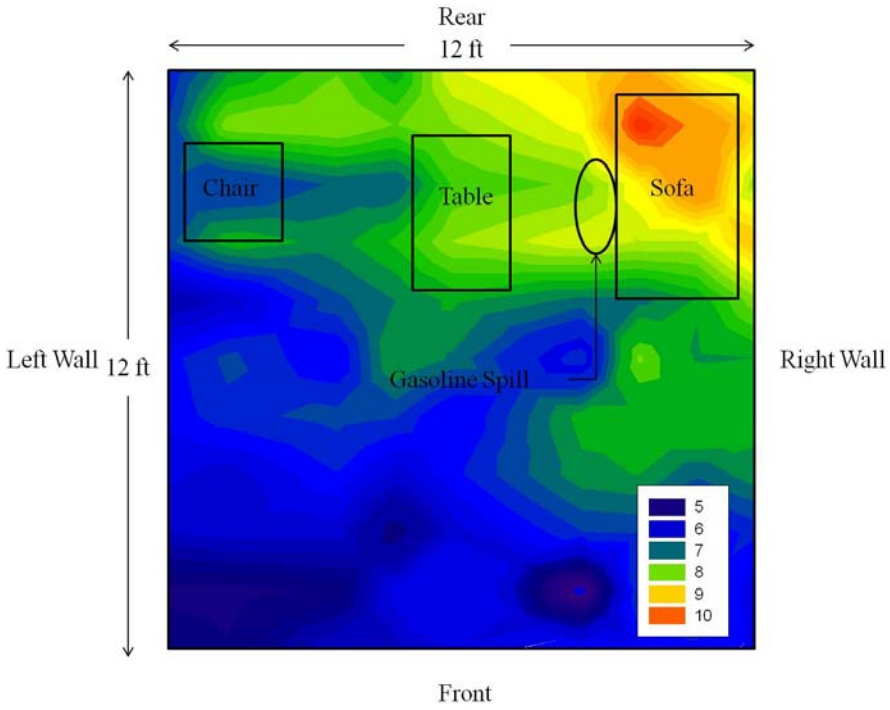

Figure 23. Calcination depth contour plot of ceiling in Test 6-2 (color-coded depths in mm).

The ceiling in this test consisted of 15.9 mm (0.625 in.) GWB. As shown in Figure 23, measured calcination depths ranged from 5–10 mm, with the most severe thermal insult occurring above the right, front corner of the upholstered sofa. Although not directly above it, this area of increased damage was near the area of origin. The increased level of damage in this corner is consistent with the fire burning the longest above the sofa compared to neighboring ceiling surfaces. For this test, the calcination depth survey was found to be very useful in that it provided insight into the area of most severe thermal damage where visually, nothing could be identified.

The relatively reduced thermal damage to the ceiling of the enclosure proximate to the vent was attributed to the localized nature of the fire scenario and the limited ventilation condition. The gasoline spill on the carpet only produced a relatively small spill fire scenario that gradually involved the upholstered sofa. However, by the time the sofa became involved, a relatively limited airflow condition had been developed within the space, which prevented the fire from spreading much beyond this general area of origin. The depth measurements collected from the ceiling of the enclosure in this test support this general growth trend.

2.3.2 Test 6-4: Gasoline on Upholstered Chair with Slit Vent Opening (with Carpet)

In Test 6-4, the fire was initiated using a 2.0 L (0.53 gal) gasoline spill with 1.5 L (0.40 gal) of gasoline poured onto the upholstered chair and 0.5 L (0.13 gal) poured onto the flooring leading from the chair to the vent. After the test burned for a period of approximately twelve minutes, the fire was manually extinguished. The ceiling in this test consisted of 15.9 mm (0.625 in.) GWB. Figure 24 shows a composite photograph of the post-fire condition. The

upholstered chair was in the back left corner. A calcination depth survey of the ceiling was conducted and a contour plot was developed to illustrate the damage profile (see Figure 25).

Figure 24. Composite photograph of fire patterns on walls and ceiling of enclosure after Test 6-4.

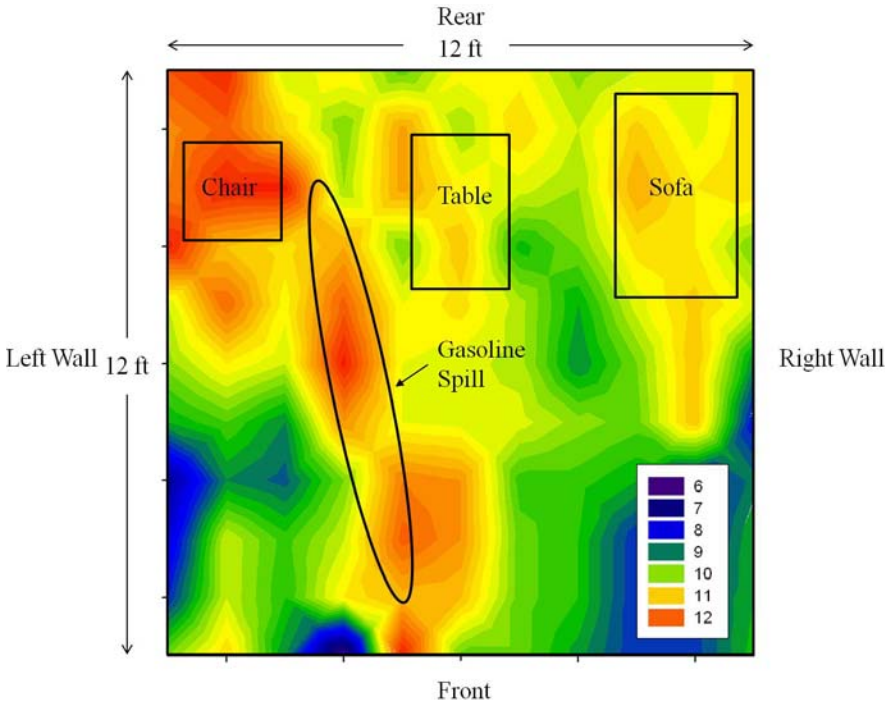

Figure 25. Calcination depth contour plot of ceiling in Test 6-4 (color-coded depths in mm).

As shown in Figure 25, measured calcination depths ranged from 6–12 mm, with the most severe thermal insult stretching from the rear, left corner of the enclosure toward the vent opening. In general, this damage area, illustrated by the calcination depth measurements, was

consistent with the area in which the initiating fire was located. Distinct areas of damage were also documented above both the upholstered sofa and wooden table. Compared to the damage measured in Test 6-2 above, it is evident that the thermal insult in this test was more severe based on the extent of calcination of the ceiling. This difference in calcination depths is consistent with the duration of the fires in these tests. The fire in Test 6-4 burned for approximately four minutes longer than that in Test 6-2, with average upper layer temperatures that were approximately 85ºC (185ºF) hotter. This added thermal insult produced a deeper, more uniform calcination layer within the GWB installed on the ceiling of the enclosure in Test 6-4 than was produced in Test 6-2. For this test, the calcination depth survey was very useful in that it provided insight into the area of most severe thermal damage where visually, it was not as clearly identified.

2.3.3 Test 6-5: Gasoline on Vinyl Floor with Full Door Opening

Test 6-5 was initiated using a 2.0 L (0.53 gal) gasoline spill on the vinyl flooring in the center of the enclosure. This initiating fire resulted in a rapidly developing, large area liquid fuel fire that quickly involved the contents of the room. The fire burned for only three minutes, but due to the full door ventilation, the fire reached flashover conditions quickly and burned at this state for approximately 2 minutes. This fire was manually extinguished. The ceiling in this test consisted of 12.7 mm (0.5 in.) GWB. A different thickness GWB was adopted in several tests to evaluate whether or not the utility of the calcination depth surveys was dependent upon the thickness of the material installed. Based on small-scale testing, such differences were not expected to have a substantial impact but the variable was evaluated nonetheless.

Patterns were observed on several of the enclosure walls and ceiling, as shown in Figure 26. The visual pattern on the ceiling in this test was generally located above the area where the initiating fire occurred; however, this pattern is partially attributed to suppression efforts (see Section 3.3.2.10).

Figure 26. Fire patterns on walls and ceiling of enclosure after Test 6-5.

A calcination depths survey of the ceiling was conducted and is shown in a contour plot in Figure 27. In this contour plot, the most severe thermal damage (i.e., greatest calcination depth) is generally located in the rear center of the enclosure above the aisle between the upholstered chair and wooden table. Although this area of highest damage was not directly above the initiating fire it was generally above the combustibles that were involved early in the development of the fire and therefore burning for the longest duration.

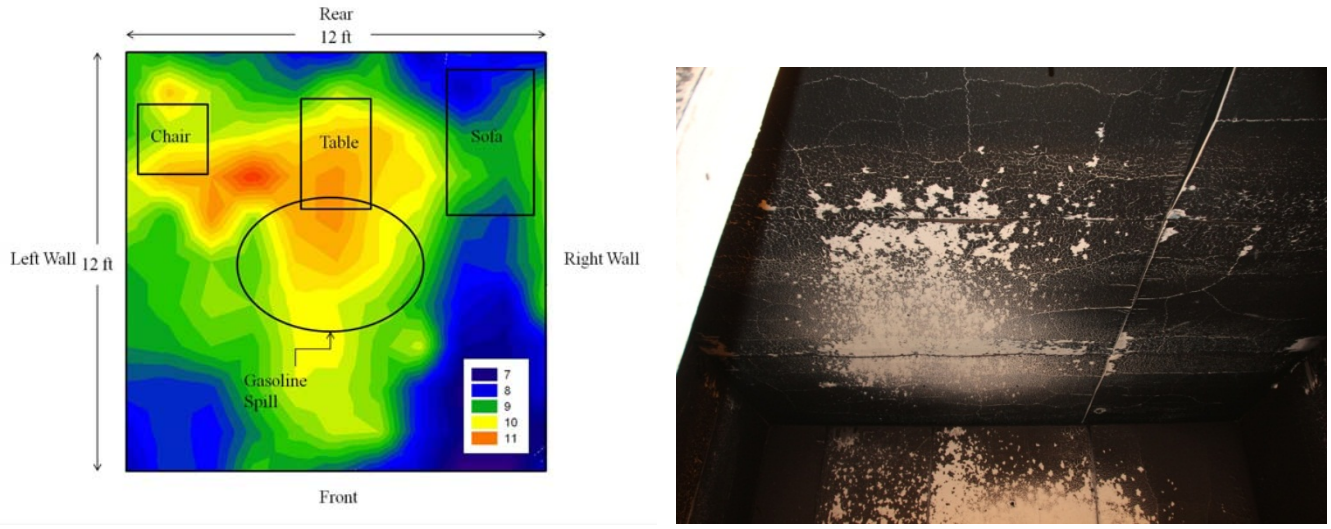

Figure 27. Calcination depth contour plot of ceiling in Test 6-5 [left] (color-coded depths in mm) and photograph of condition of ceiling [right].

Compared to the damage measured in Test 6-4 (6–12 mm depths), where flashover conditions were not achieved but extended burning continued for approximately 12 minutes, the damage severity (i.e., depth of calcination) in this test was comparable, ranging from 7–11 mm. The primary difference between the two tests was that the damage measured in Test 6-4 covered a much larger area of the ceiling due to the extended period of heating (~12 minutes), while in Test 6-5 the heating remained relatively localized due to the brevity of the test (~ 3 minutes). In both tests, the contour plots show ceiling damage associated with the ventilation flow through the vent. As noted earlier, similar damage was not identified in the survey conducted after Test 6-2 (Figure 23) which had a relatively localized fire located remote from the vent.

2.3.4 Test 6-6: Gasoline on Vinyl Floor with Slit Vent Opening

Similar to Test 6-5, Test 6-6 was initiated using a 2.0 L (0.53 gal) gasoline spill fire on vinyl flooring in the center of the enclosure, but instead of the full door vent as used in Test 6-5, the vent was narrowed to a slit vent configuration to limit ventilation. This initiating fire resulted in a rapidly developing, large area liquid fuel fire; however, due to the ventilation condition, the fire quickly became ventilation-controlled and burned at a relatively smaller, steady state for the duration of the test. In this test, the fire burned for 506 seconds (8 minutes 26 seconds) and was manually extinguished. The ceiling in this test consisted of 12.7 mm (0.5 in.) thick GWB. As shown in Figure 28, visible fire patterns on the interior surfaces of the enclosure after this test were minimal. The vast majority of the enclosure was uniformly and heavily soot stained.

Figure 28. Condition of the walls and ceiling of enclosure after Test 6-6.

Given the limited visible patterns, a calcination depth survey was performed for both the ceiling and walls. The contour plot for the ceiling of the enclosure is presented in Figure 29, while the plots for the walls of the enclosure are presented in Figure 30(a–d).

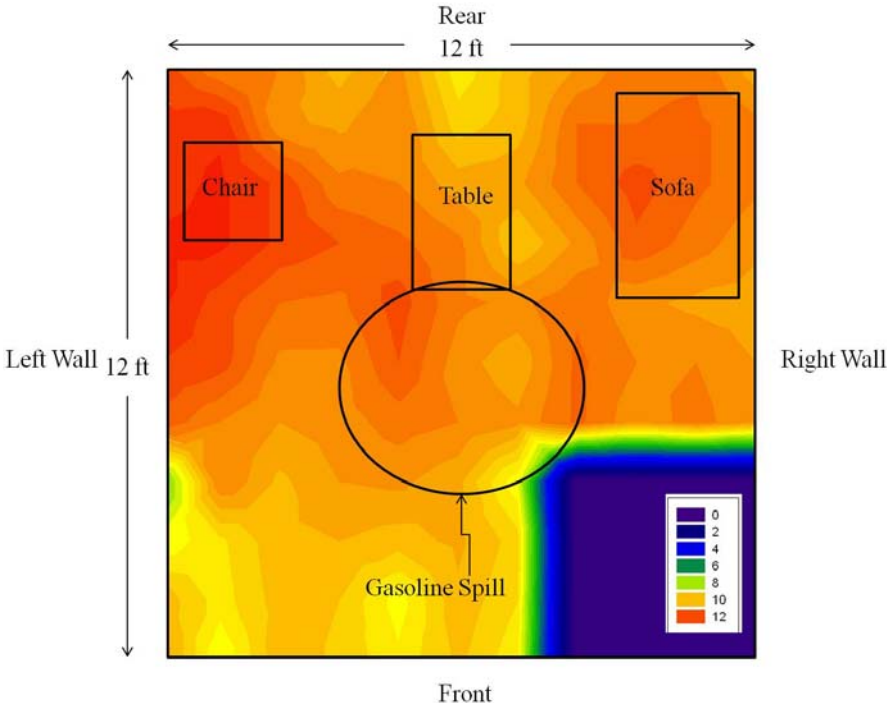

Figure 29. Calcination depth contour plot of ceiling in Test 6-6 (color-coded depths in mm).

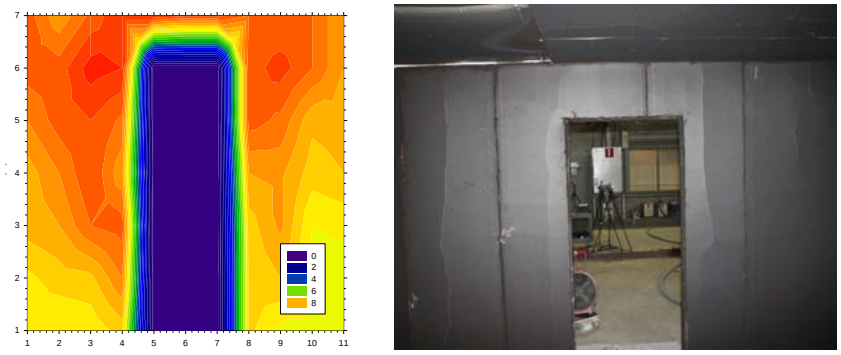

(a)

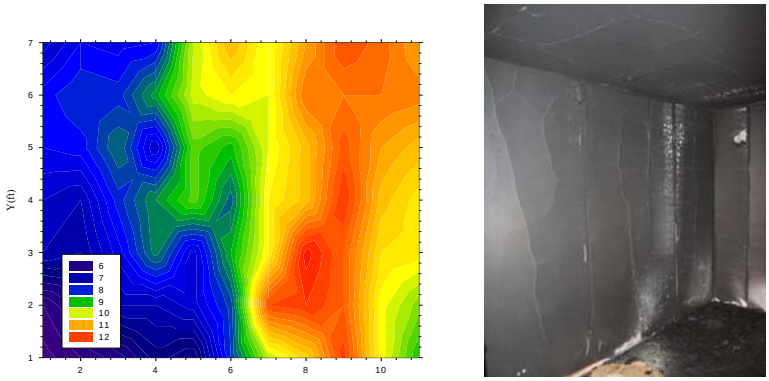

(b)

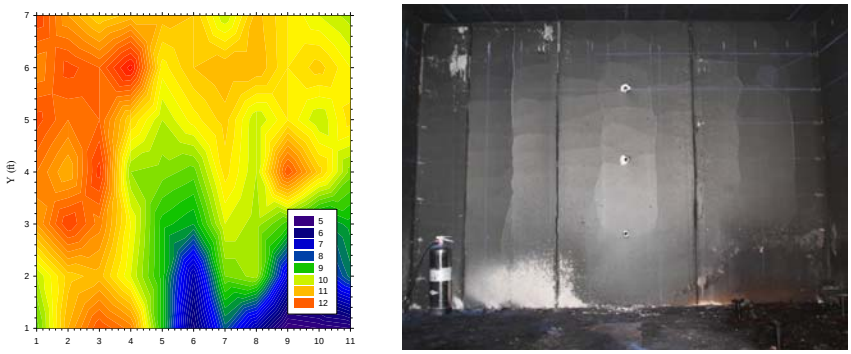

(c)

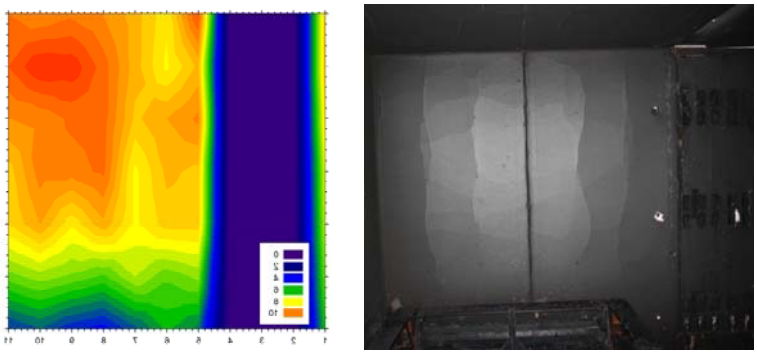

(d)

Figure 30. Contour plots for the walls of the enclosure in Test 6-6. The walls shown include (a) the front, (b) the left, (c) the back, and (d) the right (color-coded depths in mm).

The calcination depth surveys conducted on both the ceiling and the walls of the enclosure revealed differences in thermal damage to the surfaces associated with the fire development within the space. As shown in Figure 29, the damage to the ceiling was relatively uniform over the entire ceiling, but a localized area of severe damage was noted over the upholstered chair. In this test, the upholstered chair was the first item ignited and burned for the duration of the test (i.e., longest duration fire). It should be noted that the square area of zero calcination (front right corner of the enclosure) was actually a section of ceiling that fell after testing and therefore no measurements could be collected.

Similar to that of the ceiling survey results, the contour plots of the wall calcination depths (Figure 30) revealed thermal damage patterns that were not visibly identifiable. Plots (b) and (c) show that the deepest calcinations depths from floor to ceiling, located in the rear left corner of the enclosure (i.e., location of upholstered chair). The front wall contour plot shows evidence of the vent plume, and the right wall plot shows an area high in the corner above the sofa that had deep calcination. It should be noted that the large vertical sections of no calcination depth in plots (a) and (d) represent the vent and an area that was not measured due to auxiliary testing equipment, respectively.

2.3.5 Test 6-7: Gasoline on Upholstered Chair with Full Door Opening (w/Vinyl)

In Test 6-7, the fire was initiated using a 2.0 L (0.53 gal) gasoline spill with 1.5 L (0.40 gal) of gasoline poured onto the upholstered chair and 0.5 L (0.13 gal) poured onto the flooring leading from the chair to the vent. The initiating fire immediately involved the upholstered chair and wooden table. The fire reached flashover conditions approximately two minutes after ignition and burned at this state for approximately 60 seconds before being manually extinguished. The ceiling in this test consisted of 12.7 mm (0.5 in.) thick GWB. As shown in Figure 31, fire patterns on the interior surfaces of the enclosure were present on the walls in the rear left corner of the enclosure and on the center of the ceiling. A plot of the calcination depth survey of the ceiling collected after this test is provided in Figure 32.

Figure 31. Condition of enclosure ceiling after Test 6-7.

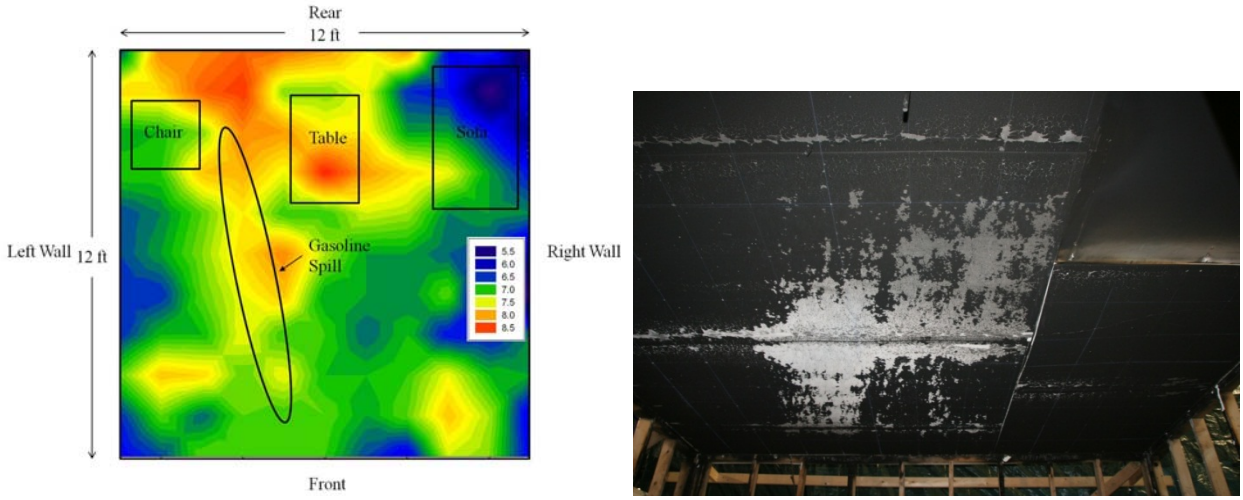

Figure 32. Calcination depth contour plot of ceiling in Test 6-7 [left] (color-coded depths in mm) and photograph of ceiling condition [right].

As shown in Figure 32 the most severe damage to the ceiling of the enclosure was located above the wooden table, between the table and upholstered chair, and along the rear wall of the enclosure. In this test, the calcination depth measurements show a pattern that is generally consistent with the spill fire pattern (i.e., near the upholstered chair and extending from the rear left corner of the enclosure towards the vent).

2.3.6 Test 6-8: Gasoline on Upholstered Chair with Slit Vent Opening (w/Vinyl)

The initiating fire used in Test 6-8 was identical to that used in Test 6-7 with the only difference between tests being the ventilation condition. In Test 6-8, the ventilation was limited using a slit vent. Similar to Test 6-7, the initiating spill fire immediately involved the upholstered chair and wooden table in Test 6-8. However, due to the limited ventilation condition, the fire did not spread beyond this initial area of involvement. The fire burned for 566 seconds (9 minutes 26 seconds) before being manually extinguished. The ceiling in this test consisted of 12.7 mm (0.5 in.) thick GWB. As shown in Figure 33, fire patterns on the interior surfaces of the enclosure were present on the walls in the rear left corner and to some extent on the ceiling of the enclosure in this corner. During this test, a small section of GWB fell from the ceiling. In the area from which this piece fell, a clean burn pattern was identified. A plot of the calcination depth survey of the ceiling collected after this test is provided in Figure 34.

Figure 33. Condition of enclosure ceiling after Test 6-8.

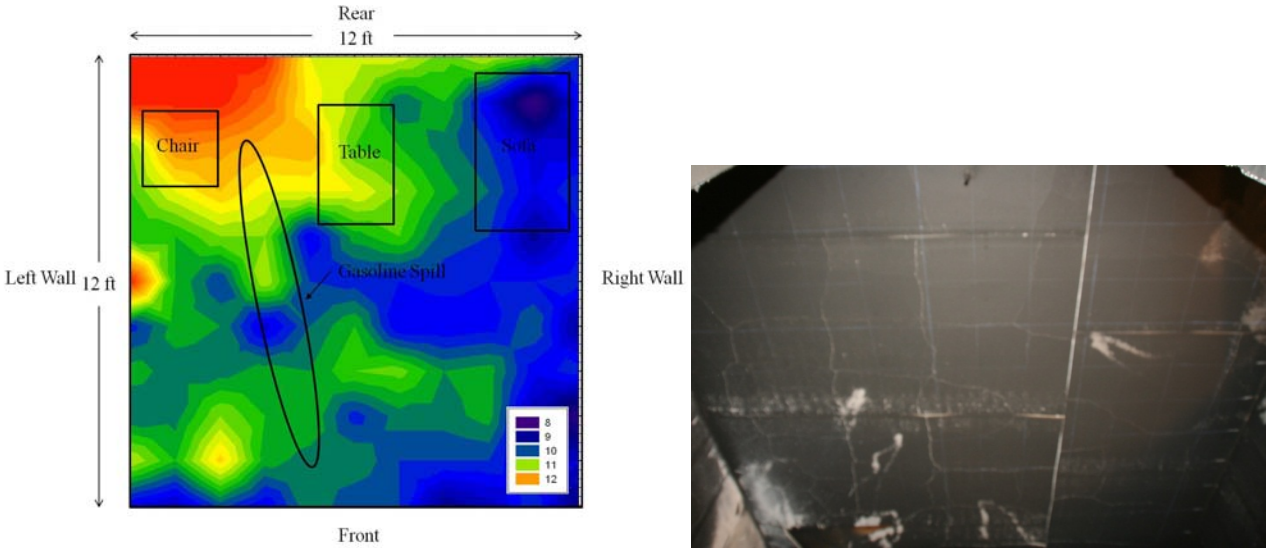

Figure 34. Calcination depth contour plot of ceiling in Test 6-8 [left] (color-coded depths in mm) and photograph of the ceiling condition [right].

The calcination depth contour plot developed from this test was generally consistent with the visual observations of fire patterns on the ceiling. The calcination depth measurements show that the most severe damage occurred in the rear left corner of the enclosure with diminishing damage moving radially outward from this area. The utility of the calcination depth survey in this test was limited due to the fact that visible patterns could be identified and correlated to the remains of burning objects within the enclosure. However, other than the clean burn patterns, the calcination depth contours provide a clearer picture of the fire intensity in the corner diminishing

away from the corner. The plot also indicates the plume from the burning baby seat against the left wall of the room.

2.3.7 Summary of Full-scale Calcination Depth Survey Analysis

Using the probing tool and technique developed from small-scale testing, a series of six calcination depth surveys were conducted on the ceilings, and in two cases on walls, of enclosures subjected to various fire scenarios. In general, the calcination depth surveys were very useful for scenarios in which the surfaces of the enclosure were heavily sooted. This soot deposition masked the thermal damage present on the GWB substrates. When probed, the resulting calcination depth profiles illustrated the areas of most severe thermal insult (i.e., highest calcination depths). The areas identified as having the greatest calcination depths were generally consistent with the area of either the initiating fire or first item ignited. This result is consistent with the calcinations depths being correlated to total heat exposures. During full-scale testing, six of the wall calcination measurement locations aligned closely with the position of a heat flux gauge. The heat flux gauges were located on the rear wall (0.6, 1.2, and 1.8 m elevations) and right wall (0.45, 1.2, and 2.0 m elevations). Using the heat flux measurements, a total heat exposure can be calculated over the duration of the test. The total heat exposure and calcination measurements allow for comparison to the correlations developed in Section 2.2.3.2. Figure 35 shows the calcination measurements (solid black data points) plotted against the heat flux correlations for 12.7 mm (0.5 in.) GWB. The measurements collected in the full-scale test generally fall within the GWB correlations developed from the cone calorimeter tests, showing that the probing method is applicable to large-scale applications as well as bench scale.

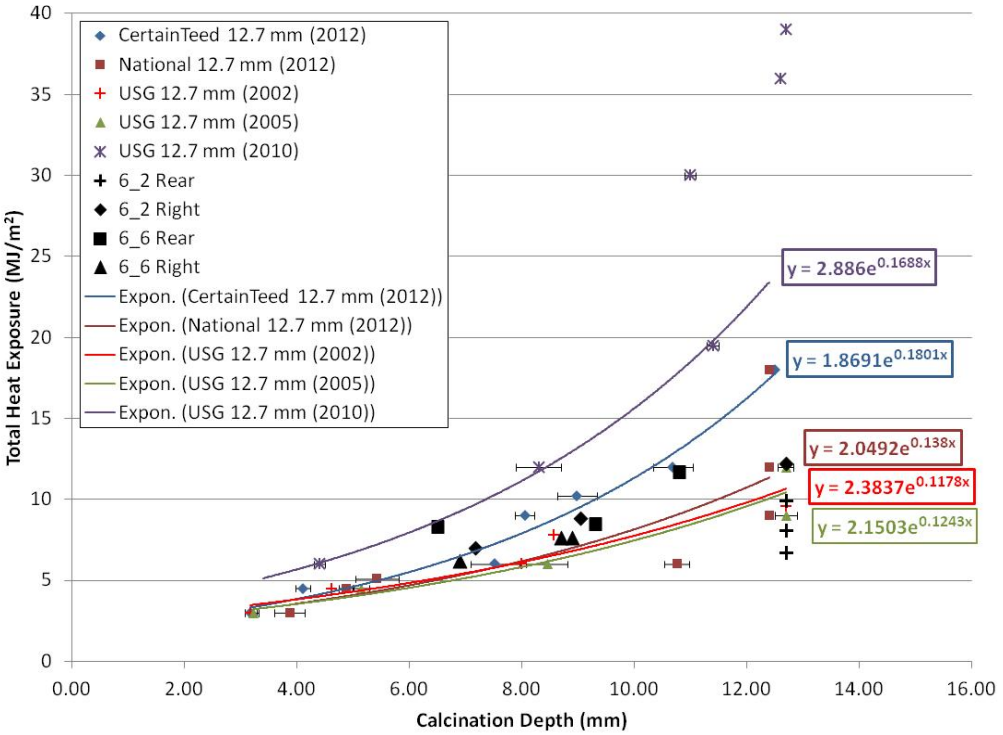

Figure 35. Full-scale calcination measurements compared to 12.7 mm (0.5 in.) GWB correlations.

2.4 Water Exposure Study

In the enclosure fires discussed above, minimal amounts of water were used to suppress the fires, and in most cases, water was not sprayed on to the ceiling. Although there was no apparent issue of water spray confounding calcinations depth surveys in the enclosure fires, this is an issue of concern for field measurements. The purpose of the work discussed in this section was to characterize the impact, if any, that water has on calcination depth measurements collected after exposing gypsum wallboard (GWB) to fire conditions. The primary variables being evaluated in these tests were the thickness of the GWB, the duration of the thermal exposure, and the duration of water application to the material after exposure.

When GWB is heated, the free- and chemically-bound water molecules within the material are driven off, leaving a relatively fragile, easily penetrated layer of calcined gypsum. However, the application of water during suppression activities can also soften GWB, thus, potentially affecting calcination measurements. Section 17.4.4 (5) of NFPA 921 [2011] warns investigators of the fact that this exposure to water could potentially impact the validity of the calcination measurements. This section of NFPA 921 states:

> "*Gypsum wallboard can be damaged during suppression, during overhaul, and post-fire by hose streams and standing water. Wetting of the calcined wallboard can soften the gypsum to the point where no reliable measurements can be made.*"

However, the impact that suppression water has on calcined GWB has not been documented in the technical literature. Based on analytical chemistry results, Schroeder [1999] stated that once the material experienced a phase change to b-anhydrate, the gypsum will not revert to its pre-fire state. The author also indicated that there is a possibility that gypsum which has been elevated to temperatures just under 200ºC (392ºF) has the potential to partially revert through rehydration, under certain environmental conditions. In his analysis, Schroeder [1999] concluded that concerns of re-hydration during and after fire suppression are valid. However, he also stated that when sufficiently heated (i.e., material properties driven to an anhydrated-β state), the thermally induced changes that occur within the material can be preserved. This conclusion was based on an analysis of the change in chemical structure of the gypsum and it is unclear if any confirmatory experimental tests were conducted. To address the uncertainties of the impact of water on calcination depth measurements, a series of intermediate-scale furnace tests were conducted to evaluate this impact.

2.4.1 Intermediate-scale Experimental Approach

The thermal exposures used to thermally degrade (i.e., calcinate) the GWB were generated using the unique intermediate-scale fire-resistance furnace located in the high bay laboratory at Hughes Associates, Inc. The wall assemblies used in this testing were constructed using dimensional lumber (i.e., 2 x 4's) and had overall dimensions of 1.2 m (4 ft) wide by 1.5 m (5 ft) tall. Each assembly consisted of a wood stud frame with a single vertical stud centered across the width of the sample. The exposed faces of the assemblies were lined with either 12.7 mm (0.5 in.) USG Ultralight Sheetrock (2012) or 15.9 mm (0.625 in.) inch USG Type X FireCode (2012) gypsum wallboard. The GWB used in these tests was purchased from a local home improvement

stored and cut to size. The GWB thicknesses evaluated represented the two most prevalent thicknesses in residential scenarios. The unexposed face was lined with 12.7 mm (0.5 in.) GWB. The test walls were constructed using drywall screws and were not sealed in any way (i.e., no drywall compound, tape, adhesives, fire caulks, etc.).

Instrumentation used during these tests consisted of the thermocouples that were used to measure both furnace gas temperatures and wall sample temperatures. Furnace gas temperatures were measured at five locations that were offset 0.15 m (6 in.) from the exposed face of the vertical wall assembly. The average of these measurements was used to control the thermal exposure.

The thermal exposure curve used in all tests was modeled after the time-temperature curve provided in ASTM E119 [2012]. Tests involving 12.7 mm (0.5 in.) GWB on the exposed face of the wall were subjected to the furnace environment for 2.5 and 5 minutes. Tests involving 15.9 mm (0.625 in.) GWB on the exposed side of the wall were subjected to the furnace environment for 7.5 and 20 minutes. The exposure times used in this testing were selected to provide quantifiable degrees of calcination in the two different thicknesses of GWB (i.e., not barely calcined but also not fully calcined). Duplicate tests were conducted at each exposure duration for each GWB thickness (i.e., total of eight tests). In these tests, peak furnace temperatures reached 567–808ºC (1053–1486°F). The exposure durations were designed to create two different levels of calcination depths within each thickness of GWB.

After each furnace exposure, the walls were immediately removed from the furnace and subjected to a water spray. Prior to applying water to the test samples, half of the sample was shielded using a single layer of 12.7 mm (0.5 in.) GWB such that water was only applied to approximately half of the wall. This approach allowed comparative data sets (i.e., wet and dry calcination depth measurements) to be collected from the same sample. Water spray exposures were either 30 or 120 seconds in duration to provide a distinct range. Water was applied to each test wall using a standard hand-held spray nozzle on a garden hose attached to the laboratory water supply. A flow rate of approximately 2 gallons per minute was used for all tests. The water spray was discharged from a distance of 0.6 m (2 ft) such that the diameter of the spray cone from the nozzle was equivalent to the width of the area being wetted (i.e., 0.6 m [2 ft]). However, this spray pattern did not impact the entire exposed surface area of the test wall at once, therefore the spray was moved vertically over the height of the test wall at a rate of approximately one pass every five seconds. For tests with a 30 second water application duration, this meant that a total of six passes (i.e., spray moving over the entire height of the sample) and 24 passes for 120 second water application duration tests. A summary of these tests and the associated test parameters is provided in Table 10. A plot comparing the furnace exposures curves for all eight tests conducted is presented in Figure 36. A heat flux characterization representative of all furnace temperature exposures was performed. Five heat flux measurements, presented in Figure 37, were taken during a single 20 minute exposure and then averaged. The total heat exposure values presented in Table 10 were calculated based on the heat flux characterization average and the duration of the exposure.

After the thermal and water exposures, the samples were permitted to cool naturally for a period of 24 hours before an initial calcination depth survey was conducted. Each survey consisted of a total of twelve measurements, six on each side (i.e., wet and dry sides) of the

GWB. Measurements were collected at 0.15 m (6 in.) intervals laterally and 0.3 m (1 ft) intervals vertically using the probing tool and technique described earlier in this report (see Figure 38).

Table 10. Summary of intermediate-scale calcination testing with water application.

Test ID	GWB Thickness (mm [in.])	Exposure Duration (min.)	Water Application Duration (min.)	Total Heat Exposure (MJ/m^2)	Water Application Density (gal/ft^2)	Total Water Exposure (gal)
1	15.9 [0.625]	7.5	0.5	24.2	1.25	3.75
2		20		74.0	1.25	3.75
3		7.5	2.0	24.2	5	15
4		20		74.0	5	15
5	12.7 [0.5]	5	0.5	16.2	1.25	3.75
6			2.0	16.2	5	15
7		2.5	0.5	7.5	1.25	3.75
8			2.0	7.5	5	15

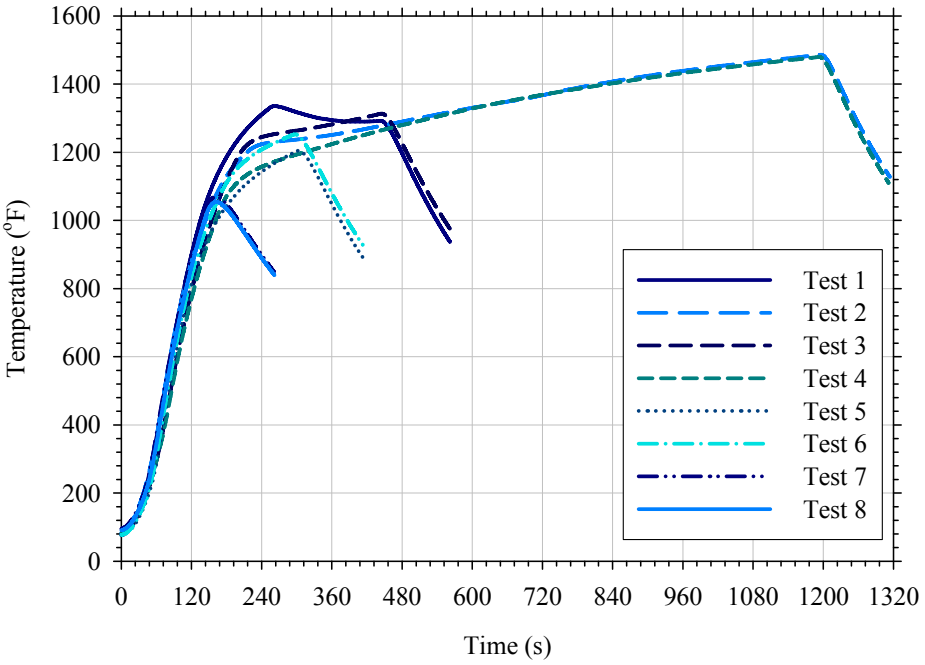

Figure 36. Summary of furnace exposure curves measured during intermediate-scale testing.

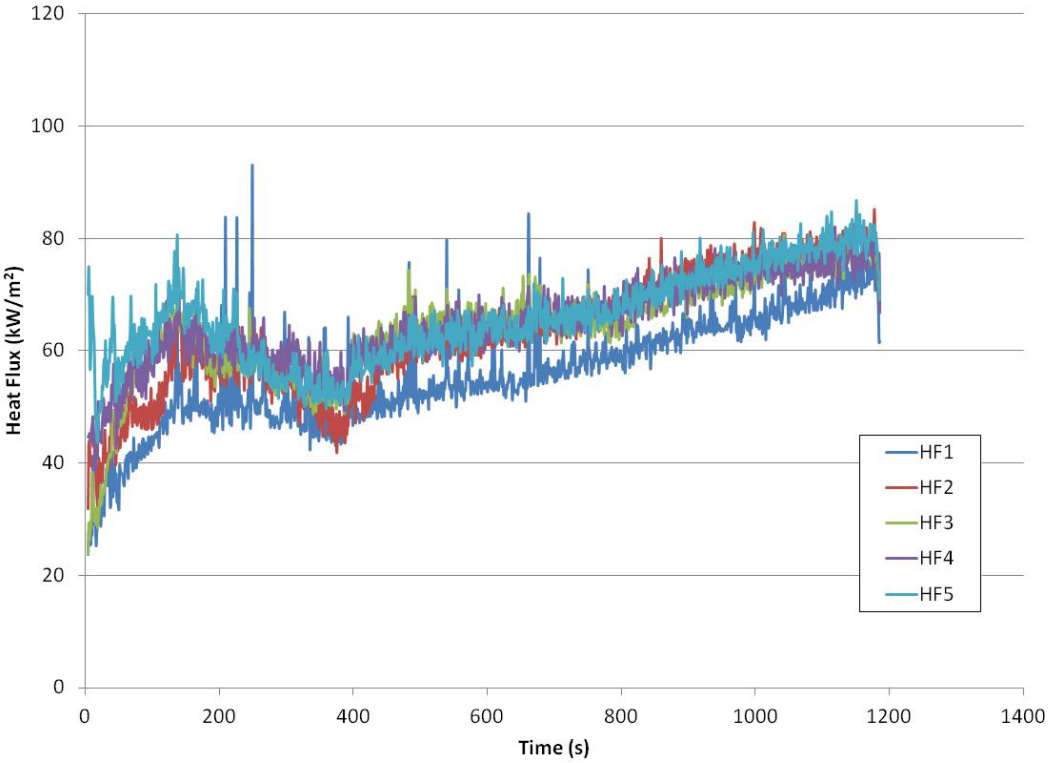

Figure 37. Heat Flux Characterization of Furnace Exposures

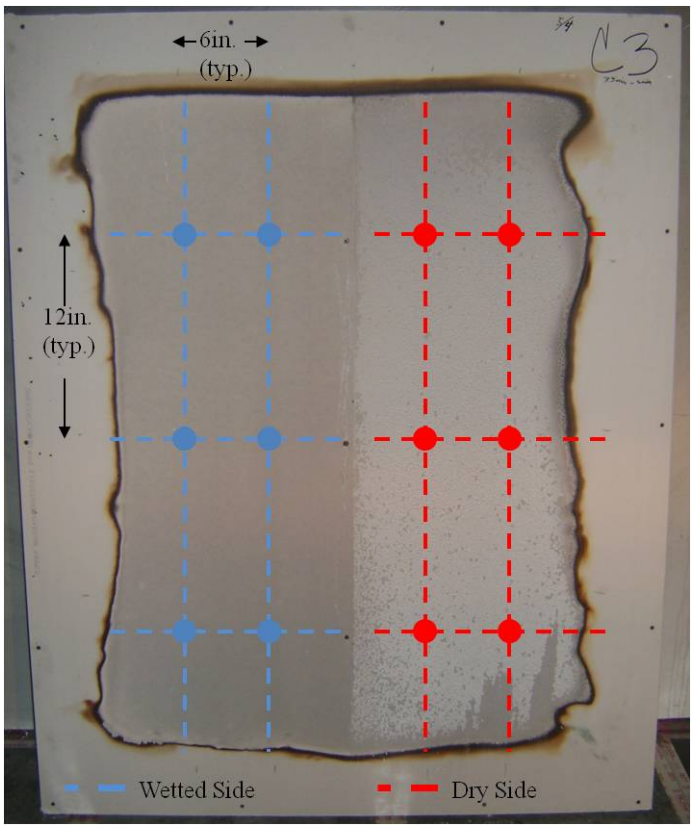

Figure 38. Probing grid used to document each intermediate-scale test wall

2.4.2 Calcination Depth Results

A summary of the average calcination depth measurements (with standard deviation) collected from both the wetted and dry sides of the test walls is provided in Table 11. Also presented in Table 11 is the difference between the wet and dry measurements. Photographs of the condition of each of the test walls are provided in Figure 39. Immediately after testing, it was noted that the walls in Tests 2 and 4 had cracked during the heating process. However, the walls were still structurally sound. The remainder of the walls showed evidence of clean burning and combustion of the exposed paper facing. After water application, the visual appearance of the majority of the walls changed in that the ash from the paper facing was washed away but physically no other changes were noted.

As shown in Figure 39, the color of the wetted side of the test walls in Tests 6 and 8 were significantly darker than the wetted side for the shorter duration water exposures (i.e., Tests 5 and 7). This darker color was attributed to the in-depth wetting that occurred due to the prolonged water exposure used after these tests. This color change was not attributed to any thermal phenomena associated with the heating and calcination of the gypsum wallboard. Photographs taken after a 30 day drying period show that the color of the walls in these tests were comparable once dry (see Figure 40).

As shown in Table 11, the calcination depth measurements collected from the intermediate-scale test walls were slightly less consistent than measured in small-scale testing. Depth measurements within a given sample had standard deviations ranging from 0–1.1 mm, which at worst, were approximately 20 percent of the average depth value. The added variability in these measurements was in part attributed to the less uniform thermal exposure imposed by the intermediate-scale furnace as compared to the cone calorimeter.

For dry calcination depth measurements collected from similar thermal exposures (e.g., test pairs 1/3, 2/4, 5/6, 7/8) the average calcination depth measurements were consistently within less than 1 mm of one another. The same was not true for the wetted samples. Differences for the wetted scenarios were as large as 1.9 mm.

Comparing the depth measurements collected on the wetted and non-wetted GWB, the wetted values were consistently greater than those measured on the dry material. The average difference between these two measurements was 1.4 mm, with differences ranging from 0.2–2.8 mm. With respect to the dry calcination depth measurement, the deeper (wetted) calcination depth values were on average eighteen percent higher with a range of differences between 4 and 34 percent. From these tests the largest differences were noted for the test walls exposed to the most severe total heat exposure and the most severe water application duration (i.e., Test 4 and 8) and the smallest differences were noted for the test walls subjected to the lower thermal exposures and shortest water exposure.

Table 11. Summary of calcination depth measurements collected 24 hrs after furnace exposure.

Test ID	GWB Thickness (mm [in.])	Exposure Duration (min.)	Total Heat Exposure (MJ/m^2)	Total Water Exposure (gal.)	Average Calcination Depth Measurements (Std. Dev.) on Dry Side (mm)	Fraction Calcined (Dry Measurement/ Total Thickness) (-)	Average Calcination Depth Measurements (Std. Dev.) on Wetted Side (mm)	Δ Depth (Wetted – Dry) (mm)	% Difference in Depth Measurement (w.r.t. Dry Side Value)
1	15.9 [0.625]	7.5	24.2	3.75	5.7 (1.1)	0.36	6.3 (0.6)	0.6	11
2		20	74.0	3.75	8.8 (0.3)	0.55	9.4 (0.6)	0.6	7
3		7.5	24.2	15	5.2 (0.4)	0.33	5.4 (0.3)	0.2	4
4		20	74.0	15	8.5 (0.3)	0.53	11.3 (0.7)	2.8	33
5	12.7 [0.5]	5	16.2	3.75	9.3 (0.4)	0.73	11.1 (0.4)	1.8	19
6			16.2	15	10.1 (0.8)	0.80	12.7 (0)	2.6	26
7		2.5	7.5	3.75	7.3 (0.2)	0.57	7.9 (0.7)	0.6	8
8			7.5	15	6.8 (0.5)	0.54	9.1 (0.7)	2.3	34

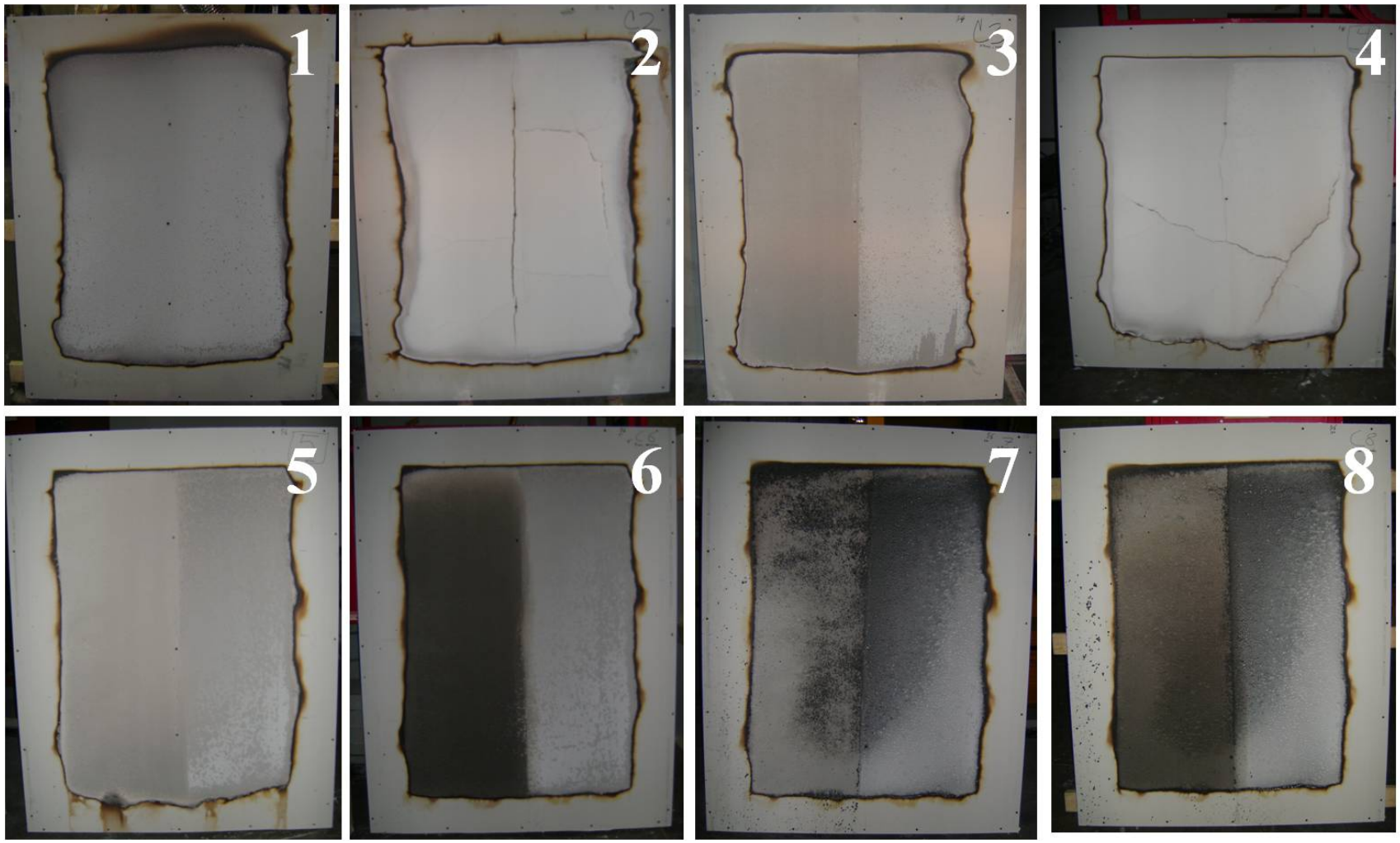

Figure 39. Condition of intermediate-scale test walls after thermal and water spray exposures (left side of each image).

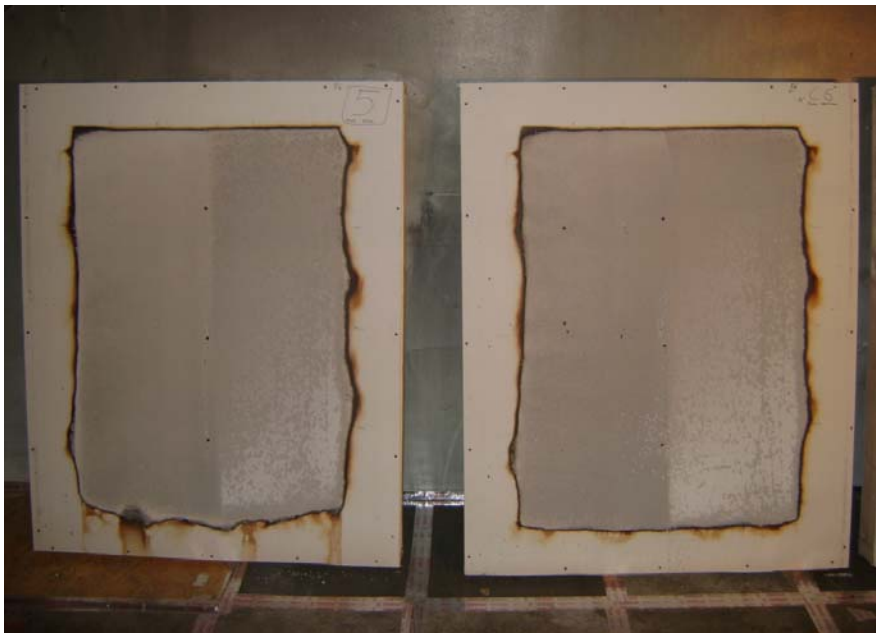

Figure 40. Comparison of test wall color (Test 5 [left] and Test 6 [right]) after 30 day drying period.

Data collected from the 15.9 mm (0.625 in.) GWB test walls suggest that the impact of water was minimal up until the most severe thermal exposure was coupled with the most severe water application duration (i.e., Test 4). In this test, an increase in depth of 33 percent was observed with the previous three exposure scenarios resulting in depth increases of ten percent or less. The susceptibility of the calcination depths, measured on the 12.7 mm (0.5 in.) GWB test walls, to water was more evident than described above for the thicker GWB. In all but one of these tests (Test 7), the wetted measurements were 19–34 percent deeper.

The impact of water application on the calcination depth measurements was associated with both the extent of calcination relative to the total thickness of the GWB and the duration of the exposure to water. Based on the testing conducted, the application of water to the calcined surface had the greatest impact in scenarios where greater than 50 percent of the thickness of the GWB was calcined and exposed to a nominal water application density of 5 gallons per square foot. For scenarios where the calcination depth was greater than 70 percent of the total thickness, the application of a water application density of as little as 1.25 gallons per square foot was found to impact the calcination depth measurements.

2.4.3 Impact of Aging on Calcination Depth Measurements

After the eight test walls described above were probed 24 hours after testing, they were stored in a conditioned space, in the vertical orientation, for a period of 30 days. During this period of time ambient conditions were maintained between 21–27ºC (70–80ºF) and a relative humidity between 45–60%. At the end of this 30-day drying period, the samples were probed using the same probing tool and technique to evaluate the impact of drying on the measurement of calcination depth. A summary of the results from this second round of measurements is provided in Table 12.

Table 12. Summary of calcination depth measurements collected 30 days after furnace exposure.

Test ID	GWB Thickness (mm [in.])	Exposure Duration (min.)	Total Heat Exposure (MJ/m^2)	Total Water Exposure (gal)	Average Calcination Depth Measurements (Std. Dev.) on dry Side (mm)	% Difference in Depth Measurement (w.r.t. 24 hr dry Measurement)	Average Calcination Depth Measurements (Std. Dev.) on Wetted Side (mm)	% Difference in Depth Measurement (w.r.t. 24hr wet Measurement)	Δ Depth (Wetted – dry) (mm)	% Difference in Depth Measurement (w.r.t. Dry Side Value)
1	15.9 [0.625]	7.5	24.2	3.75	5.1 (0.3)	-11	6.0 (0.3)	-5	0.9	18
2		20	74.0	3.75	8.7 (0.1)	-1	8.9 (0.5)	-5	0.3	3
3		7.5	24.2	15	5.4 (0.2)	4	5.3 (0.4)	-2	-0.1	-2
4		20	74.0	15	8.6 (0.3)	1	10.2 (0.4)	-10	1.7	20
5	12.7 [0.5]	5	16.2	3.75	9.1 (0.5)	-2	8.5 (0.2)	-23	-0.6	-7
6			16.2	15	9.1 (0.5)	-10	9.9 (0.4)	-22	0.9	10
7		2.5	7.5	3.75	6.7 (0.3)	-8	6.5 (0.2)	-18	-0.2	-3
8			7.5	15	6.5 (0.2)	-4	6.2 (0.3)	-32	-0.3	-5

The calcination depth measurements collected after the 30 day drying period were less varied than those collected 24 hours after the thermal exposure. After 30 days, standard deviations ranged from 0.1–0.5 mm (less than 8%), which is comparable to the range calculated during small-scale work. The difference between calcination depths measured on the wetted and dry sides of the test walls fell below 1 mm in all but one test (Test 4). It should be noted that although the difference in depths in Test 4 was not less than 1 mm, the value obtained from the 30 day drying data set decreased by more than 1 mm when compared to the difference measured 24 hours after testing (2.8 mm [24 hrs] to 1.7 mm [30 day]).

The average difference in calcination depth on the wetted side of each test wall between the 24 hour and 30 day measurements was a net reduction of 1.5 mm (15 percent), with a range of 0.1–2.9 mm. Similarly, for the dry side, an average difference of 0.3 mm (4 percent), with a range of 0–1 mm. Based on this analysis, the reduction in difference between the wetted and dry side calcination measurements after 30 days was primarily attributed to the drying of the wetted side of the test walls. These changes are likely the hardening of the material as the absorbed water was removed via natural evaporation. These results suggest that if calcination depth measurements are to be collected in an area subjected to high water application rates, the most accurate results are obtained after a period of drying.

2.4.4 Data Comparison to Calcination Correlations

The data from the furnace tests (black × data points) was plotted against the correlations established in Section 2.2.3.2 to further examine the robustness of the correlations. As shown in Figure 41, the 12.7 mm (0.5 in.) samples are in good agreement with the calcination correlations. However, the 15.9 mm (0.625 in.) samples, shown in Figure 42, are not in agreement with the correlations. No explanation has been identified for this significant difference.

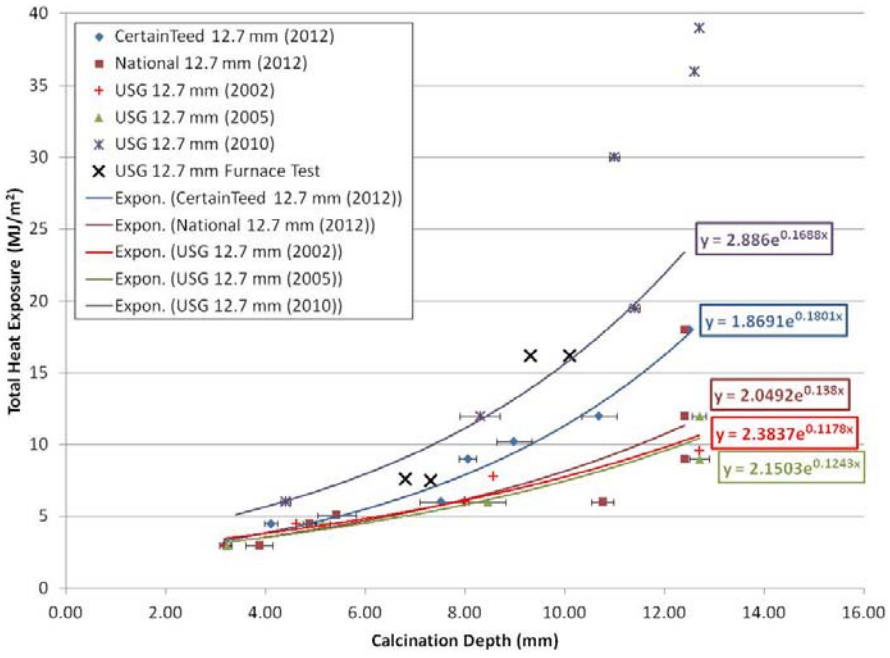

Figure 41. Furnace test comparison to calcination correlations (12.7 mm USG).

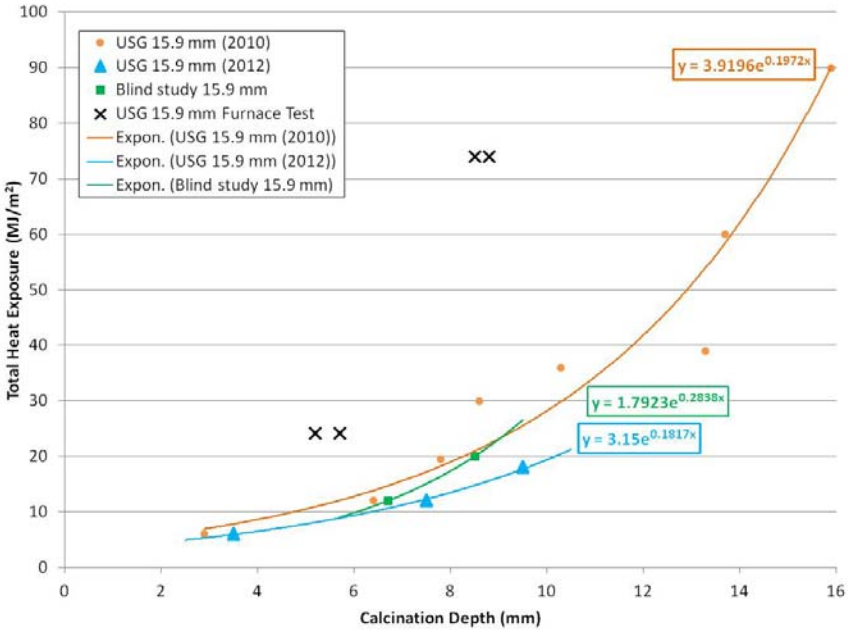

Figure 42. Furnace test comparison to calcination correlations (15.9 mm USG).

The calcination depth measurements collected after the 30 day drying period were less varied than those collected 24 hours after the thermal exposure. After 30 days, standard deviations ranged from 0.1–0.5 mm (less than 8%), which is comparable to the range calculated during small-scale work. The difference between calcination depths measured on the wetted and dry sides of the test walls fell below 1 mm in all but one test (Test 4). It should be noted that although the difference in depths in Test 4 was not less than 1 mm, the value obtained from the 30 day drying data set decreased by more than 1 mm when compared to the difference measured 24 hours after testing (2.8 mm [24 hrs] to 1.7 mm [30 day]).

The average difference in calcination depth on the wetted side of each test wall between the 24 hour and 30 day measurements was a net reduction of 1.5 mm (15 percent), with a range of 0.1–2.9 mm. Similarly, for the dry side, an average difference of 0.3 mm (4 percent), with a range of 0–1 mm. Based on this analysis, the reduction in difference between the wetted and dry side calcination measurements after 30 days was primarily attributed to the drying of the wetted side of the test walls. These changes are likely the hardening of the material as the absorbed water was removed via natural evaporation. These results suggest that if calcination depth measurements are to be collected in an area subjected to high water application rates, the most accurate results are obtained after a period of drying.

2.5 Summary of Findings from Calcination Depth Study

The calcination of gypsum wallboard (GWB) was studied with the intent to: 1) develop an objective tool and method of quantifying in situ calcination depths, 2) assess the utility of calcination depth surveys as a means to understand fire origin and fire development within an enclosure, and 3) characterize the impact of water spray on the accuracy of calcination depth measurements.

Small-scale cone calorimeter testing was used to create varying degrees of calcination within GWB samples. Using visual observations to quantify calcination depth based on color or texture variations proved inconclusive as none of these changes could be consistently correlated to calcination, more over a specific depth. However, using these samples, a hand-held tool was developed to measure calcination depth based on an evaluation which identified a probe pressure that was sufficient to penetrate all degrees of calcination but not sufficient to penetrate virgin GWB. The tool consists of a digital force gauge to which a 2 mm hex key is attached to serve as the probe. A probe force of 3 kg (6.6 lbs) was determined to be the appropriate force to completely penetrate calcined material without penetrating uncalcined material. The 3 kg force with the specified probe equates to a probe pressure of 0.86 kg/mm^2 (1175 psi). Using this probing technique, the calcination depths of all small-scale samples were measured and tabulated. The calcination depths for the corresponding total heat exposures were in good agreement to a recent study by a Mann & Putaansuu [2010], in which the authors characterized calcination depth using an FTIR chemical analysis. The similarity between the depths measured in this study and those quantified by Mann & Putaansuu [2010] serve as validation of the technique developed in this work. Additionally, a blind test performed by three separate operators validated the reliability of the technique from one operator to the next.

Correlations between calcination depth relative to total heat exposure were developed for various GWB materials, including different manufacturers, thickness and year of production. Although similar, the correlations do vary based on the variables evaluated, such that the utility of the correlations may be limited. Further work on a greater number of samples could prove fruitful in refining the correlations and expanding the utility of the correlations.

With a hand-held tool and appropriate technique developed, a series of calcination depth surveys of full-scale room fire enclosures were conducted. Surveys were conducted after six different full-scale enclosure fires with varying ignition and ventilation scenarios. The benefit of the calcination depth survey was realized primarily for the tests where visual patterns were not obvious. In these scenarios, the interior surfaces of the enclosure were heavily sooted with no visual indications of any fire patterns. However, after collecting calcination depths at set intervals and plotting these values, a contour plot of the data provided valuable insight into the areas within the enclosure that were subjected to the most severe thermal damage. In general, the areas in which the initiating (or primary first fuel) fire occurred could be identified based on differences in damage patterns relative to adjacent areas. From these full-scale calcination depth surveys, it was concluded that the utility of this technique is greatest when visible patterns are not present. In the event that visual patterns were present, calcination depth surveys provided minimal additional insight into the fire scenario. However, further study of the relationship between calcination and total heat exposure could enhance the utility of these surveys by providing fire investigators a means of estimating fire growth scenarios based on thermal damage to the GWB.

The impact of water spray on the measurement of calcination depth was also evaluated. From these tests, it was concluded that the application of water alters the measured depth of calcination. An average increase in depth of approximately 18 percent was calculated for measurements collected 24 hours after fire exposure and application of the water. This difference fell to less than five percent after the samples were left to dry for a period of 30 days. This data suggests that if measurements were to be collected in areas that have been wetted by suppression

activities for any extended period of time, it would be advisable to delay measurements until the water has been removed.

3.0 FORENSIC FIRE PATTERN ANALYSIS

3.1 Literature Review

As defined by NFPA 921 [2011], fire patterns are the visible or measurable physical changes or identifiable shapes formed by a fire event. The utility of fire patterns is dependent on the ability of the fire investigator to identify and interpret the pattern in the context of the fire event being investigated. A summary of fire effects and associated fire patterns are available in Chapter 6 of NFPA 921 [2011]. This chapter was designed to aid fire investigators in the identification and interpretation of fire patterns. In addition to the information provided in NFPA 921, there have been numerous research efforts conducted to explore the development, persistence, and utility of fire patterns. A review of this research has been summarized below.

3.1.1 Pattern Identification and Characterization

The current state of the art, with respect to fire investigation and the interpretation of fire patterns, is contained within NFPA 921 [2011]. In addition to the information contained within this guide regarding fire patterns, numerous research studies have been performed to better understand the development, repeatability, and persistence of patterns in fire environments.

The faculty at Eastern Kentucky University (EKU) have been performing full-scale room fires with the intent of fire pattern characterization. To date, the EKU researchers have investigated the reproducibility of fire patterns given an identical fuel package [Hicks et al. 2006 and 2008] as well as the persistence of and predictability of fire patterns in pre- and post-flashover fire scenarios [Hopkins et al. 2008]. Hicks et al. [2006 and 2008] concluded that pattern development can be repeatable provided influencing variables (i.e., ventilation, fuel package, etc.) are controlled. Hopkins et al. [2008] reported that in general, initial plume patterns on the boundaries of a room that are developed during the early stages of a fire will persist during post-flashover exposures and are still a viable means of assessing fire origin and development. However, it should be noted that while the patterns identified in this work persisted through post-flashover conditions, variables such as ventilation and proximity of the pattern to ventilation, were not explored and could have a major impact on pattern persistence. Most recently, the EKU researchers investigated the utility of fire patterns when the initiating fuel source is not the primary fuel source in the fire [Gorbett et al. 2010]. From this work, the author asserts that patterns generated by initiating fuel packages were persistent and identifiable, even after larger fuel packages became involved. However, the initiating fuel package used in this work (a wood crib) while providing a relatively low heat release rate, will burn for an extended period of time and is a highly radiative fire due to the complexity of the crib. These attributes could potentially create a more distinct, persistent pattern than other potential, lower heat release rate fuels that could be found in a residential setting.

Additional research examining the development/progression of fire patterns during post-flashover fires was performed by Carman [2009]. The author conducted fire tests in three identical enclosures with identical fuel loading and ignition scenarios. The primary variable

examined was the duration of the post-flashover exposure. The objective of these tests was to examine the evolution of burn patterns under varying times of exposure to full room involvement. The fuel load in all tests consisted of Class A commodities ignited using a wastebasket fire. The post-flashover durations examined were ten seconds, 111 seconds, and 140 seconds. Carman [2009] found that the longer duration, post-flashover exposures produced clean burn patterns not present in the short duration test. These patterns were produced in an area absent of a commodity fuel and were therefore attributed to the burning of volatilized fuel at a location dictated by flow patterns of incoming air. It was also noted that in the first test of short duration there was some evidence of the beginnings of a clean burn, and had the exposure been permitted to go longer, a similar pattern to the long duration would have likely formed.

Riahi et al. [2011] observed similar duration dependent pattern formation phenomena when conducting small-scale soot deposition experiments. In these tests, a gypsum wallboard wall was subjected to the same fuel source only for two different durations. Optical density contour plots of the soot deposition profiles observed by Riahi [2011] during two different duration, 0.3 m (12 in.) square gasoline pool fire exposures (e.g., 440 s and 700 s) are presented in Figure 43. The plots in Figure 43 illustrate the optical density, or extent of soot deposition, present on the GWB after each test. In these plots, areas of blue indicate areas where soot is not present with areas of red representing areas with the higher levels of soot deposition.

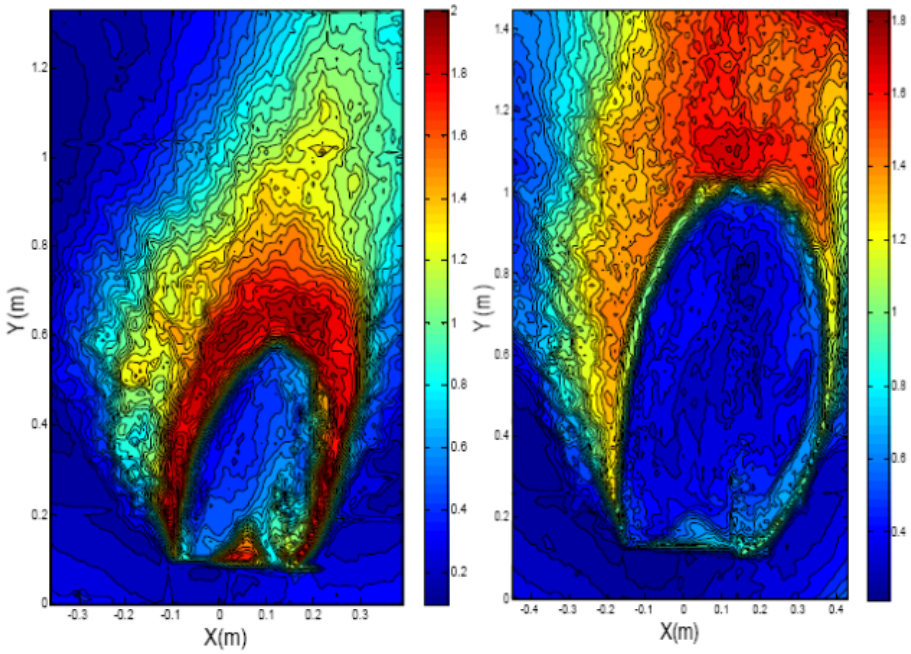

Figure 43. Optical density contour plots of soot deposition on gypsum wallboard from adjacent gasoline pool fires as presented by Riahi [2011]. Image on left represents the 440 s exposure while image on right represents 700 s exposure.

The results in Figure 43 illustrate the progression of a clean burn pattern as a function of exposure duration. The area of clean burn (i.e., central area of blue) increases from left to right not necessarily due to a larger source but simply a more prolonged exposure to the same source.

The utility of fire patterns as a tool for forensic fire investigators is an ongoing research effort being conducted by the National Institute of Standards and Technology (NIST). This research effort is the result of a recent National Research Council (NRC) publication identifying the research needs of the forensic science community [NRC 2009]. To address the recommendations of the NRC report, Madrzykowski [2010] is evaluating the repeatability of burn patterns on gypsum wallboard (GWB) exposed to a range of source fires in a pre-flashover environment. Statistical analysis of the fire pattern characterization has been performed and the repeatability of the patterns has been shown to be dependent upon both the fuel source and the proximity of the source to the wall. Madrzykowski's [2010] work is ongoing and a final report was not complete at the time of this report.

3.1.2 Ignitable Liquids and Flooring Patterns

Putorti [1997] conducted a series of four full-scale room fires to study the utility of patterns produced by fires. In this work, Putorti [1997] considered two different ignition scenarios, an incipient scenario involving flaming newspaper, and an accelerated scenario involving the use of 0.95 l (1.0 qt) of gasoline poured onto the floor of the test cell. Putorti [1997] concluded that the ventilation present during testing can have a significant impact on the pattern formation and while not discussed, the author indicated that consistent differences were observed between the fires resulting from the incipient and accelerated ignition scenarios.

Shanley [1997] was the next researcher who performed a series of controlled fire tests designed to provide a scientific basis for fire investigators to assess the propriety of their fire pattern opinions. In these tests, both laboratory and real-world enclosures were instrumented with temperature, heat flux, and gas concentration measurements. The construction and furnishing of the test enclosures were designed to be representative of real-world scenarios and the post-fire scene processing was executed in accordance with procedures outline in NFPA 921. From this work, Shanley [1997] made the following conclusions:

- the ventilation of a room greatly affects pattern formation,
- the presence of floor patterns in a flashover room is not a reliable indicator of the use of an ignitable liquid residue (ILR),
- the presence of floor patterns in a non-flashover room is a reliable indicator of the use of an ILR given that all other non-ILR materials can be ruled out,
- patterns beneath furnishings are not reliable indicators of the presence of ILR, ignitable liquids were produced during the thermal decomposition of furnishing materials located within the test enclosure, and,
- residue of ignitable liquids will remain and are detectable after a fire.

In 2001, Putorti [2001] investigated fire patterns developed on various flooring materials when a combustible/flammable liquid is spilled and burned. Putorti [2001] evaluated a total of four different flooring materials, including wood parquet, vinyl, and two different types of carpet. In this study, various quantities of liquid were poured on 1.2 m (4 ft) square sections of each flooring material and burned until the fuel was consumed. Putorti [2001] documented the

fire patterns developed from liquid fuel spill fires and developed correlations between the liquid spill area and burn pattern area.

Under a recent National Institute of Justice grant, Mealy et al. [2011] conducted a series of more than 500 liquid fuel spill fires. The goal of this work was to evaluate liquid fuel spill fire dynamics as well as to characterize the forensic fire patterns associated with these types of fires and potential Class A fuels that produce similar patterns. Several types of patterns were consistently identified for certain fuel types. Liquid fuel spill fires consistently resulted in irregularly shaped burn patterns with minimal thermal damage to the substrate, except in the case of carpet scenarios. Class A fuels constructed from plastic and foam materials consistently left an oily residue on the substrate after self-extinguishing upon fuel consumption. Based on visual pattern shapes, there were no clear indicators to differentiate between Class A and flammable liquid fuel fires. However, the extent of damage (i.e., char depths and burn through) was greater for the Class A fires compared to fuel spill fires.

Depending on the depths of fuel, a flammable liquid burning atop a substrate can contribute to the heating of the substrate or reduce the heating of the substrate. As the fuel burns, the radiant energy from the fire is absorbed by both the fuel layer and the substrate. This absorbed energy supports both the heating and volatization of the fuel as well as the heating of the substrate.

For thick fuel layers (i.e., greater than 5 mm (0.2 in.)), the temperature of the substrate will generally remain within several degrees of the boiling point of the liquid fuel burning atop it, provided the fuel layer is continuously maintained. This is due to the attenuation of the radiant heat feedback from the fire by the thick fuel layer and conduction between the fuel and substrate. For thin fuel layers (i.e., less than 5 mm (0.2 in.)), typically associated with unconfined spills, the temperature of the substrate will generally be higher due to the inability of the fuel layer to effectively attenuate radiant heat feedback. However, substrate temperatures are moderated by the fact that the temperature of the substrate, in general, cannot exceed the boiling temperature of the liquid. Therefore, depending upon the liquid that is burning, the boiling temperature may be low enough to cause relatively no thermal damage. In some cases however, for higher boiling point/multi-constituent fuels, this temperature may be high enough to thermally degrade (i.e., scorch, char, melt) the substrate. Despite the heat shielding effects of the fuel layer in both cases, damage to the substrate is likely to occur at the edge of the fuel layer because of the dry substrate material just outside the fuel area is irradiated by the flame and not shielded by the fuel.

3.2 Pattern Evaluation

The intent of this evaluation was to characterize the development and persistence of fire patterns in both open burning and enclosed conditions. In addition, this section describes under what conditions (i.e., pre- or post-flashover, etc.) various types of fire patterns can persist and be used as indicators of area of origin and the first item ignited.

3.3 Summary of Enclosure Fire Testing

This report is a companion report to the document entitled “Ignitable Liquid Fuel Fires in Buildings – A Study of Fire Dynamics” [Mealy et al. 2013]. This companion report provides the detailed descriptions of the fire scenarios, experimental setup, and fire dynamics results of the

tests used to generate the patterns described in this report. The following section provides a high-level summary of the fire dynamics associated with these tests and a detailed review of the forensic fire patterns observed after the fire was suppressed.

3.3.1 Experimental Approach

Three of the six test series conducted in this grant program will be discussed in this section: unconfined liquid fuel fires in the open, unconfined liquid fuel fires in an enclosure, and Class A fires in an enclosure. A summary of the experimental approach used in these test series is provided below.

3.3.1.1 Open Burning Substrate

A test floor for conducting unconfined liquid fuel spill fires in the open was framed with 2 x 4 inch dimensional lumber spaced 0.41 m (16 in.) on center, overlaid with a single layer of 12.7 mm (0.5 in.) plywood. The plywood served as the subfloor to either carpet or vinyl flooring. After each spill fire test, the plywood substrate was removed and a new subfloor installed. A photograph of the test floor under the hood calorimeter is provided in Figure 44.

Figure 44. Vinyl floor constructed for open burn testing.

3.3.1.2 Test Enclosure & Class A Materials

The test enclosure used was 3.7 m (12 ft) by 3.7 m (12 ft) square. The enclosure had a ceiling elevation of 2.1 m (8 ft). Identical room geometries were used by Shanley [1997] for fire pattern research and are recommended in ASTM E603 [2007]. The front wall of the enclosure was identified as the wall containing the vent and all other walls are identified accordingly (i.e., left wall to the left side upon entering through the vent opening, rear wall opposite the vent, and right wall to the right side upon entering the vent opening).

In Test Series 6, the enclosure was filled with Class A furnishings and flooring materials. The furnishings included an upholstered sofa, upholstered chair, wood-construction table, and plastic-construction car seat. Miscellaneous Class A materials including polyester blankets, plastic storage baskets, and crumpled paper were also included in these tests. The materials served as floor-level combustibles that would create fire patterns on the flooring material. A plan view of the furnished enclosure is provided in Figure 45 and a representative photograph of the Class A furnishings within the enclosure is provided in Figure 46.

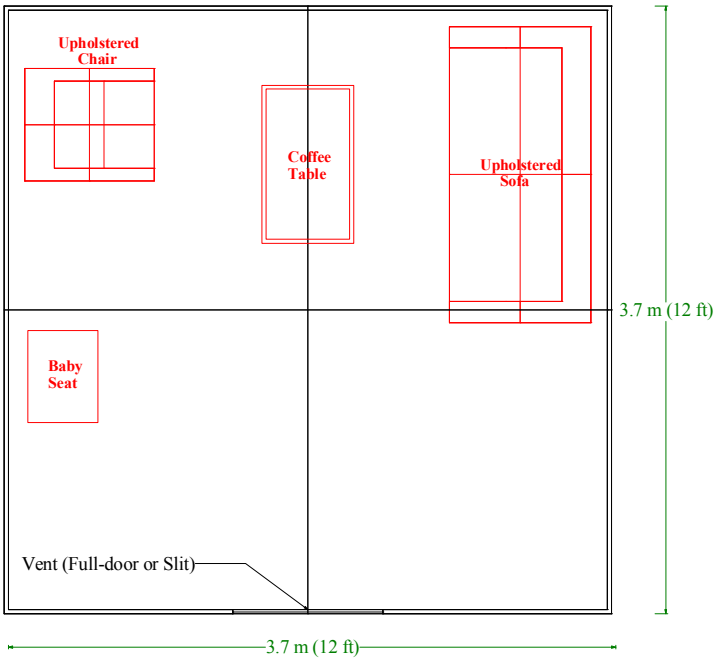

Figure 45. Plan view of test enclosure with Class A furnishings present.

Figure 46. Class A furnishing locations within test enclosure.

The flooring materials used included vinyl and carpet. The vinyl flooring system consisted of vinyl flooring applied to 12.7 mm (0.5 in.) plywood using vinyl adhesive. The vinyl used was a Congoleum Prelude vinyl sheeting with a nominal thickness of 1.2 mm (0.04 in.). The adhesive used was Robert's Premium vinyl adhesive. The vinyl adhesive was applied using a 1/16 x 1/16 x 3/32 in. notch trowel. Once applied, the adhesive was permitted to become tacky prior to the application of the vinyl sheet.

The carpet system was comprised of carpet and foam padding on 12.7 mm (0.5 in.) plywood. The carpet was a Portico Royale Plus (BP724) 100% nylon cut pile Saxony with an approximate mass per unit area of 0.85 kg/m^2 (25 oz./yd^2) and pile height of 12.5 mm (0.5 in.). The backing material of the carpet was a woven polypropylene. Foam padding was a PS53P bonded urethane foam pad with a nominal thickness of 9.5 mm (0.375 in.) and density of 88.1 kg/m^3 (5.5 lb/ft^3).

In these tests, both Class A and liquid fuel ignition scenarios were explored. The first test in this series (Test 6-0) was ignited using a small (<10 kW) Class A ignition source [Wolfe et al. 2009]. The remainder of the tests conducted in this test series were ignited using a 2.0 L (0.26 gal) gasoline spill fire. In half of the tests (Tests 6-1, 6-2, 6-5, 6-6), the entire 2.0 L (0.52 gal) of fuel was spilled directly onto the floor as illustrated in Figure 47. In the remaining four tests (Test 6-3, 6-4, 6-7, 6-8), 1.5 L (0.40 gal) of gasoline was spilled onto the upholstered chair and 0.5 L (0.12 gal) was used to create a trailer leading from the foot of the upholstered chair to the doorway. Photographs of this fuel spill scenario are provided in Figure 48.

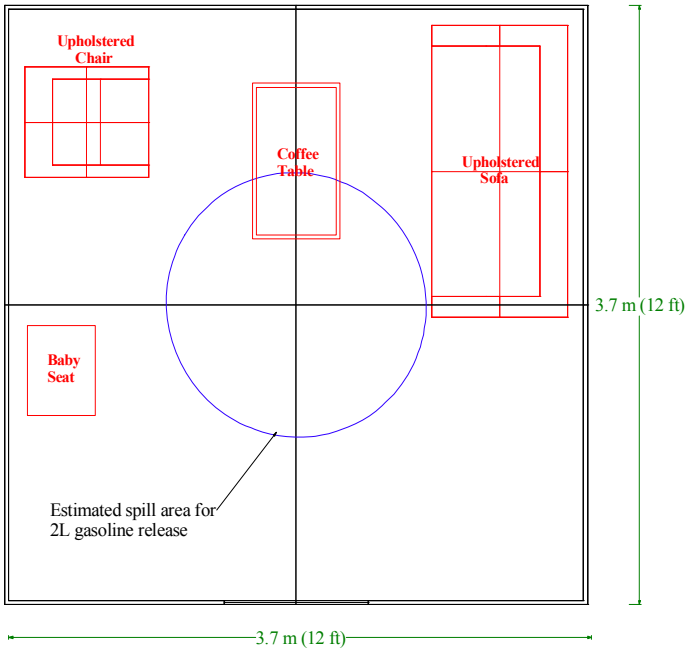

Figure 47. Illustration of gasoline spill fire scenario in center of enclosure.

Figure 48. Gasoline spill on seat of upholstered chair (left) and trailer leading from front of chair to doorway (right).

After ignition the enclosure fires were permitted to grow and burn naturally. The ventilation scheme remained fixed during each test. The duration of the tests varied based on a variety of parameters. With the exception of the first test, tests involving full-door ventilation were permitted to burn for an additional 60–120 seconds after the doorway plume was ignited (i.e., exterior flaming at the vent opening). The first test was allowed to burn for 300 seconds (5 min.) after ignition of the doorway plume. For tests involving the slit ventilation scenario, the fires were permitted to burn for between 8–12 minutes. The decision to suppress these limited ventilation scenarios was primarily based on the development of the thermal conditions within the enclosure. Once relatively steady-state conditions were achieved within the enclosure an additional 6–10 minutes of data were collected. A summary of test parameters and pertinent measurements/observations is provided in Table 13.

3.3.2 Fire Pattern Results

3.3.2.1 Test Series 1 – Unconfined Spill Fires on Carpet in the Open

When conducted in the open on carpet, the 2.0 L (0.52 gal) unconfined gasoline spill fires burned for 5–8 minutes before decaying to a stage where only flamelets existed on the perimeter of the fire pattern. Initially, this carpet spill fire scenario produced a relatively steady-state fire condition. During this steady-state period the gasoline that had been absorbed into the carpet and foam pad substrates volatized and burned. It should be noted that initially the carpet substrate remained intact (i.e., no thermal degradation) due to the evaporative cooling of the carpet by the volatizing liquid fuel. No damage to the carpet occurs because the gasoline is wicking through the carpet fibers and the thermal degradation temperature of carpet (130ºC (266ºF)) is greater than that of the boiling point of the gasoline (38–204ºC (100–400ºF)) [Chevron, 2011]. Therefore, until the bulk of the gasoline has been consumed, the temperature of the carpet cannot exceed that of the boiling point of gasoline. However, approximately 15–30 seconds after ignition, the carpet material along the perimeter of the spill began to thermally degrade due to radiant heating from the fire plume. This period of thermal degradation along the perimeter of

Table 13. Summary of test variables and results from Test Series 1, 4, and 6 [Mealy et al. 2013].

Test ID	Open/ Enclosure	Ventilation Scenario	Flooring Type	Ignition Scenario	Peak HRR (MW)	Time to Peak HRR (s)	Avg. Upper Layer Temperature (°C [°F])	Time to Exterior Flaming (s)	Test Duration (s)
1-1	Open	N/A	Carpet	Fuel Spill on Floor	0.6	25	N/A		329*
1-2			Vinyl		2.6	21			60
4-1	Enclosure		Vinyl		3.0	26	722 [1332]	N/A	88
4-2			Carpet		0.2**	282	200 [392]	N/A	330
6-0		Full Door	Carpet	Class A	6.1	429	800 [1472]	408	755
6-1		Full Door		Fuel Spill on Floor	6.3	218	655 [1211]	192	260
6-2		Slit Vent			0.9	272	415 [779]	N/A	480
6-3		Full Door		Fuel Spill on Upholstered Chair	7.2	158	715 [1319]	120	264
6-4		Slit Vent			1.8	723	500 [932]	270***	713
6-5		Full Door	Vinyl	Fuel Spill on Floor	5.0	64	755 [1391]	59	186
6-6		Slit Vent			1.1	221	413 [775]	N/A	506
6-7		Full Door		Fuel Spill on Upholstered Chair	3.7	121	715 [1319]	115	190
6-8		Slit Vent			0.9	139	605 [1121]	N/A	566

* Values based on initial 120 seconds of burning to evaluate fire size associated with gasoline spill, not contribution of carpet flooring material

** Peak heat release rate (HRR) values based on initial 90 seconds of burning (i.e., gasoline spill fire) not peak measured due to involvement of flooring material

*** Intermittent exterior flaming observed during test.

the spill pattern with the interior material remaining intact is illustrated in Figure 49. As these fires progressed, the thermal degradation front moved both radially outward due to flame spread along the carpet/foam pad flooring and radially inward due to the consumption of the gasoline. Eventually, the inward spread reached the center and self-extinguished. However, the spread of flame radially outward did not self-extinguish but instead continually grew.

Figure 49. Early stage of gasoline spill fire on carpet.

As described by Mealy et al. [2011], this mode of perimeter flaming continued to gradually spread radially outward, consuming the carpet/pad substrate. Visual observations of this growth suggest that the flame spread mechanism consists of the initial involvement of the foam pad under-layer that is relatively easily ignited and burns well. The burning foam in turn involves the carpet substrate above. However, the inherent resilience of the carpet to ignition/rapid flame spread impedes the spread of the flaming combustion on the foam pad and limits the growth of the overall fire. A photograph of this limited fire growth is presented in Figure 50.

Figure 50. Residual flaming along perimeter of carpet flooring after self-extinguishment of gasoline spill fire.

Due to the fact the carpet substrate continued to support flaming combustion after the gasoline spill fire was extinguished, the resulting fire pattern on the carpet substrate could not be directly correlated to the initial spill area. However, potential methods of discerning between the initial spill area and the area involved as a result of the continual burning of the carpet/padding material were identified by the author in previous work. [Mealy et al. 2011]. In this work, the author found that the initial spill area was generally completely consumed and had a relatively flat topography. When transitioning to the area associated with burning beyond the spill area, the topography changed to a wavier surface and the carpet/padding material was less consumed (i.e., charred by not burned to ash). Flame spread rates on carpet with padding were approximated by the author in the previous work to be 0.011 m/min. for gasoline spill fires [Mealy et al. 2011].

After being manually extinguished, the condition of the carpet flooring was evaluated. In general, the classic doughnut-shaped pattern identified in NFPA 921 [2011] was observed for all tests. The carpet and foam pad material in the center of the pattern (i.e., area where the gasoline fuel was initially poured) was the least thermally degraded. The doughnut pattern is consistent with the limited burning of material during the initial stage of the fire due to wicking of the gasoline through the carpet fibers. In some cases, the lack of thermal degradation in the center of the spill was such that the foam padding beneath the carpet substrate was still intact with no thermal degradation at all. An example of this is provided in Figure 51.

In this test, the fire did not spread uniformly, radially outward from the center of the spill due to air currents within the lab at the time of the test. However, it should be noted that the initial gasoline spill area was located in the center of the carpet flooring, which is exactly where the foam pad underlayment is the least thermally damaged (speckled green area in Figure 51) despite adjacent material being completely consumed along the path of flame spread.

Figure 51. Photograph illustrating the lack of thermal degradation in the initial spill area (center of sample) despite severe damage to adjacent carpet and padding material (upper right corner).

3.3.2.2 Test Series 1 – Unconfined Spill Fires on Vinyl in the Open

When conducted in the open on vinyl, the 2.0 L (0.52 gal) unconfined gasoline spill fires burned for 60–90 seconds before self-extinguishing. Due to the brevity of these fires and the evaporative cooling effect of the fuel, the damage to the substrate was minimal (i.e., surface charring, some cracking of the material, and negligible penetration through the vinyl layer). Involvement of vinyl adhesive and plywood subfloor was not observed in any of these tests. A representative photograph of a gasoline spill fire pattern on vinyl is presented in Figure 52.

Figure 52. 2.0 L Gasoline spill fire pattern on vinyl flooring in the open.

As shown in Figure 52, contrary to that observed for carpet spill fires, the most extensive damage on the vinyl substrate was present in the center of the spill. This difference is due to the inability of the vinyl to absorb the gasoline fuel resulting in only a thin layer (i.e., 0.5–1.5 mm) of fuel being present over the entire surface area of the spill. This relatively thin layer of fuel can only absorb a fixed amount of energy leaving the remainder of the incident heat being imposed back on the fuel surface by the fire plume to be absorbed by the vinyl substrate. Empirical data shows that the highest heat fluxes back to the fuel surface are at the center [Mealy et al. 2011, Hammins et al. 1994]. Consequently, the most severe damage to the vinyl flooring occurred in the center of the spill fire with reduced levels of damage moving radially outward. This transition from most severe to least severe damage resulting from the open burning gasoline spill fire scenario is illustrated in Figure 53. In Figure 53, four levels of thermal degradation are identified with the least severe being thermal discoloration, followed by surface charring, thermal softening of the vinyl finish, and finally surface cracking and exposure of the felt backing material.

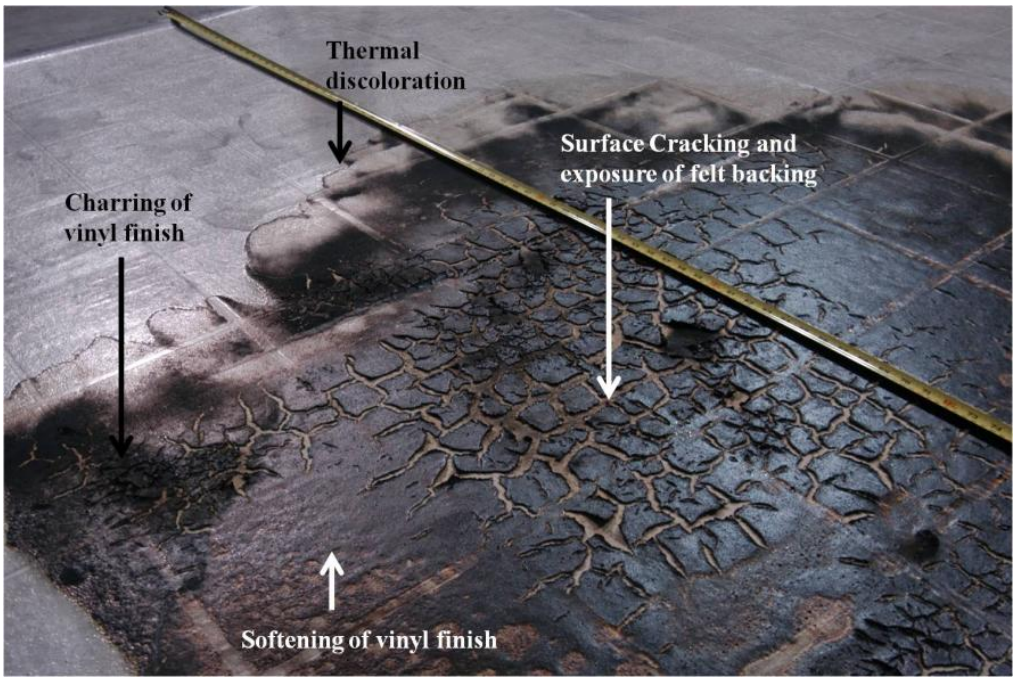

Figure 53. Illustration showing various degrees of thermal degradation of vinyl flooring due to gasoline spill fire in the open.

In all tests conducted on vinyl in the open, floor fire pattern areas were within 15 percent of the initial gasoline spill pattern areas, which ranged between 1.9–2.1 m^2 (21–23 ft^2) for the different tests. The 15 percent difference calculated in this work is consistent with the findings of previous work [Mealy et al. 2011], which consistently measured fire pattern areas that were 10 percent larger than initial spill areas for spill fires on vinyl flooring.

3.3.2.3 Test 4-1 – Unconfined Fuel Spill Fire on Vinyl in an Enclosure

The enclosed 2.0 L (0.52 gal) unconfined gasoline spill fire on vinyl burned for approximately 90 seconds before self-extinguishing. In this scenario, the damage to the vinyl flooring was extensive compared to the damage observed in the open burning scenarios. Over the course of the test, the entire enclosure floor became involved despite the fact that the initiating gasoline spill fire only covered approximately 18 percent of the floor area (i.e., 2.5 m^2 [27 ft^2]). Furthermore, the majority of the flooring surface exhibited surface cracking of the vinyl finish and exposure of the felt backing. In some areas, the vinyl finish and felt backing were completely consumed with the adhesive layer and plywood subfloor involved. An overhead photograph of the vinyl flooring after the gasoline spill fire in the enclosure is provided in Figure 54.

Figure 54. Condition of vinyl flooring after 2.0 L (0.52 gal) gasoline spill fire in enclosure.

As described in the companion report [Mealy et al. 2013], this fire scenario reached flashover conditions (i.e., upper layer temperatures in excess of 600ºC (1112ºF) and floor-level heat fluxes in excess of 20 kW/m^2) within 20 seconds of ignition. These conditions resulted in the majority of the vinyl flooring within the enclosure becoming quickly involved, notwithstanding the material already involved due to the spill fire. Consequently, there were no visual indications as to where the initiating spill fire was located because the majority of the vinyl was burning for the same period of time and the added thermal insult from the gasoline spill fire was negligible when compared to the insult from the enclosure environment.

3.3.2.4 Test 4-2 – Unconfined Fuel Spill Fire on Carpet in an Enclosure

The enclosed the 2.0 L (0.52 gal) unconfined gasoline spill fire on carpet burned for approximately 330 seconds (5.5 minutes) before being manually extinguished. Compared to the damage from the open burning scenarios, the damage to the carpet flooring was extensive. The initiating spill fire for this test covered an area that was 0.22 m^2 (2.2 ft^2). However, as shown in Figure 55, the entire substrate again became involved as a result of the enclosure effects. It should be noted that the top of Figure 45 represents the back of the enclosure (i.e., furthest from vent) while the bottom represents the front of the enclosure (i.e., nearest the vent).

Figure 55. Condition of carpet flooring after 2.0 L (0.52 gal) gasoline spill fire in enclosure.

Damage to the carpet flooring varied depending on location within the enclosure and was preferentially more damaged toward the rear of the enclosure. At the center of the substrate, a circular section of residual carpet/pad material remained. This section of material was nominally the same area (i.e., 0.2 m^2 [2.2 ft^2]) as the initiating spill fire area. This section was surrounded by completely consumed material that had burned down to and started to degrade the plywood subfloor (i.e., doughnut pattern formation). However, moving forward (i.e., toward the slit vent) in the enclosure, this area of fully consumed material transitioned to partially degraded carpet and nominally intact foam padding. The most severe damage was observed in the rear section of the carpet flooring suggesting that the fire spread to the rear of the carpet once ignited. Fire spread to the rear of the enclosure is consistent with the airflow through the slit vent causing the fire plume to bend away from the vent toward the back wall. This plume bending resulted in additional carpet becoming involved, leading to a larger fire size, which led to more severe thermal conditions being developed within the enclosure. The end result of this iterative process was complete thermal damage of the carpet flooring within the enclosure compared to the limited damage in the open burn scenario.

3.3.2.5 Test 6-0 – Class A Ignition Scenario on Sofa

Test 6-0 was a furnished room with a Class A ignition of the sofa. The ignition source in this test was centered on the seat of the upholstered sofa at the intersection of the seat and backrest. A complete description of this ignition source is provided in the companion report [Mealy et al. 2013]. This test reached flashover conditions in approximately 5.5 minutes and sustained fully-developed burning for a period 6.1 minutes. During fully developed burning, average upper layer temperatures within the enclosure were approximately 800ºC (1472ºF). Over the course of this test, approximately 70 percent of the fuel load within the enclosure (i.e., furnishings and flooring) was consumed. A stitched photograph showing the condition of the enclosure after the fire was manually extinguished is shown in Figure 56. The image shown in Figure 56 was

compiled from three different photos to illustrate the majority of the interior surfaces of the enclosure in a single image.

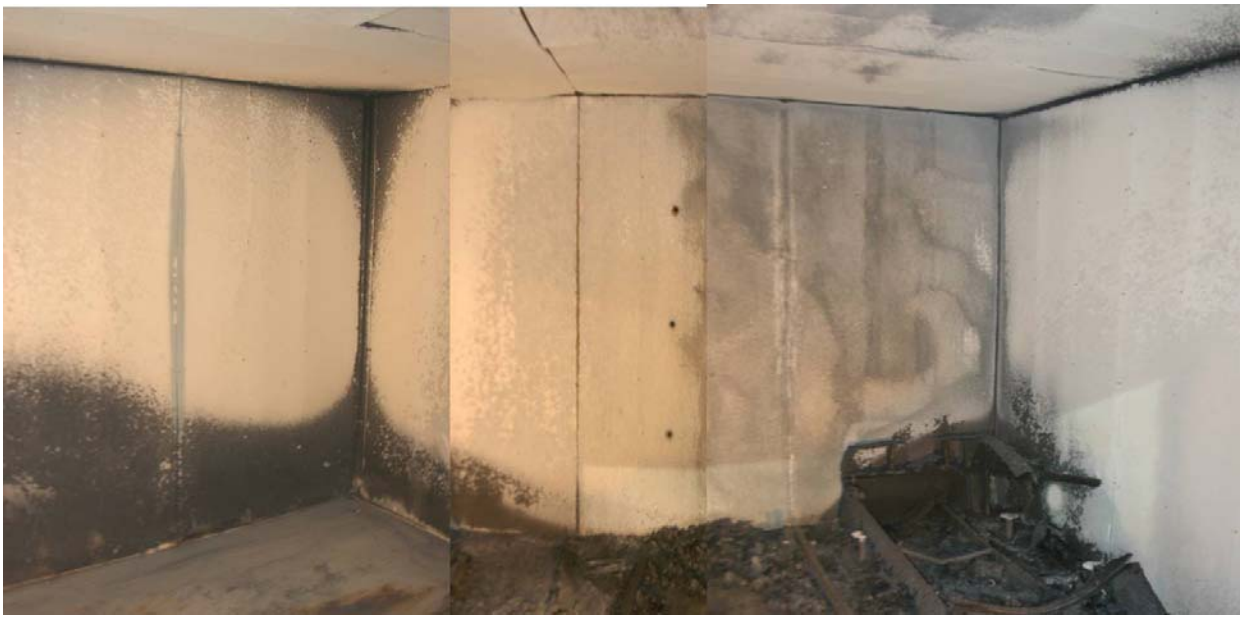

Figure 56. Composite post-test enclosure condition for Test 6-0.

Per NFPA 921 [2011], a clean burn pattern is defined as a fire pattern on surfaces where soot has been burned away [NFPA 921 2011]. For the purposes of this report, the definition of a clean burn is the relative absence of soot from a previously sooted surface due to thermal oxidation. Furthermore, since soot oxidizes over a range of temperatures (i.e., 425–1100ºC (797–2012ºF)) [Maahs 1971] the extent to which a clean burn is clean (i.e., white in color) was considered to be variable. Under this definition, the quantity of soot removed from the walls/ceiling of the enclosure and the associated qualitative color (i.e., grayscale from dark gray to white) of the surface was considered as a function of both the exposure temperature and duration.

As shown in Figure 56, three different color patterns were developed during this test: black, white, and a light green. The black areas were identified as thermally degraded gypsum wallboard paper that had been sooted during the fire. The white areas were characterized as generally having no paper present and, if present as ash, it was no longer black with soot. The green areas were characterized as having no paper with the green color originating from the calcined gypsum material. With the exception of the lower rear corners and a portion of the left wall, the majority of the interior surface area of the enclosure walls and ceiling exhibited signs of clean burn. Due to the extensive amount of clean burn created in this test, the presence of clean burns could not readily be used to identify where the most severe/prolonged burning occurred. In this test, different extents of clean burn were identified on the rear wall of the enclosure. In the left rear corner, a section of gypsum wallboard (GWB) approximately 0.6 m (2 ft) wide was white in color and originated from an elevation approximately 0.45 m (18 in.) above the floor. Moving left to right across the rear wall the next 1.2 m (4 ft) of GWB were a slightly darker shade of gray with a green tint. This section of clean burn spanned floor to ceiling and was relatively consistent in color. The last 1.8 m (6 ft) of wall was a much darker gray with a more significant green tint. The coloring in this section was not as uniform as the previously described

section with areas of dark and light coloration. In this section, a plume pattern was identified, which originated in the right rear corner of the enclosure and moved outward toward the center of the rear wall. An annotated version of Figure 56 is provided in Figure 57 to illustrate this pattern.

Figure 57. Annotated composite photograph of post-test fire condition (Test 6-0) showing location of plume pattern.

The presence of sooted areas in both rear corners was attributed to the presence of the upholstered sofa and chair in the corners of the enclosure. These objects provided both radiation and airflow obstructions, which created a means of generating both heat shadowing and smoke flow patterns.

The green tint observed in the clean burn patterns on both the rear and right hand walls of the enclosure are attributed to suppression activities that were conducted at the conclusion of this test. The suppression water used at the fire test facility is recycled and chemically treated; it is likely that the green tint to the walls is a result of the chemicals used in this treatment process. This has been noted in several previous enclosure fire test series conducted at the ATF fire test laboratory [Mealy et al. 2006, Wolfe et al. 2009].

The severity and duration of this test limited the utility of pattern analysis on both the flooring and furnishings within the enclosure. The Class A furnishings contained within the enclosure (i.e., upholstered sofa, upholstered chair, wooden table, and baby seat) were generally consumed (greater than 50 percent mass) with only charred sections of wood framing remaining. Photographs of the upholstered chair, coffee table and sofa in their post-test conditions are provided in Figure 58. It can be clearly seen, particularly with the sofa, how the furniture position against the corner resulted in the dark soot patterns in the corners.

Figure 58. Remnants of upholstered chair (left), coffee table (middle) and upholstered sofa (right) after Test 6-0.

The mass loss fraction of the upholstered sofa (0.69) was greater than that of the upholstered chair (0.54). Based on visual observations, the damage to the upholstered chair, wooden table, and baby seat was relatively uniform and appeared to have burned from the top down. A collage of close up photographs of the upholstered chair is presented in Figure 59. Debris from the coffee table and baby seat were such that only friable material remained after the test therefore further documentation was not possible.

Figure 59. Close up photographs of the topside (left) and underside (right) of the upholstered chair after Test 6-0.

This determination was made based on several different observations, including: 1) the fact that the underside of the base and legs of the upholstered chair was relatively uniformly charred. Furthermore, the main side rails of the wooden table (shown in center image of Figure 58) are in the same location as they were prior to the test, suggesting that they fell straight downward. The topside of the table and table shelf were completely consumed in this test with only small pieces of charred debris remaining between the two top rails. The uniform burn damage observed on the upholstered chair and table was not observed on the upholstered sofa. For this piece of furniture, the damage was most severe along the seat back and side of the sofa nearest the enclosure vent (as shown in Figure 60).

Figure 60. Close up photograph of upholstered sofa debris after Test 6-0.

Approximately half of the wood framing member located along the seat back of the sofa nearest the vent was completely consumed. Furthermore, the side of the sofa nearest the vent was partially collapsed after the test exposure. This was not true for the opposite side of the sofa.

For this test, the damage to the upholstered sofa was not indicative of the location of the ignition source (i.e., the damage resulting from the Class A ignition scenario did not persist through the fire). The lack of persistence is attributed to the relatively low heat release rate source used and the absence of any material that was initially involved (i.e., polyurethane foam, etc.) due to the duration of the fire. The majority of the damage to the upholstered sofa was the result of the ventilation condition present during this test. The most heavily damaged portions of the sofa in this test were those proximate to the vent with lesser damage present in more remote areas. Similar results would be expected for a Class A ignition scenario located at any location on the upholstered sofa seat, when exposed to similar enclosure fire conditions. The persistence of patterns from an initiating fire source requires that the source be sufficient to induce damage that is greater than that created by the pursuant fire scenario.

The damage to the carpet flooring was extensive with only the plywood subfloor remaining. As a result of the ventilation opening (i.e., full-open doorway), the plywood located nearest the vent was completely consumed and the extent of damage decreased moving away from the vent opening. This progression led to only the perimeter of the 3.7 m (12 ft) square subfloor remaining, as shown in Figure 61. It should be noted that the vent opening was located at the bottom of the photographs presented in Figure 61. No floor patterns were indicative of the area of origin. While the area of flooring beneath the upholstered sofa was slightly more damaged than the opposite corner of the enclosure, this difference was not significant enough to make a conclusion regarding area of origin.

3.3.2.6 Test 6-1 – Fuel Spill on Floor (Carpet) with Full Door Vent

Test 6-1 consisted of an initiating 2.0 L (0.52 gal) gasoline spill fire on carpet that was centered in front of the upholstered sofa. This test reached flashover conditions in approximately two minutes and sustained fully developed burning for a period of approximately two minutes. During fully developed burning, average upper layer temperatures within the enclosure were approximately 655ºC (1211ºF) over the duration of the post-flashover conditions. Over the course of this test, approximately 27 percent of the fuel load within the enclosure (i.e., furnishings and flooring) was consumed. Representative photographs of the condition of the enclosure after the fire was manually extinguished are shown in Figure 62.

(a)

(b)

(c)

Figure 61. Condition of flooring in Test 6-0 (a) immediately after test, (b) after removal of Class A fuels, (c) after overhaul.

Figure 62. Enclosure conditions after Test 6-1.

The most identifiable pattern observed after Test 6-1 was centered approximately 1.2 m (4 ft) from the rear right corner of the enclosure on the rear wall. This pattern was identified by the absence of soot in this area relative to neighboring walls. It extended from the floor up to a height of approximately 2.1 m (7 ft). The pattern had a width of approximately 0.3 m (1 ft) at the base and 1.1 m (3.5 ft) at the 1.8 m (6 ft) elevation. As shown in the top right and bottom left photographs in Figure 62 the lower right hand side of this pattern originated at the front face of the sofa leg rest. The pattern was also centered along the aisle that existed between the sofa and wooden table. Recall that in this test, the initiating fire was in the same aisle but was located approximately 1.1 m (3.5 ft) away from the back wall at the start of the test (see Figure 63). However, the migration of the fire to the rear of the enclosure was observed approximately 45 seconds after ignition [Mealy et al. 2013]. Based on video analysis, it was determined that the spill/carpet fire burned in this location for the duration of the test.

Figure 63. Initiating fire used in Test 6-1.

While the migration of flame toward the rear wall would support that this pattern was most likely a clean burn, a closer inspection of the pattern does show evidence of green tinting at the base of the pattern (see Figure 64). In addition, the speckled pattern around the periphery and the water drip marks through the center of the pattern are indicative of water spray. As discussed below, this pattern is also in line with the initial hose stream attack. The white area within this pattern did not have any paper ash present; however, this does not provide definitive support for either formation mechanism because both have been shown to remove the paper ash (see Test 6-0). Whether there was an initial clean burn in this area is difficult to conclude, but the evidence supports a visually similar pattern being formed/affected by water suppression activities.

Figure 64. Close up photograph of wall pattern identified in Test 6-1.

A second pattern clearly visible was on the ceiling of the enclosure. The pattern was identified because of the absence of soot in this area. However for this pattern, the area was much smaller and less uniform. A photograph showing the location of this pattern relative to the white pattern on the rear wall of the enclosure is provided in Figure 65. The center of the pattern was offset from the right wall approximately 1.2 m (4 ft) and from the rear wall approximately 1.2 m (4 ft). It was approximately 0.9 m (3 ft) in diameter.

Figure 65. Pattern on ceiling of enclosure after Test 6-1.

Despite the fact that this white pattern was above the general area where the initiating fire was located, it was determined to be unlikely that the pattern occurred as a result of the initiating fire or any other fire behavior in this test. This conclusion was based on two different evaluations: 1) an estimate of the localized heating in this area due to the initiating fire source and 2) a visual analysis of the characteristics of the pattern.

In order for this pattern to be classified as a clean burn, the absence of soot had to have been a result of thermal oxidation. Since the initiating fire did not have flame heights sufficient to impinge on the ceiling and the plume temperature associated with a fire of this size at the ceiling elevation would not be sufficient to induce thermal oxidation, it was determined to be unlikely that this fire created the pattern. Using plume centerline temperature correlations and assuming the initiating fire size was 329 kW [Mealy et al. 2013], a maximum plume temperature of 300ºC (570ºF) can be expected. Temperatures in this range are below the range of soot oxidation temperatures identified earlier in this report. The second evaluation of this pattern was a visual analysis. A close up photograph of the pattern is provided in Figure 66.

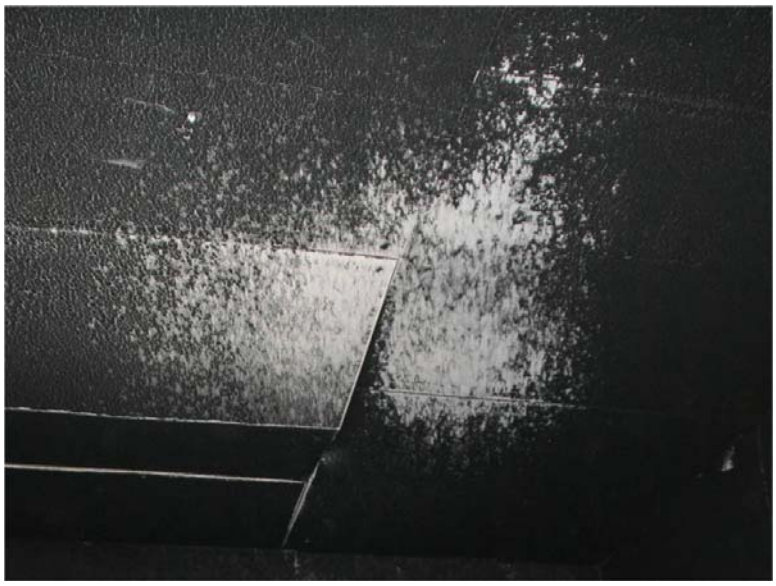

Figure 66. Close-up of ceiling pattern observed after Test 6-1.

After inspection, several aspects of the pattern were called into question regarding whether or not the pattern was the result of a thermal insult from a spill fire below. The pattern has a non-uniform speckled appearance compared to the uniform outward spreading nature of a plume. Furthermore, the presence a narrow area of soot extending into the center of the pattern is not consistent with a ceiling plume pattern. Lastly, while the pattern did not show signs of the green tinting typically associated with suppression water from the test lab, the soot that remained within the pattern appeared to be smeared or washed off as opposed to thermally degraded. This assessment was made based on comparison to patterns known to have been created by thermal oxidation (see Figure 67).

Figure 67. Examples of clean burn patterns during early stages of formation (left – Test 6-3) and after significant heating (right – Test 6-8).

After these visual evaluations, as well as reviewing test video of suppression activities, it was determined that the white ceiling pattern was most likely an artifact of suppression activities. Test video shows that during the initial attack, the hose stream was oriented upward (i.e., toward the ceiling of the enclosure). This hose stream most likely impacted the ceiling of the enclosure and removed the soot from this area. A still image showing the fire suppression attack angle is provided in Figure 68. This rationale would also support the preferential removal of soot towards the vent of the enclosure (shown in Figure 66) because the water spray would have impacted the ceiling first closer toward the vent.

Figure 68. Initial hose stream angle used to suppress the fire in Test 6-1.

In addition to the patterns described above, several other smaller patterns were characterized. A small circular pattern of less soot deposition was noted at the base of the rear wall approximately 2.1 to 2.4 m (7 to 8 ft) from the rear right corner (Figure 62). The pattern was generally in line with the left side of the coffee table, which was 0.45 m (18 in.) from the back wall. There were no other fuel packages in this area. The formation of this pattern is not associated with the burning of an object directly adjacent to the wall, as there was none there. However, it is in the close vicinity of the chair and table and may have been a result of the airflow pattern.

Above and behind the baby seat there was a heavy deposition of soot on the left sidewall. Conversely, there was no clear pattern (white or heavy soot) on the wall associated with the chair or the sofa. The wall surfaces behind the upholstered pieces of furniture were uniformly covered with heavy soot.

The front wall of the enclosure (i.e., vent wall) did not have any patterns but was also uniformly soot covered. The soot covering the walls after Test 6-1 can be described as being baked onto the walls (i.e., not friable when brushed). After this test, the majority of the interior surface area of the enclosure was soot covered (i.e., black); however, thermally discolored

gypsum wallboard (brown in color) was noted at low levels around the perimeter of the enclosure. This was primarily observed around the bases of the Class A fuels and in the corners of the enclosure and most attributed to flow conditions and shadowing preventing increased temperatures from being achieved in these areas.

Despite the severity of this fire (i.e., flashover conditions), the limited duration of the fire (4.3 minutes) resulted in relatively limited mass loss of combustibles within the enclosure. Photographs of the furnishings in their post-test conditions are provided in Figure 69.

(a) Mass Loss Fraction = 0.27

(b) Mass Loss Fraction = 0.42

(c) Mass Loss Fraction = 0.18

(d) Mass Loss Fraction = 0.28

Figure 69. Remnants of (a) upholstered chair, (b) coffee table, (c) baby seat and (d) upholstered sofa (right) after Test 6-1.

In this test, the mass loss fractions for both the upholstered sofa (0.28) and chair (0.27) were very similar. The damage to the sofa was consistent over the entire piece of furniture consisting of the complete consumption of the polyurethane foam/fabric ticking and the charring of the wood frame. No difference in thermal damage was observed in the area where the initiating fire was located (gasoline on the floor, centered in front of the sofa). With the exception of some residual foam material being present, similar damage was noted for the upholstered chair. Damage to the top of the wooden table was uniform over the entire surface. No preferential thermal decay in the area where the initiating fire was located was observed. However, the shifted location of the tabletop relative to the table shelf during post-test inspection was noted. Based on this relative position, one hypothesis was that the table fell towards the sofa at some point during the test due to the failure of the legs closest to the sofa (see Figure 70). While not necessarily indicative of the area of origin, this failure mechanism is consistent with the fire having grown larger in the area of the sofa prior to growing in the area of the chair.

The carpet flooring in this test was fully consumed in some areas of the enclosure and only thermally degraded in others. Photographs of the conditions of the floor after Test 6-1 are provided in Figure 71.

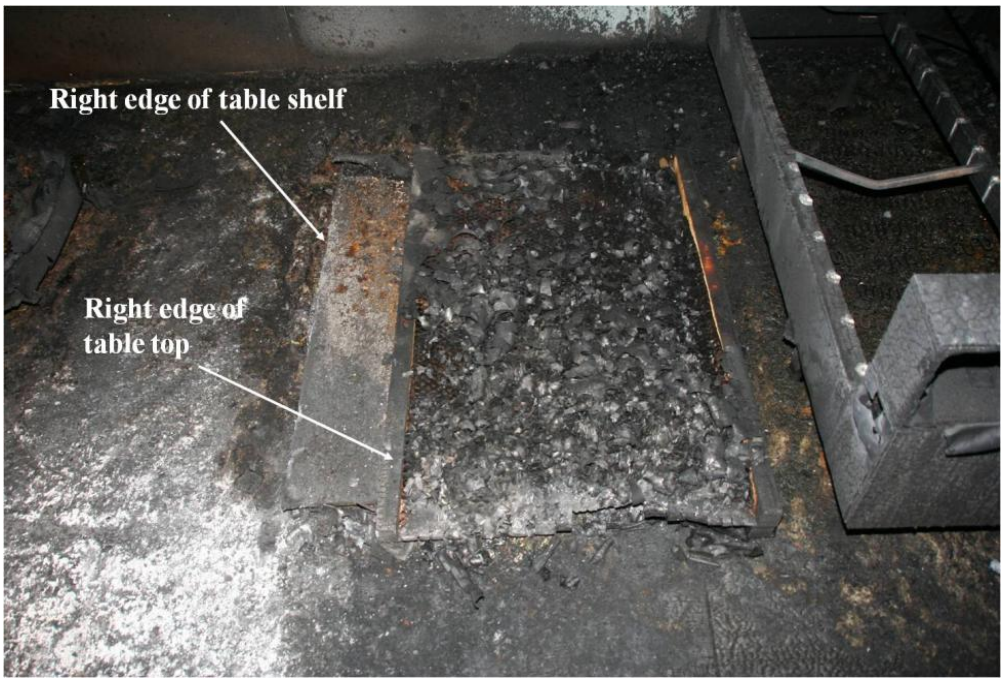

Figure 70. Location of tabletop relative to table shelf after Test 6-1.

(a) Left half of flooring (b) Right half of flooring

Figure 71. Condition of carpet flooring material after furniture debris cleared from the room in Test 6-1.

As shown in Figure 71, the areas of the most severe thermal damage to the flooring originated at the vent opening and extended into the enclosure. Two primary areas of damage were identified. The first area extended approximately 2.7 m (9 ft) into the enclosure reaching the foot of the upholstered chair. The second area extended approximately 1.5 m (5 ft) into the enclosure towards the upholstered sofa and stopped approximately 0.6 m (2 ft) from the side of the sofa nearest the vent. The geometry of these patterns was not consistent with any of the fuel loading on the floor and was therefore attributed to airflow patterns. The carpet and padding in

these areas were completely consumed and the plywood subfloor showed signs of charring. Transitions to areas in which carpet remains were present (around sofa and baby seat) included carpeting that was heavily thermally degraded but not consumed. An example of this transition is provided in Figure 72.

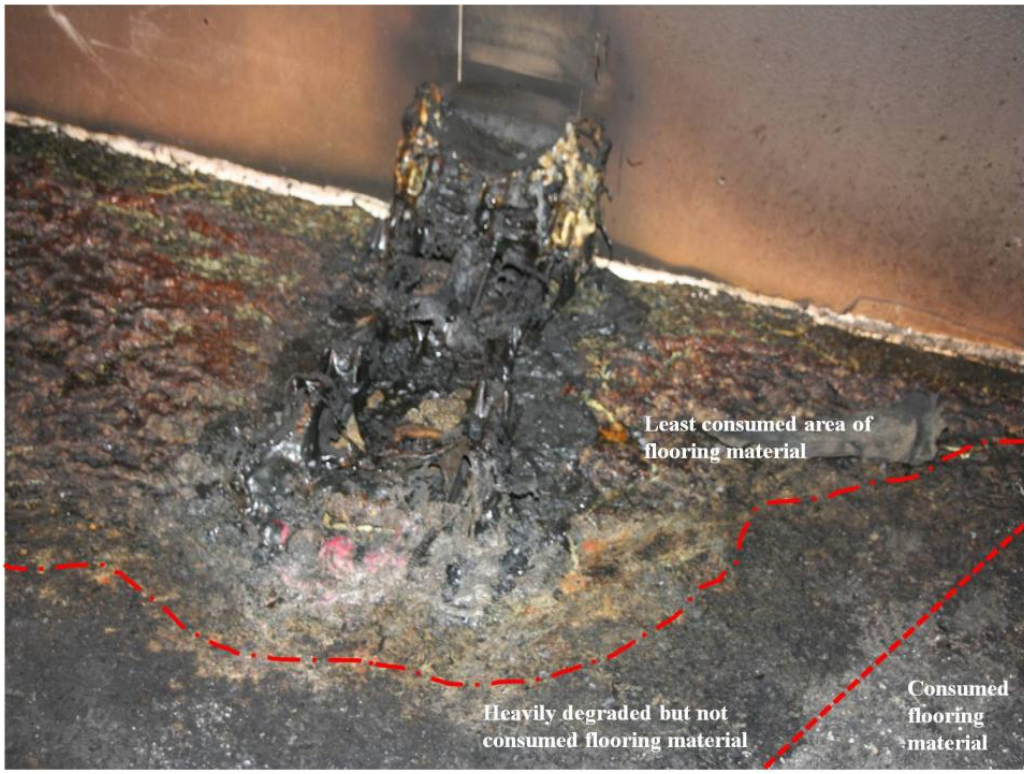

Figure 72. Annotated photograph showing various degrees of thermal degradation noted on flooring material after Test 6-1.

After overhaul (i.e., removal of all Class A fuel from the enclosure), two protection patterns were identified (see Figure 73). Both patterns were located in the vicinity of the collapsed table and were therefore identified as protection patterns. The larger protection pattern was located directly beneath the original location of the table. The pattern shown is undamaged carpet. The smaller, circular protection pattern was located in the aisle between the upholstered sofa and coffee table. The area shown in Figure 73 is undamaged plywood, the subfloor below the carpet and pad. This pattern was in the exact location where the initiating gasoline spill fire was poured. The circular pattern in the area where the initiating fire was located was a result of the evaporative cooling phenomena described in Section 3.3.2.1 coupled with the radiation block provided when the table collapsed onto this area. The section of flooring material from this location was removed with the coffee table during overhaul. The carpet and pad material was relatively undamaged and an odor of gas was apparent once removed from the underside of the table shelf.

Figure 73. Condition of flooring material after furniture debris cleared from the room in Test 6-1.

3.3.2.7 Test 6-2 – Fuel Spill on Floor (Carpet) with Slit Vent

Test 6-2 used a 2.0 L (0.52 gal) gasoline spill centered in front of the upholstered sofa as the initiating fire. This test differed from Test 6-1 in that the ventilation in this scenario was a slit vent (i.e., reduced ventilation condition). This test did not reach flashover conditions but instead burned at a relatively steady-state for approximately six minutes before being manually extinguished. During steady-state burning, a fire size of approximately 761 kW was maintained with upper layer temperatures of 415ºC (779ºF). Over the course of this test, approximately 16 percent of the fuel load within the enclosure (i.e., furnishings and flooring) was consumed. Representative photographs of the condition of the enclosure after the fire was manually extinguished are shown in Figure 74.

A range of damage to both enclosure surfaces and combustible materials within the enclosure was observed during post-test inspection. The walls of the enclosure varied in condition from thermally discolored gypsum wallboard paper (brownish coloring), located low in the space, to soot-laden and/or charred gypsum wallboard paper, located high in the space. This progression was interrupted by areas in which the soot and gypsum wallboard paper had been completely removed. The patterns on the walls after this test were different than noted in the previous two tests because they showed signs of localized combustion (i.e., enhanced damage to the gypsum wallboard and wallboard paper) at each of the vertical seams in the walls (see patterns identified in blue and red in Figure 74). With the exception of the pattern located near the far, front edge of the upholstered sofa (shown in RED ink Figure 74), the majority of these patterns originated 0.3–0.6m (1–2 ft) above the floor and ran vertically up the entire seam to the ceiling of the enclosure. The GYB seams occur at the locations of the 2 x 4 studs, which serve as a greater heat sink than the GWB by itself. As noted in fire scene investigations by the authors and in other fire

test programs, there can be greater deposition of soot on GWB along the positions backed by a stud. This may explain why there is black, charred paper along the seams. However, the repetitive clean burns around each seam is not fully understood. A close-up photograph of the damage to the wall in the vicinity of the seams in this test is provided in Figure 75. In all cases the seam was filled with fire caulk at least 24 hours prior to testing. A bead of caulk was applied to the seam between adjacent pieces of GWB and smoothed to provide a layer of caulk along the length of each seam that was approximately 6.35 mm (0.25 in.) wide.

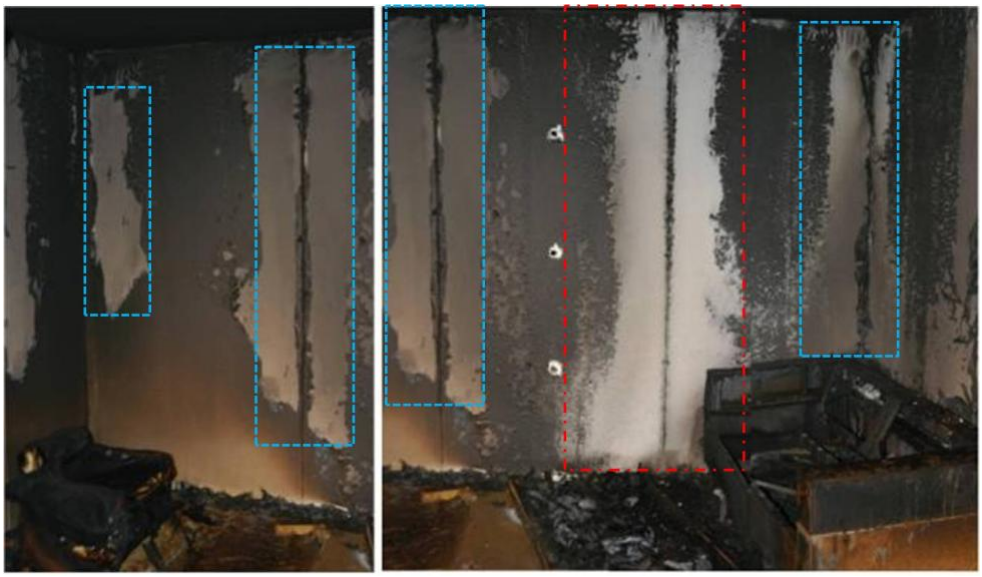

(a) (b)

(c) (d)

Figure 74. Photographs of (a) left side of rear wall, (b) right side of rear wall, (c) left wall, and (d) right wall of the enclosure after Test 6-2.

Figure 75. Close-up of seam patterns formed on rear wall of enclosure during Test 6-2.

The only wall pattern that extended to the floor of the enclosure was located approximately 1.2 m (4 ft) from the rear right corner of the enclosure on the rear wall. The pattern was widest at the base (approximately 0.6–0.75 m [2–2.5 ft]) and narrowed as it moved vertically up the seam of the GWB. This pattern was also visually more distinguishable (i.e., white in color) than the other patterns (i.e., brown/gray in color). The location of this pattern was aligned with the initiating spill fire, which was between the table and sofa. Video shows that the hose spray was minimal in this test with the stream directed downward. Therefore, this pattern was not by suppression activities.

In this test, the damage to the sofa was substantially worse than that of the upholstered chair. The mass loss fraction of the upholstered sofa (0.30) was twice that of the upholstered chair (0.15) and the majority of the other combustibles within the enclosure. The condition of these furnishings after this test is presented in Figure 76.

Figure 76. Composite photo illustrating condition of Class A furnishings after Test 6-2.

Similar to that observed in Test 6-1, the wooden table collapsed toward the upholstered sofa. In this test, the upholstered sofa had varying degrees of thermal degradation (shown in Figure 77). The location of the initiating fuel spill fire on the carpet relative to the upholstered sofa is shown

in Figure 77(a). Along the seat back of the sofa, the thermal damage decreased from the rear of the enclosure toward the vent (i.e., left to right in Figure 77(b)). This was also observed on the lower portions of the sofa. It should be noted that the localized area where a section of the upholstered sofa frame is missing is not due to low-level, localized burning, but instead is due to damage associated with the load cell support frame used to support the sofa during testing. As shown in Figure 77(b), this portion of the frame was intact immediately after testing and was apparently damaged during overhaul of the enclosure. The analysis of photographs taken before and immediately after this test enabled this damage to be justified and prevented the conclusion that the damage was attributed to a low-level fire.

(a) Spill location on carpet centered between load cell supports below sofa

(b) Sofa after removal from enclosure

(c) Area of load cell support highlighted with sofa in enclosure

Figure 77. Condition of the upholstered sofa after Test 6-2.

As shown in Figure 76, the carpet flooring was thermally degraded throughout (i.e., softening of polyolefin fibers and thermal discoloration of the material) with a localized area of complete consumption in the vicinity of the upholstered sofa. There were also several areas of protection patterns (shown in Figure 78(a)). The protection patterns were found beneath the upholstered chair, the collapsed wooden table, and the melted baby seat. The furnishings in these areas were only partially burned and consequently the carpet flooring beneath them was only thermally degraded and not consumed. The largest area of fire damage was in the rear right corner of the enclosure (i.e., the flooring material directly beneath the upholstered sofa). This carpet and pad became involved as the upholstered sofa began to burn and polyurethane foam within the sofa melted and burned beneath the sofa as a liquid fire. The duration of this test resulted in the complete consumption of the carpet and padding material to the point where the area in which the initiating fire was spilled could not be identified (shown in Figure 78(b)).

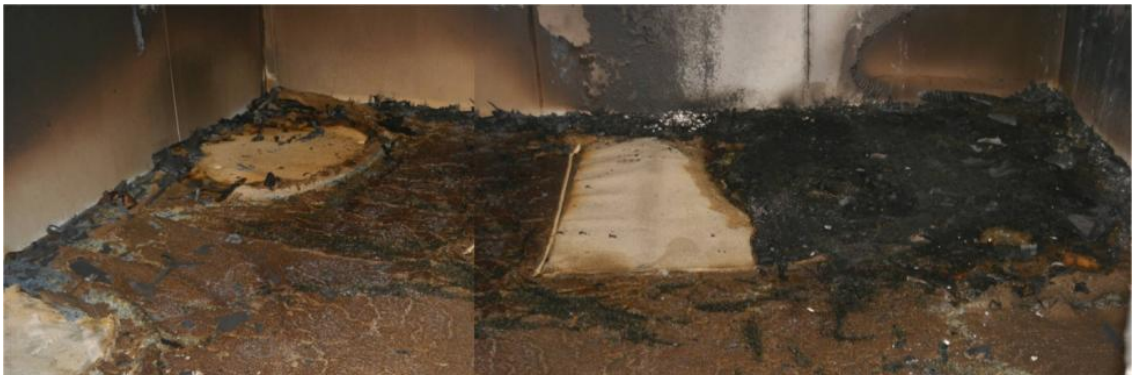

(a) View from door with protected carpet areas under chair (back left), table (center) and baby seat (bottom left corner)

(b) Floor area of initiating spill fire between table and sofa

Figure 78. Condition of the carpet flooring after Test 6-2.

3.3.2.8 Test 6-3 – Fuel Spill on Upholstered Chair (Carpet) with Full Door Vent

Test 6-3 used a 1.5 L (0.40 gal) gasoline spill on the upholstered chair and a 0.5 L (0.13 gal) trailer poured onto the carpet as the initiating fire. The gasoline trailer was poured from the base of the upholstered chair toward the door. All aspects of this test were identical to that of Test 6-1 with the exception of the ignition scenario. In this test, the first Class A fuel ignited was the upholstered chair as opposed to the upholstered sofa. This test reached flashover conditions 107 seconds (1 minute 47 seconds) after ignition and continued burning under fully developed conditions for an additional 157 seconds (2 minutes 37 seconds). During this time, average upper layer temperatures of 715ºC (1319ºF) were measured over a period of approximately 180 seconds. Over the course of this test, approximately 32 percent of the fuel load within the enclosure (i.e., furnishings and flooring) was consumed. Representative photographs of the condition of the enclosure after the fire was manually extinguished are shown in Figure 79.

Figure 79. Composite photograph of enclosure conditions after Test 6-3.

After suppression, three different areas that were absent of soot relative to neighboring wall sections were identified. Two of these patterns were along vertical GWB seams of the enclosure, one on the rear wall aligned with the space between the table and the sofa and the other on the wall directly behind the sofa. The development of these patterns proximate to the seams was similar to those in Test 6-2, but not as wide. The third white pattern was located on the left wall above the upholstered chair. The center of the pattern was approximately 1.1 m (3.5 ft) above the floor of the enclosure, which was the approximate height of the upholstered chair. The pattern was approximately 0.6 m (2 ft) wide and 0.9 m (3 ft) tall. The pattern consisted of the relative absence of soot compared to the surrounding wall with less soot present at the center of the pattern. A close up photograph of this pattern is provided in Figure 80. As can be seen in the photo, the ash from the burnt paper progresses from being dark soot coated to gray to white to absent in the middle of the pattern.

Figure 80. Close up photograph of wall pattern identified behind the upholstered chair in Test 6-3.

A pattern similar to this was identified on the ceiling of the enclosure (see Figure 81). However, it should be noted that several sections of the ceiling in this test collapsed during the fire so the full pattern could not be characterized. The pattern was generally centered in the space with the least sooted areas located in the center of the pattern gradually transitioning from white to gray to black moving from the center outward.

Figure 81. Condition of ceiling after Test 6-3.

In this test, the damage to the upholstered chair was substantially worse than that of the upholstered sofa. The mass loss fraction of the upholstered chair (0.41) was twice that of the upholstered sofa (0.23) and greater than the majority of the other combustibles within the enclosure. The damage to the sofa was most severe on the front right corner of the sofa with heavy charring of the wood frame (see Figure 82). Sections of the frame located further to the rear of the enclosure were less damaged with only surface blackening and no 'alligatoring' of the wood frame as was seen on the front corner. This preferential damage to the front right corner was attributed to the proximity of the corner to the vent and observations that this area of the sofa was the first area ignited during the test.

Figure 82. Damage to front right corner of upholstered sofa after Test 6-3.

Unlike the previous two tests (Test 6-1 and 6-2), the wooden table in this test did not fall toward either the sofa or the upholstered chair but instead, essentially remained in place during collapse. A comparison of the location of the table debris after (a) Test 6-1 and (b) this test is provided in Figure 83. This difference (i.e., not preferentially falling towards the first item ignited) was attributed to the upholstered chair being a smaller, burning fuel package than the upholstered sofa. Consequently, rather than the heat from the chair, the thermal exposure from the upper layer was the driving factor behind the thermal decay of the table, which resulted in the table being consumed from the top down.

(a) Coffee table location relative to sofa after Test 6-1.

(b) Coffee table location relative to sofa after Test 6-3.

Figure 83. Locations of coffee tables after Tests 6-1 and 6-3.

The carpet flooring was completely involved (i.e., flaming combustion) as a result of the flashover conditions that were achieved. As a result, the majority of the carpet was completely consumed with exposed subfloor material. Residual carpet material, although heavily degraded, remained in areas beneath the upholstered sofa and upholstered chair. A photograph of the condition of the floor after Test 6-3 is provided in Figure 84 and a photograph of the carpet flooring material that remained beneath the Class A furniture is provided in Figure 85.

Figure 84. Condition of carpet flooring after Test 6-3.

(a)

(b)

Figure 85. Condition of carpet flooring beneath the (a) upholstered chair and (b) upholstered sofa after Test 6-3.

Immediately after testing, with all furnishings present, no visually identifiable patterns were observed on the floor. Remaining carpet and pad and exposed plywood subfloor appeared uniformly degraded and blackened. Upon removal of all furnishings and the sweeping of the floor to remove fire debris (i.e., ash and loose charred material), the floor was again surveyed to determine if identifiable patterns were present (see Figure 86). It should be noted that the majority of the flooring material in this test was completely consumed; only remaining in ash form. Consequently, when the enclosure was swept out, a large portion of this material was removed. However, the only distinguishable floor patterns identified were protection patterns from both the wooden table and baby seat. No damage patterns associated with the gasoline spill on either the upholstered chair and/or trailer from the chair to the vent were identified. The damage sustained by the carpet material during the prolonged exposure was such that the trailer pattern did not persist. The absence of damage patterns from the gasoline spill fires on the carpet flooring was attributed to the absorptivity of the carpet and foam pad, which kept the fuel burning primarily within the flooring material, and the severity of the enclosure fire environment, which led to the eventual consumption of both the gasoline and the carpet and pad.

Figure 86. Composite photo of flooring after removal of fire debris from Test 6-3.

3.3.2.9 Test 6-4 – Fuel Spill on Upholstered Chair (Carpet) with Slit Vent

Test 6-4 used a 1.5 L (0.40 gal) gasoline spill on the upholstered chair and a 0.5 L (0.13 gal) trailer poured onto the carpet as the initiating fire. This fire scenario was the same as Test 6-3 except for the ventilation was reduced from the full door to the slit vent. Compared to Test 6-2, the test setup was the same except the gasoline fire was started at the chair instead of on the floor in front of the sofa as in 6-2. The test duration was longer than that used in Test 6-2 because conditions took longer to reach a quasi- steady-state in this test, than in Test 6-2. After an initial period of growth, this enclosure fire burned at a nominal steady-state for a period of 660 seconds (11 minutes) with an average fire size of approximately 839 kW and average upper layer temperature of 500ºC (932ºF). Over the course of this test, approximately 33 percent of the fuel load within the enclosure (i.e., furnishings and flooring) was consumed. Representative photographs of the condition of the enclosure after the fire was manually extinguished are shown in Figure 87.

Figure 87. Composite photo of the enclosure after Test 6-4.

In this test, the soot deposited on the walls during the initial portions of the test was removed from the majority of the interior surfaces of the enclosure. Initially, the 'cold' walls of the enclosure would become soot laden as a result of thermophoresis, a process by which the 'hot' soot particles within the upper layer preferentially migrate towards the 'cold' walls and become attached. Later in the fire, as enclosure temperatures reach and exceed the oxidation temperatures of soot, these deposited particles are removed. Although large areas of soot were removed during this test, several different areas where soot had been removed could be correlated to the locations of the Class A fuel packages present within the enclosure. These areas are identified in Figure 88.

Figure 88. Annotated composite photo from Test 6-4 showing location of patterns identified in sidewalls of the enclosure.

Each of the areas identified in Figure 88 show a relative absence of soot in a location where a known Class A fuel would have been burning. The absence of soot on the majority of the rear wall cannot be explained by directly adjacent burning Class A materials, but burning in the rear of the enclosure was noted in the previous tests with the slit ventilation condition. The front wall was uniformly sooted.

White patterns (absence of soot) on the ceiling were spread across the ceiling at multiple locations. However, as shown in Figure 89 the largest area absent of soot on the ceiling originated on the left hand side of the enclosure and extended to the right. Given the presence of the largest fuel item on the right hand side of the enclosure (the sofa), the prevalence of this pattern on the left is consistent with the area of origin around the chair. As shown in Figure 89, the calcination depth survey is also consistent with this point. Evidence of pattern formation as a result of fire suppression activities was not found on the enclosure surfaces after this test. This is supported by the fact that suppression activities at the end of this test were generally confined to floor level water application (i.e., directly onto burning debris).

Figure 89. Ceiling of enclosure after Test 6-4.

The damage to both the furniture and the flooring in this test was comparable to that described in Test 6-3 with respect to both damage location and severity. The upholstered chair was more severely damaged (44 percent mass loss) than the upholstered sofa (29 percent mass loss). Damage patterns on the upholstered sofa and chair were relatively uniform over the entire pieces of furniture. A photograph of the condition of the upholstered sofa after this test is provided in Figure 90.

Figure 90. Condition of upholstered sofa after Test 6-4.

The collapse of the wooden table was generally downward and not biased toward either the sofa or chair as observed in Tests 6-1 and 6-2 (see Figure 91).

Figure 91. Location of coffee table after Test 6-4 showing downward collapse, not preferential collapse towards sofa as seen in Tests 6-1 and 6-2.

Just as in Test 6-3, the carpet flooring in this test was completely involved and primarily consumed during the fire. Photographs of the condition of the floor immediately after Test 6-4 and after the enclosure was overhauled are provided in Figure 92. Compared to Test 6-3, the flooring after this test was more consumed. This was attributed to the prolonged burning duration, which permitted flooring material, even in protected areas, to become involved. As shown in Figure 92, even the area beneath the coffee table in this test was mostly consumed, whereas in previous tests, this area was relatively unburned.

(a)

(b)

Figure 92. Condition of carpet flooring (a) immediately after and (b) after overhaul (looking to the rear) of the enclosure used in Test 6.4.

The furniture was removed and the room was swept to determine if additional patterns could be identified. However, no damage patterns associated with the gasoline spill on either the upholstered chair and/or trailer from the chair to the vent were identified.

3.3.2.10 Test 6-5 – Fuel Spill on Floor (Vinyl) with Full Door Vent

Test 6-5 consisted of a 2.0 L (0.52 gal) gasoline spill fire on a vinyl floor centered in the enclosure (i.e., pour area just in front of the wooden table). A pour area in front of the sofa (as used in the carpet flooring Test 6-1) was not used due to concerns of gasoline leakage below the enclosure due to instrumentation holes in the floor for the sofa load cell supports. This test reached flashover conditions in approximately 35 seconds and sustained fully developed burning for a period of 150 seconds (2 minutes 30 seconds). During fully developed burning, average upper layer temperatures within the enclosure were approximately 755ºC (1391ºF). Over the course of this test, approximately 33 percent of the fuel load within the enclosure (i.e., furnishings and flooring) was consumed. Representative photographs of the condition of the enclosure after the fire was manually extinguished are shown in Figure 93.

Figure 93. Composite photograph of enclosure conditions after Test 6-5.

After suppression, several different wall and ceiling patterns were identified. The two most distinct patterns were located on the vent side of the sofa on the right wall of the enclosure and along the rear wall of the enclosure. These white patterns were identified due to their dramatic absence of soot relative to neighboring wall surfaces. The pattern on the sidewall of the enclosure covered the bottom half of a full sheet of GWB, 0.6 m (2 ft) of which was located behind the upholstered sofa. The rear wall pattern looked similar to that of the sidewall but was larger in area. This pattern was approximately 3.0 m (10 ft) wide and 1.8 m (6 ft) tall and was generally centered on the rear wall of the enclosure (i.e., opposite the vent). However, after review of test video and the characteristics of the patterns, the likelihood that either of these patterns were formed as a result of a thermal exposure was determined to be low. A review of test video supports that both of these patterns are most likely suppression patterns because during firefighting activity the hose stream was directed toward both of these locations. Test video also shows that the quantity of water delivered to the right wall was less than that used when directed

at the rear wall, which is consistent with the varying size of the patterns. Further support for the fact that these patterns are most likely suppression patterns is the green tint along the perimeter of these patterns (see Figure 94). As described in Section 3.3.2.5, the green tint on GWB was associated with the chemical treatment of the suppression water used at the laboratory. In addition, the perimeter of each pattern is marked by a splatter pattern consistent with the spray hose stream.

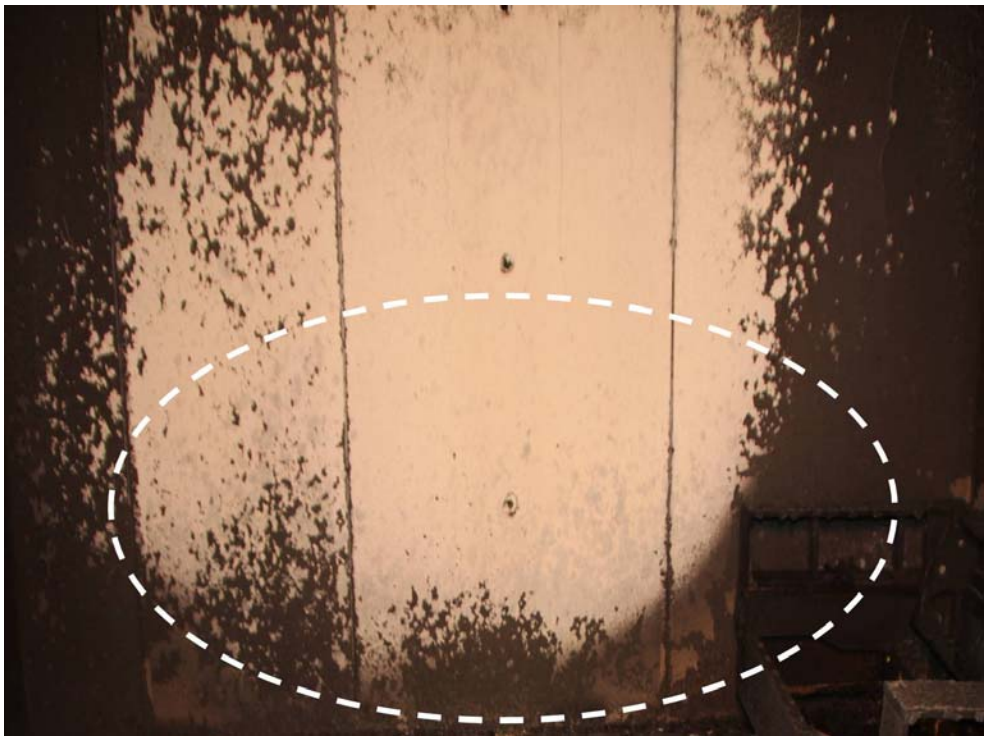

Figure 94. Photograph of pattern on rear wall with green tinting highlighted.

Additional patterns identified on the walls of the enclosure included areas above both the upholstered chair and baby seat (see Figure 95). These patterns were identified due to the decreased quantity of soot on the walls in these locations relative to neighboring areas (see Figure 95). In these locations, the soot was only partially removed from the walls of the enclosure leaving a finely speckled pattern of black and white areas. The pattern behind the baby seat originated at floor level. As shown by the baby seat debris, this fuel melted and pooled during the fire, which supports the low level exposure needed to form the left pattern shown in Figure 95. The originating height of the right pattern is consistent with the height of the upholstered chair as it decreased during the fire.

As shown in Figure 95, an additional concentrated area where soot is less prevalent (speckled) immediately to the right of the pattern attributed to the burning of the baby seat (i.e., left oval in Figure 95). This pattern was attributed to the burning of the baby seat and the associated fire plume potentially bending toward the rear of the enclosure due to ventilation or to the increasing spill fire area associated with the melting baby seat, as evidenced by the low clean burn across the base of the wall below the plume pattern.

Figure 95. Whitish patterns of relatively reduced soot that were located on the walls above the upholstered chair and baby seat after Test 6-5.

A pattern was identified on the ceiling of the enclosure located slightly left of center (see Figure 96). This pattern had a depth of approximately 1.5 m (5 ft) and a width of approximately 1.2 m (4 ft). The center of this pattern was more pronounced (i.e., more soot removed) than the pattern identified on the wall surface behind the upholstered chair and baby seat but less so than the pattern on the rear wall. The fine speckled appearance of along the perimeter of the pattern is consistent with the patterns on the left wall of the enclosure. However, the center has a splattered appearance of white spots that are similar to the patterns on the rear and right walls. The similarities between the ceiling pattern and the different patterns on both the left and rear/right walls indicate that the ceiling pattern was formed by two different mechanisms. The similarity between the perimeter of the ceiling pattern and the patterns identified behind the upholstered chair and baby seat (i.e., speckling of black/white) indicate that the initiating spill fire and the subsequent chair and table fire produced sufficient heat to oxidize soot from this section of the ceiling. However, the wide area of larger white splatter spots indicate that suppression activities altered the initial clean burn pattern.

Figure 96. Pattern identified on the ceiling of the enclosure after Test 6-5.

The condition of each of the Class A fuels present during this test is documented in Figure 97. Note that for both the upholstered sofa and coffee table presented in Figure 97, the side nearest the vent is presented on the right in the photographs. The wood frames of both the upholstered sofa and chair were uniformly charred in this test. The foam and fabric ticking for both objects was completely consumed. The top of the coffee table was fully consumed. However, the bottom shelf of the coffee table remained and showed preferential damage on the side of the shelf nearest the vent. It should be noted that this area was also intimate with the location of the initiating fire in this test. As shown in Figure 93, the coffee table collapsed onto itself in this test (i.e., not towards either the sofa of chair as was reported in other tests). This type of collapse is consistent with the table being uniformly exposed by the relatively large initiating fire. The uniformity of the damage to the upholstered furniture within the space was attributed to the location and size of the initiating fire, which resulted in the rapid involvement of the entire fuel item once ignited.

(a)

(b)

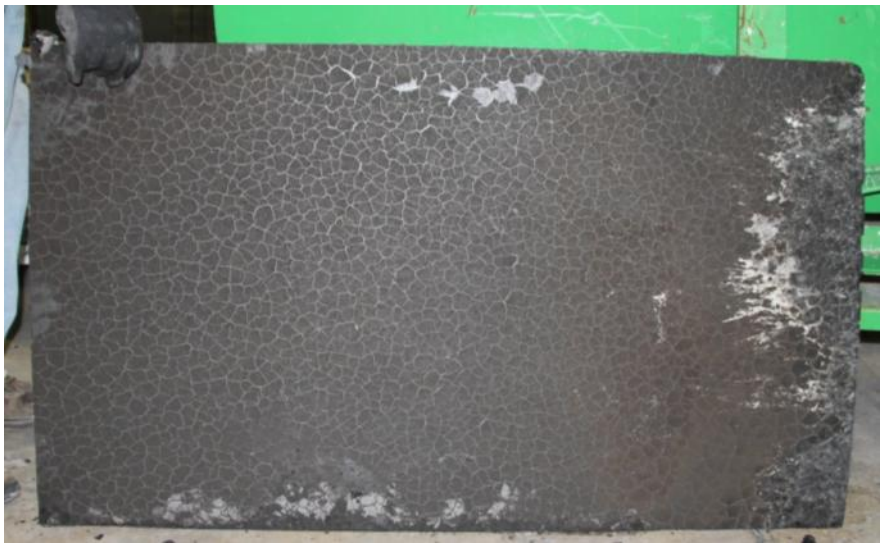

(c)

Figure 97. Post-test condition of (a) upholstered sofa, (b) upholstered chair, and (c) coffee table shelf after Test 6-5.

A photograph of the enclosure after the removal of Class A materials is provided in Figure 98. The vinyl flooring in this test was completely involved (i.e., flaming combustion). Consequently, the majority of the material was completely consumed, leaving only charred remains and ash on top of the plywood subfloor in some areas and no material in others. An annotated photograph of the condition of the floor is provided in Figure 99. Note the areas of complete consumption of vinyl flooring with only charred plywood remaining are outlined with dashed lines. Areas that are white in color at the lower edge of the photograph shown in Figures 98 and 99 represent fully consumed vinyl flooring where only soot-free ash remained. Damage to other areas of the floor ranged in severity from thermally discolored to primarily consumed.

Figure 98. Condition of vinyl flooring after Test 6-5.

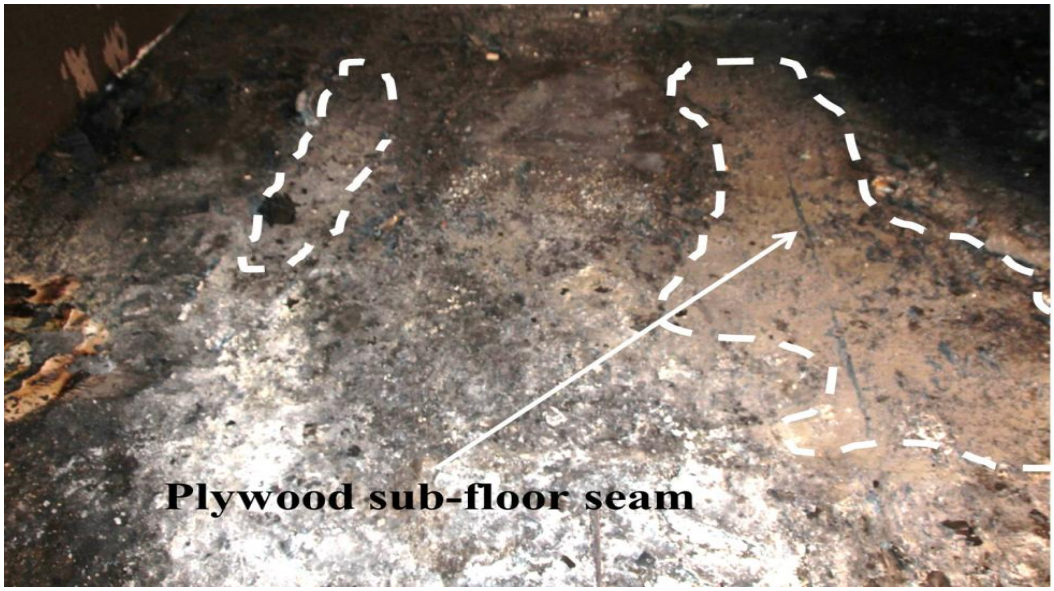

Figure 99. Annotated photograph describing condition of vinyl flooring after Class A materials were removed from Test 6-5.

As shown in Figure 98 and 99, the most severe damage to the vinyl flooring was on the right side of the enclosure. This area was generally around the perimeter of the upholstered sofa, and was characterized by the complete absence of vinyl remains and exposed plywood subfloor, indicated by the seam running down the center of the pattern. A small area of significant, but not as severe damage (i.e., some exposed plywood subfloor), was observed in front of the upholstered chair. The remainder of the flooring had charred vinyl that still remained on top of the plywood subfloor (shown in Figure 98 in a grayish, white color). The initiating fire in this scenario was a

gasoline spill that was centered in the enclosure and generally spread uniformly in all directions. The preferential degradation of the flooring material proximate to the upholstered sofa and chair was attributed to the added heat flux to the flooring material from these burning objects. Two small areas of thermally degraded, but not consumed, vinyl flooring were identified beneath the coffee table and baby seat after this test. No other protection patterns were found once the Class A fuels were removed.

No distinct patterns were identified on the front wall of the enclosure containing the vent. A conclusive pattern that occurred as a result of the initiating gasoline spill fire was not identified during post-test inspection. Any patterns formed by the initiating gasoline spill fire did not persist through the involvement of the contents of the room. The damage to vinyl flooring in this test was comparable to the test conducted with only vinyl floor (i.e., no furniture) in all locations other than those proximate to the Class A fuels. In these locations, the damage to the vinyl floor was more severe.

3.3.2.11 Test 6-6 – Fuel Spill on Floor (Vinyl) with Slit Vent

Test 6-6 used a 2.0 L (0.52 gal) gasoline spill fire on vinyl centered in the enclosure (i.e., pour area just in front of the wooden table). This test used the same ignition scenario used in Test 6-5 only with a slit vent (i.e., a more limited ventilation condition). After an initial period of growth, this enclosure fire burned at a nominal steady-state for a period of 300 seconds (5 minutes) with an average fire size of approximately 1.1 MW and average upper layer temperature of 413ºC (775ºF). Later in the test, upper layer temperatures exceeded 600ºC (1112ºF) and floor heat flux levels exceeded 20 kW/m^2 (only in the back), but these conditions did not persist for the full remainder of the fire. Over the course of this test, approximately 37 percent of the fuel load within the enclosure (i.e., furnishings and flooring) was consumed. Representative photographs of the condition of the enclosure after the fire was manually extinguished are shown in Figure 100.

Figure 100. Composite photograph of enclosure conditions after Test 6-6.

As shown in Figure 100, the limited ventilation condition and the consequent lack of fire and temperature development within the enclosure resulted in minimal pattern formations on the interior surface of the enclosure. The majority of the walls and ceiling were heavily soot stained. The texture of the interior surfaces was very smooth and glossy as opposed to rough and matted. The GWB paper remained but was heavily sooted and appeared to be baked. Upon touching the walls of the enclosure, the soot was not readily removed. These surface characteristics were attributed to the temperatures within the enclosure (i.e., 225–550ºC (437–1022ºF)) from 0.6–2.4 m (2–8 ft) being in the general range of soot oxidation temperatures without grossly exceeding them. Several different areas with a relative absence of soot were identified on the walls of the enclosure after this test. These white areas were located on the left and rear wall of the enclosure. One pattern was located on the base of the rear wall, approximately 0.9 m (3 ft) from the left corner. Figure 101 shows the low level burning of the upholstered chair (left) and coffee table (center) that was documented during Test 6-6. Based on test observations, it is unlikely that the soot in this location was impacted by suppression activities. Consequently, this pattern is deemed a clean burn pattern.

Figure 101. Low level burning in left, rear corner of the enclosure during Test 6-6 (view from vent at 215 s after ignition).

The second pattern identified was located behind and above the upholstered chair on the left wall and ceiling (see Figure 102). This clean burn pattern extended from the chair up to the ceiling and was characterized by white speckling. The pattern continued across the ceiling for approximately 0.9–1.2 m (3–4 ft) into the middle of the enclosure. As shown in Figure 102, the absence of soot in this area was far less prominent in this location than was observed on the rear wall. Two low level, circular areas of speckling were observed on opposite sides of the GWB seam. The damage to the paper of the GWB paper along the seam increased with increasing elevation.

Figure 102. Photograph of absence of soot noted on left wall of the enclosure behind the upholstered chair.

There was also a clean burn pattern at the base of the left wall associated with the melted plastic remains of the baby seat (see Figure 103). As shown in Figure 103, the area located behind the baby seat suggests that the fire plume from the burning baby seat was potentially bending towards the rear corner of the enclosure. This migration of the fire towards the rear of the enclosure has been noted in previous testing.

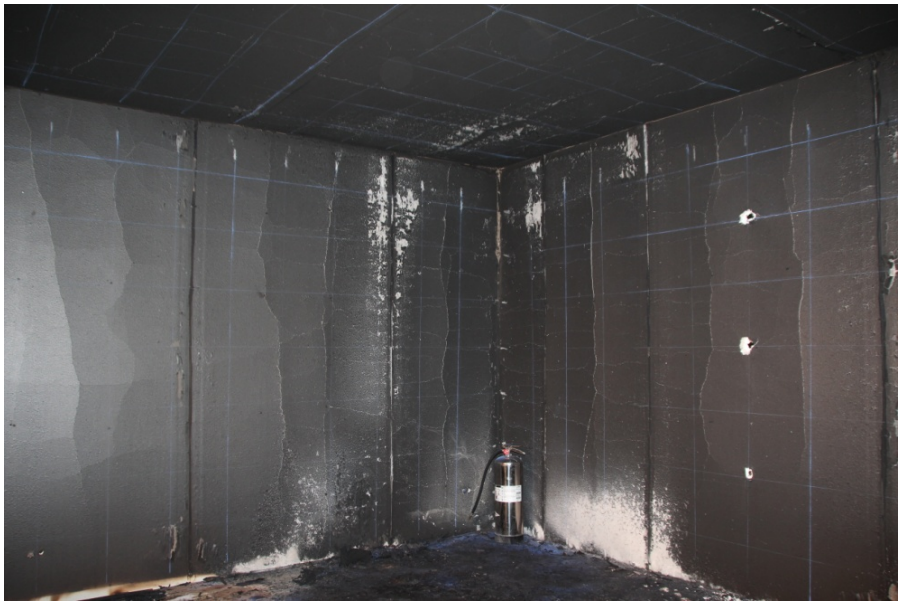

(a)

(b)

Figure 103. Clean burn pattern and area of the melted baby seat (bottom left corner).

In this test, the majority of the areas identified as being at least partially vacant of soot were found in the rear left corner of the enclosure. For tests with slit vents, the fire banked down due to the development of a deep, vitiated upper layer within the enclosure. The deep layer created an inflow of air along the floor that caused the fires in these tests to migrate towards the rear of the enclosure. This sort of vent flow caused the fire plume to bend toward the rear left corner of the enclosure. This bending resulted in the involvement and continued burning of the combustibles in this corner more so than in other areas of the enclosure. The prolonged burning in this location was sufficient to oxidize all soot that was initially deposited thus producing the white area.

Damage to the furnishings in this test was very biased towards the upholstered chair (0.64) and wooden table (0.66) compared to the upholstered sofa (0.18). During the inspection of the furnishings after this test, the frame of the upholstered sofa was found to have no evidence of charring while the frame of the chair and table were heavily charred. None of the damage to the furnishings was indicative of an initiating fire location or directional heat exposure. The damage to each piece was relatively uniform on that given piece of furniture. This evidence is consistent with the fact that the fuel spill preferentially involved the chair and table first before the sofa.

The vinyl flooring in this test was thermally degraded but less so than was noted in Test 6-5. The majority of the material was still present and generally only blackened with limited charring/cracking of the material to expose the plywood subfloor. A photograph of the condition of the vinyl flooring after Test 6-6 is provided in Figure 104.

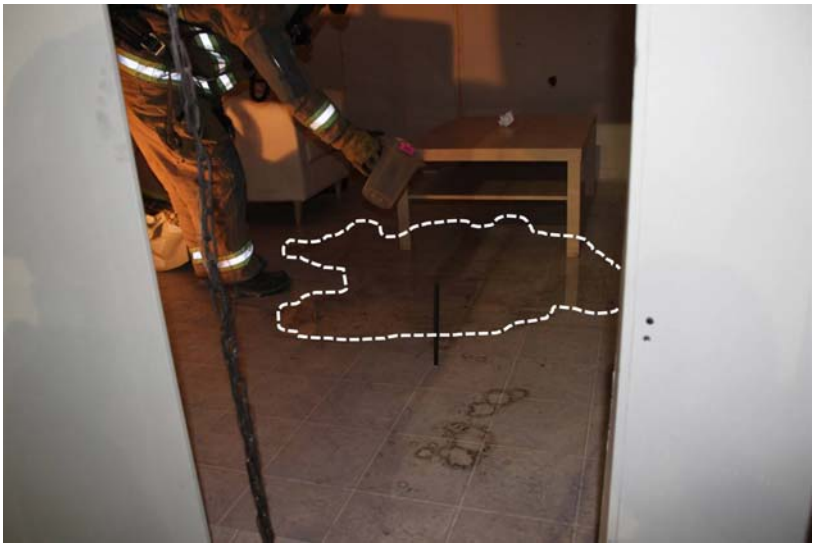

(a)

(b)

Figure 104. Photograph of (a) initial spill area and (b) condition of vinyl flooring after Test 6-6.

As shown in Figure 104, the primary areas of cracking of the vinyl flooring are located in front of the location of where the wooden table was and moving toward the front right corner of the enclosure (i.e., lower right corner of the photograph). Other areas of flooring within the photograph are relatively uniformly blackened and intact (i.e., flat against the enclosure floor). Although this area of increased damage is consistent with the general area where the initiating spill fire was released, the entire fuel spill area is not characterized the same damage. Other factors such as the burning of the coffee table and the effect of the ventilation condition may have contributed to this preferential degradation. Despite the fact that additional fuel loading was present during this test compared to the test where only vinyl flooring was present within the enclosure during the 2.0 L gasoline spill fire, the damage to the flooring in this test was less severe. This difference is attributed to the limited, slit ventilation, which limited the fire development compared to the full door vent in the vinyl flooring only scenario. It was also noted that damage to the flooring material in the rear, left corner beneath the clean burn pattern was no more severe than that noted in the majority of the enclosure flooring and less than that described above.

3.3.2.12 Test 6-7 – Fuel Spill on Upholstered Chair (Vinyl) with Full Door Vent

Test 6-7 used a 1.5 L (0.40 gal) gasoline spill on the upholstered chair and a 0.5 L (0.13 gal) trailer poured onto the vinyl flooring as the initiating fire. This test reached flashover conditions 115 seconds (1 minute 55 seconds) after ignition and continued burning under fully developed conditions for an additional 60 seconds (1 minute). During this time, average upper layer temperatures of 715ºC (1319ºF) were measured over a period of approximately 60 seconds. Over the course of this test, approximately 27 percent of the fuel load within the enclosure (i.e., furnishings and flooring) was consumed. Representative photographs of the condition of the enclosure after the fire was manually extinguished are shown in Figure 105. It should be noted that the white areas on the rear wall of the enclosure, shown in Figure 105, are due to reflection of the camera flash and are not actually white in color, but are gray.

Multiple different patterns were identified on the enclosure walls and ceiling after Test 6-7. The largest pattern was on the rear wall of the enclosure. The pattern originated approximately 0.6 m (2 ft) from the rear, left corner at floor level and extended to the ceiling. The top edge of the pattern was consistently at this elevation over the entire width (i.e., 2.4 m (8 ft)), while the bottom edge of the pattern increased in elevation above the floor from left to right. The pattern was identified because of the glossy nature of this section of wall relative to the matted black color of the neighboring GWB. The GWB paper in this location was consumed. The soot staining and glossy appearance was on the gypsum material.

(a)

(b)

(c)

Figure 105. Photographs of composite enclosure (a) left wall (b), and rear wall (c) conditions after Test 6-7.

The second pattern identified was an area behind the upholstered chair (see Figure 106) where soot was less prevalent than in neighboring areas. Given that the chair was the initiating fire source, soot would have been deposited onto the wall in this location early in the test due to thermophoresis. As the chair fire developed, the thermal exposure was sufficient to oxidize soot and start a clean burn pattern as shown in Figure 106. The relative absence of soot in this area was identified in several of the earlier tests conducted (6-3 and 6-5).

Figure 106. Condition of wall behind upholstered chair after Test 6-7.

The third pattern identified was a white area absent of soot on the ceiling of the enclosure (see Figure 107). The pattern was centered approximately 1.8 m (6 ft) inside the enclosure from the vent and was irregular in shape with portions of the pattern extending towards the rear of the enclosure and portions extending towards the vent. The pattern was located above area of the chair and table, extending to the front edge of the wooden table, which is the area where the gasoline trailer terminated.

Figure 107. White area identified on ceiling of enclosure after Test 6-7.

After this test, sections of foam were still present on both the upholstered sofa and upholstered chair. Photographs of these two pieces of furniture are provided in Figure 108. One main difference between the furnishings was the extent of thermal degradation on the legs of the upholstered chair compared to the lower sections of the upholstered sofa. The chair legs were heavily charred (see charring on front leg of upholstered chair in Figure 108(b)) despite the fact that there was polyurethane foam still attached to the topside of the chair. This is consistent with the initiating spill fire in front of the chair. The upholstered sofa frame was only thermally discolored (i.e., blackened) with no evidence of charring. Only the top surface of the wooden table was consumed with sections of the honeycomb core material still present.

(a)

(b)

Figure 108. Condition of (a) upholstered sofa and (b) upholstered chair after Test 6-7.

The damage to the vinyl flooring in this test varied significantly. The perimeter of the enclosure was thermally degraded and blackened while the flooring in the center of the enclosure was completely consumed exposing the plywood subfloor. A photograph of the condition of the vinyl flooring after Test 6-7 is provided in Figure 109. A close-up of the difference in damage to the flooring material that is highlighted in Figure 109 is provided in Figure 110.

Figure 109. Condition of vinyl flooring after Test 6-7.

Figure 110. Close up of difference in damage to flooring after Test 6-7.

As shown in Figure 109, the damage in the center of the enclosure was relatively uniform. Based on this fact, the damage was not directly attributed to the initiating fire (i.e., gasoline spill fire near chair and trailer toward door). If the damage was a result of the spill fire, it would be expected that the damage would be biased to the left (i.e., where the spill fire was poured). Given that the damage is generally centered in the enclosure this damage is attributed to ventilation effects more so than the initiating fire. No distinct patterns were identified in the area where the gasoline trailer was poured (i.e., area between the table and upholstered chair). The pattern generated during the initial stages of the fire did not persist in this test.

3.3.2.13 Test 6-8 – Fuel Spill on Upholstered Chair (Vinyl) with Slit Vent

Test 6-8 used a 1.5 L (0.40 gal) gasoline spill on the upholstered chair and a 0.5 L (0.13 gal) trailer poured onto the vinyl flooring as the initiating fire. This test was identical to Test 6-7 with the exception of the slit vent ventilation condition. In this test, the gasoline spill fire on the floor burned for the initial 60 seconds but then self-extinguished, leaving only the upholstered chair burning within the enclosure. As the upholstered chair became fully involved relatively steady-state conditions were developed within the enclosure. These conditions were maintained for approximately 540 seconds (9 minutes) with an average fire size of approximately 755 kW and average upper layer temperature of 605ºC (1121ºF). Over the course of this test, approximately 24 percent of the fuel load within the enclosure (i.e., furnishings and flooring) was consumed. Representative photographs of the condition of the enclosure after the fire was manually extinguished are shown in Figure 111.

Figure 111. Composite photograph of enclosure conditions after Test 6-8.

A single primary pattern was identified on the walls of the enclosure. The pattern was located in the rear, left corner of the enclosure and covered approximately 0.6 m (2 ft) of the left and rear wall extending outward from the corner. The pattern was characterized by the absence of soot in this area relative to neighboring wall sections. Given that the primary fuel burning in the test was the upholstered chair located in this corner of the enclosure, it was concluded that this clean burn pattern was formed as a result of thermal exposure. Except for a small white patch high on the

right side of the back wall, the majority of the interior surface of the enclosure was uniformly soot-laden with the soot being matted as opposed to glossy, which had been observed in previous tests.

The mass loss fraction of the upholstered chair in this test was far more severe (0.56) than any of the other Class A furnishings. The upholstered sofa and table each loss less than ten percent of their original mass. Photographs of these pieces of furniture are provided in Figure 112.

(a)

(b)

Figure 112. Comparison of damage to the (a) upholstered sofa and (b) upholstered chair after Test 6-8.

As shown in Figure 112, the chair was completely consumed other than the wooden base which was heavily charred. The sofa had sections of polyurethane foam and fabric ticking remaining. The wood frame of the sofa was thermally discolored with only slight evidence of charring noted. The wooden table was partially charred, more so than the upholstered sofa frame but less than that of the upholstered chair. In this test, the coffee table collapsed in place (i.e., not preferentially towards either piece of upholstered furniture).

The vinyl flooring in this test was most damaged in an area stretching from the upholstered chair to the front of the wooden table. The vinyl in this area was either completely charred and in the form of ash or was completely consumed with exposed subfloor present. The degree of damage decreased moving outward from this area with the majority of the vinyl flooring being partially consumed and a small area around the perimeter of the enclosure with only thermal discoloration. A photograph of the condition of the vinyl flooring after Test 6-8 is provided in Figure 113.

Figure 113. Condition of vinyl flooring after Test 6-8.

The most severe area of flooring damage, observed in the area between the upholstered chair and wooden table, was consistent with the gasoline trailer used as the initiating fire in this test. However, it was not readily apparent that this damage was a direct result of the gasoline spill. In fact, test observations indicate that the spill fire only burned for a period of approximately 60 seconds before self-extinguishing. This short burning duration suggests that the floor damage was not due primarily to the gasoline spill fire. The preferential damage to this area of flooring relative to other areas within the enclosure was in part due to the spill fire, which based on open burning fire observations will thermally degrade, discolor, and slightly char the vinyl veneer, but also due to the involvement of the larger Class A furnishing around this area. The combustion of these larger fuel packages resulted in enhanced radiation feedback to the floor in this area, which would further degrade and potentially ignite the flooring material.

3.4 Characteristics of Patterns

A variety of patterns were described in the previous section. The majority of these patterns were characterized by the relative absence of soot in a given area when compared to neighboring areas. When formed as a result of a thermal exposure, these types of areas are traditionally referred to as clean burn patterns, indicating that the soot, once deposited on the surface of the substrate was thermally oxidized (i.e., removed). However, there were several instances in this testing where it was determined through either test observations or post-test analysis that an area of relatively less soot (white or gray area) was due to suppression activity, not thermal oxidation. This section characterizes the patterns produced by both of these mechanisms to establish criteria to differentiate between a clean burn and suppression pattern.

As stated above, the majority of the patterns described for each test were identified due to the absence of soot on otherwise sooty surfaces. This absence of soot resulted in the area appearing lighter in color (i.e., white or gray) as opposed to black. Upon closer inspection of the patterns, it was determined that the absence of soot correlated to the absence of the GWB paper. However, it should be noted that paper ash can still be present even after a pattern transitions to being white in color. The absence of the GWB paper was attributed to either thermal degradation resulting in ash or clean gypsum or suppression activity (i.e., water spray removing ash).

As a fire develops, even if close to a wall [Riahi 2011], soot is initially deposited on the GWB. In the case of thermal degradation, as the fire imposes a greater heat flux on the GWB, the paper facing pyrolizes or burns and turns to ash. The ash can be soot covered and black, but with additional heat, the soot burns and the ash can turn white. In addition, as the ash flakes off the GWB surface and gypsum is exposed, the surface also appears to turn white. This gradual degradation of the GWB paper can result in a speckled pattern initially being formed in areas subjected to relatively severe thermal exposures. An example of the formation of the speckled black/white area and the gradual degradation/consumption of the sooted GWB is provided in Figure 114.

Figure 114. Example of sooted GWB paper that was partially consumed during Test 6-5.

The intermediate-scale furnace test samples from the calcination study (see Section 2.4), show that GWB paper ash can remains after soot has been oxidized. An example of this is provided in Figure 115. As shown in the close-up photo in Figure 115(b), the white material on the right side of the GWB sample in Figure 115(a) is ash. This sample was exposed to 10 MJ/m^2 of heat in the furnace. Figure 116 shows a close up photograph of another GWB sample exposed to only 4 MJ/m^2 of heat in the furnace that has black soot covered ash.

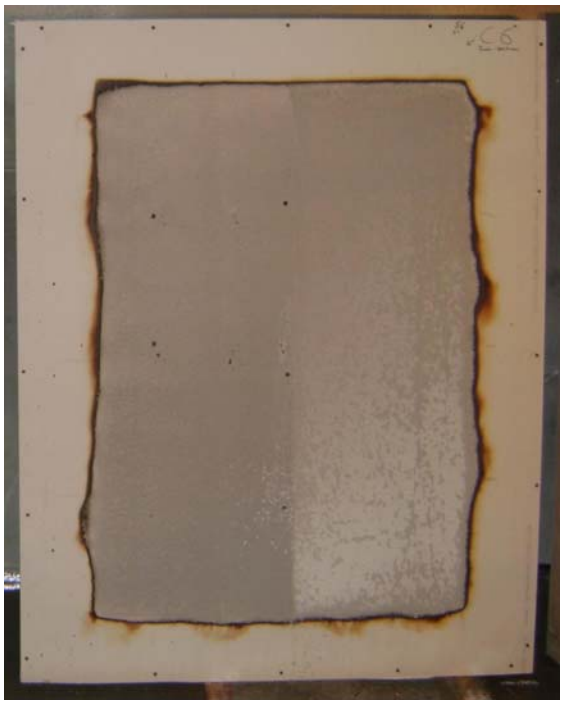

(a) Clean burn pattern on lower right hand corner of GWB with paper ash still present.

(b). Close up photograph of paper ash on gypsum wallboard.

Figure 115. Intermediate-scale furnace exposure sample (Test 6).

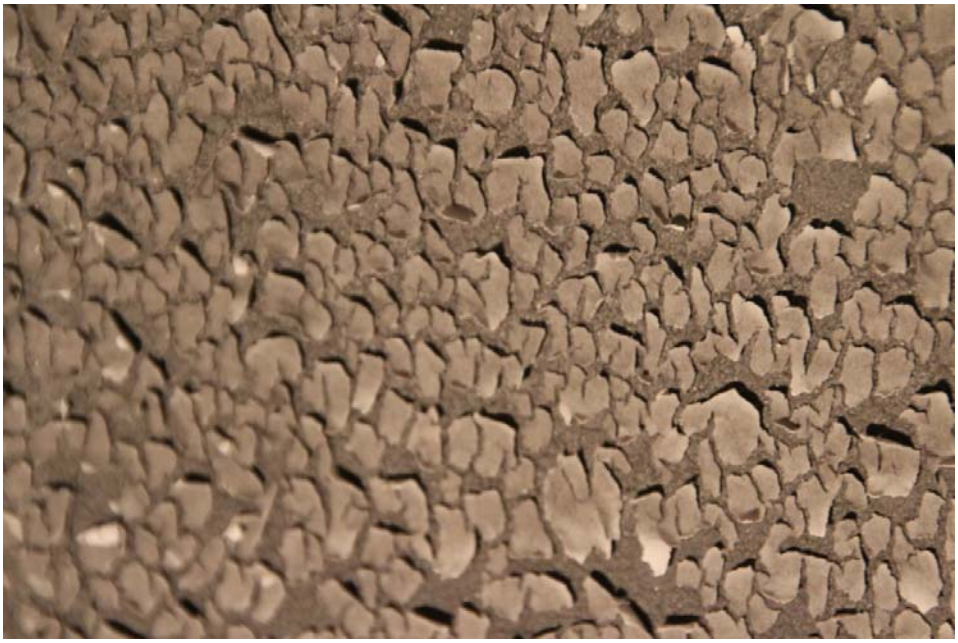

Figure 116. Close up photograph of paper ash on gypsum wallboard still covered with soot (Test 7).

In the case of suppression activity, the momentum of the water spray impacting the friable ash layer forcefully removes the material. As shown in Figure 117, the structure of the water spray can produce a spray pattern that has similarities to a speckled clean burn. However, the patterns can be distinguished based on the splatter pattern formed by the impacting water and the areas of smeared soot as well as the clean removal of ash and soot.

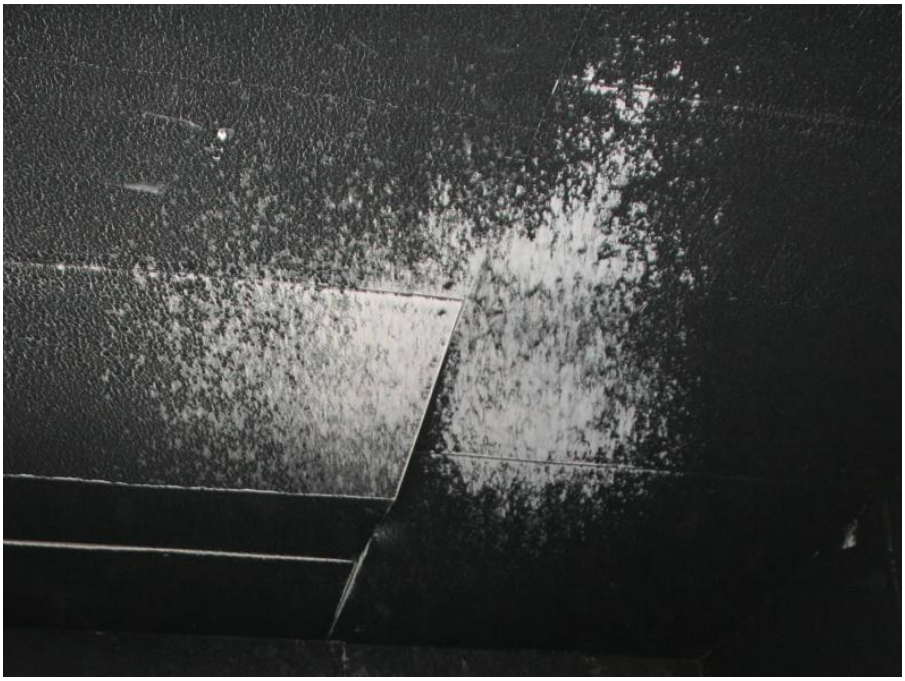

Figure 117. Suppression pattern from Test 6-1.

In some cases, two pattern formation mechanisms (i.e., thermal and suppression) may exist. For example, consider the ceiling pattern from Test 6-5 (shown in Figure 118); it is possible to distinguish between the speckling and the water splatter that are present. Figure 118 is annotated to show the distinction. The speckling on the perimeter of the pattern is relatively fine with a crazed appearance, similar to that shown in Figure 114. The water splatter in the center of the pattern consists of larger areas of soot removal and has the smeared, directional appearance. In this fire, the clean burn pattern was initially formed in this location but at the time of suppression, the pattern was altered due to water spray.

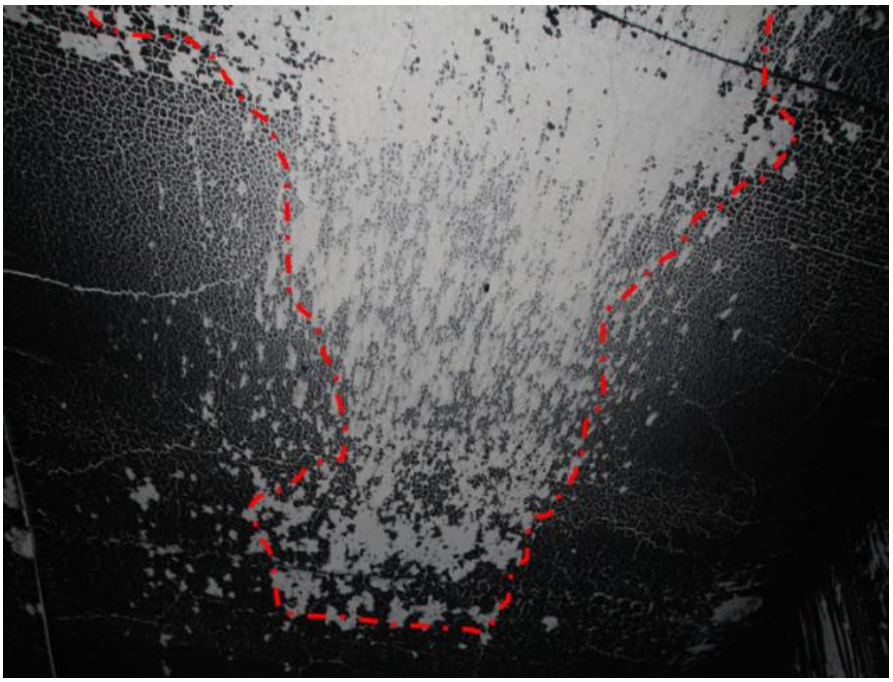

Figure 118. Annotated photograph of ceiling pattern produced by both thermal (fine speckle outside dashed line) and suppression activity (splatter pattern inside line) in Test 6-5.

3.5 Summary of Fire Pattern Findings

Gasoline spill fire scenarios were conducted on carpet and vinyl flooring in the open and in rooms with other Class A combustibles. The enclosure fires in this study included flashover conditions (full door vented fires) and fully involved fires that did not actually flashover (slit vent cases). In both types of fires, most combustibles in the room had pyrolized or burned. Exposure durations ranged from 60–300 seconds for open burning scenarios, 1–6 minutes for post-flashover scenarios, and 7–12 minutes for the limited ventilation scenarios.

In general, the utility of floor patterns was minimal for all scenarios except those conducted in the open. Due to the extensive thermal damage within the enclosure fires, patterns initially formed by gasoline spill fires were destroyed. For vinyl floor scenarios, the brevity of the spill fire was such that the surface charring and thermal discoloration produced by the spill fires were quickly overwhelmed by the ignition and burning of the material. Furthermore, the impermeable nature of the vinyl was such that the subfloor was not impacted in any way by the initial spill

fire, therefore when the vinyl flooring was consumed, the subfloor showed no evidence of the initiating fire scenario.

For carpet scenarios, the persistence and utility of the patterns was slightly better than that of vinyl floors. In both the open burning and enclosed scenario with no Class A materials present, the carpet flooring showed evidence of the gasoline spill fire in the form of a doughnut pattern. However, this type of pattern was not observed in any of the enclosure tests conducted with Class A fuels present. In these tests, patterns remaining on the flooring materials were primarily a result of the burning Class A materials inducing ignition and flame spread on the flooring material. As a result of this, when the carpet flooring was not completely thermally degraded, the largest and most severe areas of burning were generally located proximate to the larger Class A furnishings (i.e., upholstered sofa and chair).

Based on these flooring evaluations, the persistence of a fire pattern from an initiating fire source requires that the damage from the source be greater than that from the pursuant enclosure fire and that the substrate be resilient enough to survive both exposures. Spill fires in rooms with large volumes relative to the fire size are candidate scenarios in which fuel spill patterns may have a chance to persist, particularly for floor materials that can absorb liquid fuel. Unless there are areas of undamaged or marginally damaged flooring, initial spill fire patterns are not expected to remain post-fire. Based on the tests conducted with fully involved, limited ventilation fires and full door vented flashed over fires, spill patterns did not persist due to the widespread thermal degradation of the floor.

In the nine Class A fire enclosure tests, the most easily identifiable patterns were characterized by the relative absence of soot compared to adjacent areas. Traditionally, these patterns are referred to as clean burns and are associated with the thermal oxidation of soot (i.e., removal of soot due to high temperature exposure). Clean burns are also typically associated with areas that are stark white in contrast to adjacent areas that are blackened due to soot deposition. However, clean burns can exhibit a range of colors from dark gray to white as the pattern forms with increasing heat exposure. These patterns will also range from a finely speckled appearance to fully cleared areas of white gypsum.

Numerous wall patterns were identified behind the smaller fuel packages (i.e., upholstered chair and baby seat) which were offset from the enclosure wall. These patterns were not completely clean (white) but showed signs of soot oxidation. Within the boundary of these clean burn patterns, soot was still present, but to varying degrees of gray. As the fire exposed the gypsum wallboard, the paper face would pyrolize (thermally degraded, char). Pyrolysis of materials can transition to flaming combustion, but it can also progress as charring or smoldering combustion. The result of the pyrolysis or burning of the gypsum wallboard paper was ash. Ash was present both with and without soot (i.e., black and white). Clean burns occurred with white ash present and sometimes with no ash at all, just the underlying gypsum.

These tests showed that clean burn patterns can be formed on walls in areas that do not have a Class A fuel source directly adjacent to them. As noted by other investigators, clean burns can be formed on walls and ceilings in areas dictated by the supply of air due to local ventilation flows. In several of the tests, large areas in which soot had been removed were not associated with fire exposure. Although these white patterns had similar appearances to clean burn patterns,

they had notable differences upon closer examination. These patterns were characterized by a splatter appearance (larger whitish spots) around the periphery with the center consisting of larger areas of soot removal, sometimes with signs of a smeared, directional appearance. These patterns were the result of suppression activities on both walls and ceilings. In some cases, particularly walls, watermarks were observable (i.e., water drip marks). Besides the characteristics noted above, the suppression patterns were also verified by the visual presence of a green tint to the pattern that was associated with the chemical treatment of the suppression water at the fire lab. The means of differentiating clean burn and suppression patterns based on the characteristics described in this report would be enhanced by further systematic testing. These tests showed that the characteristics are distinct. However, for the case of complete soot and ash removal with large white patterns, there may be circumstances that the absence of either the speckled pattern associated with clean burn development or splatter patterns associated with water extinguishment cause uncertainty in determining the source of the white pattern. In addition, depending on the quality and resolution of photographs, it is possible to have water spray patterns appear as indistinguishable from clean burns in photos.

4.0 IGNITABLE LIQUID RESIDUE IN FIRE DEBRIS

NFPA 921 [2011] contains guidelines for conducting a fire scene investigation and more specifically, in Chapter 16, outlines the handling, collection, preservation, and analysis of physical evidence from a fire scene. Several recommendations are made for the collection and preservation of samples suspected to contain an ignitable liquid residue (ILR), including: the collection of comparison samples, the use of metal cans when collecting solid/liquid samples, and the proper identification of samples once collected. The document also recommends that samples be identified and labeled in accordance with ASTM E1188 [2005] and ASTM E1459 [2005]. However, there is very limited information/guidance that is provided to an investigator regarding where samples should be collected from and how a fire environment can impact the persistence of an ignitable liquid residue. One goal of this study was to characterize the persistence of ignitable liquid residues within fuel spill patterns from liquid fuels burning in the open and in enclosure fire scenarios involving other Class A materials. To address this goal a series of small- and large-scale fire tests were conducted whereby fire debris samples were generated under both controlled and realistic conditions.

4.1 Fire Debris Analysis Literature Review

4.1.1 Fire Debris Analysis

Evidence from fire scenes is routinely provided to forensic laboratories to determine the chemical make-up of the evidence and more often than not determine whether or not an ignitable liquid is present within the debris. Although a wide variety of analytical techniques are available, the technique most often used in forensic science laboratories to establish the presence of an ignitable liquid is based upon the principle of heated headspace enrichment. The standard practice for this technique is ASTM E1412 [2007] and the test method outlining the analysis of the extracts obtained from ASTM E1412 protocols is ASTM E1618 [2006]. This analytical approach generally consists of the adsorption of an ignitable liquid residue onto a porous polymer/charcoal media, the elution of the residue into a solvent, and analysis of the eluted material using a gas-chromatograph-mass-spectrometer (GC/MS). Once analyzed, the chemical

signature of the material analyzed is compared to existing libraries and/or comparison samples. This comparison is traditionally performed by a fire debris chemist to identify the contents of the fire debris and to determine whether or not ignitable liquids are in fact present in the fire debris. More often than not, ignitable liquid residue analysis is performed to qualitatively identify the chemical constituents within fire debris. Quantitative measurements of concentration are not typically made.

4.1.2 Ignitable Liquid Residue Studies

4.1.2.1 Comparison Sample Collection

In addition to the collection of an ILR sample from within a pattern of interest, NFPA 921 [2011] also recommends that a comparison sample be collected to rule out the presence of a naturally occurring ILR within the material collected or ILR from other known sources within a space. Several studies dating back to the late 1970s [Clodfelter 1977, Nowicki 1990, Lentini et al. 2000] have demonstrated that various common household materials, when thermally decomposed, can produce volatile components due to the use of petroleum-derived liquids during manufacturing.

4.1.2.2 Impact of Suppression Activities

Due to the fact that fire debris is often saturated with water during fire suppression activities, it is important to understand the impact this has on analytical results. Ren & Bertsch [1999] determined that in general the presence of water only had a moderate influence on the analytical results producing a slight shift toward higher molecular weight components.

4.1.2.3 Adsorption Media Selection

Charcoal media is used more often than porous polymers due to the relatively effective retention of the ILR once adsorbed [Bertsch 1997, Williams et al. 2005]. The adsorption of ILR onto the charcoal media is accomplished using either static or dynamic methods. Static adsorption is the more recently developed and effective means of ILR adsorption. In both cases, when the fire debris is heated, the ILR is volatized and adsorbed onto the media material suspended in the headspace of the can. To date, several studies have been conducted to identify optimal adsorption techniques for ILR analysis [Kurz 1984, Newman et al. 1996, Williams et al. 2005]. Newman et al. [1996] investigated the impact of time, temperature, strip size, and sample concentration on the use of activated charcoal strips for ILR analysis. Fuel volumes ranging from 0.3–20 µL were evaluated. Charcoal media ranged in size from 16–128 mm^2. The author also investigated temperatures ranging from 60–120^oC and heating durations ranging from 2–48 hrs. From this series of tests, the author found that at lower heating temperatures, higher molecular weight compounds are not sufficiently volatized for adsorption and at higher temperatures, light end compounds can be significantly distorted due to increased volatization of high molecular weight compounds. Newman et al. [1996] also concluded that the size of the charcoal media does not have an impact on the resolution of the accelerant adsorption but can result in distortion of results if higher concentrations of ILR are present. As the concentration of accelerant within the sample increased, so did the extent of the distortion for a given size charcoal media. Based upon these conclusions, Newman et al. developed an analysis scheme for the extraction of ILR

from fire debris for analysis. The authors recommend a temperature range of 50–70ºC, a soak time of 16–24 hours, and a minimum strip size of 64 mm^2.

A follow-up study to the work conducted by Newman et al. [1996] was conducted by Williams et al. [2005] nearly a decade later. The purpose of this follow up study was to better understand adsorption saturation and chromatographic distortion effects within commercial containers. Experimental variables included activated charcoal disc sizes (12.6–99 mm^2), liquid fuel volumes (12–720 µL), and type of liquid fuel (stock hydrocarbon solution and un-weathered gasoline). The authors established that the size of the activated charcoal plays an important role in identifying the ILR present in a fire debris sample. Williams et al. [2005] found that as the surface area of activated charcoal available for adsorption decreases, saturation of the media occurs sooner and more pronounced distortion of the ILR chromatogram occurs. For the scenarios evaluated using the ASTM E1412 [2007] recommended activated charcoal strip size of nominally 100 mm^2, distortion was observed for ILR volumes of 24 µL or larger. Based upon these findings, the authors showed through experimentation that distortion effects can be overcome by simply heating the container and cooling it back to room temperature prior to taking a sub-sample (i.e., a smaller sample of the debris from within the can), placing it in another evidence can and analyzing, such that hydrocarbon components are uniformly distributed in the container.

4.1.2.4 Internal Standards

In the context of this work, an internal standard is an analyte, with known characteristics and concentration that is added to either the fire debris itself or the eluting solution. The addition of an internal standard(s) to fire debris prior to ILR analysis is not standard operating procedure in most analytical laboratories [TWGFEX 2008]. However, this technique is often used in laboratory quality control to monitor the extraction and analysis of target analytes from a given sample. ASTM E1412 [2007] suggests the use of either 3-phenyltoluene (3PT) or diphenlymethane as an internal standard added to the eluting solution. Locke et al. [2009] evaluated eight different compounds for their use as an internal standard in the analysis of fire debris. The extraction efficiency and interference potential of these standards were evaluated at both room temperature and 60ºC (140ºF). From this work, the author recommended the use of two internal standards in combination, one with a low boiling point and one with a higher boiling point. Locke et al. also recommended that the internal standard be delivered directly into the solvent used to elute the charcoal strip (i.e., substrate onto which fire debris was adsorbed). Tetrachloroethylene (PCE) was identified as the best choice for the low boiling point standard.

4.1.3 Quantitative Analysis and Ignitable Liquid Residue (ILR) Persistence

To date, only a limited amount of research has been conducted to evaluate the persistence and prevalence of ignitable liquid residues within fire debris samples and fire patterns. Only one study was identified which attempted to determine an optimal location within a fire pattern to collect a fire debris sample for ILR analysis.

O'Donnell [1985] conducted a pair of tests on carpet flooring to evaluate the distribution of ignitable liquid residue within a pour pattern after the accelerant was primarily consumed. Gasoline was used as the liquid fuel in these tests. The fuel was manually distributed within a

0.9 m (3 ft) diameter circle. After an unspecified period of burning, the gasoline spill fire was manually extinguished using a carbon dioxide extinguisher. After extinguishment, the pattern was divided into 0.1 m (4 in.) x 0.15 m (6 in.) sections and analyzed for ILR using pentane extraction. A plot of the findings of this work is presented in Figure 119.

O'Donnell [1985] concluded that the highest concentrations of residue were present at the edges of the burn pattern. In this work the author did not specify where exactly along the edge (i.e., including neighboring virgin material or not) of the pattern the samples were collected. The author justified these findings using basic principles of fire dynamics in that a temperature profile of the flame would show that the fire is much hotter toward the center than it is at the edges. Based upon this limited data set, O'Donnell recommended that ILR samples be collected at the periphery of a pattern. Similar recommendations are put forth by Stauffer et al. [2008] who references the work of O'Donnell [1985] as well as by IAAI [2001]. In these works, it is recommended that the fire debris samples from within suspected ignitable liquid patterns be collected at the edges of patterns, with the sample consisting of one-half burned and one-half unburned material. As stated earlier, NFPA 921 [2011] does not offer any recommendation as to where an ILR sample should be collected from within a pattern.

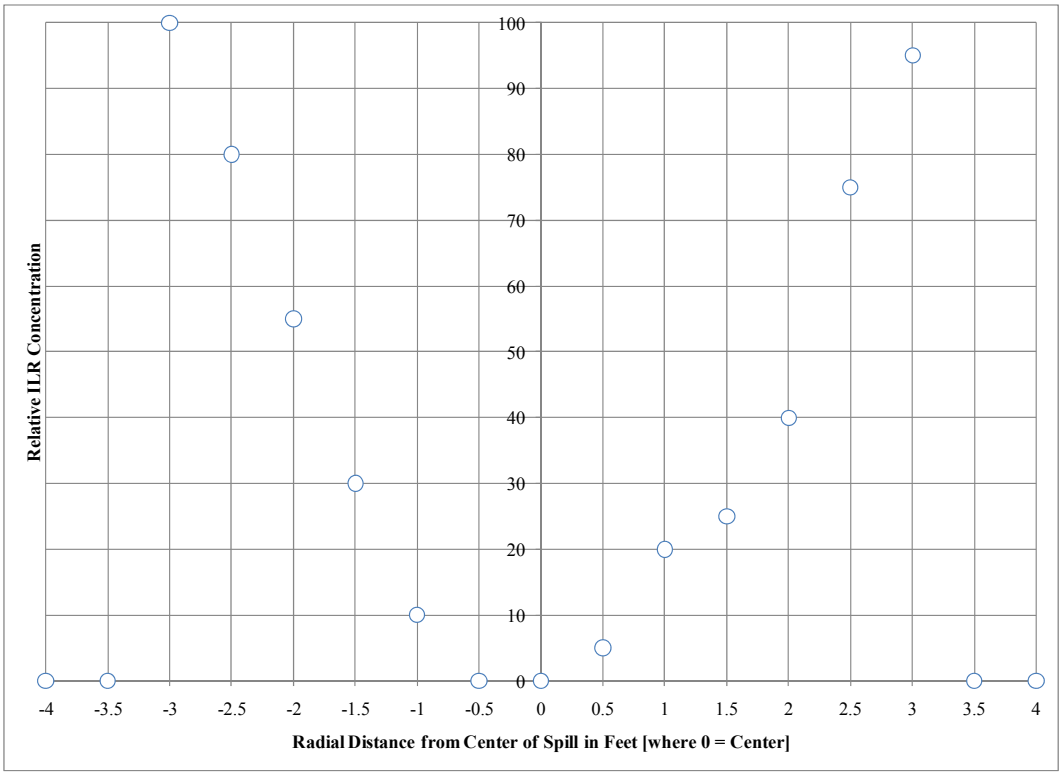

Figure 119. Graphical representation of O'Donnell [1985] ILR sampling findings.

4.2 Sample Collection and Analytical Approach

4.2.1 Sample Collection Procedure

All ILR samples were collected in accordance with generally accepted procedures of the forensic fire investigation community. In this work, samples were collected in two different

forms. Samples collected from small-scale cone calorimeter testing were collected in the state in which they were tested (i.e., 0.1 m (4 in.) square sections). Samples removed from the free-burning or enclosure fire tests were collected in the form of a 45 cm^2 (7 $in.^2$) core of the flooring substrate. Samples were removed from the flooring assembly using a 0.08 m (3 in.) diameter hole-saw. Samples collected along the perimeter of the burn pattern were removed such that the material collected includes approximately half of the consumed flooring/furnishing material and half of the relatively unconsumed flooring/furnishing material. All samples were collected within 24 hours of testing.

Multiple hole-saws were used during sample extraction. After each use, the tool was soaked in a solution of dish detergent and water as described by Dement [1996] in order to prevent sample contamination. Furthermore, during all sample collection, sampling personnel wore new gloves during the extraction of each sample. After sample collection, gloves were discarded.

Once extracted from the flooring system or removed from the cone calorimeter test frame, samples were stored in an unlined, metal paint can with an internal volume of 950 cm^3 (1 qt). The cans were purchased new and were not reused. After filling, the cans were sealed and labeled with a unique identifier associated with the test date, test ID, and sample location. Evidence cans were stored at ambient temperatures (i.e., average temperatures of 21±3ºC (70±5ºF) and 50±10 percent relative humidity) prior to analysis.

4.2.2 Analytical Procedure

The standard test method for the forensic analysis of fire debris is ASTM E1618 [2006], "Standard Test Method for Ignitable Liquid Residues in Extracts from Fire Debris Samples by Gas Chromatography-Mass Spectrometry." The test method does not specify equipment settings but instead provides an acceptable range such that the user can determine settings based upon specific need. The setting ranges specified in the standard include:

- Sample Inlet System: Splitless
- GC Oven Temperature: 50–300ºC (122–572ºF)
- Mass Spectrometer Setting: 40–400 *m/z*

After being collected, the samples were submitted to a commercial analytical laboratory for analysis (Applied Technical Services). This analysis was performed in accordance with the extraction procedures outlined in ASTM E1412 [2007] and the analysis procedures outlined in ASTM E1618 [2006]. In this analysis, an activated carbon strip (10 mm x 10 mm) was suspended in the headspace of each collection can using a paperclip and un-waxed dental floss. The size of the activated carbon strip identified for this analysis was based upon the minimum size strip recommended in ASTM E1412 [2007] as well as based upon the data put forth by Williams et al. [2005] indicating that a strip of this size can capture vapor concentrations up to approximately 20 µL/L without distortion of the fuel chromatograph.

Each sample was spiked with 20 µL of a 2.5 percent solution of 3-phenyltoluene (3PT) in ether prior to the adsorption step (i.e., placement into the oven). The addition of this internal standard was used to verify the ILR extraction process (i.e., verify that the debris was releasing any ILR present). The sealed can was then heated for 18 hours at 87ºC (188ºF). Once cooled to room temperature, the activated carbon strip was removed from the can and cut in half. One half

was archived by the test laboratory and the other was eluted in a vial of 0.5 ml of diethyl ether ($C_4H_{10}O$) for analysis using gas chromatography/mass spectroscopy (GC/MS). The diethyl ether was spiked with 0.1 percent (100 ppm) of Tetrachloroethylene (PCE) to characterize the efficiency with which the sample is inserted into the GC/MS. The GC/MS equipment used for all testing was an Agilent Model 6890N Gas Chromatograph coupled with an Agilent Model 5973 Mass Spectrometer. High purity helium (He) was used as the carrier gas in all tests. A constant flow of helium was passed through the GC/MS column at a flow rate of 1.2 mL/min. The injection volume in these analyses was 1μL with an injection temperature of 280ºC (536ºF).

All samples were injected into the GC/MS column in split mode with a 20:1 split ratio. The heating profile used in all tests consisted of the following:

- 55ºC (131ºF) for 2.5 minutes
- 20ºC (68ºF) per minute to 115ºC (239ºF) for 2 minutes
- 10ºC (34ºF) per minute to 285ºC (545ºF) for 2.5 minutes
- Total Run Time of 27 minutes

The transfer line between the gas chromatograph and mass spectroscopy equipment was maintained at a temperature of 280ºC (536ºF). The mass spectrometer scan range was set to 33–400 amu. With this analysis, an assessment (Positive/Negative) as to whether or not ILR was present within each sample was made. This assessment was based on the guidance provided in Section 10.2.1 of ASTM E1618 [2011].

4.3 Small-scale Ignitable Liquid Residue Persistence Study

A series of small-scale tests were conducted to systematically characterize the persistence of an ignitable liquid on various substrates when exposed to varying thermal conditions. The variables considered were substrate, liquid spill volume, total heat exposure, and sample collection time. For the purposes of this study, the total heat exposure (MJ/m^2) was defined as the product of the incident heat flux to the sample surface (kW/m^2) and the exposure duration(s). The variables were explored using the ASTM E1354 [2011] cone calorimeter, a small-scale fire test apparatus used to characterize the response of materials when exposed to a controlled level of radiant heat.

4.3.1 Experimental Approach

The variables evaluated in these tests were developed to be similar to the full-scale fire testing of Test Series 6, described in the companion report [Mealy et al. 2013]. The substrates evaluated represent typical construction materials on which ignitable liquids may be spilled in a fire involving an accelerant and include: carpet (with padding and plywood sub-layer), vinyl (with plywood sub-layer), plywood, and representative furniture sections (i.e., 100 percent cotton fabric, polyester batting, and 57 mm (2.25 in.) thick polyurethane foam layer). A more detailed description of the composition of these substrates is provided in the companion report [Mealy et al. 2013].

Gasoline was the ignitable liquid used in all tests. The gasoline used in these tests was from the same batch of gasoline used in all of the full-scale tests. Two different liquid spill scenarios were developed based on the type of substrates evaluated. The spill scenario used for vinyl and

plywood substrate testing consisted of 5.0 mL (0.2 oz.) of gasoline being poured onto the 0.1 m (4 in.) square sample surface resulting in a liquid depth of approximately 0.5 mm (0.02 in.). To prevent fuel from running over the edges of the small-scale samples, the perimeter of the samples was diked using high temperature RTV. A bead of RTV with a nominal height of 6.35 mm (0.25 in.) was added to the perimeter of each sample. The 0.5 mm (0.02 in.) average fuel thickness described above was deemed conservative (i.e., less than the spill thicknesses typically measured on these substrates during full-scale testing) and therefore the persistence of fuel in these tests would represent the lower bound of expected persistence,

The spill scenario used for carpet testing consisted of 20.0 mL (0.7 oz.) of gasoline being poured onto the 0.1 m (4 in.) square sample surface. The absorbent nature of the carpet made estimating spill depths challenging. Based on and earlier study by Mealy et al. [2011] the spill coverage area on carpet per volume of liquid released was 0.19 m^2/L (7.6 ft^2/gal). For the cone tests, an average coverage area of 0.00387 m^2 (0.042 ft^2) was measured. This area correlates to within two percent of the area per unit volume data provided in the previous study. Average coverage areas for the tests involving the furniture substrates were 0.0054 m^2 (0.048 ft^2) which correlates to area per unit volume of gasoline of 0.27 m^2/L (10.8 ft^2/gal).

The thermal exposures used were designed to represent the conditions generated by a burning substrate in the absence of an external radiant heat source and the conditions generated by a burning substrate within an enclosure fire (i.e., radiant exposure from the burning substrate as well as external heating from hot upper layer). To simulate the presence of a hot upper layer, the cone calorimeter heater was set to produce an incident heat flux of 35 kW/m^2 at the sample surface. The exposure durations used in this testing were two minutes and ten minutes. For the purposes of these tests, the exposure duration was defined as the time the samples were permitted to burn and be exposed to external radiant heating. The durations were designed to represent expected burning times for residential house fire scenarios. These times were determined by selecting bounding fire department response times for residential house fires based on a USFA study [USFA 2006].

After each exposure, the samples were collected in unlined, steel quart cans. The sample collection times used in this testing were 4 hours and 48 hours. The durations were selected to be representative of a rapid-fire scene investigation and evidence collection scenario as well as a longer period. A summary of the tests conducted is provided in Table 14

Table 14. Summary of small-scale ignitable liquid persistence testing.

Test ID	Substrate	Thermal Exposure	Exposure Duration (min.)	Collection Time (hr)
C1 / W1 / V1 / F1	Carpet/Wood/Vinyl/ Furniture Sample	Burning sample only	2	4
C2 / W2 / V2 / F2				48
C3 / W3 / V3 / F3			10	4
C4 / W4 / V4 / F4				48
C5 / W5 / V5 / F5		Burning sample + 35kW/m^2	2	4
C6 / W6 / V6 / F6				48
C7 / W7 / V7 / F7			10	4
C8 / W8 / V8 / F8				48

In these tests, a 0.1 m (4 in.) sample was placed beneath a conical shaped heater that provided a uniform irradiance to the sample surface. The sample mass was constantly monitored using a load cell and the effluent from the sample was collected in the exhaust hood above the heater. Oxygen consumption calorimetry was performed in the duct, downstream of the hood, via flow rate and gas specie (O_2, CO_2, and CO) measurements that are continuously monitored. Prior to testing, the test apparatus was calibrated and an external heat flux, when appropriate was set. Two minutes of background data was collected prior to the start of each test. The liquid fuel was poured onto the substrate thirty seconds prior to ignition/exposure. The start of a test consisted of placing the substrate beneath the cone heater and manually igniting the material using a small propane flame. Substrates were permitted to burn for the prescribed duration and then manually extinguished. Extinguishment was achieved by placing a section of insulation board over top of the burning material and removing the substrate from beneath the heater. The substrate was then placed in an exhaust hood until placed in the evidence can.

4.3.2 Cone Calorimeter Results

A total of 32 small-scale gasoline spill fire tests were conducted beneath the cone calorimeter. Data from these tests is summarized in Table 15. In this table, the total heat exposure for each of the samples was calculated. This value is the product of the thermal exposure and the exposure duration and represents an approximation of the total quantity of heat to which the sample was subjected over the duration of the test. The re-radiation from the flame plume of the burning sample was approximated as 30 kW/m^2 based on cone calorimeter testing conducted by McKinnon [2012] at fluxes of both 25 and 60 kW/m^2. In these tests, the author measured the heat feedback to the surface of burning cone samples at two different fluxes and approximated the additional heat flux from the fire. Heat release rate curves for the various substrates and scenarios evaluated are provided in Figure 120.

The gasoline spill fires conducted on these small-scale samples behaved similar to those conducted at larger scales. Under ambient conditions (i.e., no external heat flux) the spill fires on impermeable (vinyl) and slightly permeable (plywood) substrates grew rapidly to a peak value and decayed in a similar time frame. As shown in Figure 120(a) and (c), in the absence of an external heat flux these fires only burned for 60–90 seconds before self-extinguishing. The substrates under these conditions were not involved and only slight thermal degradation of the material was noted. With an incident heat flux of 35 kW/m^2 applied, these samples exhibited a similar initial peak but did not self-extinguish. Instead, the flooring material became involved and continued to burn until manually extinguished.

Table 15. Summary of cone calorimeter results for small-scale gasoline spill fire tests.

Test ID	Substrate	Thermal Exposure	Exposure Duration (min.)	Total Heat Exposure (MJ/m^2)	Mass Loss Fraction	Peak HRR (kW/m^2)	Total Heat Released (kJ)
C1	Carpet	Flame Plume (~30kW/m^2)	2	3.6	0.07	341	29
C2					0.07	329	26
C3			10	18	0.26	344	85
C4					0.28	321	88
C5		Flame Plume + External (~65kW/m^2)	2	7.8	0.15	1052	59
C6					0.14	931	57
C7			10	39.	0.50	906	145
C8					0.56	787	138
W1	Plywood	Flame Plume (~30kW/m^2)	2	3.6	0.10	436	19
W2					0.05	263	9
W3			10	18.	0.35	305	9
W4					0.43	322	17
W5		Flame Plume + External (~65kW/m^2)	2	7.8	0.20	355	23
W6					0.20	342	25
W7			10	39.	0.81	362	79
W8					0.80	337	82
V1	Vinyl	Flame Plume (~30kW/m^2)	2	3.6	0.09	316	11
V2					0.09	329	11
V3			10	18.	0.33	199	5
V4					0.34	271	10
V5		Flame Plume + External (~65kW/m^2)	2	7.8	0.19	569	26
V6					0.17	563	28
V7			10	39.	0.66	574	75
V8					0.66	575	75
F1	Furniture Material	Flame Plume (~30kW/m^2)	2	3.6	0.33	183	10
F2					0.36	548	34
F3			10	18.	0.54	142	15
F4					0.47	664	43
F5		Flame Plume + External (~65kW/m^2)	2	7.8	0.47	216	19
F6					0.44	682	51
F7			10	39.	0.97	212	22
F8					0.92	603	87

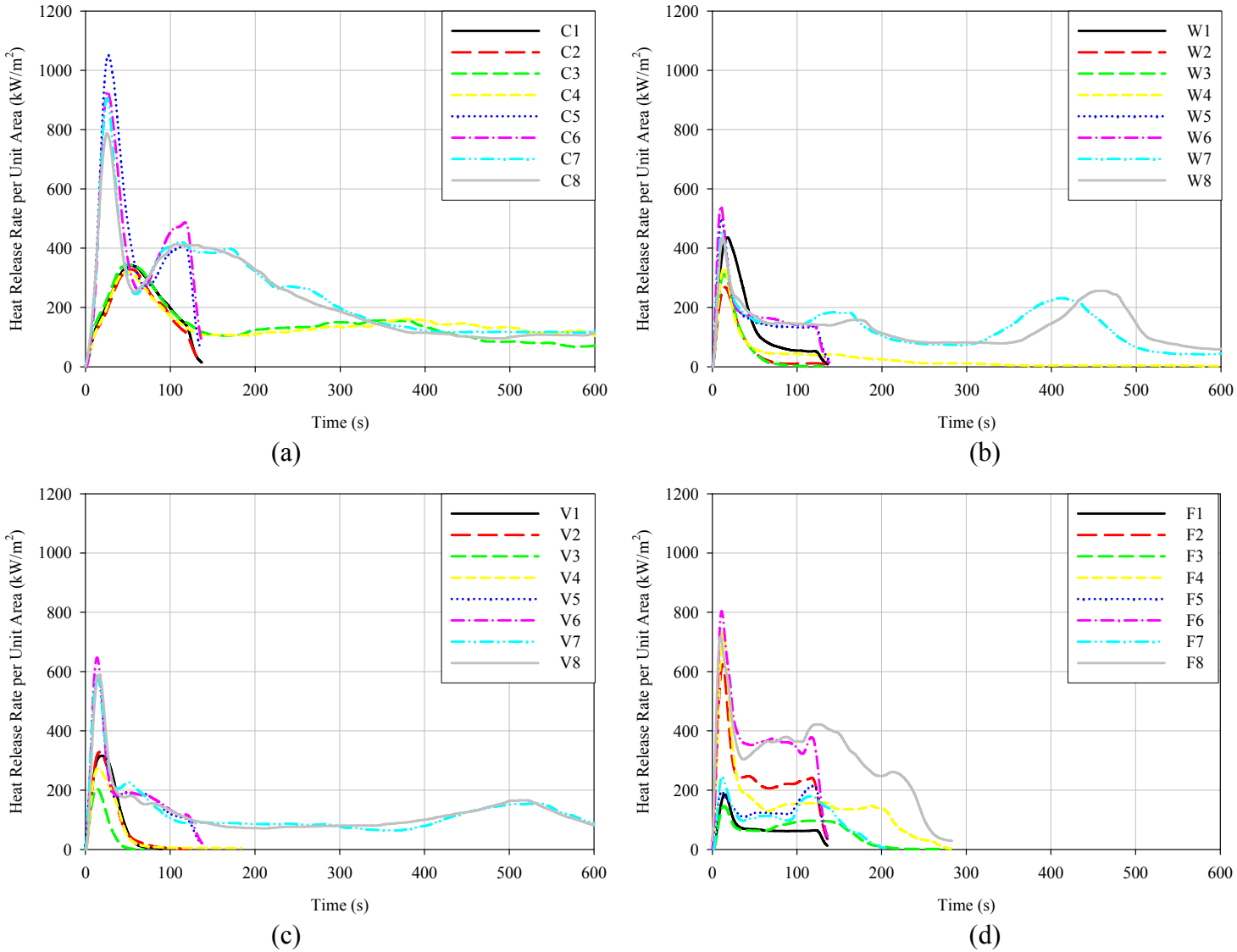

Figure 120. Heat release rate profiles from small-scale gasoline spill fire testing in a cone calorimeter on (a) carpet, (b) plywood, (c) vinyl, and (d) furniture material.

With the exception of the 3.6 MJ/m^2 total heat exposure, a common trend in damage severity was observed for the substrates evaluated. This trend consisted of the furniture material being the most damaged (i.e., highest mass loss fraction), followed by the plywood, vinyl, and carpet flooring material (i.e., lowest mass loss fractions). When exposed to 3.6 MJ/m^2 of total heat, the plywood, vinyl, and carpet flooring materials were degraded to a similar extent with the furniture remaining as the most degraded material. A plot illustrating this trend at each of the total heat exposures is provided in Figure 121. Equations for the linear best fit for each substrate are also presented in Figure 121.

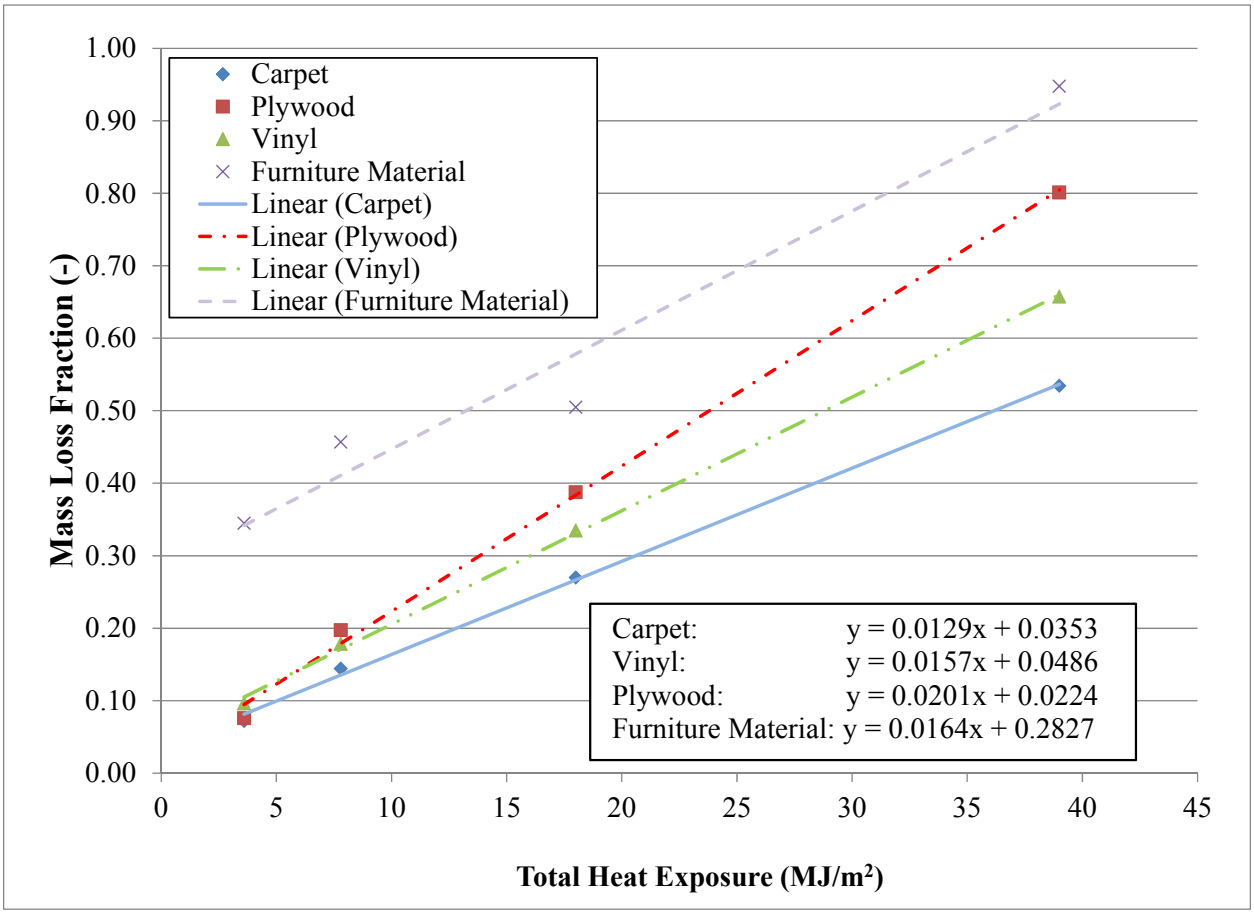

Figure 121. Extent of damage to substrate material as a function of estimated total heat exposure to substrate from combustion of gasoline spill and substrate material burning.

4.3.3 Ignitable Liquid Residue Persistence Results

Each of the samples listed in Table 15 were evaluated for ignitable liquid residue (ILR) using the analytical procedures described in Section 4.2.2. The persistence of the gasoline on the substrates varied with both substrate and exposure duration. Table 16 and Figure 122 present the persistence results. Gasoline was found to be the most persistent when spilled onto the carpet substrate. The fuel was positively identified for all total heat exposures evaluated. The persistence of the fuel on plywood was the next most prevalent with gasoline positively identified in all samples except the most severe (i.e., 39 MJ/m^2 of total heat exposure). The vinyl flooring and furniture material proved to be the most challenging spill substrate to positively

identify ILR. For these materials, gasoline was only identified after the least severe exposure (i.e., 3.6 MJ/m^2).

It should be noted that in addition to the variables identified in Table 16, the time to collection was also varied. For each total heat exposure, a 4-hour and 48-hour collection time were considered. However, for the time frames considered, the delay in sample collection did not impact the identification of the presence of gasoline in the fire debris.

Table 16. Summary of ASTM E1618 ILR evaluation results from small-scale persistence study.

Test ID	Substrate	Thermal Exposure Severity	Exposure Duration (min.)	Total Heat Exposure (MJ/m^2)	Mass Loss Fraction	Detectable ILR (Y/N)
C1	Carpet	Flame Plume (~30kW/m^2)	2	3.6	0.07	Y
C2					0.07	Y
C3			10	18	0.26	Y
C4					0.28	Y
C5		Flame Plume + External (~65kW/m^2)	2	7.8	0.15	Y
C6					0.14	Y
C7			10	39	0.50	Y
C8					0.56	Y
W1	Plywood	Flame Plume (~30kW/m^2)	2	3.6	0.10	Y
W2					0.05	Y
W3			10	18	0.35	Y
W4					0.43	Y
W5		Flame Plume + External (~65kW/m^2)	2	7.8	0.20	Y
W6					0.20	Y
W7			10	39	0.81	N
W8					0.80	N
V1	Vinyl	Flame Plume (~30kW/m^2)	2	3.6	0.10	Y
V2					0.10	Y
V3			10	18	0.33	N
V4					0.34	N
V5		Flame Plume + External (~65kW/m^2)	2	7.8	0.19	N
V6					0.17	N
V7			10	39	0.66	N
V8					0.66	N
F1	Furniture Material	Flame Plume (~30kW/m^2)	2	3.6	0.33	Y
F2					0.36	Y

Test ID	Substrate	Thermal Exposure Severity	Exposure Duration (min.)	Total Heat Exposure (MJ/m^2)	Mass Loss Fraction	Detectable ILR (Y/N)
F3			10	18	0.54	N
F4					0.47	N
F5		Flame Plume + External (~$65kW/m^2$)	2	7.8	0.47	N
F6					0.44	N
F7			10	39	0.97	N
F8					0.92	N

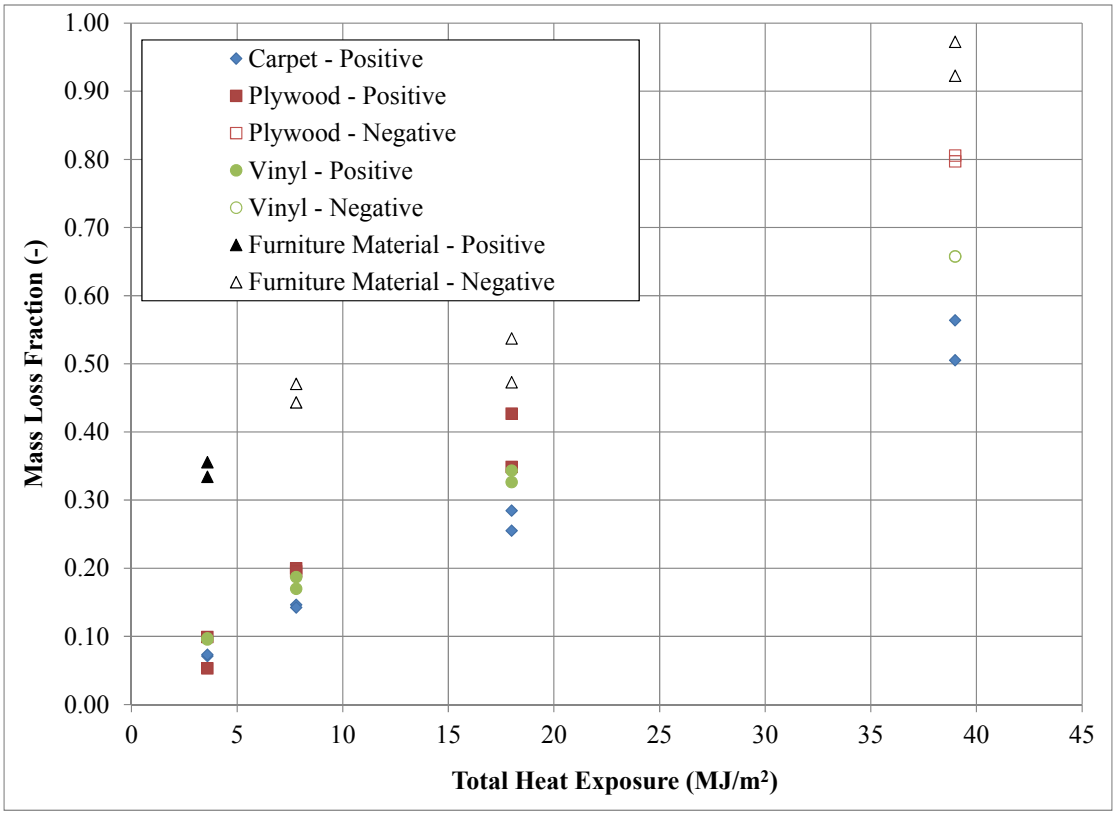

Figure 122. Persistence of ILR relative to mass loss fraction and total heat exposure (data from Table 4.3).

Based on the data provided in Table 16, a material degraded by more than 60 percent consistently provided a negative indication of ILR (i.e., no gasoline residue identified despite the fact that it was initially present), for all substrates considered. For the vinyl and furniture materials, this threshold was found to be as low as 17 and 44 percent, respectively. An upper bound (i.e., maximum extent of degradation before all ILR consumed) could not be determined from the testing conducted. The carpet substrate exhibited the highest degree of thermal degradation (i.e., 56 percent consumed) with positive ILR indications identified.

The persistence of the gasoline in the carpet substrate is most likely due to the absorptivity of the carpet material itself, as well as the polyurethane foam padding and plywood underlayment. The porous nature of these materials channels the gasoline away from the surface of the substrate thus shielding the fuel from the radiant exposure and prolonging the duration in which the ILR can remain within the substrate. This logic is generally supported by the results obtained for the plywood substrate. In the case of the vinyl substrate, since the material is relatively impermeable, the gasoline could not be absorbed/protected and was progressively degraded prior to and while the substrate was degraded. The lack of persistence of the gasoline residue when applied to the furniture material is attributed to the combustible nature of the materials that made up this substrate. When compared to the other three substrates, the furniture material was relatively easily ignited and burned vigorously with very little charring or residual material after combustion. This type of combustion does not lend itself to preserving the gasoline residue after even moderate thermal exposures.

Based on these results, when tested at small-scale, gasoline was found to be most persistent when spilled onto carpet flooring. The likelihood of the residue remaining on various other substrates was found to be progressively less probable for plywood, vinyl, and furniture material, respectively. From these tests, it was determined that the absorptivity and combustibility of the substrate were the factors that most impacted the persistence of the gasoline on the substrate. The results indicate that an evaluation of the degree of fuel consumption can be used to assess the expectation of being able to detect ILR. Consequently, a negative ILR result is not conclusive that an accelerant was not present, but a positive ILR result is conclusive of its presence.

4.4 Ignitable Liquid Residue Sampling Location Study

An objective of this study was to determine optimal locations to collect ILR samples within a fire pattern for given fire scenarios. Factors considered in the testing included the total heat exposure to the spill substrate, the burning environment, the location of the pattern relative to burning objects, the location of the pattern relative to ventilation openings, and the sampling location within the pattern. This objective was accomplished by way of full-scale testing in the open and in a compartment. Open burning spill fire tests were conducted to evaluate the persistence of ILR at various locations within a fuel spill fire pattern when only subjected to radiant heating from the fire plume. Full-scale enclosure fire testing was performed to evaluate the impact of the enclosure, ventilation, and adjacent burning objects.

Stauffer et al. [2008] indicated that fuel volatility will dictate the potential for a fuel having detectable ILR quantities that survive a fire. The author concluded that highly volatile fuels will be consumed quickly in a fire and be less likely to survive post-fire activities while low volatility fuels will be consumed at a slower rate and have a higher likelihood of surviving post-fire exposures. Based on this conclusion, gasoline was selected as the fuel in all tests conducted for this study to provide a conservative assessment of where residue is most prevalent after a fire. Gasoline was deemed a conservative fuel choice because the fuel is highly volatile meaning the fuel is readily depleted during fire events. Therefore, in instances where the fuel persists it is a reasonable assumption that less volatile fuels would also persist only with a greater prevalence on the substrate.

For the full-scale enclosure fire scenarios, the impact of pattern location was evaluated based on the proximity of the pattern to both the enclosure vent as well as neighboring Class A combustibles that were involved in the fire. Where applicable, samples were collected along the perimeter of patterns from an area proximate to and remote from these locations to determine what effect, if any, they have on the persistence of ILR on the flooring material. Finally, the location of the sample within the pattern was evaluated to determine where ILR was most prevalent, thus establishing an optimal sampling location. Exposure durations were evaluated by allowing fires to burn for different periods of time.

4.4.1 Sampling and Documentation

After each test, ILR samples were collected from various locations within a given pattern. The number and location of samples collected was dependent upon the conditions of the test. An overview of the general methodology used to collect samples from both open burning and enclosed fire tests is described below. Photographs were used to document the fire patterns present in the enclosure after each test.

4.4.1.1 Open Burning Tests

For open burning tests, samples were collected from various locations within the spill fire pattern in each test. It should be noted that heat release rate data was not collected for the open burning tests discussed in this ILR study. The ten tests conducted for this report were conducted strictly for ILR evaluation. For all tests, the sampling locations included samples collected at the edges of the pattern, the midpoint between the edge and center, and at the center of the pattern. In these tests, and all tests evaluated in this study, edge sampling consisted of collecting material from both the consumed and virgin material at the edge of the pattern as recommended by Stauffer et al. [2008]. Photographs of representative sampling locations for each substrate type are provided in Figure 123.

Figure 123. Representative ILR sample locations on vinyl (left) and carpet (right) flooring for open burning tests.

4.4.1.2 Enclosure Fire Tests without Class A Fuels

Two different enclosure fire tests were conducted without any Class A fuels present within the enclosure, except flooring material (Test Series 4). The flooring material used in these tests was the same carpet and vinyl systems used in all previous testing. In these tests, a 2.0 L (0.53 gal) gasoline spill fire was ignited in the center of the enclosure. In each test, a total of nine ILR samples were collected. A greater amount of samples were collected in these tests because of the additional fuel spill volume as well as the added variable of the impact of the vent on the burning behavior of the spill fire. In these tests, sampling locations were based on both a visual assessment of the spill fire pattern on the flooring material, when present, as well as the knowledge of the location the spill from pre-test observations, when patterns did not persist through the test exposure. An ideal representation of the sampling locations, as well as a photograph of actual sampling locations from the carpet spill fire is provided in Figure 124. A description of the sample locations is described in Table 17.

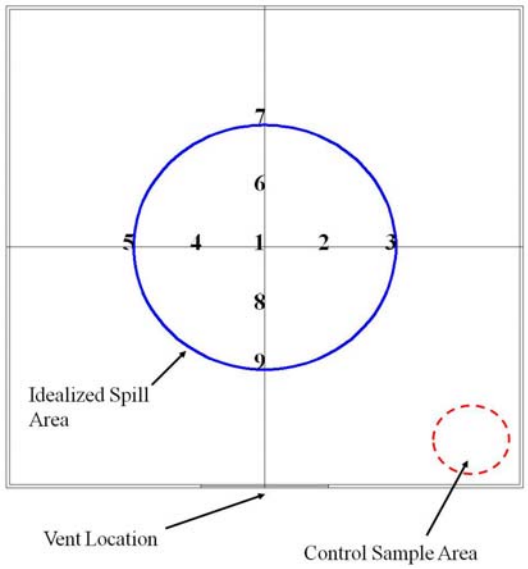

(a)

(b)

Figure 124. Ideal representation (a) and photograph (b) of actual ILR sampling locations for a gasoline spill fire on carpet flooring within the test enclosure (Test 4-2).

Table 17. Rationale for ILR sampling locations on flooring materials in Test Series 4.

Location(s)	Sampling Location
3/5/7/9	Edges of pattern/Recommended location [Stauffer et al. 2008]
2/4/6/8	Midpoint between edge and center of pattern
1	Center of Pattern

The sample locations described above were used to identify optimal locations via several different comparisons. Comparing results from locations 3/5/7/9 to results from locations 2/4/6/8 were selected to provide insight into which location, edge or mid-point has a higher likelihood of ILR being present. These locations were also compared to the center location to identify an optimal location within the entire pattern. The impact of ventilation was also evaluated by comparing results from locations 8/9 to locations 6/7 with the proximity of 8/9 to the vent relative to 6/7 being deeper in the compartment.

4.4.1.3 Enclosure Fire Tests w/Class A Fuels

In Test Series 6, between four and eight samples were collected from both the fire patterns and Class A materials present within the enclosure. The number of samples collected was based primarily on the spill area created in each fire scenario. A brief summary of the scenarios evaluated in Test Series 6 is provided in Table 18. For a complete description of these tests, the reader is referred to the companion report [Mealy et al. 2013].

Table 18. Summary of tests conducted in Test Series 6 from Mealy et al. [2013].

Test ID	Ventilation Scenario	Flooring Type	Ignition Scenario
6-0	Full Door	Carpet	Class A
6-1	Full Door		Fuel Spill on Floor
6-2	Slit Vent		
6-3	Full Door		Fuel Spill on Upholstered Chair
6-4	Slit Vent		
6-5	Full Door	Vinyl	Fuel Spill on Floor
6-6	Slit Vent		
6-7	Full Door		Fuel Spill on Upholstered Chair
6-8	Slit Vent		

In general, three different pattern scenarios were created during the execution of the nine tests listed in Table 18. For Tests 6-1 and 6-2, the spill fire pattern on the floor was relatively confined due to the absorptivity of the carpet flooring. This limited spill fire pattern size

prevented the need for collecting multiple samples from the pattern. In Tests 6-5 and 6-6, the vinyl flooring allowed the gasoline spill to spread over a large area of the flooring. This large fire area provided sufficient debris that multiple samples could be collected and evaluated. In Tests 6-3, 6-4, 6-7, and 6-8, samples were collected from the upholstered chair, beneath the upholstered chair, and on the flooring where the trailer was poured. Representative photographs of these spill scenarios are provided in Figure 125 through Figure 127, respectively. Illustrations and photographs of sample locations for each test are provided in the discussion of results below.

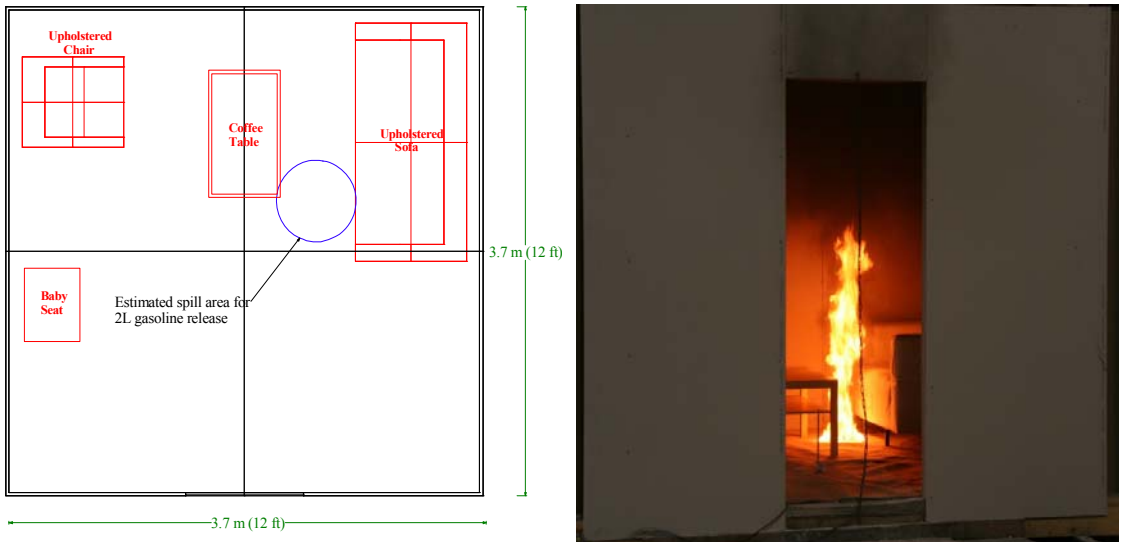

Figure 125. Localized spill fire on carpet (Test 6-1).

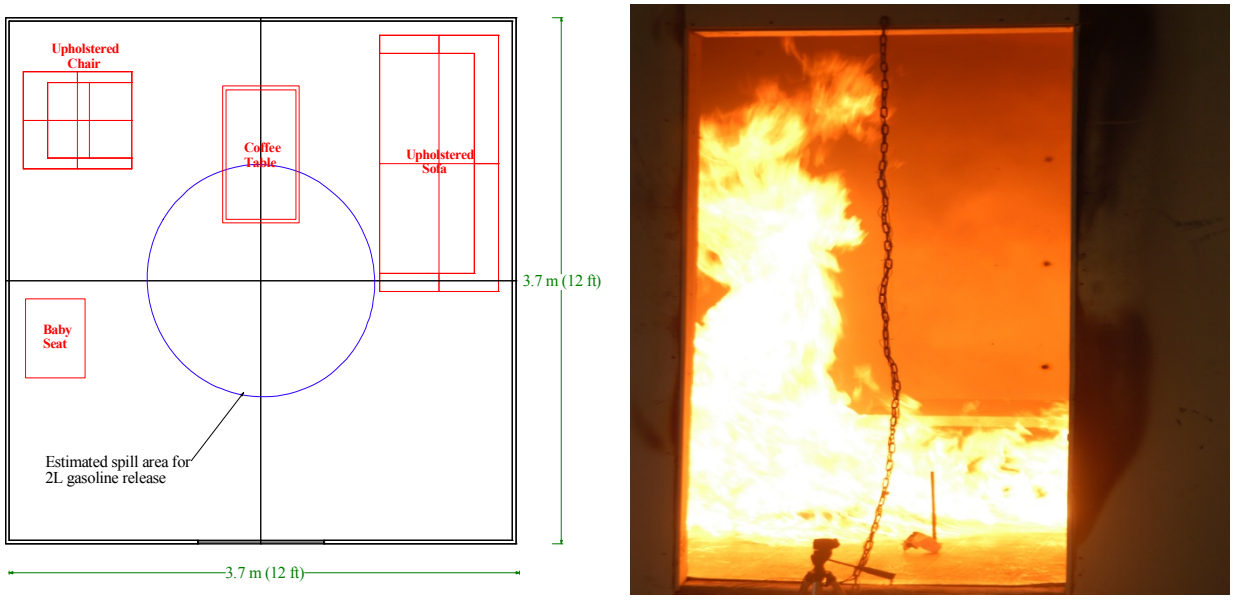

Figure 126. Large spill fire on vinyl flooring (Test 4-1).

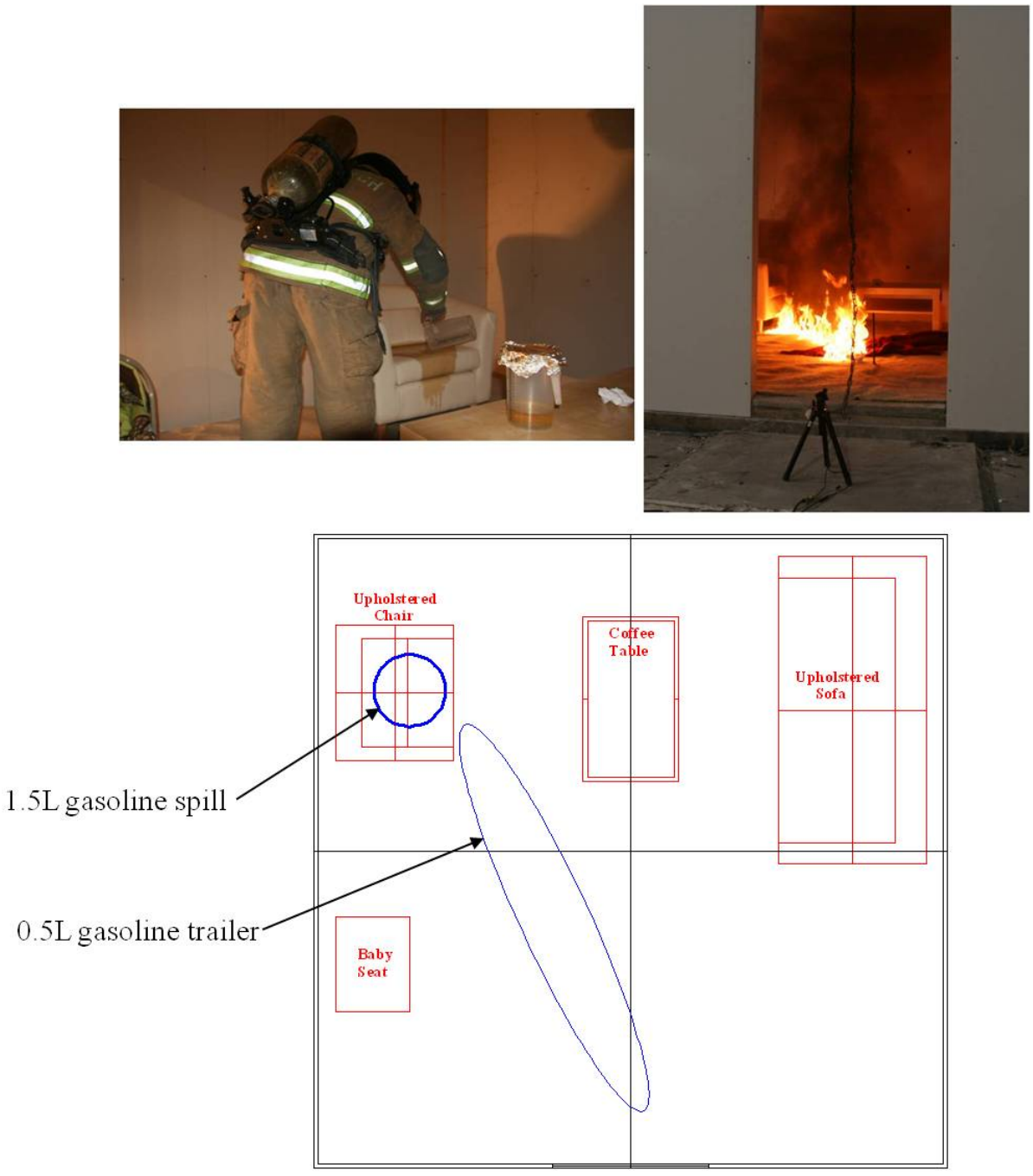

Figure 127. Gasoline spill on seat of upholstered chair (left) and trailer leading from front of chair to doorway (right) (Test 6-3).

4.4.1.4 Control Samples

It has been demonstrated that numerous common household materials contain detectable levels of petroleum products [Lentini et al. 2000]. Furthermore, in the event of a fire, the thermal decomposition of these materials could result in the presence of ILR signatures on neighboring materials. Consequently, it is necessary to collect and analyze control samples for comparison.

The collection of control samples is recommended in numerous publications and standards of care [Lentini et al. 2000, NFPA 921 2011]. In this study, control samples were collected at the same time ILR samples were collected. Control samples were collected from areas as remote from the burn pattern as was possible.

4.5 Open Burning Test Results

A series of ten 0.5 L (0.13 gal) open burning gasoline spill fires were conducted on carpet and vinyl substrates. These spill fires were manually poured in the center of a 1.2 m (4 ft) square substrate sample. The vinyl samples were permitted to burn to self-extinguishment which was on average 46 seconds. The carpet samples were manually extinguished with a hand-held carbon dioxide extinguisher with burning durations of 156 seconds (2.5 minutes). Fires were extinguished once the primary fire was out and there was only a residual ring of flamelets. ILR samples were collected 24 hours after the spill fire was extinguished. A summary of the results from the ILR analysis on these samples is provided in Table 19. Tests C1–C5 were replicate open burn fires conducted on carpet flooring and Tests V1–V5 were open burn fires conducted on vinyl flooring. These tests were conducted strictly for the ILR sampling study (i.e., heat release data was not collected in any of these tests). The total heat exposures in these tests were calculated using the measured burning durations and the assumed heat feedback to the substrate based on heat flux data collected for similar spill fires on similar substrates by Mealy et al. [2011].

Table 19. Summary of ILR results from open burning spill fire testing.

Test ID	Total Heat Exposure (MJ/m^2)	Sample ID	Sample Collection Location	Detectable ILR (Y/N)
C1	5.9	C1-1	Edge	Y
		C1-2	Midpoint	Y
		C1-3	Center	Y
		C1-4	Midpoint	Y
		C1-5	Edge	Y
C2	5.9	C2-1	Edge	Y
		C2-2	Midpoint	Y
		C2-3	Center	Y
		C2-4	Midpoint	Y
		C2-5	Edge	Y
C3	5.0	C3-1	Edge	Y
		C3-2	Midpoint	Y
		C3-3	Center	Y
		C3-4	Midpoint	Y
		C3-5	Edge	Y
C4	5.0	C4-1	Edge	Y
		C4-2	Midpoint	Y
		C4-3	Center	Y
		C4-4	Midpoint	Y
		C4-5	Edge	Y

Test ID	Total Heat Exposure (MJ/m^2)	Sample ID	Sample Collection Location	Detectable ILR (Y/N)
C5	1.8	C5-1	Edge	Y
		C5-2	Midpoint	Y
		C5-3	Center	Y
		C5-4	Midpoint	Y
		C5-5	Edge	Y
V1	3.4	V1-1	Edge	Y
		V1-2	Midpoint	Y
		V1-3	Center	N
		V1-4	Midpoint	Y
		V1-5	Edge	Y
V2	3.5	V2-1	Edge	Y
		V2-2	Midpoint	Y
		V2-3	Center	N
		V2-4	Midpoint	Y
		V2-5	Edge	Y
V3	2.5	V3-1	Edge	Y
		V3-2	Midpoint	Y
		V3-3	Center	Y
		V3-4	Midpoint	Y
		V3-5	Edge	Y
V4	2.6	V4-1	Edge	Y
		V4-2	Midpoint	Y
		V4-3	Center	Y
		V4-4	Midpoint	Y
		V4-5	Edge	Y
V5	3.2	V5-1	Edge	Y
		V5-2	Midpoint	Y
		V5-3	Center	N
		V5-4	Midpoint	Y
		V5-5	Edge	Y

In general, the results obtained for both the carpet and vinyl flooring material were similar for these open burning scenarios in that the majority of samples collected were positively identified as containing ILR. The thermal exposures produced by these spill fire scenarios were not sufficient to completely consume the ILR present on the flooring materials. This conclusion is consistent with the cone calorimeter results in Table 16, where gasoline on plywood persisted for total heat exposures of 7.8 MJ/m^2 and more and gasoline on vinyl persisted for exposures as low as 3.6 MJ/m^2. The maximum estimated total heat exposures in these spill tests were 5.9 MJ/m^2 for the plywood and 3.5 MJ/m^2 for the vinyl. Both values are less than the threshold values

identified in the small-scale testing (Table 16) as being sufficient to completely consume ILR on the given substrate.

The total heat exposure for the spill fires was estimated using the burning durations for each test and the radiant heat feedback values obtained from the literature. Burning durations measured during spill fires on vinyl flooring ranged from 38–53 seconds and for the carpet scenarios ranged from 60–196 seconds. For the vinyl tests, the radiant heat feedback to the fuel/substrate surface was estimated to be 66 kW/m^2. This value was taken from heat flux data collected by Mealy et al. [2011] when conducting 1.0 L (0.26 gal) gasoline spill fires on vinyl substrates. The value represents an average of four tests with the heat flux being collected from the center of the spill. For the carpet tests, the radiant heat feedback to the fuel/substrate surface was estimated to be 30 kW/m^2. Although similar scenarios (i.e., spill fires on carpet) were conducted by Mealy et al. [2011], radiant heat feedback data was not collected by the author in these tests. Consequently, the 30 kW/m^2 value used in this work was based on literature data for similarly sized (i.e., 0.3 m [1 ft] diameter) heptane pool fires. [Hammins et al. 1994]. The gasoline spill fires in this study ranged from 0.3– 0.45 m (12–18 in.) in diameter.

In three of the five vinyl spill fire tests (V1/V2/V5), ILR was not identified in the sample taken from the center of the spill pattern. The absence of ILR at this location in three separate tests suggests that the consumption of ILR within the fire pattern begins at the center of the pattern, where the thermal exposure to the substrate from the fire plume is most severe. This is consistent with the results of O'Donnell (see Section 4.1.3). The burning durations in these tests were also the longest of the five vinyl tests conducted with the corresponding total heat exposure values being the closest to the 3.9 MJ/m^2 threshold identified in small-scale testing.

4.6 Full-scale ILR Sampling Test Results

A total of nine full-scale enclosure fires were conducted using a 2.0 L (0.53 gal) gasoline spill fire as the ignition scenario. These fires were conducted using two different ventilation conditions such that differing thermal conditions could be achieved using the same initiating fire source. Two of the nine tests (Tests 4-1 and 4-2) were conducted with only flooring material present within the enclosure. A summary of the thermal conditions developed and duration of the fire exposures in these tests is provided in Table 20. For a complete description of the test scenarios and thermal conditions developed in these tests, the reader is referred to the companion report [Mealy et al. 2013].

As discussed earlier in this report (Fire Pattern Analysis) for the majority of these tests, the spill fire patterns on the flooring material did not persist through the fire scenario. Consequently, the locations of the ILR sample collections were determined based primarily on pre-test knowledge of the location of the initiating fire.

Table 20. Summary of thermal conditions developed during full-scale enclosure fire testing.

Test ID	Ventilation Scenario	Flooring Type	Ignition Scenario	Peak HRR (MW)	Avg. Upper Layer Temperature (ºC [ºF])	Test Duration (s)
4-1	Full Door	Vinyl	Fuel Spill on Floor	3.0	705 [1301]	88
4-2	Slit Vent	Carpet		0.9	385 [725]	330
6-1	Full Door	Carpet	Fuel Spill on Floor	6.3	655 [1211]	260
6-2	Slit Vent			0.9	415 [779]	480
6-3	Full Door		Fuel Spill on Upholstered Chair	7.2	715 [1319]	264
6-4	Slit Vent			1.8	500 [932]	713
6-5	Full Door	Vinyl	Fuel Spill on Floor	5.0	755 [1391]	186
6-6	Slit Vent			1.1	413 [775]	506
6-7	Full Door		Fuel Spill on Upholstered Chair	3.7	715 [1319]	190
6-8	Slit Vent			0.9	605 [1121]	566

4.6.1 Enclosed Spill Fires without Class A Fuels

Eighteen ILR samples, nine from each flooring system, were collected from these two enclosure fires. Of these eighteen samples, only three were positively identified as containing ignitable liquid residue, all from the carpet flooring material. No positive identifications were made for the debris collected from the vinyl flooring. Carpet samples containing ILR were collected from the center, right mid-point, and front mid-point of the carpet spill pattern. A summary of the sample locations evaluated and the associated ILR results is provided in Table 21. A comparison of the average floor heat flux profiles measured during each test is provided in Figure 128.

Table 21. Summary of ILR results from enclosed gasoline spill fires without Class A fuels present.

Flooring Substrate	Sample Collection Location	Detectable LR (Y/N)
Carpet	Center	Y
	Right Mid-Point	Y
	Right Edge	N
	Left Mid-Point	N
	Left Edge	N
	Rear Mid-Point	N
	Rear Edge	N
	Front Mid-Point	Y
	Front Edge	N
Vinyl	Center	N
	Right Mid-Point	N
	Right Edge	N
	Left Mid-Point	N
	Left Edge	N
	Rear Mid-Point	N
	Rear Edge	N
	Front Mid-Point	N
	Front Edge	N

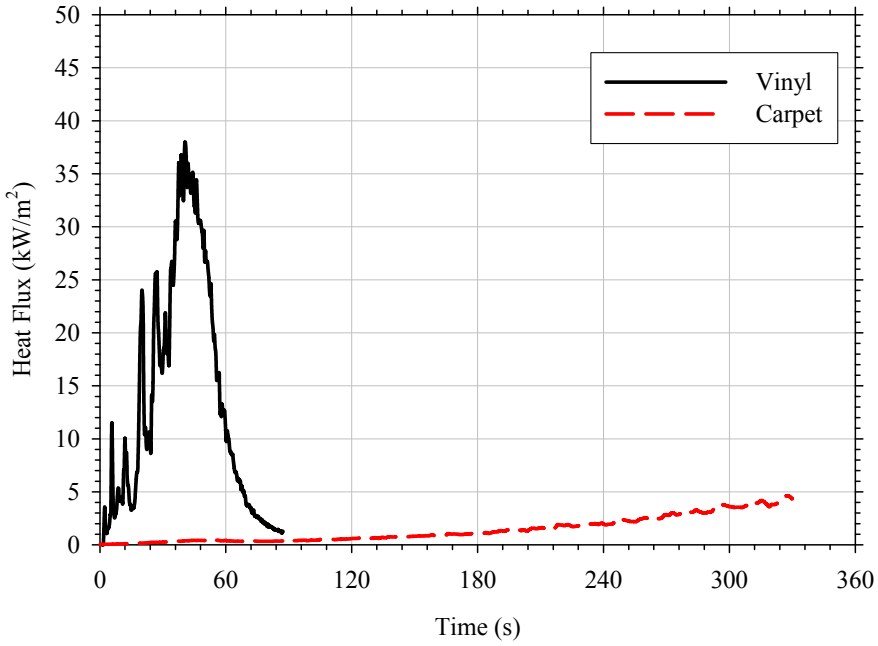

Figure 128. Comparison of average floor heat fluxes measured for 2.0 L (0.53 gal) gasoline spill fires on vinyl and carpet flooring.

Based on the data provided in Figure 128, the total heat exposure from the hot upper layer to the carpet flooring was calculated to be approximately 0.5 MJ/m^2 while for the vinyl flooring test the value was 1.2 MJ/m^2. These values only account for the radiant heat exposure from the flame plume to the extent the heat flux gauges in the corners of the enclosure see this heat, which would actually be greater in the center of the spill fire. For discussion purposes, the radiant heat feedback from the fire plume to the substrates in these tests was approximated for each substrate type.

For the vinyl test, the radiant heat feedback to the fuel/substrate surface was estimated to be 66 kW/m^2. This value was taken from heat flux data collected by Mealy et al. [2011] for 1.0 L (0.26 gal) gasoline spill fires on vinyl substrates. The value represents an average of four tests with the heat flux being collected from the center of the spill. Using this approximation, the total heat exposure to the vinyl flooring system was estimated to be 7.3 MJ/m^2 (6.1 MJ/m^2 from the spill fire and 1.2 MJ/m^2 from the enclosure environment). As shown in Table 16 for the cone calorimeter tests, ILR was positively identified for vinyl samples subjected to 3.6 MJ/m^2 but not 7.8 MJ/m^2. The estimated value of 7.3 MJ/m^2 for the compartment test is consistent with the small-scale persistence results.

For the carpet test, the radiant heat feedback to the fuel/substrate surface was estimated to be 30 kW/m^2. Although similar scenarios were conducted by Mealy et al. [2011] (i.e., spill fires on carpet), radiant heat feedback data was not collected by the author in those tests. Consequently, the 30 kW/m^2 value used in this work is based on literature data for similarly sized liquid fuel fires [Hammins et al. 1994]. Using the 30 kW/m^2 and the measured incident heat flux to the carpet flooring from the hot upper layer, the total heat exposure was estimated at 11.1 MJ/m^2. As shown in Table 4.3 for the small-scale tests, ILR from gasoline spill fires on carpet flooring persisted for total heat exposures of 3.6 to 39 MJ/m^2. Although the compartment spill fire estimate of 11 MJ/m^2 is within the range for expected ILR persistence, only three samples had positive measurements for gasoline. An illustration of the areas in which positive and negative identifications were made is provided in Figure 129. Although the outer sample locations were within the burn pattern, they were outside of the initial spill pattern. The locations with positive ILR measurements were the center sample and the adjacent front and right samples that were within the initial spill area. The geometrically similar samples to the left and back of the center had no measured ILR. This may be a result of the total heat exposure in this area being much higher than estimated due to the fire plume bending toward the back of the compartment and radiating those areas to a greater degree. This leaning plume effect was visually observed during the test but could not be adequately documented due to loss of visibility within the enclosure. The bending of the plume toward the rear of the enclosure is also evident in the fire pattern shown in Figure 129 by the greater extent of burning between the center of the spill and the rear wall. Also shown in Figure 129 is an idealized spill area overlaid on the post-test photograph. The movement of the fire in this direction would have subjected the flooring material in these areas to greater thermal exposures that were potentially sufficient to completely consume the liquid fuel and associated residue.

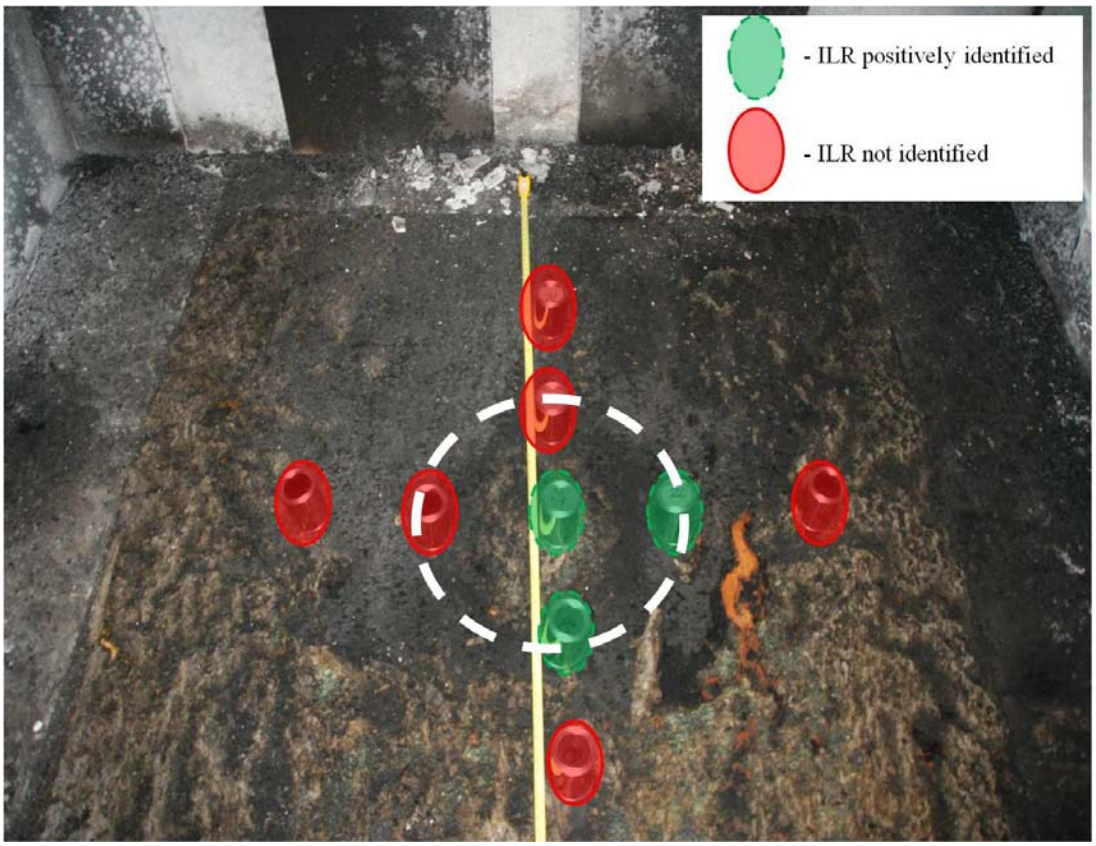

Figure 129. Locations of positive and negative ILR identification after enclosed gasoline spill fire on carpet flooring test without Class A fuels present.

The outer edge samples were collected from these locations based on the recommendation in the literature that fire debris samples be collected from the edges of patterns. The pattern was identified based on the visual observation of the line of demarcation between blackened and partially degraded carpet material. The absence of ILR in the edge samples was expected based on observations of the initiating spill fire. As described in the companion report [Mealy et al. 2013], the initiating spill fire only covered an area of approximately 0.2 m^2 (2.2 ft^2), an area far less than the visual pattern observed in Figure 129. The difference in the area between the initiating fuel spill area and the fire pattern on the carpet flooring was attributed to the carpet flooring at the edges of the spill fire igniting and gradually propagating outwards. Similar patterns and fire growth were described for open burning spill fires on carpet in previous testing [Mealy et al. 2011].

As indicated above, the results from these compartment tests are consistent with the findings of the small-scale persistence study described in Section 4.3. Full-scale gasoline spill fire testing showed that the persistence of ILR on vinyl when subjected to even relatively brief thermal exposures within an enclosure can be minimal. The impermeable nature of the flooring material limits the extent to which the fuel can be preserved/protected when subjected to a thermal exposure. Consequently, the volatile nature of the fuel leads to it being consumed. Comparing the results of Table 19 for gasoline fires on vinyl in the open to the compartment fires clearly demonstrates that the added effect of the hot layer, even from a brief fire, is sufficient to eliminate ILR. In the open burning tests, ILR persisted for most samples except a few in the

center of the spill fires. In the compartment fire, there was no ILR at any location. Based on the total heat exposure to the floor, it is possible to estimate whether ILR would be expected to persist. Consequently, there may be a range of compartment volume to fire size scenarios that may result in ILR persistence. The larger the room relative to the fire size the greater the possibility for ILR to be detected.

Contrary to the results obtained from the vinyl flooring, ILR was identified in several of the carpet samples that were exposed to a slightly more severe enclosure fire. This preservation is attributed to the absorptivity of the flooring material, which enabled the fuel to be channeled away from the exposed surface thus preventing immediate and complete combustion. Although ILR was found, the persistence of the residue was found to be non-uniform and positive samples were collected from locations that were not traditionally recommended samplings areas (i.e., midpoint between the center and edge of pattern). Although positive ILR measurements were made, the compartment fire environment did yield a lower probability of persistence than in the open spill fire scenarios, where all sample locations had positive measurements for gasoline. Consequently, the greater the total heat exposure to the substrate in a compartment fire, the less chance there will be to positively identify ILR.

4.6.2 Gasoline on Carpet Floor with Full Door Opening (Test 6-1)

As described in Section 4.4.1.3, the gasoline spill fire scenario used in this test consisted of a localized spill directly onto the carpet flooring between the upholstered sofa and wooden table. The spill area was approximately 0.14 m^2 (1.5 ft^2). A complete description of the evolution of this enclosure fire test can be found in the companion report [Mealy et al. 2013]. However, it should be noted that during post-fire inspection of the enclosure, a section of flooring was identified beneath the collapsed wooden table that was protected during the test. This protection came when the table collapsed towards the upholstered sofa, as shown in the left image of Figure 130. The time at which the table collapsed could not be determined based on test video or observations. After collapsing, the wooden table shielded the initial spill area from any additional heating for the duration of the test. This protected area was identified when the table was removed from the enclosure during overhaul procedures and the flooring material was found to be attached to the underside of the table when the table was lifted out of the enclosure. A photograph of the space within the enclosure where this protected area was identified is provided in the right image of Figure 130. In this image both protected areas were found beneath the collapsed table. Several samples were collected from this single section of flooring material that was attached to the wooden table. Flooring ILR samples were collected from the plywood subfloor removed from the small circular pattern shown in Figure 130. The carpet, the foam padding underlayment, and a section of the wooden table itself were all collected and analyzed individually.

Figure 130. Condition of wooden table and flooring after Test 6-1 prior to overhaul (left) and after overhaul (right).

A total of eight ILR samples were collected in this test, three samples were taken directly from flooring material in the area of the spill, three samples were collected from neighboring Class A fuels (i.e., wooden table) and flooring material that had melted to the table, one sample was collected in the vicinity of the debris from the baby seat, and a single control was taken from the front right corner. An annotated photograph of the flooring after Test 6-1, with sampling locations identified, is provided in Figure 131. In the figure, samples shown in red were collected from the flooring material, while samples shown in blue were collected from the debris that was attached to Class A materials removed from the enclosure during overhaul. A summary of the ILR results from these samples is provided in Table 22. Six of the eight samples collected were identified as containing ILR from gasoline. All of the flooring samples and all of the debris samples collected from the protected area beneath the wooden table contained ILR.

Figure 131. ILR sampling locations for Test 6-1.

Table 22. Summary of ILR findings from Test 6-1.

Test ID	Sample ID	Sample Collection Location	Detectable ILR (Y/N)
6-1	1	Edge of Pattern furthest from Doorway	Y
	2	Center of Pattern	Y
	3	Edge of Pattern nearest Doorway	Y
	4	Control	N
	5	Edge of Baby Seat Melt	N
	6	Padding Melted to Table from Protected Area	Y
	7	Carpet Melted to Table from Protected Area	Y
	8	Section of Table that Created Protected Area	Y

The absence of ILR in samples 4 and 5 in this test scenario demonstrate that the combustion of both flooring material and Class A materials constructed from plastics (i.e., baby seat) did not produce compounds that could be mistaken as ILR from gasoline. The presence of ILR in samples 1–3 and 6–8 suggest that the collapse of the wooden table onto the area of the carpet flooring where the initial fuel spill occurred protected the fuel that was absorbed into the carpet but not yet combusted or only partially combusted. The collapse of the table onto the initial fuel spill area limited the extent to which the fuel could be consumed over the course of the fire. Consequently, ILR was identified in all samples collected from the vicinity of the initial spill. During overhaul of the table and flooring material in this area, the odor of gasoline was detected.

4.6.3 Gasoline on Carpet Floor with Slit Vent Opening (Test 6-2)

The spill fire scenario in this test was identical to that described for Test 6-1 in Section 4.6.2, except with a smaller vent. Only four ILR samples were collected from this test. Three samples were collected from the gasoline spill area between the upholstered sofa and wooden table and a single control sample was collected from the front right corner of the enclosure. Just as in Test 6-1, the wooden table collapsed at some point during the enclosure fire. However, in this test, the table collapsed in a manner that did not completely cover the area of flooring on which the initiating spill fire was poured. As shown in Figure 132(a), the table collapsed towards the rear right corner of the enclosure leaving some portion of the front of the spill area exposed. Based on visual observation of the spill just prior to ignition, an outline of the spill (dashed line) relative to the centerline of the sofa (solid line) is provided in Figure 132(a).

(a) Remains in place

(b) Remains removed

Figure 132. Position of collapsed wooden table after Test 6-2.

As shown in Figure 132(b), the carpet in the area between the upholstered sofa and wooden table was heavily charred but still present after Test 6-2. After the condition of the enclosure was documented, the Class A fuels within the space were removed and flooring samples were taken for analysis. An annotated photograph showing sample collection areas in this test is provided in Figure 133. A summary of the ILR analysis results for the samples collected from this test is provided in Table 23.

Figure 133. ILR sampling locations for Test 6-2.

Table 23. Summary of ILR findings from Test 6-2.

Test ID	Sample ID	Sample Collection Location	Detectable ILR (Y/N)
6-2	1	Front Edge of Pattern nearest Doorway	N
	2	Center of Pattern	Y
	3	Rear Edge of Pattern furthest from Doorway	Y
	4	Control	N

The absence of ILR in sample 4 was expected because it was collected as a control, but again demonstrates that the thermal degradation/combustion of the flooring material does not produce compounds that could be mistaken as ILR. The presence of ILR in samples 2 and 3 suggest that the collapse of the wooden table onto the area of the carpet where the initial fuel spill occurred protected the fuel that was absorbed into the carpet but had not yet been combusted or was only partially combusted. Given the presence of ILR in samples 2 and 3, the absence of ILR in sample 1 was investigated further. One hypothesis as to why no ILR was found at this location was that the thermal exposure from this test may have been sufficient to completely consume the fuel spill, had the table not collapsed onto the majority of the initial fuel spill area. Based solely on the radiant heat from the hot upper layer (3.0 MJ/m^2) and estimating the radiant heat from the fire plume over the duration of the test (30 kW/m^2 over 480 seconds ~ 14 MJ/m^2) the total heat

exposure to the floor is estimated at 17 MJ/m^2. This value is within the range of total heat exposures for which ILR persisted in small-scale test samples (Table 16). However, the value does not take into account radiant fluxes from neighboring Class A fuels burning (i.e., the upholstered sofa and wooden table) which when burning can produce fires as large as 1.2 and 0.6 MW, respectively [Mealy et al. 2013].

4.6.4 Gasoline on Upholstered Chair with Full Door Opening (with Carpet) (Test 6-3)

As described in Section 4.4.1.3, the gasoline spill fire scenario used in this test consisted of a 1.5 L (0.40 gal) spill directly onto the upholstered chair and a 0.5 L (0.13 gal) trailer from the chair toward the doorway. A complete description of the evolution of this enclosure fire test can be found in the companion report [Mealy et al. 2013]. A total of six ILR samples, consisting of four flooring material samples, one upholstered chair sample, and one control sample were collected after this test. Figure 134 shows the general location of the flooring and upholstered chair samples collected.

The samples were collected prior to the overhaul of the enclosure and the cans shown in Figure 134 were staged for illustrative purposes. The control sample was collected from the same general area (i.e., front right corner of the enclosure) as for all enclosure tests conducted. The upholstered chair sample that was collected was taken from the center of the wood base of the chair. This wooden base was essentially the only remaining structure of the upholstered chair after this test.

Figure 134. ILR sampling locations for Test 6-3.

Although a visible pattern of the trailer was not present after this test, the trailer path was noted prior to ignition such that samples could be collected from within an area that was known to have gasoline present at the start of the test. A summary of the ILR analysis results for the samples collected from this test is provided in Table 24.

Table 24. Summary of ILR findings from Test 6-3.

Test ID	Sample ID	Sample Collection Location	Detectable ILR (Y/N)
6-3	1	Trailer (near door)	N
	2	Trailer (near table)	N
	3	Trailer (in front of chair)	N
	4	Flooring at foot of chair	Y
	5	Wood base of chair	Y
	6	Control	N

As shown in Table 24, ILR was only identified in two of the six samples collected. The absence of ILR in the control sample was expected. ILR was not found in the any of the trailer samples that were collected but was found in the flooring sample collected from underneath the upholstered chair as well as the sample taken from the wood base of the upholstered chair. The absence of ILR in any of the trailer sample areas was partly attributed to the relatively minimal amount of liquid applied. However, upon review of the trailer pattern (see Figure 135), it appears that the trailer ILR samples were not actually on the trailer location. This illustrates the difficulty of identifying appropriate locations for ILR due to the lack of clear patterns associated with a spill or trailer. This indicates how critical it is to systematically survey a larger area to increase the probability of sampling an actual ILR location.

4.6.5 Gasoline on Upholstered Chair with Slit Vent Opening (with Carpet) (Test 6-4)

The spill fire scenario in this test was identical to that described for Test 6-3 in Section 4.6.4. A total of seven ILR samples were collected after this test except with a smaller vent. Four samples were collected from various locations within the trailer, a single sample was collected from the wooden base of the upholstered chair, a single sample was collected from flooring material directly beneath the upholstered chair, and a control sample was taken. An annotated photograph showing sample collection areas is provided in Figure 136. All samples were collected at the centerline of the gasoline trailer. A summary of the results from ILR analysis of the samples shown is provided in Table 25.

(a)

(b)

Figure 135. Gasoline trailer created in Test 6-3 prior to and immediately after ignition.

(a)

(b)

Figure 136. Initial gasoline spill fire (a) and ILR sampling locations (b) for Test 6-4.

Table 25. Summary of ILR findings from Test 6-4.

Test ID	Sample ID	Sample Collection Location	Detectable ILR (Y/N)
6-4	1	Trailer (near door)	N
	2	Trailer (near table)	N
	3	Trailer (between table/chair)	Y
	4	Trailer (in front of chair)	Y
	5	Flooring material underneath chair	Y
	6	Wood base of chair	Y
	7	Control	N

ILR was positively identified in four of the seven samples collected. Samples 3–6 were all found to contain ILR while samples 1 and 2 did not. The absence of ILR in locations 1 and 2 is consistent with the greater thermal environment in the front of the enclosure. The limited ventilation conditions used in this test (i.e., slit vent) created a ventilation controlled environment whereby later in the fire, flaming combustion generally occurred in the vicinity of the vent due to the availability of combustion air. The heat flux profiles measured during the test (shown in Figure 137) show floor level values in the front of the enclosure being upward of ten times greater than those measured in the rear. Photographs in Figure 113 in Mealy et al. [2013] show the transition of the fire to the front of the enclosure in the second half of the fire, consistent with the heat flux profiles.

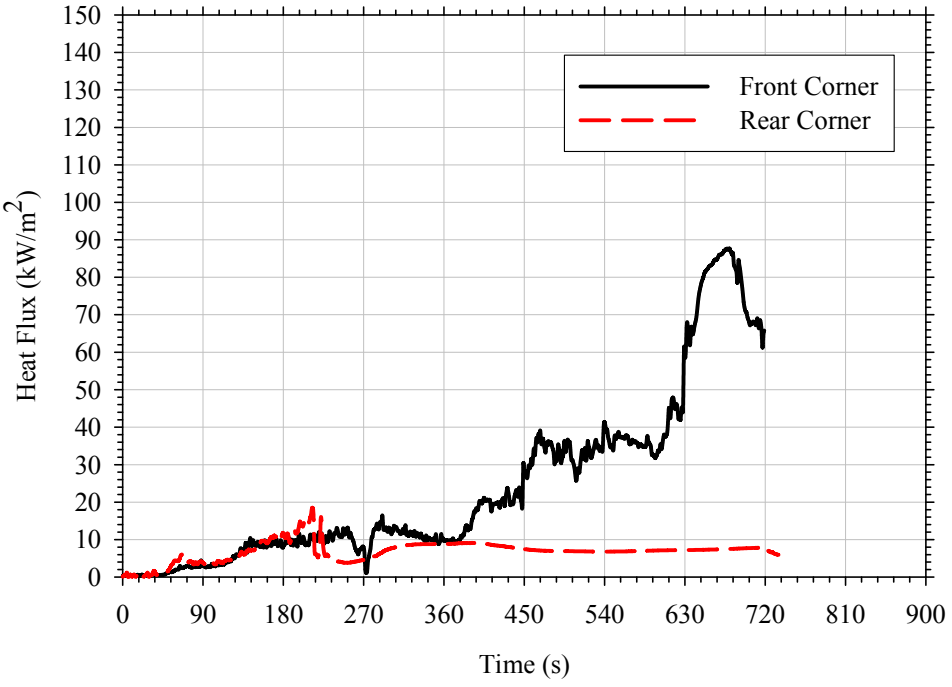

Figure 137. Floor level heat flux measurements collected during Test 6-4.

4.6.6 Gasoline on Vinyl Floor with Full Door Opening (Test 6-5)

The ignition scenario for this test produced a large area (1.6 m^2 [17 ft^2]) spill fire on the vinyl flooring. The spill was poured in the center of the enclosure, which was approximately 0.15 m (6 in.) in front of the wooden table on the vent side of the table. A complete description of the evolution of this enclosure fire test can be found in the companion report [Mealy et al. 2013]. Seven ILR samples were collected after this test. All samples were collected from the floor of the enclosure with five samples taken from within the initial spill area, a single sample taken from an area next to the upholstered sofa, and a single control sample. The sample removed from the flooring adjacent to the upholstered sofa (Sample 6) was collected because a decorative plastic bin was placed at this location prior to testing. The purpose of this sample was to determine if thermally degraded Class A materials, more specifically a melted polystyrene plastic bin, could yield a false-positive ILR sample. An annotated photograph showing sample collection areas is provided in Figure 138. A summary of the results from ILR analysis of the samples is provided in Table 26.

Figure 138. ILR sampling locations for Test 6-5.

Table 26. Summary of ILR findings from Test 6-5.

Test ID	Sample ID	Sample Collection Location	Detectable ILR (Y/N)
6-5	1	Edge of Pattern nearest Doorway	N
	2	Mid-point of Pattern nearest Doorway	N
	3	Center of Pattern	N
	4	Leftmost Edge of Pattern	Y
	5	Edge of Pattern furthest from Doorway	N
	6	Location of polystyrene container at edge of sofa	N
	7	Control	N

Out of the seven samples collected in this test, a positive indication of the presence of ILR was only found in one of the samples. The absence of ILR in samples 6 and 7 was generally expected but did confirm that in the scenario tested, the thermally degraded flooring/adhesive material (i.e., vinyl) as well as the Class A plastics do not create false-positive ILR samples. Of the remaining five samples, all of which were collected from within the initial fuel spill area, only one sample (Sample 4) contained ILR. Based on the small-scale and enclosure fire testing that was conducted without Class A materials present, the absence of ILR in the majority of the sampling locations was attributed to the complete combustion of all fuel present. Based on floor level heat flux measurements collected during the test, the total heat exposure in this test was estimated at 19 MJ/m^2. This value was well above the exposures identified in small-scale testing as being sufficient to completely consume any ILR on vinyl. The presence of ILR in sample 4 illustrates the potential for residue to remain under severe thermal conditions. The fact that this sample was located along the edge of the spill fire pattern supports the current recommendation to fire investigators that edge samples be collected [Stauffer et al. 2008].

4.6.7 Gasoline on Vinyl Floor with Slit Vent Opening (Test 6-6)

The fire scenario for this test was the same as that used in Test 6-5 except with a smaller vent. Seven ILR samples were collected. All samples were collected from the floor of the enclosure with five samples taken from within the initial spill area, a single sample taken from an area next to the upholstered sofa, and a single control sample. As described in Section 4.6.6, the sample removed from the flooring adjacent to the upholstered sofa (Sample 6) was collected to explore the potential for Class A plastic materials to create compounds that could be mistaken for ILR. An annotated photograph showing sample collection areas for this test is provided in Figure 139. A summary of the results from ILR analysis of the samples shown is provided in Table 27.

Figure 139. ILR sampling locations for Test 6-6.

Table 27. Summary of ILR findings from Test 6-6.

Test ID	Sample ID	Sample Collection Location	Detectable ILR (Y/N)
6-6	1	Edge of Pattern nearest Doorway	N
	2	Mid-point of Pattern nearest Doorway	N
	3	Center of Pattern	N
	4	Leftmost Edge of Pattern	N
	5	Edge of Pattern furthest from Doorway	N
	6	False positive taken near polystyrene container at edge of sofa	N
	7	Control	N

Positive ILR results were not reported for any of the samples collected from Test 6-6. The absence of ILR in this test was attributed to the prolonged thermal exposure to which the flooring material and fuel were subjected. The estimated total heat exposure to the flooring material over the duration of this test was calculated to be 44 MJ/m^2, a value that is well above any previous thermal exposure considered in either small- or full-scale testing for which ILR is expected to persist on vinyl.

4.6.8 Gasoline on Upholstered Chair with Full Door Opening (with Vinyl) (Test 6-7)

As described in Section 4.4.1.3, the gasoline spill fire scenario used in this test consisted of a 1.5 L (0.40 gal) spill directly onto the upholstered chair and a 0.5 L (0.13 gal) trailer from the chair to the doorway. A representative photograph of the gasoline trailer spill area when released onto the vinyl flooring is provided in Figure 140. Due to the impermeable nature of the vinyl flooring, although poured as a trailer, the gasoline naturally spread, resulting in more of wide patter as opposed to the traditional thin, line trailer pattern. A complete description of the evolution of this enclosure fire test can be found in the companion report [Mealy et al. 2013].

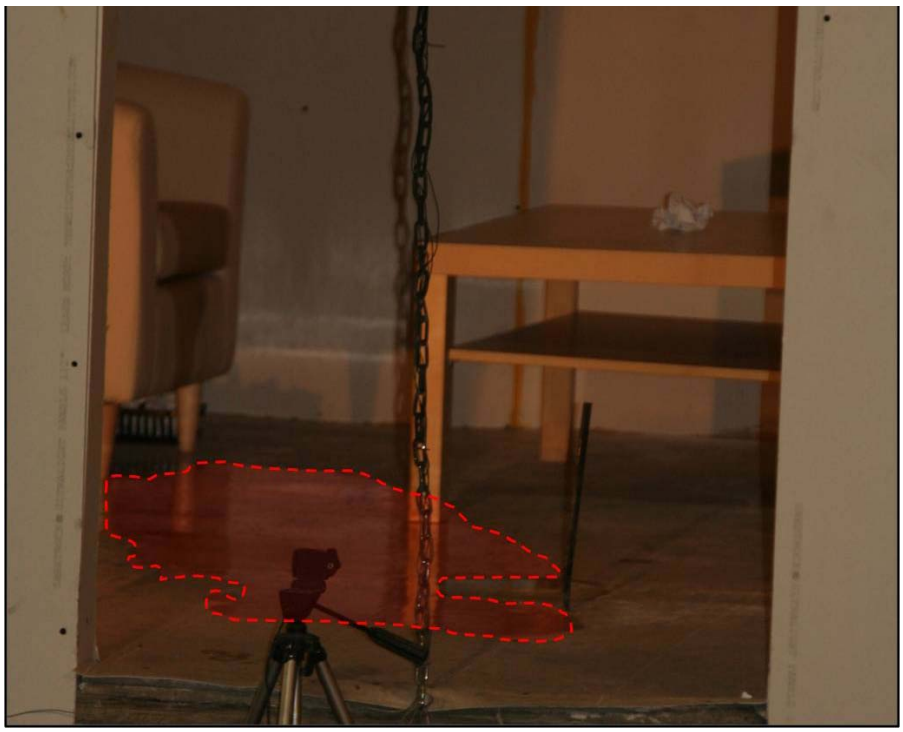

Figure 140. Annotated photograph showing representative gasoline trailer spill area on vinyl flooring.

Seven ILR samples consisting of five flooring material samples, one sample from the upholstered chair, and one control sample were collected. Figure 141(a) shows the general location of the flooring and upholstered chair samples collected. Figure 141(b) shows the damage to the flooring. A floor pattern extending from the left back corner toward the vent can be seen in Figure 141(b); however, it should be noted that the pattern is significantly broader than the initiating spill area. The control sample was collected from the same general area (i.e., front right corner of the enclosure) as for all enclosure tests conducted. The upholstered chair sample that was collected was taken from center of the wood base of the chair. This wooden base was essentially the only remaining structure of the upholstered chair after this test. A summary of the ILR results from this test are provided in Table 28.

(a)

(b)

Figure 141. ILR sampling locations (a) and condition of flooring proximate to vent (b) for Test 6-7.

Table 28. Summary of ILR findings from Test 6-7.

Test ID	Sample ID	Sample Collection Location	Detectable ILR (Y/N)
6-7	1	Trailer (near Door)	N
	2	Trailer (2 ft from Door)	N
	3	Trailer (near Table)	Y
	4	Trailer (center of Trailer)	Y
	5	Flooring at base of chair	N
	6	Upholstered chair debris	Y
	7	Control	N

Positive ILR identifications were made for two of the flooring samples taken from within the trailer and the sample collected from the wood base of the upholstered chair. The trailer samples containing ILR were taken from areas at the midpoint of the trailer proximate to the wooden table. As indicated earlier in this section, the location of the sampling points is based on the pre-test knowledge of the spill pattern. Samples taken near both the upholstered chair as well as the vent did not contain ILR. The non-uniformity of ILR presence within the trailer was consistent with the intensity of the burning at the vent and the duration of the upholstered chair burning negatively impacting the persistence of ILR in these areas. In this test, the upholstered chair burned for the duration of the test which in turn exposed the flooring material immediately in front of the chair, more so than in other locations, to a prolonged radiant exposure. Supporting data for this rationale was provided in Test 6-3, where the upholstered chair did not burn for such an extended period of time and ILR results at this location were positive. However, a different type of flooring was present in Test 6-3 (i.e., carpet) which has been shown to preserve ILR more efficiently than vinyl. Similarly, the vent burning that was observed for the last 75 seconds of this test, would have created a severe thermal exposure to the flooring material in this general area. The severity of the thermal exposure to the vinyl flooring in the vicinity of the vent is shown in Figure 141. In this photograph, large sections of vinyl are absent (i.e., consumed) as a result of the exposure. Thermal exposures in the central area of the trailer (Samples 3 and 4) were likely not as severe and therefore ILR was able to persist in these areas.

4.6.9 Gasoline on Upholstered Chair with Slit Vent Opening (with Vinyl) (Test 6-8)

The fire scenario for this test was the same as that used in Test 6-7 with the primary difference being the change to a more limiting ventilation scenario. Seven ILR samples were collected from the debris in this test. With the exception of Sample 6, all samples were collected from the floor of the enclosure with five samples taken from within the initial spill area (i.e., trailer and runoff from the spill on the upholstered chair) and a single control sample. An annotated photograph showing sample collection areas is provided in Figure 142. A summary of the ILR analysis for this test is provided in Table 29.

Figure 142. ILR sampling locations for Test 6-8.

Table 29. Summary of ILR findings from Test 6-8.

Test ID	Sample ID	Sample Collection Location	Detectable ILR (Y/N)
6-8	1	Trailer (near door)	N
	2	Trailer (2ft from slit vent)	N
	3	Trailer (near table)	N
	4	Flooring beneath chair	Y
	5	Trailer (in front of chair)	N
	6	Edge of the molten upholstered chair debris	Y
	7	Control	N

Only one of the flooring samples collected from within the trailer spill area was positively identified. The second sample positively identified was that taken from the upholstered chair debris. The presence of ILR in both of these samples was attributed to the absorption of gasoline into the chair components and the protection given to the ILR by the upholstered chair itself. In the case of the sample taken from the flooring beneath the chair, the upholstered chair served to shield the flooring material, to some extent, from the radiant heating generated by the upholstered chair/liquid fuel fires as well as the hot upper layer. The absence of ILR in any of the trailer pattern sample locations was attributed to the thermal exposure generated during this test. A total heat exposure of 14 MJ/m^2 was calculated for this test based on the heat flux measurements collected at floor level and the estimated radiant heat feedback from the vinyl spill

fire. This value is greater than the values identified in the small-scale testing as being sufficient to completely consume ILR on vinyl.

4.6.10 Analysis of ILR Sampling Location Study for Enclosure Fire Scenarios

The impact of the enclosure, ventilation scenario, and proximity of burning Class A materials was shown in the results presented in Sections 4.5 and 4.6.1–4.6.9. Each of these variables was found to impact the persistence of ILR in spill fire patterns in different ways for different substrates.

4.6.10.1 Impact of Enclosure

ILR results from the open burning and enclosed spill fire (without Class A materials) testing were compared and the impact of the enclosure was evaluated. For open burning scenarios, the presence of ILR on both carpet and vinyl samples was found to be prevalent, more so on carpet than on vinyl. In these tests, the fires burned to either self-extinguishment (vinyl) or until the fire decayed and transitioned to the burning of pad and carpet around the perimeter of the burned area. However, when similar fires were within a test enclosure measuring 3.7 m (12 ft) square by 2.4 m (8 ft) tall, the persistence of ILR on these substrates diminished dramatically with only select locations remaining.

The greater absence of ILR in the enclosure test is attributable to the added incident heat flux created by the hot upper layer as well as added radiant heat from other Class A fires. The increased heating of the floor in the enclosure is quite evident by the increased damage of the flooring that occurs across the whole compartment beyond the initial fuel spill area. For example, in the open, there was minimal damage on vinyl, and what was damaged was isolated to the initial spill area. In the compartment fires, the whole vinyl floor in the room was thermally damaged. Total heat exposures calculated in the open burning vinyl floor tests ranged from 3.0–4.7 MJ/m^2. This range of values falls between the exposures tested at small-scale that produced positive and negative ILR results. As stated in Section 4.5, in three of the five open burn tests, the center sample location produced negative ILR results with positive indications identified at midpoint (i.e., between center and edge) and edge locations. The fact that ILR was beginning to be consumed in some of the longer duration open spill fires indicates that the added heat provided by the enclosure is more than enough to consume any remaining ILR within the initial spill pattern. Based on the total heat exposure to the floor, it is possible to estimate whether ILR would be expected to persist. Consequently, there may be a range of compartment volume to fire size scenarios that may result in ILR persistence. The larger the room relative to the fire size the greater the possibility for ILR to be detected.

For the full-scale fire tests, ILR was identified more often in carpet samples than in vinyl, even though they were tested under similar fire scenarios. This effect was observed in the cone calorimeter testing that showed the critical total heat exposure for gasoline ILR in carpet to be much higher than that on vinyl (above 39 MJ/m^2 for carpet compared to below 8 MJ/m^2 on vinyl). This preservation is attributed to the absorptivity of the flooring material, which enabled the fuel to be channeled away from the exposed surface, thus preventing immediate and complete combustion. Although ILR was found in the compartment fires, the compartment fire environment yielded a lower probability of persistence than in the open spill fire scenarios,

where all sample locations had positive measurements for gasoline. Similar to the gasoline on vinyl fires, the greater the total heat exposure to the substrate in a compartment fire, the less chance there will be to positively identify ILR.

4.6.10.2 Potential for False-Positive Results from Thermally Degraded Materials

A total of twelve samples, not exposed to an ignitable liquid, were collected from the compartment fires. Eight of these samples were taken as controls, two were removed from the debris of a thermally degraded baby seat, and two were removed from the debris of a thermally degraded polystyrene tray. The control samples collected in this work consisted of thermally degraded flooring material, four carpet samples and four vinyl samples degraded to varying degrees. None of these samples were positively identified as containing ILR.

4.7 Summary of ILR Persistence and Sampling Location

A total of 52 small- and full-scale fire tests were conducted to study the persistence of an ignitable liquid residue on several different substrates subjected to varying fire conditions and to identify optimum locations from within fire patterns for ILR sampling. The focus of the small-scale testing was to characterize the persistence of an ignitable liquid residue on four different substrates exposed to four different total heat exposures. The substrates evaluated varied in porosity and propensity to burn and represented typical building materials (composite furniture materials, plywood, vinyl and carpet/pad). The results from this testing demonstrated that the likelihood of an ILR persisting within a given substrate was dependent upon both the total heat exposure and the ability of the substrate to absorb the ignitable liquid. Absorbent materials such as carpet flooring and plywood retained ILR under more severe thermal exposures than impermeable substrates, such as vinyl.

The absorbency of the ignitable liquid substrate was not the only factor identified as playing a key role in the persistence of ILR on the material. The combustibility of the material (i.e., how readily it burns) impacted the persistence of the ILR. The prime example of this was the composite furniture material. This material was the most absorbent material tested, however, it was also the most readily combusted (i.e., greatest mass loss at a given heat flux), which resulted in the material being the least likely to contain ILR after the thermal exposure. Based on the small-scale test results, gasoline was most persistent when spilled onto carpet and pad flooring. The likelihood of residue remaining on the other substrates tested was found to be progressively less probable for plywood, vinyl, and the furniture material, respectively. From these tests, approximate total heat exposure thresholds were calculated based on the exposure severity and exposure duration. The thresholds were calculated to provide estimates of the total amount of heat needed to consume the ILR present within the samples tested. A threshold was not established for carpet (i.e., ILR was always identified for the four total heat exposures considered, up to 39MJ/m^2). The threshold for plywood is between 18–39 MJ/m^2. The threshold for vinyl and the furniture material was between 3.6–7.8 MJ/m^2. It should be noted that this threshold is most likely dependent on the volume of ILR applied to the substrate with greater volumes requiring larger total heat exposures and vice versa. However, this variable was not explored in this work.

Full-scale testing was conducted to identify optimum sampling locations within fuel spill fire patterns. Open-burning and enclosed scenarios, with and without Class A furnishings, were evaluated. ILR results from open burning tests showed that in these scenarios the thermal insult from the spill fire alone is generally not sufficient to consume the ignitable liquid residue present within a given pattern. Samples were collected at edge, mid-point, and center locations for both carpet and vinyl substrates.

The results from open burning spill fires on carpet showed that in the absence of an external heat source, samples can be collected from anywhere within the original spill area to obtain positive ILR results. It should be noted that in many cases, even open burns with extended burning duration, the initial spill area is not readily identifiable. Consequently, for carpet scenarios, sampling from the center of the pattern provides the highest likelihood of positive ILR identification, if an ignitable liquid was initially present. This approach is supported by the fire dynamics that are required to form the doughnut pattern, a well established fire pattern associated with liquid fuel spills on carpet flooring (see Section 3.3.2.1). The phenomenon that forms this pattern requires that the ILR persist the longest at the center of the pattern to the limited burning of material during the initial stage of the fire because of wicking of the gasoline through the carpet fibers. Essentially, the liquid fuel keeps the center of the spill area cool even though it has the greatest incident heat flux from the flame compared to the edges of the fire area. The higher probability of ILR in the center is contrary to the conclusion of O'Donnell. In O'Donnell's tests, the carpet flooring did not have padding beneath it (i.e., less absorption), and his results are not consistent with the formation of doughnut patterns.

For the open burning spill fires on vinyl, the majority of the sampling locations were positively identified as containing ILR. However, in three of the tests, ILR was not identified at the center sampling location. These results indicate that for impermeable substrates, sampling along the edge, or at least away from the center should provide the highest likelihood of positive ILR identification if an ignitable liquid was initially present. This result is consistent with the recommendations of Stauffer et al. [2008]. The preferential degradation of the ILR at the center of the vinyl spill fire pattern is attributed to greater heat fluxes in the center than at the edges.

Within an enclosure without additional Class A combustibles present, the presence of ILR was found to be substantially less prevalent than was observed for open burning tests. This decrease in ILR persistence is attributed to the additional heat imposed by the hot upper layer within the enclosure. This hot layer not only caused additional fuel to be evaporated from the substrate, but also resulted in the involvement of the substrate in the fire. For the vinyl substrate, despite the fact that a 2.0 L (0.53 gal) gasoline spill was used, no positive ILR samples were identified. For the carpet scenarios, three of the nine samples collected were identified as containing ILR. All of these samples were collected from the center of the pattern which is consistent with the findings of the open-burning tests. These tests demonstrated the negative impact that an enclosure has on the persistence of ILR.

Within an enclosure with Class A combustibles present, the persistence of ILR on both carpet and vinyl flooring was dependent on numerous factors that affect the total heat exposure to the material with the ILR. These factors can include the hot upper layer, radiation from fire plumes of burning Class A material and ventilation that creates intensified combustion regions. From these tests, it was determined that identifying ILR sampling locations from enclosure fires with

severe fire conditions (i.e., near or post-flashover) is very challenging for two primary reasons: the first being that the patterns created by the spill fires did not persist through the fire event; and the second being the thermal exposure created by the enclosure fire consumed the ILR in many samples. In general, upholstered furnishing debris (i.e., wood/particle board framing materials) had the highest likelihood of retaining an ILR when compared to samples collected from flooring materials (i.e., carpet or vinyl). Based on the fact that fuel spill patterns generally may not be identifiable at fire scenes with substantial damage (e.g., flashed over conditions), areas should be surveyed for ILR using a systematic approach (i.e., a grid network across the whole space) to ensure representative results. However, particular attention may be given to areas around furniture or other fuel sources that were known to exist in the room. Without a systematic survey approach, the chances are high that an investigator will miss a positive ILR sample location if relying on a visual indicator. This concept reinforces the findings of this work that the absence of ILR in samples collected from a fire scene is not a confirmation that an ignitable liquid was not initially present.

5.0 CONCLUSIONS

This report addresses the forensic analysis of ignitable liquid fuel fires in buildings relative to pattern formation, evaluation of the utility of calcination measurements of gypsum wallboard, and the persistence of ignitable liquid residues (ILR). Based on both small-scale testing and full-scale enclosure fires, an improved understanding of pattern formation and the use of several fire scene analysis tools and methods have been developed. This work establishes a technical basis for interpreting the causes of fire scene patterns, how they relate to area of origin and fire dynamics and the degree that patterns and ILR can be used to substantiate or dismiss the presence of liquid fuel during a fire.

The calcination of gypsum wallboard (GWB) was studied with the intent to 1) develop an objective tool and method of quantifying in situ calcination depths, 2) assess the utility of calcination depth surveys as a means to understand fire origin and fire development within an enclosure, and 3) characterize the impact of water spray on the accuracy of calcination depth measurements. Based on the results of this study, visual observations of GWB cross-sections are not an accurate method to quantify calcination depth based on color or texture variations. Although variations in these characteristics did change, they were not consistently correlated to calcination, moreover a specific depth. A hand-held tool was developed to measure calcination depth based on an evaluation which identified a probe pressure that was sufficient to penetrate all degrees of calcination but not sufficient to penetrate virgin GWB (i.e., uncalcined material). The tool consists of a digital force gauge to which a 2 mm hex key is attached to serve as the probe. A probe force of 3 kg (6.6 lbs) was determined to be the appropriate force to completely penetrate calcined material without penetrating uncalcined material. The 3 kg force with the specified probe equates to a probe pressure of 0.86 kg/mm^2 (1175 psi). Using this probing technique, the calcination depths for a range of GWB samples exposed to varying total heat exposures were in good agreement to a recent study by Mann & Putaansuu [2010], in which the authors characterized calcination depth using an FTIR chemical analysis. The similarity between the depths measured in this study and those quantified by Mann serve as validation of the technique developed in this work. In addition, the probe pressure identified by Mann was 0.9 kg/mm^2 (1230 psi), which is within 5% of the value identified in this study. Correlations were established between the depth of calcination relative to the total heat input to the GWB. A total heat

exposure of approximately 36 MJ/m^2 was required to achieve complete calcination of GWB samples with a thickness of 12.7 mm (0.5 in.) and approximately 90 MJ/m^2 was required to achieve complete calcination of samples with a thickness of 15.9 mm (0.625 in.) samples.

Calcination depth surveys of GWB in full-scale room fires were conducted and contour plots of the depths were compared to visual patterns and the area of origin of the fire. The benefit of the calcination depth survey was realized primarily for the tests where visual patterns were not obvious. In these scenarios, the interior surfaces of the enclosure were heavily sooted with no visual indications of any fire patterns. However, the contour plots provided valuable insight into the areas within the enclosure that were subjected to the most severe thermal damage. In general, the areas in which the initiating (or primary first fuel) fire occurred could be identified based on differences in damage patterns relative to adjacent areas. In the event that visual patterns were present, calcination depth surveys provided minimal additional insight into the fire scenario. However, further study of the relationship between calcination and total heat exposure could enhance the utility of these surveys by providing fire investigators a means of estimating fire growth scenarios based on thermal damage to the GWB. Further work should include documenting transient heat fluxes to walls and ceilings from typical fuel sources (i.e., the total heat exposure). In addition, future work should also continue to evaluate the calcination of lightweight GWB from different manufacturers and to assess the suitability of the 3 kg force probe measurement procedure on these boards.

The impact of water spray on the measurement of calcination depth was evaluated in this study. The results of the testing show that the application of water alters the measured depth of calcination. An average increase in depth of approximately 18 percent was calculated for measurements collected 24 hours after fire exposure and application of the water. This difference fell to less than five percent after the samples were left to dry for a period of 30 days. This data suggests that if measurements are to be collected in areas that have been wetted by suppression activities for any extended period of time, it would be advisable to delay measurements until the water has been removed. However, based on the limited water application (1.25 and 5 gal/ft^2), even at 24 hours, the expected error (~18%) is reasonable if the main purpose of the depth survey is to identify heat patterns.

Gasoline spill fire scenarios were conducted on carpet and vinyl flooring in the open and in rooms with other Class A combustibles. The enclosure fires in this study included flashover conditions (full door vented fires) and fully involved fires that did not actually flashover (slit vent cases). In both types of fires, most combustibles in the room had pyrolized or burned. Exposure durations ranged from 60–300 seconds for open burning scenarios, 1–6 minutes for post-flashover scenarios, and 7–12 minutes for the limited ventilation scenarios.

In general, the utility of floor patterns was minimal for all scenarios except those conducted in the open. Due to the extensive thermal damage within the enclosure fires, patterns initially formed by gasoline spill fires were destroyed. For vinyl floor scenarios, the brevity of the spill fire was such that the surface charring and thermal discoloration produced by the spill fires were quickly overwhelmed by the ignition and burning of the material. Furthermore, the impermeable nature of the vinyl was such that the subfloor was not impacted in any way by the initial spill fire, therefore when the vinyl flooring was consumed, the subfloor showed no evidence of the initiating fire scenario.

For carpet scenarios, the persistence and utility of the patterns was slightly better than that of vinyl floors. In both the open burning and enclosed scenario with no Class A materials present, the carpet flooring showed evidence of the gasoline spill fire in the form of a doughnut pattern. However, this type of pattern was not observed in any of the enclosure tests conducted with other Class A fuels present (i.e., furniture). In these tests, patterns remaining on the flooring materials were primarily a result of the burning Class A materials inducing ignition and flame spread on the flooring material. As a result of this, when the carpet flooring was not completely thermally degraded, the largest and most severe areas of burning were generally located proximate to the larger Class A furnishings (i.e., upholstered sofa and chair).

Based on these flooring evaluations, the persistence of a fire pattern from an initiating fire source requires that the damage from the source be greater than that from the pursuant enclosure fire and that the substrate be resilient enough to survive both exposures. Spill fires in rooms with large volumes relative to the fire size are candidate scenarios in which fuel spill patterns may have a chance to persist, particularly for floor materials that can absorb liquid fuel. Unless there are areas of undamaged or marginally damaged flooring, initial spill fire patterns are not expected to remain post-fire. Based on the tests conducted with fully involved, limited ventilation fires and full door vented flashed over fires, spill patterns did not persist due to the widespread thermal degradation of the floor.

In the nine Class A fire enclosure tests, the most easily identifiable patterns were characterized by the relative absence of soot compared to adjacent areas. Traditionally, these patterns are referred to as clean burns and are associated with the thermal oxidation of soot (i.e., removal of soot due to high temperature exposure). Clean burns are also typically associated with areas that are stark white in contrast to adjacent areas that are blackened due to soot deposition. However as demonstrated in this work, clean burns can exhibit a range of colors from dark gray to white as the pattern forms with increasing heat exposure. These patterns will also range from a finely speckled appearance to fully cleared areas of white gypsum. Further work would be valuable to correlate the different stages of clean burn formation with the visual pattern characteristics, the depth of calcination and the total heat exposure. This work would result in refined methodology of pattern interpretation that could be used to evaluate area of origin and fire growth scenarios.

A range of visual characteristics for clean burn patterns were observed in this study. Numerous wall patterns were identified behind the smaller fuel packages (i.e., upholstered chair and baby seat) which were offset from the enclosure wall. These patterns were not completely clean (white) but showed signs of soot oxidation. Within the boundary of these clean burn patterns, soot was still present, but to varying degrees of gray. As the fire exposed the gypsum wall board, the paper face would pyrolize (thermally degrade, char). Pyrolysis of materials can transition to flaming combustion, but it can also progress as charring or smoldering combustion. The result of the pyrolysis or burning of the gypsum wallboard paper was ash. Ash was present both with and without soot (i.e., black and white). Clean burns occurred with white ash present and sometimes with no ash at all, just the underlying gypsum. These tests showed that clean burn patterns can be formed on walls in areas that do not have a Class A fuel source directly adjacent to them. As noted by other investigators, clean burns can be formed on walls and ceilings in areas dictated by the supply of air due to local ventilation flows.

In several of the tests, large areas in which soot had been removed were not associated with fire exposure. Although at first glance these white patterns had similar appearances to clean burn patterns, they had notable differences upon closer examination. These patterns were characterized by a splatter appearance (larger whitish spots) around the periphery with the center consisting of larger areas of soot removal, sometimes with signs of a smeared, directional appearance. These patterns were the result of suppression activities on both walls and ceilings. In some cases, particularly walls, water marks were observable (i.e., water drip marks). Besides the characteristics noted above, the suppression patterns were also verified by the visual presence of a green tint to the pattern that was associated with the chemical treatment of the suppression water at the fire lab. It is not expected that this color effect will be seen in the field unless similar water treatments are used. The means of differentiating clean burn and suppression patterns based on the characteristics described in this report would be enhanced by further systematic testing. These tests showed that the characteristics are distinct. However, for the case of complete soot and ash removal with large white patterns, there may be circumstances where the absence of either the speckled pattern associated with clean burn development or splatter patterns associated with water extinguishment cause uncertainty in determining the source of the white pattern. In addition, depending on the quality and resolution of photographs, it is possible to have water spray patterns appear as indistinguishable from clean burns in photos.

A total of 52 small- and full-scale fire tests were conducted to study the persistence of an ignitable liquid residue on several different substrates subjected to varying fire conditions and to identify optimum locations from within fire patterns for ILR sampling. The focus of the small-scale testing was to characterize the persistence of an ignitable liquid residue on four different substrates exposed to four different total heat exposures. The substrates evaluated varied in porosity and propensity to burn and represented typical building materials (composite furniture materials, plywood, vinyl and carpet/pad). The results from this testing demonstrated that the likelihood of an ILR persisting within a given substrate was dependent upon both the total heat exposure and the ability of the substrate to absorb the ignitable liquid. Absorbent materials such as carpet flooring and plywood retained ILR under more severe thermal exposures than impermeable substrates, such as vinyl.

The absorbency of the ignitable liquid substrate was not the only factor identified as playing a key role in the persistence of ILR on the material. The combustibility of the material (i.e., how readily it burns) impacted the persistence of the ILR. The prime example of this was the composite furniture material. This material was the most absorbent material tested, however, it was also the most readily combusted (i.e., greatest mass loss at a given heat flux), which resulted in the material being the least likely to contain ILR after the thermal exposure. Based on the small-scale test results, gasoline was most persistent when spilled onto carpet and pad flooring. The likelihood of residue remaining on the other substrates tested was found to be progressively less probable for plywood, vinyl, and the furniture material, respectively. From these tests, approximate total heat exposure thresholds were calculated based on the exposure severity and exposure duration. The thresholds were calculated to provide estimates of the total amount of heat needed to consume the ILR present within the samples tested. A threshold was not established for carpet (i.e., ILR was always identified for the four total heat exposures considered, up to 39MJ/m^2). The threshold for plywood is between 18–39 MJ/m^2. The threshold for vinyl and the furniture material was between 3.6–7.8 MJ/m^2. It should be noted that this threshold is most likely dependent on the volume of ILR applied to the substrate with greater

volumes requiring larger total heat exposures and vice versa. However, this variable was not explored in this work.

Full-scale testing was conducted to identify optimum sampling locations within fuel spill fire patterns. Open-burning and enclosed scenarios, with and without Class A furnishings, were evaluated. ILR results from open burning tests showed that in these scenarios the thermal insult from the spill fire alone is generally not sufficient to consume the ignitable liquid residue present within a given pattern. Samples were collected at edge, mid-point, and center locations for both carpet and vinyl substrates.

The results from open burning spill fires on carpet showed that in the absence of an external heat source, samples can be collected from anywhere within the original spill area to obtain positive ILR results. It should be noted that in many cases, even open burns with extended burning duration, the initial spill area is not readily identifiable. Consequently, for carpet scenarios, sampling from the center of the pattern provides the highest likelihood of positive ILR identification, if an ignitable liquid was initially present. This approach is supported by the fire dynamics that are required to form the doughnut pattern, a well established fire pattern associated with liquid fuel spills on carpet flooring. The phenomenon that forms this pattern requires that the ILR persist the longest at the center of the pattern to the limited burning of material during the initial stage of the fire because of wicking of the gasoline through the carpet fibers. Essentially, the liquid fuel keeps the center of the spill area cool even though it has the greatest incident heat flux from the flame compared to the edges of the fire area. The higher probability of ILR in the center is contrary to the conclusion of O'Donnell. In O'Donnell's tests, the carpet flooring did not have padding beneath it (i.e., less absorption), and his results are not consistent with the formation of doughnut patterns.

For the open burning spill fires on vinyl, the majority of the sampling locations were positively identified as containing ILR. However, in three of the tests, ILR was not identified at the center sampling location. These results indicate that for impermeable substrates, sampling along the edge, or at least away from the center should provide the highest likelihood of positive ILR identification if an ignitable liquid was initially present. This result is consistent with the recommendations of Stauffer et al. [2008]. The preferential degradation of the ILR at the center of the vinyl spill fire pattern is attributed to greater heat fluxes in the center than at the edges.

Within an enclosure without additional Class A combustibles present, the presence of ILR was found to be substantially less prevalent than was observed for open burning tests. This decrease in ILR persistence is attributed to the additional heat imposed by the hot upper layer within the enclosure. This hot layer not only caused additional fuel to be evaporated from the substrate, but also resulted in the involvement of the substrate in the fire. For the vinyl substrate, despite the fact that a 2.0 L (0.53 gal) gasoline spill was used, no positive ILR samples were identified. For the carpet scenarios, three of the nine samples collected were identified as containing ILR. All of these samples were collected from the center of the pattern which is consistent with the findings of the open-burning tests. These tests demonstrated the negative impact that an enclosure has on the persistence of ILR.

Within an enclosure with Class A combustibles present, the persistence of ILR on both carpet and vinyl flooring was dependent on numerous factors that affect the total heat exposure to the

material with the ILR. These factors can include the hot upper layer, radiation from fire plumes of burning Class A material and ventilation that creates intensified combustion regions. From these tests, it was determined that identifying ILR sampling locations from enclosure fires with severe fire conditions (i.e., near or post-flashover) is very challenging for two primary reasons: the first being that the patterns created by the spill fires did not persist through the fire event and the second being the thermal exposure created by the enclosure fire consumed the ILR in many samples. In general, upholstered furnishing debris (i.e., wood/particle board framing materials) had the highest likelihood of retaining an ILR when compared to samples collected from flooring materials (i.e., carpet or vinyl) Based on the fact that fuel spill patterns generally may not be identifiable at fire scenes with substantial damage (e.g., flashed over conditions), areas should be surveyed for ILR using a systematic approach (i.e., a grid network across the whole space) to ensure representative results. However, particular attention may be given to areas around furniture or other fuel sources that were known to exist in the room. Without a systematic survey approach, the chances are high that an investigator will miss a positive ILR sample location if relying on a visual indicator. This concept reinforces the findings of this work that the absence of ILR in samples collected from a fire scene is not a confirmation that an ignitable liquid was not initially present.

The section below provides a bulletized summary of the major findings and conclusions of this research program. The work is presented in three major categories of 1) Calcination of gypsum wallboard, 2) Pattern formation, and 3) Ignitable liquid residue.

Calcination of gypsum wallboard (GWB)

1) Calcination depth measurements
    a. Visual observations of color or texture variations in GWB cross-sections are not an accurate method to quantify calcination depth
    b. Best procedure is to use a digital force gauge with a 2 mm hex key probe applied at a probe force of 3 kg (6.6 lbs), which will penetrate calcined material without penetrating uncalcined material (this may not apply to lightweight GWB for which a lower force may be needed).

2) Field Surveys
    a. Calcination depth survey includes a systematic array of measurements in a grid pattern, such as 1 ft spacing, across a wall or ceiling.
    b. Plotting the depth measurements as a contour plot for each wall or ceiling surface can reveal areas of greater heat flux (i.e., larger and/or longer fire exposures).
    c. Contour plots of calcination depths may resemble visual patterns that can be captured in photographs. However, they can provide more detailed patterns of thermal effects where surfaces have been covered with soot or firefighting water sprays have potentially altered surfaces or washed away soot, creating patterns that may be misinterpreted as clean burn.
    d. Contour plots of calcination depths on ceilings showed the greatest depths above areas in which the initiating (or primary first fuel) fire occurred. This evidence

was particularly useful in aiding the area of origin determination when the ceiling was covered with soot.

e. Correlations were established between the depth of calcination relative to the total heat input to the GWB. A total heat exposure of approximately 10 to 25 MJ/m^2 was required to achieve complete calcination of GWB samples with a thickness of 12.7 mm (0.5 in.) and approximately 90 MJ/m^2 was required to achieve complete calcination of samples with a thickness of 15.9 mm (0.625 in.) samples. With additional testing of heat fluxes to walls and ceiling from specific fuel sources burned next to these surfaces, the correlations can aid in the evaluation of understanding the fire size and duration of burning.

f. Although correlations of calcination depth to total heat input is dependent on the specific brand, the evaluation of GWB from three manufacturers and over a multi-year period shows that the correlations are reasonably similar.

g. The surface damage on GWB can be used to estimate the total heat input to the surface. With increasing heat exposure, the exposed surface of the GWB changes from a brown discoloration of the paper to black sooty ash to white ash with a grey surface to white ash with a white gypsum surface. These phase changes have been correlated to specific total heat exposures expressed in MJ/m^2 as noted above for the depth of calcination correlations.

h. The impact of water spray on the accuracy of calcination depth measurements

i. Water application increases the measured depth of calcination. An average increase in depth of approximately 18 percent was calculated for measurements collected 24 hours after fire exposure and application of the water (1.25 and 5 gal/ft^2). This difference fell to less than five percent after the samples were left to dry for a period of 30 days. Based on the limited water application, even at 24 hours, the expected error (~18%) is reasonable if the main purpose of the depth survey is to identify heat patterns.

Pattern formation

1) Liquid Fuel Spill Fires

a. The utility of floor patterns may be minimal for fires in which most combustibles in the room have pyrolized or burned (i.e., full involvement). Therefore, patterns initially formed by gasoline or other liquid spill fires can be easily destroyed.

b. For vinyl floor scenarios (as with other relatively impermeable surfaces), the brevity of the spill fire is such that the surface charring and thermal discoloration produced by the spill fire is quickly masked by the ignition and burning of the material. Typical spill fires will only burn for approximately 1 minute.

c. For carpet scenarios, the persistence and utility of spill fire patterns was slightly better than that of vinyl floors. In both the open burning and enclosed scenario with no Class A materials present, the carpet flooring showed evidence of the gasoline spill fire in the form of a doughnut pattern. However, in a room fire with

other combustibles involved, the patterns remaining on the flooring materials were primarily a result of the burning of the other combustibles, such as upholstered furniture.

d. Unless there are areas of undamaged or marginally damaged flooring, initial liquid fuel spill fire patterns are not expected to remain post-fire. Based on these flooring evaluations, the persistence of a fire pattern from an initiating fire source requires that the damage from the source be greater than that from the pursuant enclosure fire and that the substrate be resilient enough to survive both exposures.

2) Clean Burns

a. Clean burns are traditionally associated with the thermal oxidation of soot (i.e., removal of soot due to high temperature exposure) and often are associated with areas that are white in contrast to adjacent areas that are blackened due to soot deposition.

b. Clean burns can exhibit a range of colors from dark gray to white as the pattern forms with increasing heat exposure. These patterns will also range from a finely speckled appearance to fully cleared areas of white gypsum.

c. Stages of clean burn formation can include the formation of ash from the gypsum wallboard paper.

d. Ash can be present both with and without soot (i.e., black and white). Clean burns occurred with white ash present and sometimes with no ash at all, just the underlying gypsum.

e. There is currently no established correlation to compare the different stages of clean burn formation with the visual pattern characteristics, the depth of calcination and the total heat exposure. Such correlations would result in a refined methodology of pattern interpretation that could be used to evaluate area of origin and fire growth scenarios. Based on the bench-scale calcination study, clean burn may be associated with total heat exposures of about 20 MJ/m^2 and higher. At these heat exposures, GWB will be fully calcined.

f. Clean burn patterns can be formed on walls and ceilings in areas that do not have a Class A fuel source directly adjacent to them. These clean burn patterns can be dictated by the supply of air due to local ventilation flows.

g. Water sprays can produce patterns that may be confused with clean burn. The water effect patterns were characterized by a splatter appearance (larger whitish spots) around the periphery with the center consisting of larger areas of soot removal, sometimes with signs of a smeared, directional appearance. In some cases, particularly walls, water marks were observable (i.e., water drip marks).

h. Depending on the quality and resolution of photographs, it is possible to have water spray patterns appear as indistinguishable from clean burns in photos. The addition of calcination depth surveys may prove useful in differentiating between water spray patterns and clean burn patterns.

Ignitable liquid residue (ILR)

1) Persistence of ignitable liquid residue (ILR)
    a. The likelihood of an ILR persisting within a given substrate is dependent upon both the total heat exposure and the ability of the substrate to absorb the ignitable liquid.
    b. Absorbent materials such as carpet flooring and plywood retained ILR under more severe thermal exposures than impermeable substrates, such as vinyl.
    c. The greater the total heat exposure the lower the persistence.
    d. The combustibility of the material (i.e., how readily it burns) impacted the persistence of the ILR. Materials that readily burn (i.e., greatest mass loss at a given heat flux) are least likely to contain ILR after the thermal exposure. Polyurethane foam, as used in upholstered furniture, is an example of a materially with a relatively high mass loss rate.
    e. Gasoline was most persistent when spilled onto carpet and pad flooring. The likelihood of residue remaining on the other substrates tested was found to be progressively less probable for plywood, vinyl, and the furniture material, respectively.
    f. Approximate total heat exposure thresholds were calculated to provide estimates of the total amount of heat needed to consume the ILR present within the samples tested.
        i. A threshold was not established for carpet since ILR was always identified for the four total heat exposures evaluated, up to 39MJ/m^2.
        ii. The threshold for plywood is between 18–39 MJ/m^2.
        iii. The threshold for vinyl and the furniture material was between 3.6–7.8 MJ/m^2.
    g. It should be noted that the thresholds are most likely dependent on the volume of ILR applied to the substrate with greater volumes requiring larger total heat exposures and vice versa. However, this variable was not explored in this work.

2) Optimum sampling location for ILR
    a. For open burning spill fires (also applies to fires that are relatively small compared to room volume), the thermal insult from the spill fire alone is generally not sufficient to consume all of the ignitable liquid residue present within a given pattern.
        i. For open burning spill fires on carpet, ILR samples can be collected from anywhere within the original spill area to obtain positive ILR results. It should be noted that in many cases, even open burns with extended burning duration, the initial spill area is not readily identifiable. Consequently, for carpet scenarios, sampling from the center of the pattern provides the highest likelihood of positive ILR identification, if an ignitable liquid was initially present.

ii. For open burning spill fires on vinyl, the majority of the sampling locations were positively identified as containing ILR. However, in three of the tests, ILR was not identified at the center sampling location. These results indicate that for impermeable substrates, sampling along the edge, or at least away from the center should provide the highest likelihood of positive ILR identification if an ignitable liquid was initially present.

b. Within an enclosure without additional Class A combustibles present, the presence of ILR was found to be substantially less prevalent than was observed for open burning tests.

   i. This decrease in ILR persistence is attributed to the additional heat imposed by the hot upper layer within the enclosure. This hot layer leads to more fuel evaporation and involvement of the substrate in the fire.

   ii. For the vinyl substrate with a 2.0 L (0.53 gal) gasoline spill, no positive ILR samples were identified.

   iii. For the carpet scenarios, only three of the nine samples collected were identified as containing ILR. All of these samples were collected from the center of the pattern, which is consistent with the findings of the open-burning tests.

c. Within an enclosure with Class A combustibles present, the persistence of ILR on both carpet and vinyl flooring was dependent on numerous factors that affect the total heat exposure to the material with the ILR.

   i. Factors include the hot upper layer, radiation from fire plumes of burning Class A material and ventilation that creates intensified combustion regions.

   ii. For enclosure fires with severe fire conditions (i.e., post-flashover or fully-involved without flashover), positive measurement of ILR is very challenging for two primary reasons:

      1. patterns created by liquid fuel spill fires do not persist through the fire event

      2. ILR does not persist as readily due to thermal exposure.

   iii. Based on the fact that fuel spill patterns generally may not be identifiable at fire scenes with substantial damage, areas should be surveyed for ILR using a systematic approach. A grid network across the whole space should be used to take multiple ILR test samples.

   iv. Without a systematic survey approach, the chances are high that an investigator will miss a positive ILR sample location if relying on visual indicators.

The absence of ILR in samples collected from a fire scene is not a confirmation that an ignitable liquid was not initially present.

6.0 REFERENCES

ASTM E1188 (2005), *Standard Practice for Collection and Preservation of Information and Physical Items by a Technical Investigator*, American Society of Testing and Materials, West Conshohocken, PA.

ASTM E1412 (2007), *Standard Practice for Separation of Ignitable Liquid Residues from Fire Debris Samples by Passive Headspace Concentration with Activated Charcoal*, American Society of Testing and Materials, West Conshohocken, PA.

ASTM E1459 (2005), *Standard Guide for Physical Evidence Labeling and Related Documentation*, American Society of Testing and Materials, West Conshohocken, PA.

ASTM E1618 (2006), *Standard Test Method for Ignitable Liquid Residues in Extracts from Fire Debris Samples by Gas Chromatography-Mass Spectrometry*, American Society of Testing and Materials, West Conshohocken, PA.

Bertsch, W. (1997), "Analysis of accelerants in fire debris – data interpretation," Forensic Science Review, **9** (1), pp. 2–21.

Carman, S.W. (2009), "Progressive Burn Pattern Development in Post-Flashover Fires," *Proceedings: Fire and Materials 2009, 11th International Conference and Exhibition*, January 26–28, 2009, San Francisco, CA, p. 971.

Chevron (2011), *Unleaded Regular Gasoline – Material Safety Data Sheet*.

Chu, N.N., 2004, "Calcination of Gypsum Plasterboard under Fire Exposure," Fire Engineering Research Report 04/6.

Clodfelter, R.W. and Hueske, E.E. (1977), "A comparison of decomposition products from selected burned materials with common arson accelerants," *Journal of Forensic Science*, **22** (1), pp. 116–118.

DeHaan, J.D. (1997), *Kirk's Fire Investigations*, 3rd Edition, Prentice Hall.

Dement, J.L. (1996), *Cross Contamination*, Bureau of Alcohol Tobacco and Firearms, Hyattsville, MD.

Stauffer, E., Dolan, J., and Newman, R. (2008), *Fire Debris Analysis*, Academic Press.

Flynn, J.D. (2009), "Intentional Fires," National Fire Protection Association.

Gorbett, G., Hicks, W., Hopkins, R., and Kennedy, P. (2010), "Fire Patterns Analysis with Low Heat Release Rate Initial Fuels," *ISFI 2010 Proceedings*: *International Symposium on Fire Investigation Science and Technology,* Marriott Kingsgate Conference Center, Cincinnati, OH, September 27–29, 2010, pp. 269–294.

Gorbett, G.E., Hicks, W., Kennedy, P.M., and Hopkins, R.L. (2006), "Full-Scale Room Burn Pattern Study," *ISFI 2006 Proceedings*: *International Symposium on Fire Investigation Science and Technology,* Marriott Kingsgate Conference Center, Cincinnati, OH, June 26–28, 2006, pp. 207–220.

Gottuk, D.T. and White, D.A. (2002), "Liquid Fuel Fires," Section 2/Chapter 15, *The SFPE Handbook of Fire Protection Engineering*, Third Edition, DiNenno, P.J. (ed.).

Hammins, A., Fischer, S., Kashiwagi, T., Klassen, M., and Gore, J. (1994), "Heat Feedback to the Fuel Surface in Pool Fires," *Combustion Science and Technology*, **97** (1–3), pp. 37–62.

Hicks, W., Gorbett, G., Hopkins, R., Kennedy, P., and Abney, W. (2006), "Advanced Fire Pattern Research Project: Single Fuel Package Fire Pattern Study," *ISFI 2006 Proceedings*: *International Symposium on Fire Investigation Science and Technology,* Marriott Kingsgate Conference Center, Cincinnati, OH, June 26–28, 2006, pp. 221–232.

Hicks, W., Gorbett, G., Hopkins, R., Kennedy, P., and Abney, W. (2008), "Full-Scale Single Fuel Package Fire Pattern Study," *ISFI 2008 Proceedings*: *International Symposium on Fire Investigation Science and Technology,* Marriott Kingsgate Conference Center, Cincinnati, OH, May 19–21, 2008, pp. 209–220.

Hopkins, R.L., Gorbett, G., and Kennedy, P.M. (2008), "Fire Pattern Persistence and Predictability in Pre and Post Flashover Compartment Fires," *ISFI 2008 – Proceedings of the International Symposium on Fire Investigation Science and Technology*, National Association of Fire Investigators, Sarasota, FL.

IAAI (2001), "The Pocket Guide to Accelerant Evidence Collection," International Association of Arson Investigators.

Kennedy, J. and Kennedy, P.M. (1962), *Fire and Arson Investigation*, Investigations Institute, Chicago, IL.

Kennedy, P.M., Kennedy, K.C., and Hopkins. R.L. (2003), "Depth of Calcination Measurement in Fire Origin Analysis," *8th International Conference and Exhibition – Fire and Materials 2003,* San Francisco, CA, January 28, 2003, 12 p.

Kurz, M.E., Jakacki, J., and McCaskey, B. (1984), "Effects of container size and volatility on relative detectability of accelerants by purge and trap versus heated headspace method," *Arson Analysis Newsletter*, **8** (1), pp. 1–14.

Lentini, J.J., Dolan, J.A., and Cherry, C. (2000), "The petroleum-laced background," *Journal of Forensic Science*, **45** (5), pp. 968–989.

Maahs, H. (1971), "Oxidation of Carbon at High Temperatures: Reaction-rate Control or Transport Control," No. NASA-TN-D-6310, NASA Technical Note.

Madrzykowski, D. (2010), "Fire Pattern Repeatability: A Laboratory Study on Gypsum Wallboard," *ISFI 2010 Proceedings*: *International Symposium on Fire Investigation Science and Technology*, Marriott Kingsgate Conference Center, Cincinnati, OH, September 27–29, 2010, 12 pp.

Mann, D.C. and Putaansuu, N.D., 2010, "Studies of the Dehydration/Calcination of Gypsum Wallboard," *Fire and Arson Investigator*, **61** (1), pp. 38–44.

McGraw, J.R. (1998), "Flammability and Dehydration of Painted Gypsum Wallboard Exposed to Fire Heat Fluxes," University of Maryland.

McNair, H.M., and Bonelli, E.J. (1968), "Basic Gas Chromatography," Varian Aerograph, p. 158.

Mealy, C.L. and Gottuk, D.T. (2013), "Ignitable Liquid Fuel Fires in Buildings – A Study of Fire Dynamics," Grant No. 2009-DN-BX-K232, Office of Justice Programs, National Institute of Justice, Department of Justice.

Mealy, C.L., Benfer, M., and Gottuk, D.T. (2011), "Fire Dynamics and Forensic Analysis of Liquid Fuel Fires," Grant No. 2008-DN-BX-K168, Office of Justice Programs, National Institute of Justice, Department of Justice.

Mealy, C.L. and Gottuk, D.T. (2006), "A Study of Unventilated Fire Scenarios for the Advancement of Forensic Investigations of Arson Crimes," 98IJCXK003, Office of Justice Programs, National Institute of Justice, Department of Justice.

Modak, A.T. (1981), "Ignitability of High-Fire-Point Liquid Spills," EPRI NP-1731, Factory Mutual Research Corporation.

Newman, R.T., Dietz, W.R., and Lothridge, K. (1996), "The Use of Activated Charcoal Strips for Fire Debris Extractions by Passive Diffusion. Part I: The Effects of Time, Temperature, Strip Size, and Sample Concentration," *Journal of Forensic Sciences,* **41** (3), pp. 361–370.

NFPA 921 (2011), "Guide for Fire and Explosion Investigations," National Fire Protection Association.

Nowicki, J.F. (1990), "An accelerant classification scheme based on analysis by gas chromatography/mass spectrometry," *Journal of Forensic Science*, **35** (5), pp. 1064–1086.

NRC (2009), "Strengthening Forensic Science in the United States: A Path Forward," National Research Council.

O'Donnell, J.F. (1985), "The Sampling of Burned Areas for Accelerant Residues Analysis, *Fire and Arson Investigator*, **35** (4), pp. 913–923.

Posey and Posey (1983), James E. Posey, Eleanor P. Posey, "Using Calcination of Gypsum Wallboard to Reveal Burn Patterns," The Fire and Arson Investigator, IAAI, St. Louis, MO.

Putorti, A. (2001), "Flammable and Combustible Liquid Spill/Burn Patterns," NIJ Report No. 604-00, National Institute of Justice.

Putorti, A.D. (1997), "Full-scale Room Burn Pattern Study," NIJ Report No. 601-97, National Institute of Justice.

Ren, Q.L. and Bertsch, W. (1999), "A comprehensive sample preparation scheme for accelerants in suspect arson cases," *Journal of Forensic Science*, **44** (3), pp. 504–515.

Riahi, S. (2011), "New Tools for Smoke Residue and Deposition Analysis," Dissertation submitted to The George Washington University.

Schroeder, R.A. (1999), "Post-Fire Analysis of Construction Materials, Doctor of Engineering Dissertation, University of California Berkeley.

SFPE Engineering Guide for Piloted Ignition, 2002, (p. 14).

Shanley, J.H. (1997), "Report of the United States Fire Administration Program for the Study of Fire Patterns," FA 178, Federal Emergency Management Administration, United States Fire Administration.

Stensaas, J.P. et al. (1999), "Determination of fire patterns on floor coverings due to liquid accelerants," Report No. STF22 F98864, Norwegian Fire Research Laboratory.

Williams, M.R., Fernandes, D., Bridge, C., Dorrien, D., Elliott, S., Sigman, M. (2005), "Adsorption Saturation and Chromatographic Distortion Effects on Passive Headspace Sampling with Activated Charcoal in Fire Debris Analysis," *Journal of Forensic Science,* **50** (2), pp. 1–9.

Wolfe, A., Mealy, C.L., and Gottuk, D.T. (2009), "Fire Dynamics and Forensic Analysis of Limited Ventilation Compartment Fires," Grant No. 2007-DN-BX-K240, National Institute of Justice, Department of Justice.

APPENDIX A – VISUAL SUMMARY OF TESTING

A visual summary of each sample is provided below. Each sample summary contains: (a) a pre-exposure face view, (b) a post-exposure face view, and (c), (d), a view of each cross section analyzed.

A.1 CertainTeed 12.7 mm (0.5 in.) (2012)

Total Heat Exposure: 3 MJ/m^2 (10 kW/m^2 for 5 minutes)

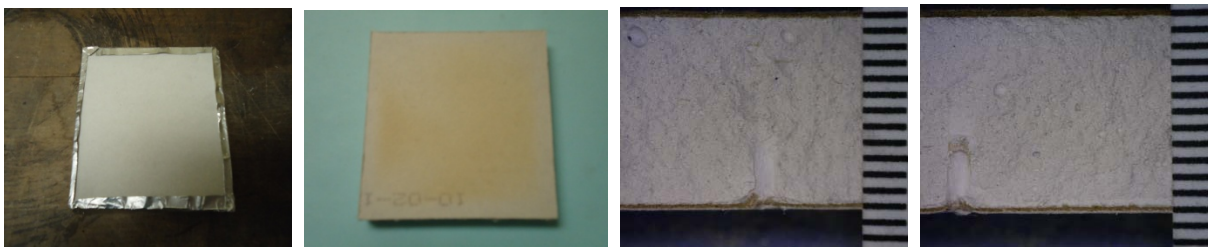

(a) (b) (c) (d)

Total Heat Exposure: 4.5 MJ/m^2 (10 kW/m^2 for 7.5 minutes)

(a) (b) (c) (d)

Total Heat Exposure: 6 MJ/m^2 (20 kW/m^2 for 5 minutes)

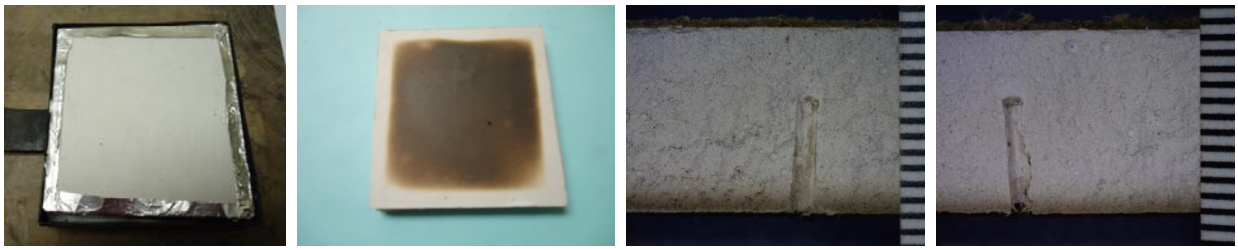

(a) (b) (c) (d)

Total Heat Exposure: 9 MJ/m^2 (20 kW/m^2 for 7.5 minutes)

(a) (b) (c) (d)

Total Heat Exposure: 10.2 MJ/m^2 (20 kW/m^2 for 8.5 minutes)

(a) (b) (c) (d)

Total Heat Exposure: 12 MJ/m^2 (20 kW/m^2 for 10 minutes)

(a) (b) (c) (d)

Total Heat Exposure: 18 MJ/m^2 (20 kW/m^2 for 15 minutes)

(a) (b) (c) (d)

Total Heat Exposure: 39 MJ/m^2 (65 kW/m^2 for 10 minutes)

(a) (b) (c) (d)

Total Heat Exposure: 90 MJ/m^2 (100 kW/m^2 for 15 minutes)

(a) (b) (c) (d)

A.2 National Gypsum 12.7 mm (0.5 in.) (2012)

Total Heat Exposure: 3 MJ/m^2 (10 kW/m^2 for 5 minutes)

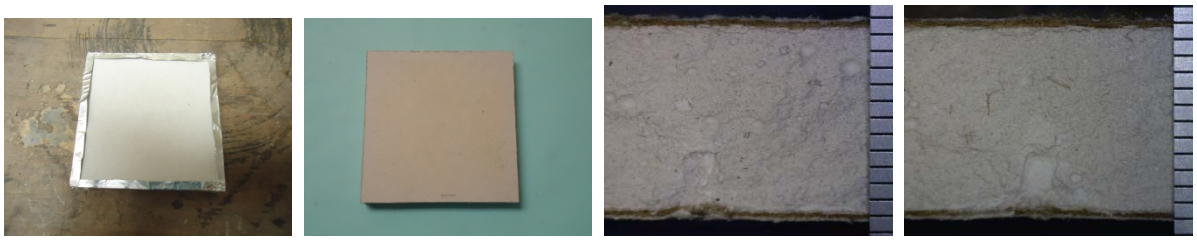

(a) (b) (c) (d)

Total Heat Exposure: 4.5 MJ/m^2 (10 kW/m^2 for 7.5 minutes)

(a) (b) (c) (d)

Total Heat Exposure: 5.1 MJ/m^2 (10 kW/m^2 for 8.5 minutes)

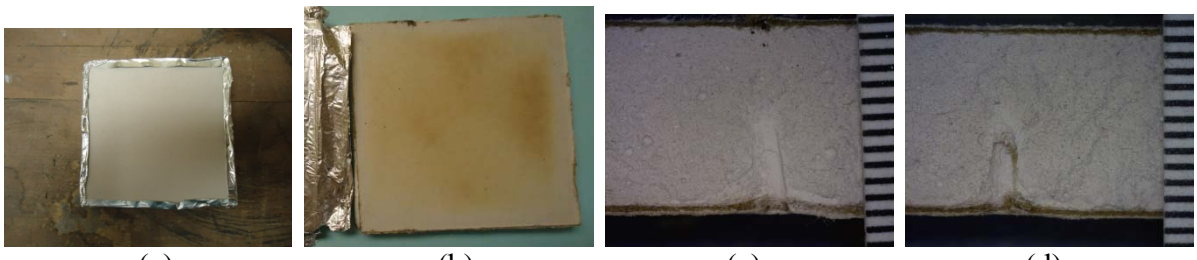

(a) (b) (c) (d)

Total Heat Exposure: 6 MJ/m^2 (20 kW/m^2 for 5 minutes)

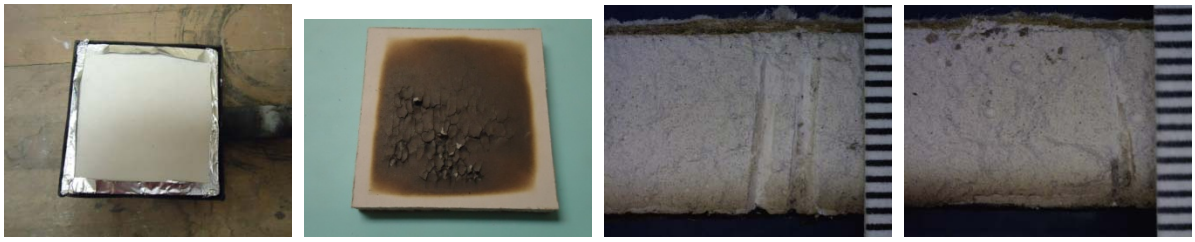

(a) (b) (c) (d)

Total Heat Exposure: 9 MJ/m^2 (20 kW/m^2 for 7.5 minutes)

(a) (b) (c) (d)

Total Heat Exposure: 12 MJ/m^2 (20 kW/m^2 for 10 minutes)

(a) (b) (c) (d)

Total Heat Exposure: 18 MJ/m^2 (20 kW/m^2 for 15 minutes)

(a) (b) (c) (d)

A.3 United States Gypsum (USG) 12.7 mm (0.5 in.) (2002)

Total Heat Exposure: 3 MJ/m^2 (10 kW/m^2 for 5 minutes)

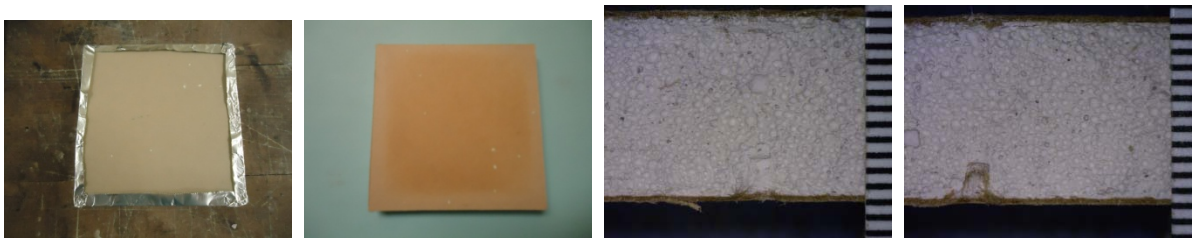

(a) (b) (c) (d)

Total Heat Exposure: 4.5 MJ/m^2 (10 kW/m^2 for 7.5 minutes)

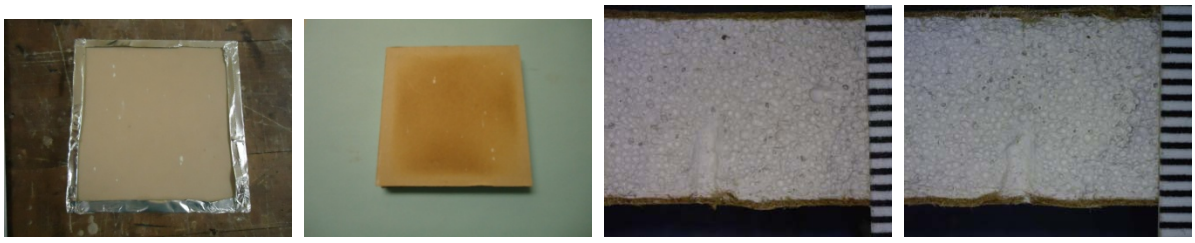

(a) (b) (c) (d)

Total Heat Exposure: 6 MJ/m^2 (20 kW/m^2 for 5 minutes)

(a) (b) (c) (d)

Total Heat Exposure: 7.8 MJ/m^2 (20 kW/m^2 for 6.5 minutes)

(a) (b) (c) (d)

Total Heat Exposure: 9.6 MJ/m^2 (20 kW/m^2 for 8 minutes)

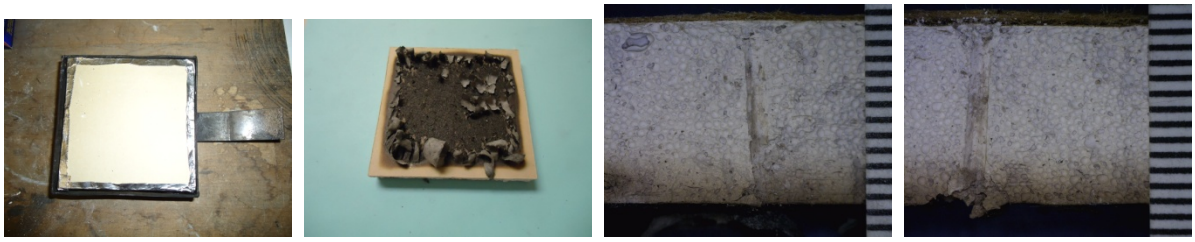

(a) (b) (c) (d)

A.4 USG 12.7 mm (0.5 in.) (2005)

Total Heat Exposure: 3 MJ/m^2 (10 kW/m^2 for 5 minutes)

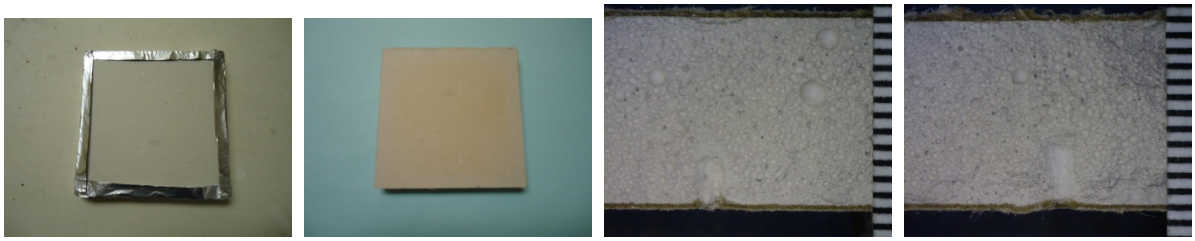

(a) (b) (c) (d)

Total Heat Exposure: 4.5 MJ/m^2 (10 kW/m^2 for 7.5 minutes)

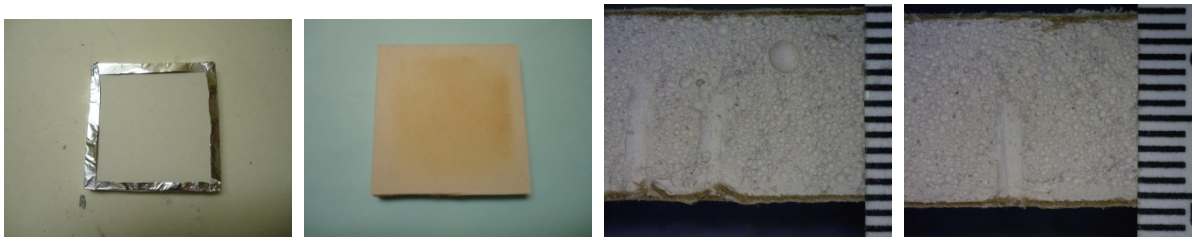

(a) (b) (c) (d)

Total Heat Exposure: 6 MJ/m^2 (20 kW/m^2 for 5 minutes)

(a) (b) (c) (d)

Total Heat Exposure: 9 MJ/m^2 (20 kW/m^2 for 7.5 minutes)

(a) (b) (c) (d)

Total Heat Exposure: 12 MJ/m^2 (20 kW/m^2 for 10 minutes)

(a) (b) (c) (d)

A.5 USG 15.9 mm (0.625 in.) (2012)

Total Heat Exposure: 6 MJ/m^2 (10 kW/m^2 for 10 minutes)

(a) (b) (c) (d)

Total Heat Exposure: 6 MJ/m^2 (20 kW/m^2 for 5 minutes)

(a) (b) (c) (d)

Total Heat Exposure: 12 MJ/m^2 (20 kW/m^2 for 10 minutes)

(a) (b) (c) (d)

Total Heat Exposure: 12 MJ/m^2 (40 kW/m^2 for 5 minutes)

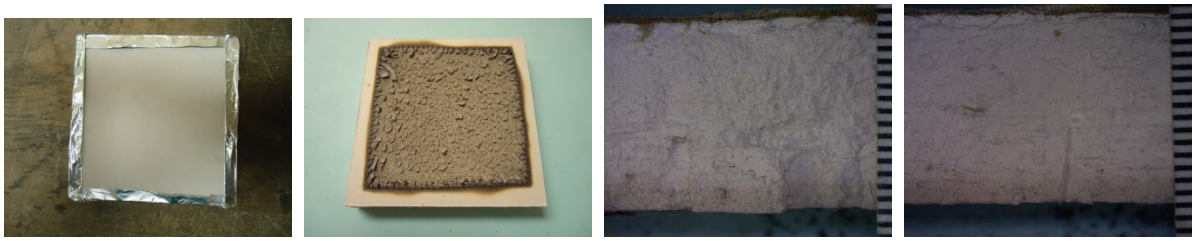

(a) (b) (c) (d)

Total Heat Exposure: 18 MJ/m^2 (30 kW/m^2 for 10 minutes)

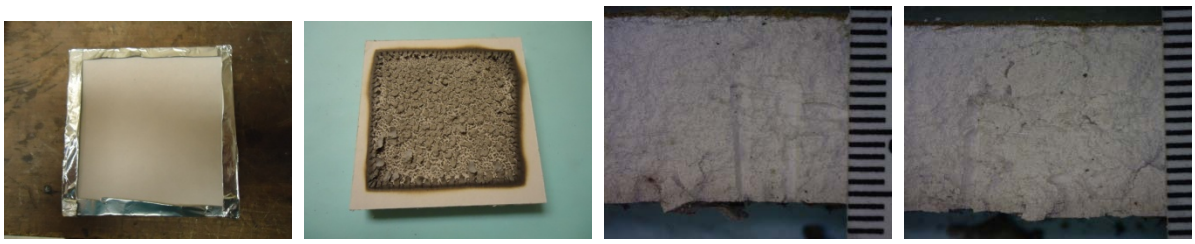

(a) (b) (c) (d)

Total Heat Exposure: 18 MJ/m^2 (60 kW/m^2 for 5 minutes)

(a) (b) (c) (d)

A.6 USG 12.7 mm (0.5 in.) Ultralight (2011)

Total Heat Exposure: 6 MJ/m^2 (20 kW/m^2 for 5 minutes)

(a) (b) (c) (d)

Total Heat Exposure: 10.2 MJ/m^2 (20 kW/m^2 for 8.5 minutes)

(a) (b) (c) (d)

Total Heat Exposure: 15 MJ/m^2 (20 kW/m^2 for 12.5 minutes)

(a) (b) (c) (d)